

**CHARACTERISATION OF CYTOCHROME
P450s IN *ANOPHELES GAMBIAE***

**Submitted to the University of Sheffield for the
degree of
Doctor of Philosophy**

By

Michael Olugbenga Kusimo



**Department of Molecular Biology and Biotechnology
University of Sheffield
England, United Kingdom**

November, 2014

Declaration

This thesis is the result of my work. The material contained within this thesis has not been presented, nor is currently being presented, either wholly or in part for any other degree or qualification.

The research work was undertaken both at the University of Sheffield and at Liverpool School of Tropical Medicine. DNA sequence confirmation for plasmid used in the purification of 5xHist-tagged CYP6Z2 was done at the Core Genomic Facility, Medical School, University of Sheffield and the purification steps were carried out in Professor David Hornby's lab in Sheffield. All the mutagenesis work on CYP6 family in this thesis were carried out in Dr. Mark Paines lab at Liverpool School of tropical medicine and the DNA confirmation of the mutants and wild type confirmed by Source BioScience LifeSciences labs across UK.

Dedication

This Thesis is dedicated to my mum, Mrs Sussana Abosede Kusimo, who was denied formal education by her parents but who gave all to ensure all her children could gain the knowledge she was denied. The achievement in this thesis is an evidence of what she would have become if given the opportunity.

Abstract

Cytochrome P450s provide a natural mechanism by which insects defend themselves against the relatively small number of insecticides approved by WHO in fighting malaria vectors. Three dimensional structures of these enzymes are important to aid our understanding of the mechanism of their action in dissipating the harmful effects of such insecticides. However, to date no coordinates of any insect P450 structure have been deposited in the Protein Data Base. In this study a C-terminally, His-tagged, recombinant CYP6Z2, CYP for cytochrome P450, was constructed genetically and its expression and biochemical properties evaluated in an attempt to produce material suitable for crystallisation trials and ultimately X-ray structural analysis.

The recombinant enzyme was purified in a soluble form through the introduction of a range of chemical agents including sodium cholate. A series of truncating mutants were constructed to determine the minimum set of primary structural elements that create a barrier to crystallisation. Genetically engineered truncations (11 amino acids and 22 amino acids) of the N-terminal hydrophobic region did not produce holoprotein. The N-terminal region appears to be essential to ensure the proper folding of insect P450 investigated, which may be the principal reason underpinning the lack of success in producing crystal structures for this group of enzymes.

The homology model of CYP6Z2 used in this thesis, compared with those of the confirmed pyrethroid metabolisers; CYP6D1 and CYP6P3, revealed three key amino acid differences at their active sites. Single and double mutations of these three amino acids were constructed to explore their individual and joint roles in the metabolic activities of CYP6Z2. The single mutants, CYP6Z2 (Y102F) and CYP6Z2 (F212L) retained similar affinities as wild type for both benzyloxyresorufin (BR) and methoxyresorufin (MR) fluorescent probes. However, the

turnover number of CYP6Z2 (Y102F) was 1.7-fold lower than the wild type for BR but shows improved activity with MR achieving 2-fold increase in turnover. CYP6Z2 (F212L) maintained the same turnover number with the wild type against BR but attained a 3.9-fold increase in activity against the methoxy derivative. Deletion of the positively charged arginine in CYP6Z2 (R210A) significantly improved the activity of the enzyme. The turnover number increased by 3-fold against BR and the enzyme effectiveness also increased by 2-fold. To further investigate the roles of these residues, the same mutations were introduced into CYP6P3. The addition of a hydroxyl group in CYP6P3 (F110Y) changed the kinetic behaviour of the enzyme drastically: the mutant lost activity with the resorufin probe and the affinity for the DEF probe was lowered by 7-fold. Conversely, introduction of benzyl ring in CYP6P3 (L216F) did not affect the affinity, but the enzyme's activity increased by 15-fold with DEF. CYP6P3 (L216F) also improved the pyrethroid metabolising ability of the enzyme. These experiments clearly point to the important contribution of these amino acids in modulating the metabolic characteristics of these P450s. Similar studies were carried out to investigate the function of F115 in CYP6Z2 and CYP6Z3. This residue is frequently found close to the heme in P450s, where it is believed to play a key stabilising role in substrate recognition. A range of mutants were prepared and all produced holoproteins except F115H. The results presented in this thesis, point to a significant role in metabolic function for this residue, F115A, in CYP6Z3, and a rationalisation of the data is presented.

Finally, the metabolic activities of CYP6Z2 and CYP6Z3 were compared in this study. Results presented here, suggest that both act independently in the presence of cytochrome *b*₅ in their activities against the resorufin fluorescent probes but their activities with diethyl fluorescein (DEF) probe increased significantly when cytochrome *b*₅ is present. CYP6Z3 has 2-fold turnover rate and 5-fold greater efficiency more than CYP6Z2 in dealkylation of BR

and 8-fold and 10-fold in turnover and efficiency respectively for MR. These metabolic comparisons suggest strongly that CYP6Z3 is an improved “version” of CYP6Z2.

Acknowledgements

Meeting Prof. David Hornby will forever be one of the best things to happen to me. I narrowly would have missed the opportunity to meet him. My admission into the department of Molecular Biology and Biotechnology was probably the last he did as the HOD. Everything about my studentship was not desirous. Old, poor and worst still coming back to science after spending over 10years in banking! Only very few supervisors would take the risk of accepting my studentship. But he supported me and gave me equal opportunity in his lab to prove my worth. My in-road into LSTM, where I did my bench work with Dr. Mark Paine would not have been possible if he did not care.

I will never forget my first meeting with Dr. Mark Paine in LSTM. Prof. Dave Hornby arranged the meeting for us to discuss my project on P450 enzymes. I was blank throughout the meeting. He gave me 2ul of samples to take back with me to Sheffield to start working with. It was when I got to Sheffield to start working with the plasmids that I realised he only gave me 2ul! I was coming from banking where we work in millions an billions. I concluded he gave me small volume as an excuse to discard me. However, when I transformed the plasmids I realised he had actually given me too much. The content of this thesis is a testimony of how much he has invested in me on P450 enzymes. He did not just give me a bench place to work; he made my stay in LSTM a memorable one. I almost forgot I belong to University of Sheffield.

A big thank you to all my contacts and friends in Sheffield; Linda Harris, Dr Qiaser Sheikh, Paul E Brown, Asma Abdalgalel, Alison Nwokeoji, Ashraf Ahmed, Oluyinka Iyiola, Taib Hamar Soor. I definitely have more friends to thank in Liverpool, all members of ECG group, especially Dr. Cristina Yunta Yane, all members of Vector group standing out in this group is

Sulaiman Sadi, all the Yr 10 & Yr 12 students of Liverpool Life Sciences UTC 2013/2014. I appreciate you all.

My family members both in Nigeria and in the UK have been more than supportive. They cared and supported me my kids and wife which made this journey easier. These family members included all my siblings, my wonderful friends, Mr. & Mrs Victor Akintunde, Mr. & Mrs Segun Adegbite, Mr. & Mrs Julius Okedele, my parish pastors, Admiral Eyitayo and Professor Aboaba, all members of RCCG Pavilion Parish VI Lagos.

Finally to the Hornby family, I say thank you for your love. I was not only considered as Prof. Hornby's student but as part of the wonderful family. Mrs. Derby Hornby welcomed me into her home with open arms. I am most grateful.

Table of contents

Declaration.....	I
Dedication.....	II
Abstract	III
Acknowledgements	VI
Table of contents.....	VIII
List of tables	XII
List of figures.....	XIV
List of abbreviations.....	XVIII
Chapter 1	1
1.1 The economic and medical importance of insects	1
1.1.1 Beneficial insects	1
1.1.2 Insect pests and vectors.....	2
1.2 Vector control.....	2
1.2.1 Major insecticides used in vector control.....	3
1.3 Mechanisms of insecticide resistance	8
1.4 The Cytochrome P450 family of enzymes	10
1.4.1 Functional Roles of P450s.....	11
1.4.2 Nomenclature of P450 Enzymes	12
1.4.3 Classification of P450s based on the nature of their redox partners.....	13
1.4.4 Structure of the active site of P450 enzymes	16
1.4.5 Schematic illustrations of P450 catalytic cycle	18
1.4.6 P450 redox partners	24
1.4.7 Reactions Catalyzed by P450s.....	29
1.4.8 P450 Distribution in Nature	30
1.5 Mutagenesis	35
1.5.1 Site directed mutagenesis (SDM)	35
1.6 Protein 3-dimensional modelling.....	38
1.7 Aims of this project.....	39
Chapter 2	40
2 Site directed mutagenesis to validate the roles of the amino acid residues identified by homology modelling in the active sites of CYP6P3 & CYP6Z2.....	40

2.1	Introduction	40
2.2	Materials & Methods	43
2.2.1	Site directed mutagenesis	43
2.2.2	Co-expression of CYP6Z2, wild and mutants with P450 reductase	45
2.2.3	P450 quantification of the CYPs expressed	47
2.2.4	Enzyme assay	47
2.2.5	Thermostability assay	48
2.2.6	Inhibition assay	48
2.2.7	HPLC analysis	48
2.3	Results	49
2.3.2	Wild type CYP6P3 and mutants, CYP6P3 (Y110F) and CYP6P3 (L216F).....	65
2.4	Discussion.....	72
Chapter 3		76
3	Investigating the role of Phe ¹¹⁵ in the CYP6Z subfamily and comparing kinetic parameters and pyrethroid activities of CYP6Z2 and CYP6Z3	76
3.1	Introduction	76
3.2	Materials & Methods	79
3.2.1	Site directed mutagenesis	79
3.2.2	Thermostability assay	79
3.2.3	Effects of a range of concentrations of cytochrome <i>b</i> ₅ on CYP6Z family.....	79
3.2.4	Cloning and expression of CYP6Z1 in JM109.....	81
3.3	Results	83
3.3.1	P450 contents of expressed mutant isoforms of CYP6Z2	83
3.3.2	Specific activities of CYP6Z2 and mutants against resorufin & DEF probes ..	83
3.3.3	Optimisation of cytochrome <i>b</i> ₅ concentration for metabolic assay	86
3.3.4	Comparison of specific activities of wild type CYP6Z2 and wild type CP6Z3 with resorufin probes and DEF with and without cytochrome <i>b</i> ₅	87
3.3.5	Comparing kinetic parameters of CYP6Z2 and CYP6Z3	90
3.3.6	Thermostability of CYP6Z2, CYP6Z3 and CYP6P3 compared	93
3.3.7	Pyrethroid insecticides metabolic profiles of CYP6Z2 and CYP6Z3 compared with CYP6P3	94
3.3.8	Effect of mutating F115 on the kinetic parameters of CYP6Z2 and CYP6Z3..	95
3.3.9	Effect of mutating F115 on pyrethroid insecticide metabolic profiles of CYP6Z3 ⁹⁷	

3.3.10	Comparison of the thermostability of mutant CYP6Z3 (F115A), CYP6Z2 (Y102F), CYP6Z2 (F212L) and CYP6Z2 (R210A)	98
3.4	Discussion.....	100
Chapter 4	103
4	Establishing suitable expression and purification methods for full length 5xHis-tagged CYP6Z2 & the N-terminal truncated isoforms.....	103
4.1	Introduction	103
4.2	Materials & Methods	106
4.2.1	Transformation and plasmid preparation and analysis	106
4.2.2	Primer design for pB13 insert sequencing	106
4.2.3	Modification to the histidine sequence attached to the CYP6Z2 gene.	107
4.2.4	SDM procedure for the plasmid modification.....	107
4.2.5	Construction and cloning of truncated versions of 5xHis-tagged CYP6Z2....	108
4.2.6	Expression of the full length 5xHis-tagged CYP6Z2 and the truncated isomers	109
4.2.1	Affinity chromatography and purification of full length 5xHis-tagged CYP6Z2	109
4.2.2	Ion exchange purification of the partially purified full length 5xHis-tagged CYP6Z2	110
4.2.3	SDS-PAGE analysis.....	110
4.2.4	Immunoblotting	111
4.2.5	Bradford total protein quantification	111
4.2.6	P450 quantification of the full length 5xHis-tagged CYP6Z2 expressed	112
4.3	Results	113
4.3.1	Confirmation of Insert and Plasmid	113
4.3.2	Expressed full Length 5xHis-tagged CYP6Z2 and the truncated isoforms	114
4.3.3	SDS-PAGE and immunoblotting of expressed 5xHis-tagged CYP6Z2	117
4.4	Discussion.....	119
Chapter 5	124
5	General discussion and conclusions.....	124
5.1	The N-terminal hydrophobic region of insect P450s may be a requirement for structural stability and integrity.....	124
5.2	Site directed mutagenesis of amino acid residues at the active sites of CYP6Z2 and CYP6P3 predicted to be involved in metabolic activity, by <i>in silico</i> modelling.	127

5.3	The role of cytochrome <i>b</i> ₅ in P450 metabolism depends on both the substrates and the P450 enzymes	129
5.4	Phenylalanine residue 4.0 Å to porphyrin may be involved in stabilising coupling of the oxygen on the haem iron.	132
5.5	CYP6Z3 has higher metabolic activity than CYP6Z2	135
5.6	Conclusions	136
5.7	Recommendations.....	137
	References	140
	Appendix 1: Plasmid pB13.....	160
	Appendix 2: DNA Sequence confirmation of SDM of CYP6Z2(R210A).....	161
	Appendix 3: PCR reactions	163
	Appendix 4: CPR quantification graphs and total protein evaluations	164
	Appendix 5: Amino Acid sequence confirmation of double mutant CYP6Z2 (F212L, Y102F)	166
	Appendix 6: Amino acid sequence confirmation of double mutant CYP6Z2(F212L, Y102A)	167
	Appendix 7: Resorufin standard curve.....	168
	Appendix 8: DNA sequence alignments of documented alleles of CYP6Z2 amino acid with the gene used in this project.	169
	Appendix 9: Analysis of mutations observed in the polymorphism of CYP6Z2	170
	Appendix 10: Amino acid sequence confirmation of CYP6P3	173
	Appendix 11: HPLC Chromatograms	174
	Appendix 12: No of nucleotide change and the effects on enzyme activities.	179
	Appendix 13: Amino acids sequence alignment of CYP6Z1, CYP6Z2 & CYP6Z3.....	180
	Appendix 14: Amino acids sequence alignment of CYP6Z1, CYP6Z2 & CYP3A4	181
	Appendix 15: % amino acids identities between CYP6Z1, CYP6Z2, CYP6Z3 and CYP3A4	182
	Appendix 16: DNA Sequence confirmation of ompACYP6Z1	183
	Appendix 17: DNA Sequence confirmation of SDM of CYP6Z3 (F115A)	185
	Appendix 18: Protein standard curve	186

List of tables

Table 1.1: Beneficial insects and their advantage to man.....	1
Table 2.1: Amino acids differences at the active sites of CYP6Z2 and CYP6P3.....	42
Table 2.2: Mutagenic primers for the creation of double mutants CYP6Z2(F212L,Y102A), CYP6Z2(F212L,Y102F) and CYP6Z2(R210A).....	44
Table 2.3: Specific activities of CYP6Z2, CYP6Z2 (Y102F) and CYP6Z2(F212L) against resorufin probes.....	53
Table 2.4: Benzyloxyresorufin kinetics of CYP6Z2 (wild), CYP6Z2(Y102F) & CYP6Z2(F212L).....	55
Table 2.5: Methoxyresorufin kinetics of CYP6Z2(Y102F) & CYP6Z2(F212L).....	56
Table 2.6: Specific activities of CYP6Z2(R210A) against the four resorufin probes.....	57
Table 2.7: Specific activity of CYP6Z2 (R210A) with the DEF probe.....	58
Table 2.8: Benzyloxyresorufin kinetics of CYP6Z2(R210A) compared with the wild type CYP6Z2 and mutants Y102F and F212L.....	60
Table 2.9: Specific Activities of CYP6P3 and CYP6P3(L216F) with or without b_5 against BR & PR.....	66
Table 2.10: Specific Activities of CYP6P3 and CYP6P3(L216F) with or without b_5 against DEF.....	67
Table 2.11: Kinetic parameters for DEF by CYP6P3, F110Y and L216F.....	69
Table 2.12: Pyrethroid insecticides depletion assay.....	71
Table 3.1: Phe ¹¹⁵ mutagenic primers for CYP6Z2 and CYP6Z3.....	80
Table 3.2: Comparison of dealkylation of resorufin probes between CYP6Z3 and CYP6Z2.....	87
Table 3.3: Specific activities of CYP6Z3 and CYP6Z2 against BR with or without b_5	88
Table 3.4: Specific activities of CYP6Z3 and CYP6Z2 against DEF with or without b_5	89

Table 3.5: Kinetic parameters of BR dealkylation by CYP6P3 & CYP6Z2.....	91
Table 3.6: Kinetic parameters for MR dealkylation of CYP6Z2 & CYP6Z3	92
Table 3.7: Insecticide metabolic activities of CYP6Z3 and CYP6Z2 compared with CYP6P3 as control.....	94
Table 3.8: Kinetic parameters for BR dealkylation of CYP6Z2, CYP6P6Z2 (F115A), CYP6Z3 and CYP6Z3(F115A).....	96
Table 3.9: Metabolic assay with pyrethroid insecticides.....	97
Table 4.1: Primers and template for the creation of truncated 5xHis-tagged CYP6Z2.....	108
Table 5.1: Comparisons of the amino acid sequences of the N-terminal hydrophobic domain of CYP2B sub-family with CYP6Z2.....	125
Table 5.2: Predicted phenylalanine in some P450s and their closeness to the porphyrin of the haem.....	133

List of figures

Figure 1.1: Dichlorodiphenyltrichloroethane (DDT).....	4
Figure 1.2: Malathion.....	4
Figure 1.3: Bendiocard.....	5
Figure 1.4: Permethrin and etofentrox.....	6
Figure 1.5: Deltamethrin and cypermethrin.....	6
Figure 1.6: Biochemical target sites of synthetic insecticides.....	7
Figure 1.7: Detoxification of deltamethrin by P450-mediated oxidation.....	9
Figure 1.8: The typical P450 haem iron with all the six ligands coordination.....	11
Figure 1.9: P450 nomenclature chart.....	12
Figure 1.10: Typical class 1 P450s in both eukaryotic system and prokaryotic system.....	13
Figure 1.11: Typical class 2 P450s in both eukaryotic system and prokaryotic system.....	14
Figure 1.12: Electron transfer through the cytochrome P450–cytochrome P450 reductase Complex.....	15
Figure 1.13: The typical conserved P450 fold illustrating the helices, haem iron centre and the arrangement of the substrate recognition sites.....	17
Figure 1.14: Resting state of P450, binding of substrate displacing water molecule and acceptance of the first electron.....	18
Figure 1.15: Peak at 450nm as seen when P450s are artificially reduced by sodium dithionite in the presence of CO.....	19
Figure 1.16: Binding of oxygen and rearrangement of electrons resulting to formation of ferric superoxide.....	20
Figure 1.17: Acceptance of second electron.....	20
Figure 1.18: Protonation steps.....	21
Figure 1.19: Electron rearrangement between the haem and the bound atom for the formation of the activated oxygen.....	21
Figure 1.20: Product formation and release.....	22
Figure 1.21: The catalytic cycle of P450.....	23

Figure 1.22: Crystal structure of rat CPR domain showing the arrangement of the FMN and FAD domains.....	25
Figure 1.23: Some of the reactions catalysed by P450s.....	29
Figure 1.24: Pie charts of P450 distributions in nature.....	30
Figure 2.1 Structural alignment of the homology models of CYP6P3 and CYP6Z2.....	42
Figure 2.2: A-Fe ²⁺ -CO vs Fe ²⁺ difference spectrum CYP6Z2 and the single mutants.....	50
Figure 2.3: Fe ²⁺ -CO vs Fe ²⁺ difference spectrum CYP6Z2 and the double mutants	51
Figure 2.4: Specific activities of CYP6Z2 (wild), CYP6Z2 (Y102F) and CYP6Z2 (F212L) with the resorufin probes.....	53
Figure 2.5: Michaelis-Menten plot of CYP6Z2 (wild) CYP6Z2(Y102F) & CYP6Z2(F212L)-benzyloxyresorufin kinetics.....	55
Figure 2.6: Michaelis-Menten plot of CYP6Z2 (wild), CYP6Z2 (Y102F) & CYP6Z2 (F212L)-methoxyresorufin kinetics.....	56
Figure 2.7: Michaelis-Menten plot of CYP6Z2(R210A)-benzyloxyresorufin kinetics.....	60
Figure 2.8: Inhibition assay of CYP6Z2-mediated methoxyresorufin O-debenzylation (MROD) reaction with deltamethrin as inhibitory ligand.....	61
Figure 2.9: Inhibition assay of CYP6Z2(Y102F) -mediated MROD reaction with deltamethrin as inhibitory ligand.....	62
Figure 2.10: Inhibition assay of CYP6Z2(F212L) -mediated MROD reaction with deltamethrin as inhibitory ligand.....	62
Figure 2.11: Deltamethrin Metabolism comparison of wild Type CYP6Z2 and mutants F212L & Y102Y from freshly prepared enzymes.....	63
Figure 2.12: Deltamethrin Metabolism comparison of wild Type CYP6Z2 and mutant R210A from freshly prepared enzymes.....	64
Figure 2.13: Bar chat of specific activities of CYP6P3 and CYP6P3(L216F) with or without <i>b</i> ₅ against BR and PR.....	66
Figure 2.14: Bar chat of the specific activities of CYP6P3, F110Y and L216F with or without <i>b</i> ₅ against DEF probe.....	66
Figure 2.15: Michaelis-Menten plot of CYP6P3, F110Y and 216F -DEF kinetics.....	69
Figure 2.16: Thermostability test of CYP6P3, CYP6P3(F110Y) and CYP6P3(L216F) using DEF substrate.....	70

Figure 2.17: Homology models of CYP6P3 overlaid with CYP6Z2 and deltamethrin.....	73
Figure 2.18: Homology models of CYP6Z2 with permethrin docked in the active site, and CYP6D1 with permethrin docked in the active site.....	73
Figure 3.1 Homology model of CYP6Z2 viewed with Pymol showing the haem in rainbow colour and Phe ¹¹⁵ residue in yellow at a 7.1 Å to the haem center and 3.1 Å to the pyrrole of the haem.....	78
Figure 3.2: Homology model of CYP6P3 showing the haem in red colour, Phe ¹¹⁰ in green and Phe ¹²³ in blue. Phe ¹¹⁰ is 12.1 Å and 13.6 Å to the nearest pyrroles of the haem, while Phe ¹²³ is 4.1 Å close to the nearest pyrrole of the haem. Phe ¹²³ of CYP6P3 occupies the same position as Phe115 of CYP6Z2 when compared.....	79
Figure 3.3: Fe ²⁺ -CO vs Fe ²⁺ difference spectrum of CYP6Z2 and the mutants, F115A, F115L and F115Y.....	84
Figure 3.4: A- Fe ²⁺ -CO vs Fe ²⁺ difference spectrum CYP6Z2 and F115A, F115L, and F115Y- P450 contents in (µM).....	84
Figure 3.5: Specific activities of CYP6Z, F115A, F115L, F115Y and F115W against BR...	85
Figure 3.6: Serial dilution of cytochrome <i>b</i> ₅ concentrations against 1 pmol of P450 in DEF dealkylation reaction.....	86
Figure 3.7: Effect of <i>b</i> ₅ on P450 activity. Bar chat of specific activities of CYP6Z3 and CYP6Z2 against BR with or without <i>b</i> ₅	88
Figure 3.8: The influence of cytochrome <i>b</i> ₅ on the specific activity of CYP6Z3 and CYP6Z2 against DEF, with or without <i>b</i> ₅ investigating effect of addition of cytochrome <i>b</i> ₅ to the reactions.....	89
Figure 3.9: Michaelis-Menten plot of CYP6P3 & CYP6Z2 -BR kinetics.....	91
Figure 3.10: Michaelis-Menten plot of CYP6P3 & CYP6Z2 -MR kinetics.....	92
Figure 3.11: Thermostability of CYP6Z2, CYP6Z3 and CYP6P3 compared as a percentage of activity against DEF at room temperature.....	93
Figure 3.12: Michaelis-Menten plots: A- CYP6Z2 and CYP6Z2(115A), B- CYP6Z3 and CYP6Z3(F115A). -BR kinetics.....	96
Figure 3.13: Thermostability assay of: CYP6Z3 and mutant F115A, CYP6Z2 and mutants Y102Y,F212L and CYP6Z2 and mutant R210A.....	99
Figure 4.1: 1% agarose gel the digested CYP6Z2 sample with standard DNA markers....	113
Figure 4.2: The P450 yield of at different incubation temperature, shaking and time.....	115

Figure 4.3: Fe ²⁺ CO vs Fe ²⁺ difference spectrum of the full length 5xHis-tagged CYP6Z2 and the 2 truncated isoforms, CYP6Z2(Δ3-13) & CYP6Z2(Δ3-25) showing the P450 & P420 folding patterns.....	116
Figure 4.4: The SDS-PAGE of the expressed CYP6Z2 stained with coomassie with the protein ladder	117
Figure 4.5: SDS-PAGE stained with coomassie and western blot of the purified CYP6Z2 on affinity chromatography and further purification on SP sepharose.....	118
Figure 4.6: Homology model of CYP6Z2 showing the three dimensional structure of the full length CYP6Z2. The N-terminal hydrophobic domain truncated is the extended domain in blue.....	121
Figure 5.1: One step dealkylation reaction of P450 against resorufin derivative probes.....	130
Figure 5.2: Two-step dealkylation reaction of P450 against fluorescein derivative probes..	130
Figure 5.3: Predicted phenylalanine that may be involved in π-π interactions with the porphyrin of the haem in CYP6Z1, CYP6Z2, CYP6Z3, CYP6P3, CYP6M2 and CYP2D6.....	134

List of abbreviations

A	Adenine
aa	Amino acid
ALA	δ -Aminolevulinic acid
amp	Ampicillin
<i>An. gambiae</i>	<i>Anopheles gambiae</i>
ATP	Adenosine triphosphate
<i>b₅</i>	Cytochrome <i>b₅</i>
bp	Base pair(s)
BR	Benxyloxyresorufin
BSA	Bovine serum albumin
C	Cytosine
cDNA	Complementary Deoxyribonucleic acid
CPR	Cytochrome P450 reductase
C-terminus	Carboxyl terminus
dATP	Deoxyadenosine Triphosphate
DDT	Dichlorodiphenyltrichloroethane
DEF	Diethyl-Fluorescein
DMSO	Dimethyl sulfoxide
DNA	Deoxyribonucleic acid
dNTP	Deoxynucleoside triphosphate
dsDNA	Double strand
DTT	Dithiothreitol
<i>E.coli</i>	<i>Escherichia coli</i>
EDTA	Ethylenediaminetetra acetic acid
ER	Ethoxyresorufin
EtBr	Ethidium bromide
EtOH	Ethanol
exo	Exonuclease

G	Guanine
HPLC	High-performance liquid chromatography
IPTG	Isopropyl -1- thio- β -D- galactoside
Kb	Kilo base pair (1000bp)
<i>kcat</i>	Overall Enzymatic Catalytic Rate
kDa	KiloDalton
LB	Luria Bertani Medium
MR	Methoxyresorufin
mRNA	Messenger ribonucleic acid
mt	Mutant type
MW	Molecular weight
NADP	Nicotinamide adenine dinucleotide phosphate
N-terminus	Amino terminus
O/N	Over night
OD	Optical density
Oligo	Oligodeoxynucleotide
Ori	Origin of replication
P450	Cytochrome P450
PAGE	Polyacrylamide gel electrophoresis
PBS	Phosphate-buffered saline
PCR	Polymerase Chain Reaction
pfu pol	<i>Pyrococcus furiosus</i> Polymerase
pol	Polymerase
PR	Pentoxeresorufin
rpm	Revolutions per minute
SDM	Site-directed mutagenesis
SDS	Sodium dodecyl sulphate
ss	Single strand
T	Thymine
TAE	Tris-acetic acid-EDTA
TB	Terrific broth

TEMED	Tetramethylethylenediamine
Tet	Tetracycline
TSE	Tris-Sucrose-EDTA
UV	Ultraviolet
W/T	Wild type

Chapter 1

1.1 The economic and medical importance of insects

Insects belong to a class of invertebrates within the arthropod phylum (Chapman, 2009). They have a chitinous exoskeleton, three body parts, head, thorax and abdomen, three pairs of jointed legs, compound eyes and a pair of antennae. There are more than a million species described and they represent more than half of all known living organism (Chapman, 2009). Insects are considered to be both beneficial and harmful to humans.

1.1.1 Beneficial insects

Insects described as beneficial to man, are those that add value to the human race. Some of the beneficial insects are listed in Table 1.1

Table 1.1: Beneficial insects and their advantage to man.

Insect	Benefit(s)
Bees	Honey, wax, pollination (Losey and Vaughan, 2006)
Silkworm	Silk (Losey and Vaughan, 2006)
Ladybugs	Predator of pest insects (Gullan and Cranston, 2009)
Maggot	Wound treatment (Whitaker et al., 2007)
Cicada	Source of protein (Gullan and Cranston, 2009)
Dung beetles	Decomposition and burial of dung (Losey and Vaughan, 2006)
Lac Insects	Shellac (used in dye, wood finishing, polish, food glazes etc)

1.1.2 Insect pests and vectors

Insect pests are those considered to cause significant damage to farm produce, such as the locust, infrastructure, such as termites and those that are parasitic, including lice and bed bugs (Bale et al., 2008). Insect vectors transmit infectious pathogens to another living organism (Roberts and Janovy, 2005) and have been reported to be responsible for close to 20% of all infectious diseases affecting people in developing countries (David et al., 2013). Mosquitoes are carriers of parasites and viruses responsible for human diseases typified by malaria and dengue (World Health Organization, 2010).

Malaria is prevalent in tropical and subtropical regions (Caraballo and King, 2014) and presents a major hindrance to economic development in these regions. In 2005, it was estimated that over £8 billion is lost annually in Africa as a consequence of the widespread distribution of malaria (Greenwood et al., 2005). Malaria in man is caused by infection with any of the five species of the single cell *Plasmodium* parasites: *P. falciparum*, *P. vivax*, *P. ovale*, *P. malariae* and *P. knowlesi* (Collins, 2012, Mueller et al., 2007). The primary causative agent of fatal mortality rate is *P. falciparum*, since *P. vivax*, *P. ovale*, *P. malariae* elicit milder type of malaria disease (Caraballo and King, 2014). Infection is transmitted by bites from an infected female mosquito of the *Anopheles* species, especially from *An. gambiae* and *An. funestus*.

1.2 Vector control

The World Health Organisation (WHO), other organisations and many countries have initiated several programmes to eradicate malaria. The two major strategies deployed to date are the development of drugs and vector control programs. However, the available drugs are expensive and the parasites are developing resistance at a significant pace (Djimdé et al., 2001, Price and Nosten, 2001, Wellems and Plowe, 2001). Chloroquine (CQ) drug was discovered in 1940 and

became first-line drug for the treatment of malaria. It was effectively used to treat and eradicate malaria in the 1950s. However, its use diminished and was banned in some countries as first-line drug because of the emergence of malaria parasite developing resistance to the drug (Klein, 2013). Combination of sulfadoxine/pyrimethamine (SP) replaced CP but did not last long as front-line drug because of the wide spread of parasite resistance that emerged quickly (Roper et al., 2003). Artemisinin class drugs are currently the first-line malaria drug. However, there have been reports of a delayed-clearance phenotype, which is the first sign that resistance to the drug may emerge soon (Dondorp et al., 2010, Phyo et al., 2012). Vaccination, which would have been a practicable option to fight malaria parasite is still the subject of clinical trials (Agnandji et al., 2011). Therefore, developing a sustainable and effective vector control management program to prevent the transmission of the parasite is of paramount importance.

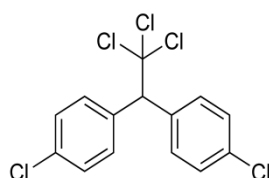
Vector control includes the large-scale distribution of long lasting insecticide treated nets (LLINs) and insecticide residual sprays (IRS) in endemic regions (Bassat et al., 2008, Riveron et al., 2013). LLINs are impregnated with pyrethroid insecticides and are wash resistant (up to 20 washes) (Atieli et al., 2010). Pyrethroid insecticides are the only group of insecticides approved by WHO to be used in conjunction with LLINs (Hougard et al., 2003). Whereas the four different insecticides groups approved by WHO: chlorinated hydrocarbons, pyrethroids, carbamates and organophosphates can be used in IRS (David et al., 2013). The vector control program is currently offering the most effective means of preventing malaria transmission (Stevenson et al., 2011). However, pyrethroid and DDT resistance in *An. gambiae* is reported to be spreading across Africa (Yadouleton et al., 2010).

1.2.1 Major insecticides used in vector control

Insecticides are substances that have the capability to kill or debilitate insects (Stephenson et al., 2006). The various classes of insecticides are described below.

1.2.1.1 Organochlorides

This is the most widely used class of insecticides and includes dichlorodiphenyltrichloroethane, DDT. The insecticidal effect of this compound was discovered in 1939 and it has been used to control malaria morbidity and mortality since then (Dunlap, 1981).



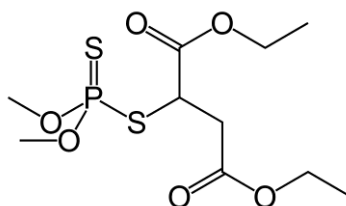
DDT

Figure 1.1: Dichlorodiphenyltrichloroethane (DDT). An organochloride insecticide.

Its environmental effects on wild life, including egg shell thinning has led to a banning order for agricultural purposes, limiting its use to disease vector control (van den Berg, 2009).

1.2.1.2 Organophosphates & carbamates

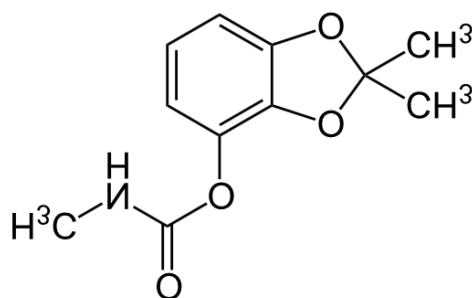
Organophosphates are esters of phosphoric acid and act as insecticides by interfering with acetylcholinesterase and other cholinesterases. They kill or disable insects by disrupting nerve impulses. These insecticides, unlike organochlorides, degrade at a significant rate with time, and do not cause bioaccumulation (Connell et al.). However, they have cumulative toxic effect to wild life. Malathion is one example of this class of insecticide.



Malathion

Figure 1.2: Malathion. An organophosphate insecticide.

Carbamates, such as Bendiocarb (Figure 1.3) exhibit a similar mode of action as the organophosphates, causing reversible inhibition of acetylcholinesterases. Organophosphate irreversibly inactivate acetylcholinesterases (Robert, 2002).



Bendiocarb

Figure 1.3: Bendiocarb. A carbamate insecticide.

1.2.1.3 Pyrethroids

Pyrethroid insecticides are important in malaria control programs because they are the only insecticide class recommended by WHO for use in the manufacturing of LLINs, and remain widely used in indoor residual spray formulations. They are preferred to other insecticide classes, especially in household insecticides (Robert, 2002), because they are non toxic to humans at low concentration (less than 1/100th pound of active ingredient per acre (Pears and Cranshaw, 2010)) required to be effective on insect and are easily degraded by sunlight under normal atmospheric conditions (Gilbert et al., 2005).

Pyrethroids are synthetic analogues of pyrethrins from the pyrethrum flower. There are two classes of these insecticides based largely on their mode of binding to sodium channels (Figure 1.6) and the presence of α -cyano group in their chemical structures (Gilbert et al., 2005).

Type 1 pyrethroids bind preferentially to closed sodium-channels and do not have an α -cyano group examples are shown below.

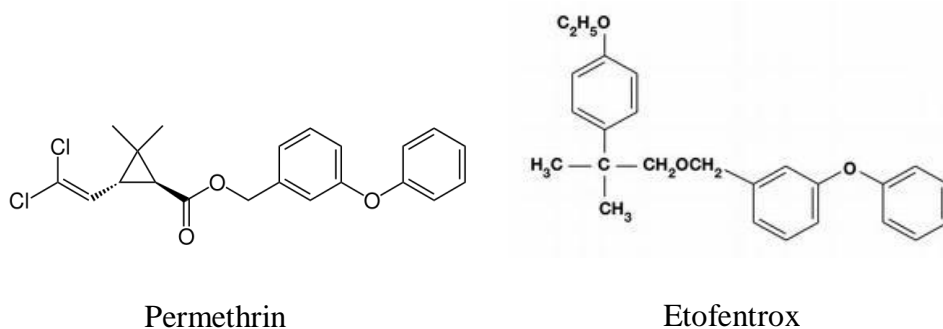


Figure 1.4: Permethrin and etofenrox. Examples of type 1 pyrethroid insecticides.

Type 2 pyrethroids bind preferentially to open sodium-channels and have an α -cyano group (Figure 1.5)

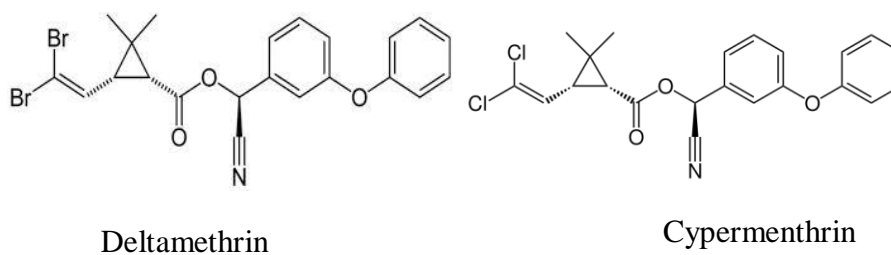


Figure 1.5: Deltamethrin and cypermethrin. Examples of type 2 pyrethroid insecticides

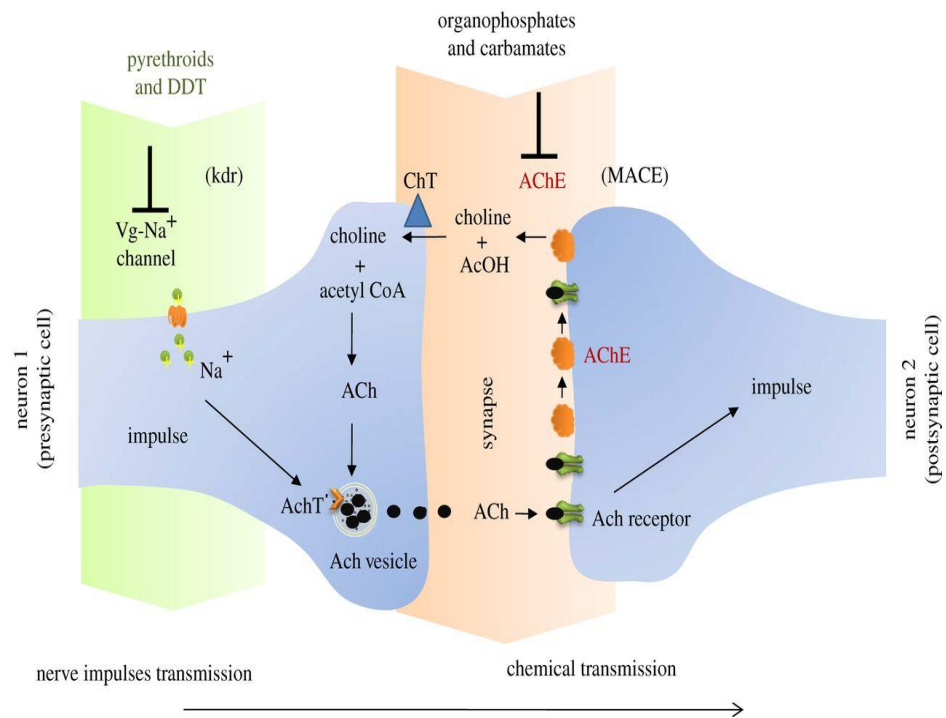


Figure 1.6: Biochemical target sites of synthetic insecticides. Pyrethroids and DDT exert their toxic effect by blocking voltage-gated sodium channels, which generally produces fast knock-down properties (kdr). Organophosphate (OP) and carbamate insecticides inhibit acetylcholinesterase (AChE) which plays an important role in terminating nerve impulses. The reduced sensitivity of AChE as a result of a gene mutation (MACE) causes resistance to OP and carbamate insecticides. ACh, acetylcholine; AchT, Ach transporter; AcOH, acetic acid; ChT, choline transporter; MACE, modified acetylcholinesterase; Vg-Na⁺ channel, voltage-gated sodium channel; kdr, knock-down resistance (diagram taken from (David et al., 2013))

1.3 **Mechanisms of insecticide resistance**

Insecticide resistance in general, is the inherited ability of a strain of insects to survive doses of an insecticide that would ordinarily kill the majority of individuals in a normal population of the same species (World Health Organization, 1982). The mechanisms responsible for insect resistance are complex and include behavioural and/or physiological changes of insects. This might include, avoiding the insecticides, sequestration of the insecticide, altered penetration, target site alteration and bio-degradation (Gilbert et al., 2005). Mosquitoes use target site modification and metabolic resistance as their insecticide resistance mechanisms (David et al., 2013). Target site resistance involves mutation that leads to well-defined target site alteration and resistance to insecticides (David et al., 2013, Donnelly et al., 2009). Metabolic resistance involves increased bio-degradation of the insecticides via overproduction of detoxification enzymes which includes P450s, glutathione s-transferases and carboxyesterases or cholinesterases (Hemingway and Ranson, 2000): these enzymes can act alone or in concert with each other (Fig. 1.7). P450s, however, are the major enzyme family out of the detoxification enzyme groups that have been extensively reported to be associated with insecticide resistance (David et al., 2013).

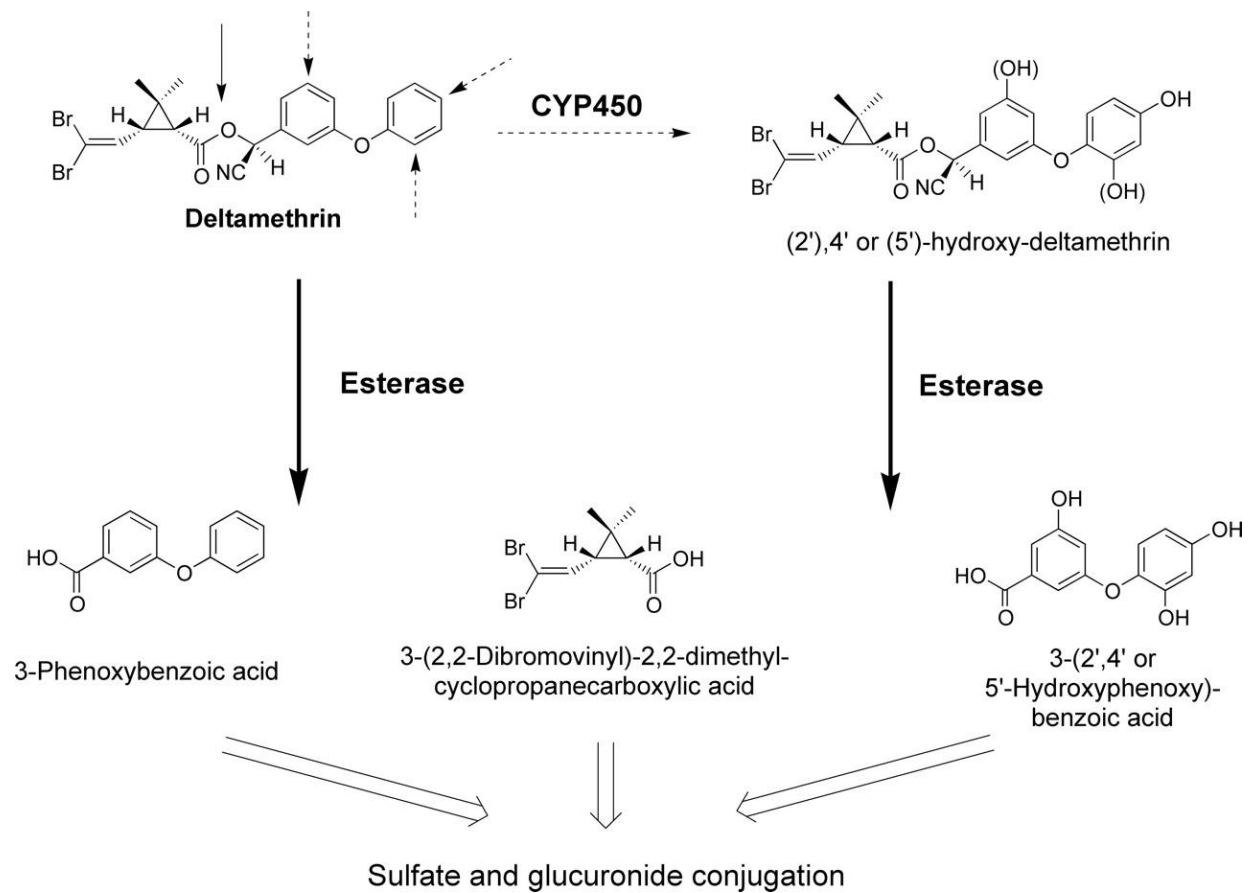


Figure 1.7: Detoxification of deltamethrin by P450-mediated oxidation (dotted arrows) in combination with esterase-mediated hydrolysis (solid arrows) and followed by conjugation, figure taken from (Anand et al., 2006).

1.4 The Cytochrome P450 family of enzymes

Cytochrome P450s have been given several names based on their functions since they were first described by Hayaishi in 1955, who measured an enzymatic activity involved in the oxidative cleavage of catechol to mucronic acid. He named the enzyme “pyrocatechase” (Hayaishi et al., 1955). Pyrocatechase thus became one of the first enzymes to be discovered capable of incorporating atmospheric oxygen in the cleavage of the carbon chains of substrates (Denisov et al., 2005). These enzymes are called monooxygenases because they could incorporate hydroxyl groups into substrates; mixed function oxidases because each of the atoms of the atmospheric oxygen is used simultaneously, one incorporated into substrate and the other forming a water molecule; polysubstrate monooxygenases because they usually are not substrate specific; microsomal oxidases because they are usually found in the microsomes of eukaryotic cells; and haem thiolate proteins, because haem is anchored to the protein via a cysteine thiolate ligand (Feyereisen, 1999). Presently, the unambiguous simple name “P450” without modifier is being used because of the characteristic peak at 450 nm (Estabrook, 1996).

P450 enzymes are a large group of haem thiolate proteins, now known to be ubiquitous in Nature. Unlike other haem containing proteins, they absorb light maximally at 450 nm in the reduced carbon monoxide bound state. The molecular basis of cytochrome P450 absorbance in this range is the unusual structural environment of its liganding to the haem iron. Four ligands are provided by nitrogens on the haem ring. There are two vacant ligands above and below the plane of the haem: the fifth and sixth ligands. In cytochrome P450, the fifth ligand is occupied by a thiolate anion (Figure 1.8). The sulphur is derived from a conserved cysteine at the haem binding region of the active site. The sixth ligand position is usually temporarily occupied by a water molecule, which is displaced when the substrate binds to the active site (Shaik et al., 2005).

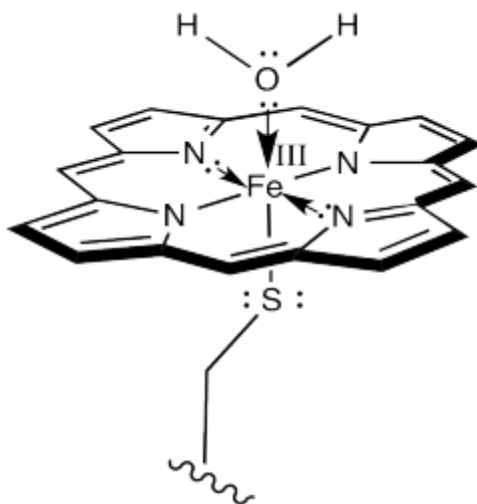


Figure 1.8: The typical P450 haem iron with all the six ligands coordinated. (<http://employees.scsbsju.edu/cschaller/Reactivity/oxygen/O RO SP450rest.png>).

1.4.1 Functional Roles of P450s

There are two main functions performed by P450s. They metabolise xenobiotic compounds, which are exogenous to the organisms. They do these by either making the compound water soluble or they degrade the compound into non toxic metabolites (Hammock et al., 1985). The second function is important in the biosynthesis of signalling molecules which in turn are important for the control of development and homeostasis (Denisov et al., 2005). Drugs and xenobiotic removal, steroid hormones and fat soluble vitamin synthesis including conversion of polyunsaturated fatty acids into biologically active molecules are performed by P450s in mammalian tissues. The same roles are performed in insects where control of development and resistance to insecticides have been linked to P450s (Agosin, 1985, Feyereisen, 1999)

1.4.2 Nomenclature of P450 Enzymes

Cytochrome P450 (CYP) is a ubiquitous class of enzyme in Nature but there exist numerous variants of CYP isoforms which are classified according to the similarities of their amino-acid sequences as follows:

- Families - CYP *families* contain genes that have at least 40% sequence homology.
- Subfamilies - Members of a *subfamily* must have at least 55% identity.
- Individual genes – Specific Isoform

Illustrated as follows:

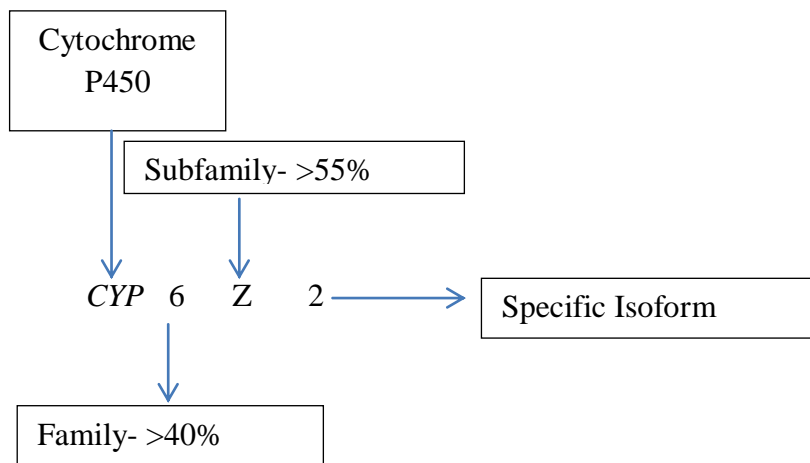


Figure 1.9: P450 nomenclature chart

1.4.3 Classification of P450s based on the nature of their redox partners

P450s are generally classified into two major classes. The classifications depend on the nature of the other protein(s) involved in their redox reactions (Nebert and Gonzalez, 1987).

Class I P450- This class is made up of a two-component shuttle system consisting of an iron-sulfur protein (ferredoxin) and ferredoxin reductase. This class is found on the membranes of mitochondria or in bacteria and is shown diagrammatically in Figure 1.10.

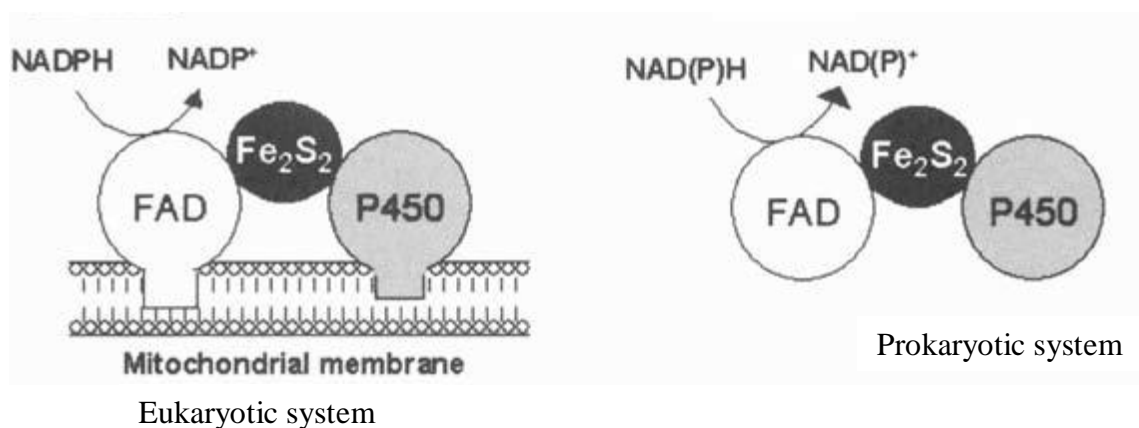


Figure 1.10: Typical class 1 P450s in both eukaryotic and prokaryotic systems. Electrons are transferred from NAD(P)H via an FAD-containing ferredoxin reductase and an iron-sulphur containing ferredoxin to P450 (Paine et al., 2005).

Class II P450- This class is a single membrane-bound enzyme containing FAD and FMN cofactors. This class is typified by the liver microsomal enzymes in mammalian cells:

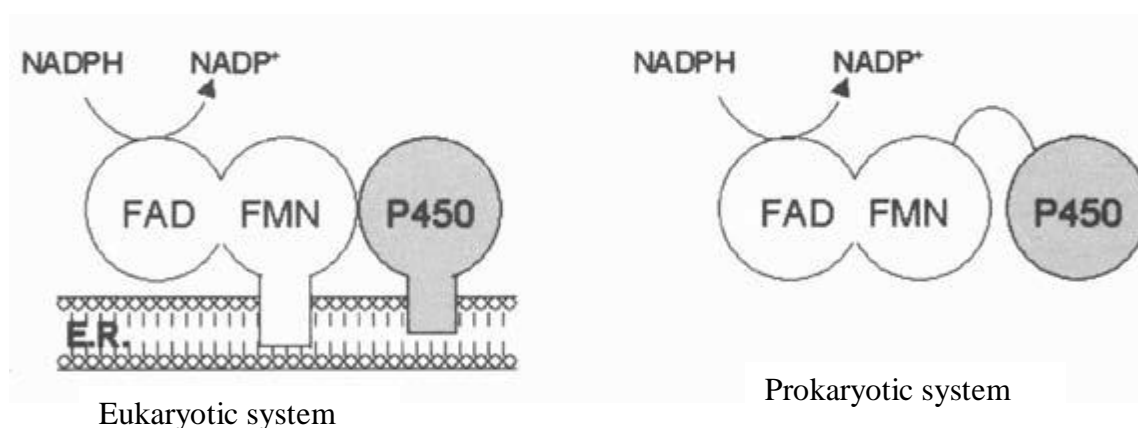


Figure 1.11: Typical class 2 P450s in both eukaryotic system and prokaryotes. Electrons are transferred from NADPH via diflavin (FMN and FAD) containing reductases. The reductases are bound to the endoplasmic reticulum in eukaryotes but fused to the P450s in prokaryotes e.g. P450 BM3 (Paine et al., 2005).

There are some groups of P450s that can act alone (i.e. without a redox partner) such as CYP74A (Brash, 2009). P450 BM3 has a unique structure in which P450 is fused to CPR, thereby making it self sufficient: it possesses the highest catalytic activity among the known P450s (Munro et al., 2002).

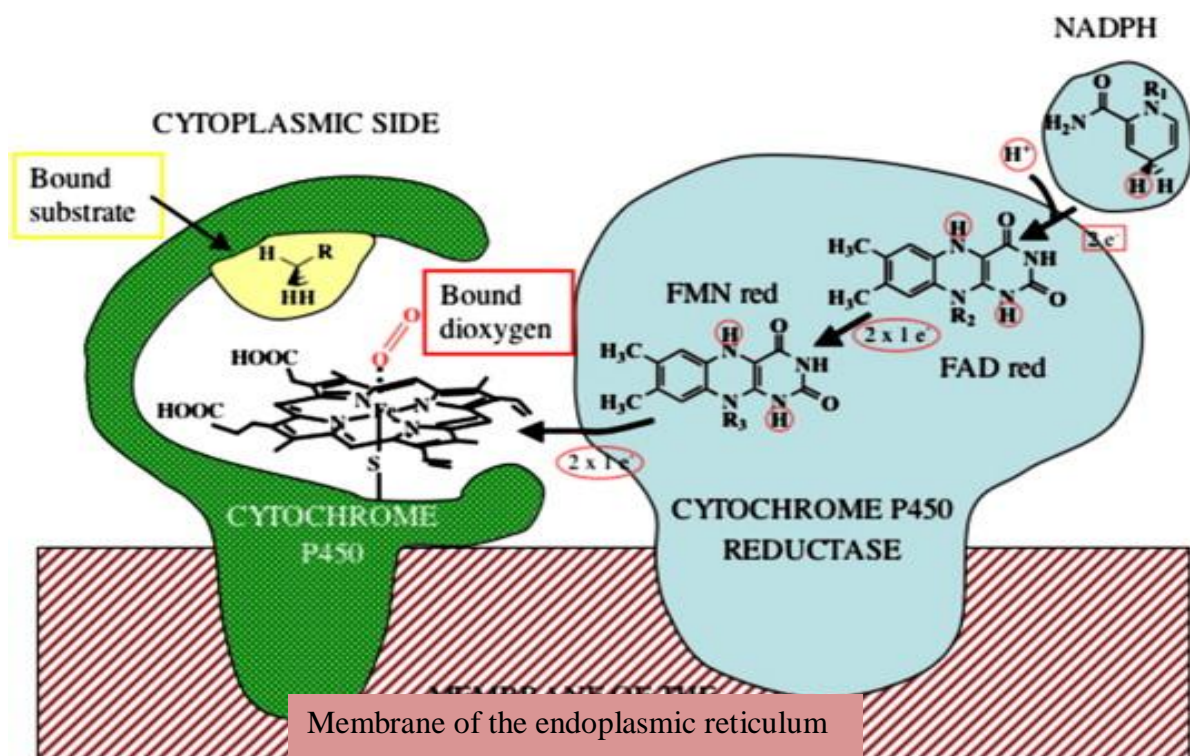


Figure 1.12: Electron transfer through the cytochrome P450–cytochrome P450 reductase complex taken from (Ricoux et al., 2007).

1.4.4 Structure of the active site of P450 enzymes

P450 enzymes have a common overall structural topology even though their sequence identity is less than 20% across the gene superfamily (Hasemann et al., 1995). The structural core of P450s is made up of four helices, with three parallel helices indicated as D, L and I as shown in Figure 1.13. Helix E is anti-parallel to the other helices (Presnell and Cohen, 1989). The prosthetic haem group is confined between the distal I helix and proximal L helix and bound to the adjacent Cys-haem-ligand loop which has the conserved amino acid sequence FxxGx(H/R)xCxG, the P450 signature. The cysteine is the proximal ligand to the iron in the haem. The sulphur in the cysteine forming the fifth ligand in the haem iron, which is a thiolate, and is the origin of the characteristic 450-nm Soret band observed for the ferrous-CO complex from where the P450 is named (Dawson et al., 1976).

There are six substrate recognition sites in P450s which are regarded as flexible region of the active site that allow binding of substrates of different sizes (Gotoh, 1992). SRS1 is located at the B' helix region, SRS2 and SRS3 are parts of the F and G helices, SRS4 is part of I-helix, SRS5 is at β 4 hairpin and SRS6 is at K helix β 2 connecting region. Substrates bind to these SRS regions in an induced-fit mechanism for subsequent catalytic activity (Pylypenko and Schlichting, 2004). These SRSs have been shown through SDM to contribute to the functions of the P450s. SRS1, SRS4, SRS5, and SRS6 participating in formation of the catalytic site, while SRS 2 and SRS3 participate in the formation of the substrate access channel (Schuler and Berenbaum, 2013).

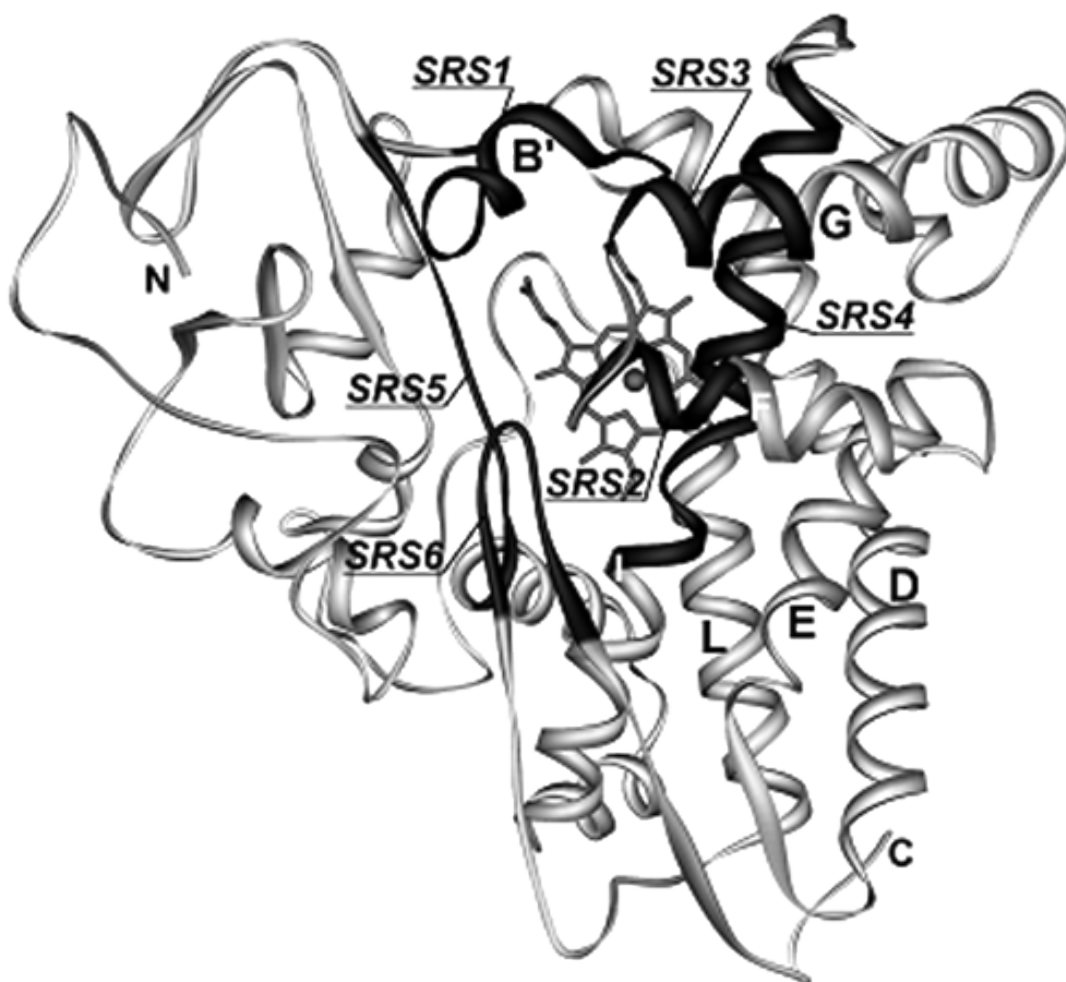


Figure 1.13: The typical conserved P450 fold illustrating the helices, haem iron centre and the arrangement of the substrate recognition sites (Denisov et al., 2005).

1.4.5 Schematic illustrations of P450 catalytic cycle

When a P450 is at its “resting” state, it is mostly in the ferric Fe^{3+} form, owing to the relatively low reduction potential of the $\text{Fe}^{3+}/\text{Fe}^{2+}$ couple: the presence of the proximal thiolate ligand helps to maintain this low redox potential (Fantuzzi et al., 2004). In the absence of substrates, water coordinates at the sixth ligand to stabilise the low state of the ferric iron (Raag and Poulos, 1989). Substrate binding to the enzyme displaces the water molecule at the sixth distal ligand position and causes a shift of the resting low spin of the haem iron to high spin (Sligar, 1976). The displacement of the water molecule at the sixth ligand thermodynamically destabilises the ferric state to be easily reduced by the presence of the first electron to the ferrous state (Haines et al., 2001).

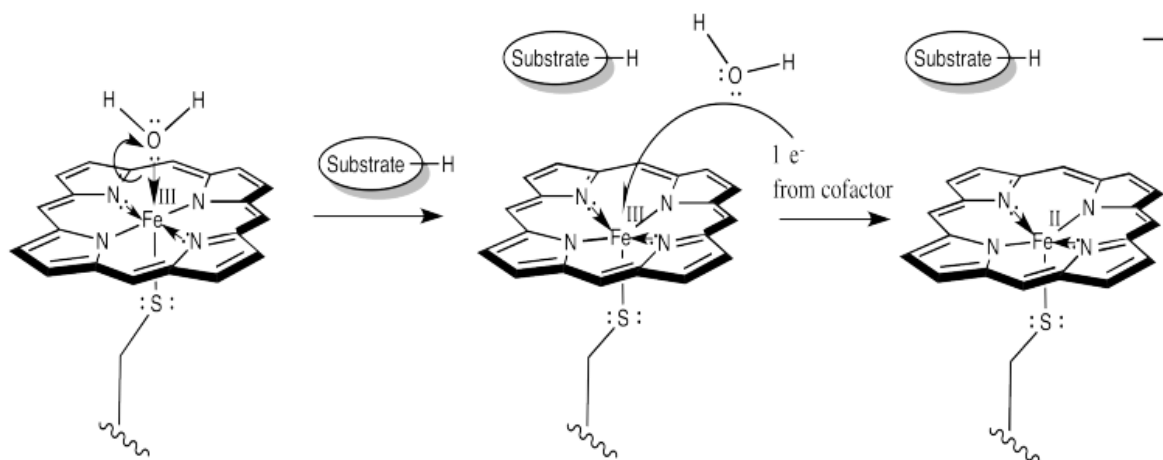


Figure 1.14: Resting state of P450, binding of substrate displacing water molecule and acceptance of the first electron. (<http://employees.scsbsju.edu/cschaller/Reactivity/oxygen/OROSP450bind.png>).

Oxygen and carbon monoxide do not bind to the ferric form of the haem iron. However, they do bind when a reducing agent such as dithionite or P450 reductase reduces (using NADPH) the ferric haem iron to ferrous form. The ferrous CO versus ferrous difference spectrum is based on the ability of the P450 to bind CO when reduced and form the complex that specifically gives a spectrum with a peak at 450nm which is due to the signature cysteine thiolate to the 5th ligand of the haem iron of the P450 (Klingenberg, 1958). Omura et al developed the extinction coefficients which enables the in vitro quantification of the P450s possible using sodium dithionite as reducing agent (Omura and Sato, 1962).

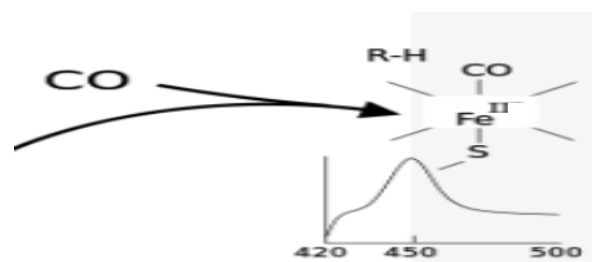


Figure 1.15: Peak at 450nm as seen when P450s are artificially reduced by sodium dithionite in the presence of CO

Oxygen on the other hand binds to the reduced P450 to give the ferrous dioxygen complex $\text{Fe}^{2+}\text{-OO}$ or ferric superoxide complex $\text{Fe}^{3+}\text{-OO}^-$ because the iron is able to transfer an electron to the bound dioxygen (Momenteau and Reed, 1994).

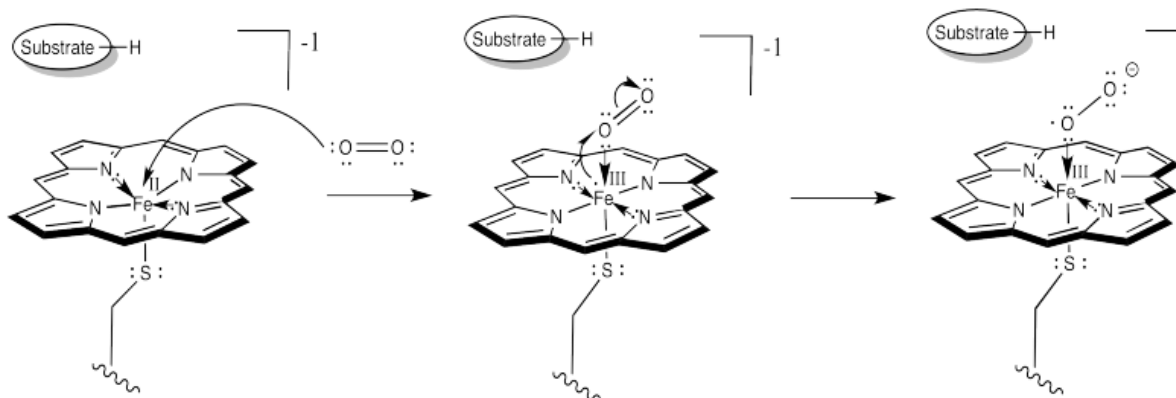


Figure 1.16: Binding of oxygen and rearrangement of electrons resulting to formation of ferric superoxide. (<http://employees.scsbsju.edu/cschaller/Reactivity/oxygen/O OSP450bind.png>).

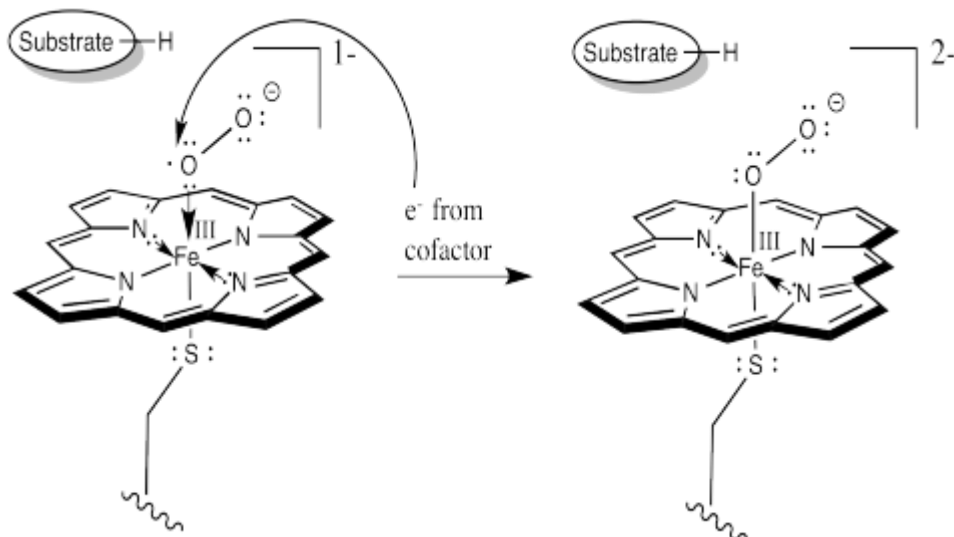


Figure 1.17: Acceptance of second electron. The ferric superoxide is reduced with a second electron provided by the cofactor(s) to become ferric peroxide ion. (<http://employees.scsbsju.edu/cschaller/Reactivity/oxygen/O OSP450peroxo.png>).

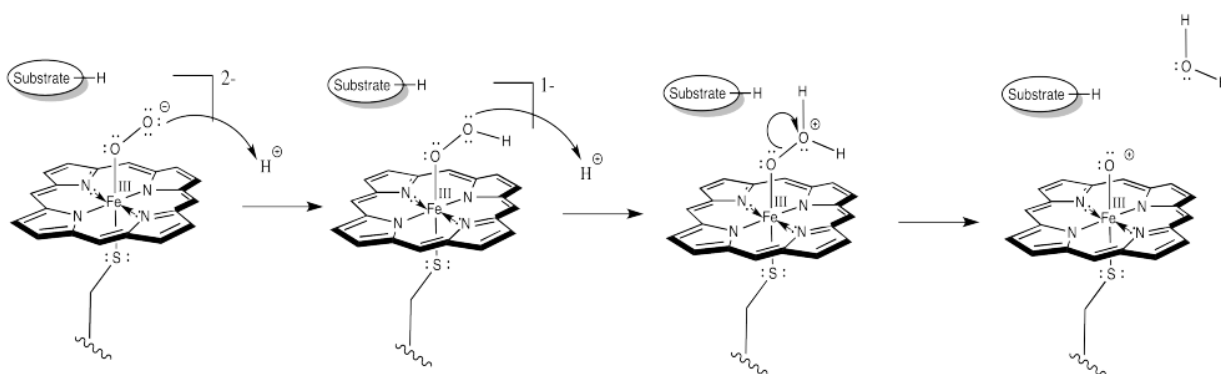


Figure 1.18: Protonation steps. The ferric peroxide formed is protonated twice at the distal oxygen atom on the haem iron causing the heterolytic cleavage of the O-O bond and the release of water. This leaves an atom of electron-deficient oxygen on the haem. (<http://employees.scsbsju.edu/cschaller/Reactivity/oxygen/O OSP450proton.png>).

The heterolytic cleavage of the O-O bond forms the ferryl-oxo porphyrin complex, which now possesses electron deficient oxygen. The iron in the haem has reservoir of electrons and could donate one electron to form iron (IV) or two to form iron (V) oxide complex. Porphyrin plays a key role in the activation of the oxygen on the haem iron at this point by donating an electron for the O-O bond cleavage (Dolphin et al., 1997, Goh and Nam, 1999, Stillman, 2000).

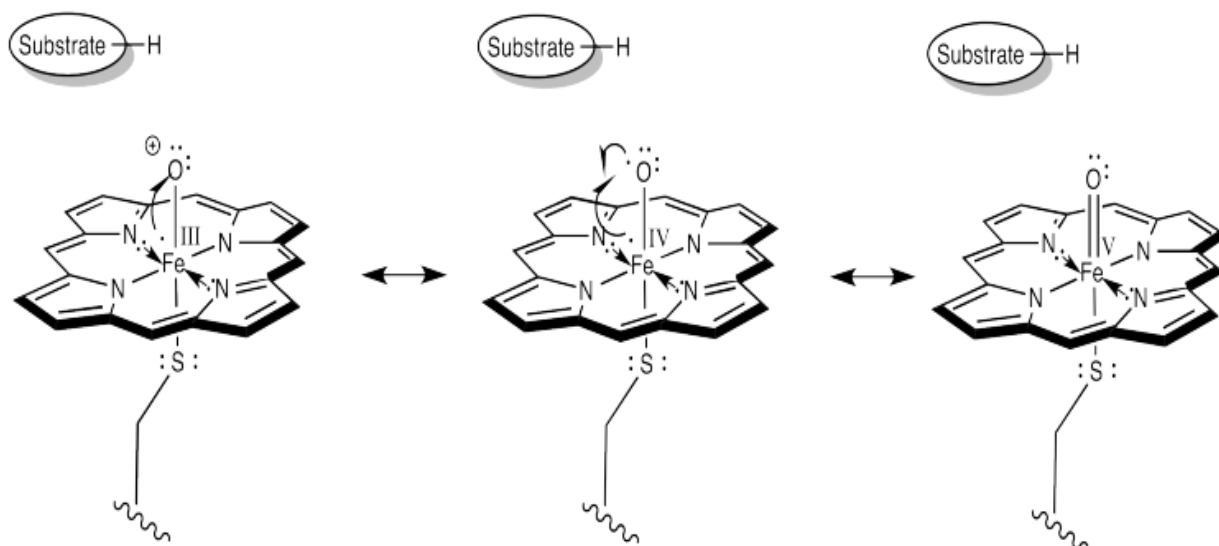


Figure 1.19: Electron rearrangement between the haem and the bound atom for the formation of the activated oxygen. (<http://employees.scsbsju.edu/cschaller/Reactivity/oxygen/O OSP450active.png>).

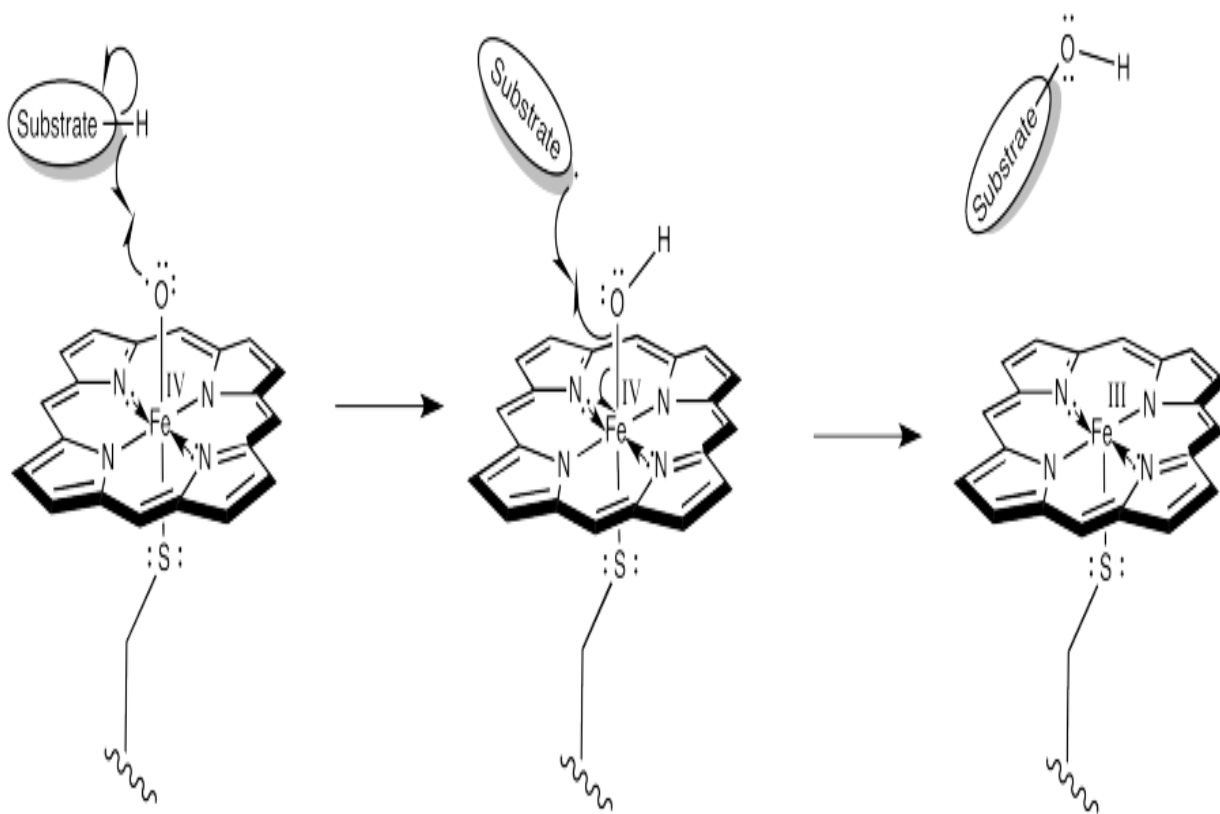


Figure 1.20: Product formation and release. The unpaired electron of the oxygen on iron (IV) is a radical which P450 uses to carry out its various catalytic activities. (<http://employees.scsbsju.edu/cschaller/Reactivity/oxygen/O OSP450CHAct.png>).

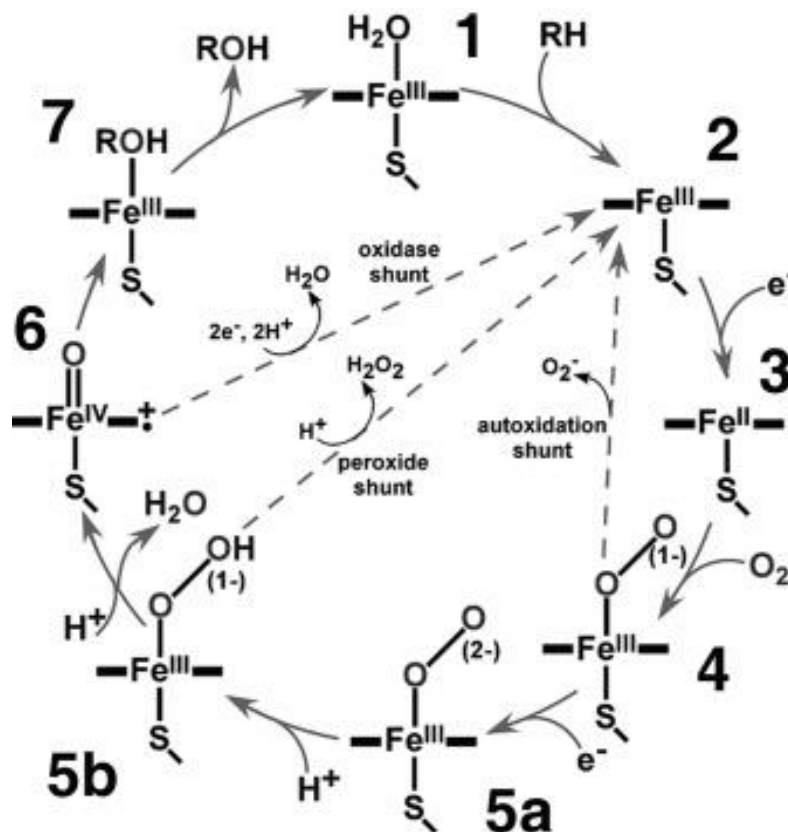


Figure 1.21: The catalytic cycle of P450 (Denisov et al., 2005)

There are three possible abortive steps in the catalytic cycle which are:

- I. Autoxidation of the oxy-ferrous complex in step 4- Here the oxygen is released as superoxide anion and the haem-iron goes back to step 1.
- II. Peroxide shunt in step 5 (a, b) – The peroxide or the hydroperoxide coordinated to the haem iron dissociates, forming hydrogen peroxide.
- III. Oxidase uncoupling in step 6- Instead of oxygenating the substrate the iron (V) oxide complex is oxidized to water.

1.4.6 P450 redox partners

The transfer of each of the two electrons required for the effective functioning of P450s is provided by NADPH-cytochrome P450 reductase (CPR) alone or with contributions from cytochrome *b*₅.

1.4.6.1 NADPH-cytochrome P450 reductase

CPR is a membrane-bound flavoprotein that transfers two electrons in a sequential process from NADPH to P450 (Paine et al., 2005). CPR is usually present at a molar ratio of one tenth to one twentieth that of P450 (Feyereisen et al., 1990). CPR like P450s has an N-terminal hydrophobic region with which it interacts with the membrane and P450s (Black et al., 1979, Paine et al., 2005).

The catalytic region of CPR has three domains which are made up of the FMN-binding domain, the NADPH/FAD binding domain and a linker domain located in between the NADPH/FAD sequence and considered to be serving structural role of positioning the other two major domain correctly for direct electron transfer (Paine et al., 2005).

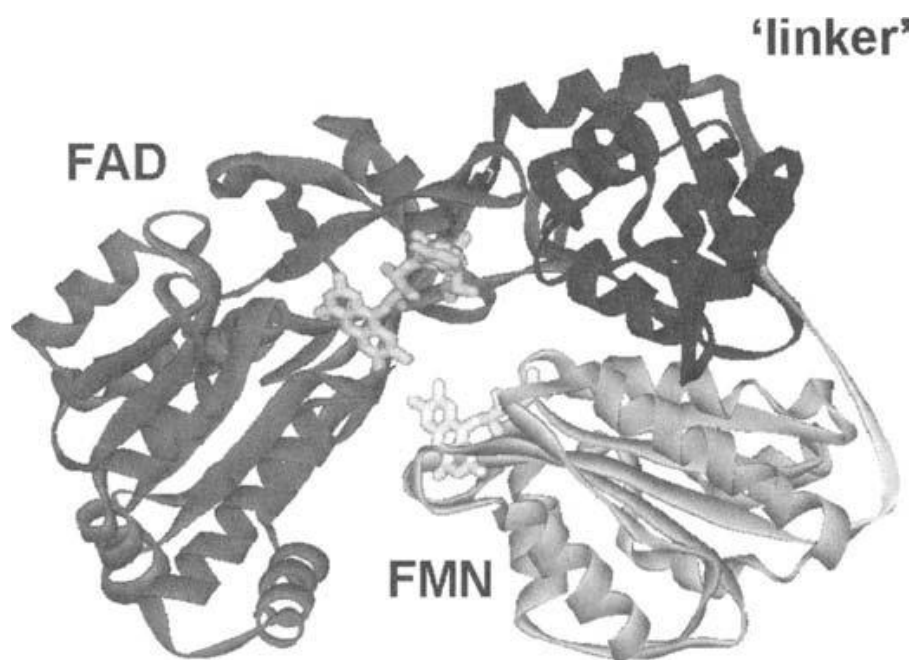


Figure 1.22: Crystal structure of rat CPR domain showing the arrangement of the FMN and FAD domains with the linker in between (Paine et al., 2005)

Electrons are transferred from NADPH to FAD and from FAD to FMN and finally passed on to the P450 enzyme (Paine et al., 2005). CPR can also transfer electron to cytochrome b_5 (Enoch and Strittmatter, 1979, Paine et al., 2005). The effects of the combination of CPR with cytochrome b_5 in P450 reactions are discussed further below and also shown in Chapter 3 of this thesis.

1.4.6.2 Cytochrome *b*₅

Cytochrome *b*₅ (*b*₅) is a haemoprotein ubiquitous in Nature and contains protoporphyrin IX (Schenkman and Jansson, 1999). This haemoprotein is relatively low molecular weight, cylindrical and contains 6 helices and 5 β -strands (Lu et al., 1995). It is an acidic protein folded into two domains. The main and larger domain is the cytosolic haem containing the, amino-terminal hydrophobic domain. The second domain is the smaller region joined to the globular region by a proline-rich motif of about 7 amino acid residues followed by 7 polar amino acids ending the polypeptide chain. The second domain has a net hydrophobic surface and forms the membrane binding carboxyl part comprising between 14 -18 amino acid residues (Scott Mathews, 1985). This haemoprotein, unlike P450, cannot interact with CO or oxygen, because the haem iron is coordinated both at the fifth and the sixth position by two histidines. However, it can act as an electron transfer intermediate between reductases and oxidative proteins (Schenkman and Jansson, 2003). The involvement of cytochrome *b*₅ in P450 mediated reactions depends on the type of the P450 and the substrates involved (Kuwahara and Omura, 1980). Substrates influence the affinity of P450 for NADPH-cytochrome P450 reductase (Tamburini et al., 1986), and also influence affinity between P450 and cytochrome *b*₅ (Bonfils et al., 1981).

1.4.6.2.1 Functions of cytochrome b_5

1.4.6.2.2 Increased delivery of the second rate limiting electron

Cytochrome b_5 , in ferric form, can be reduced by NADH-cytochrome b_5 reductase or CPR and this ferrous cytochrome b_5 could provide the second electron to the oxyferrous P450 (Correia and Mannering, 1973). This rate-limiting step was observed in ferrous cytochrome b_5 increasing the disappearance of oxyferrous complex (Noshiro et al., 1980).

1.4.6.2.3 Increasing the coupling of activated oxygen on the haem iron

Cytochrome b_5 acts, depending on the substrate and the P450, to increase coupling of the activated oxygen on the haem iron by reducing the rate of release of superoxide which in turn results in an increased product with lower formation of hydrogen peroxide (Qian et al., 1998). Cytochrome b_5 performs this function by modulating the increase in the input of the second electron thereby reducing the uncoupling due to slow incorporation of the electron by NADPH-cytochrome P450 reductase alone (Yoshio, 1981).

1.4.6.2.4 Facilitating 2-electron uptake from NADPH by forming two-haemoprotein complex with P450

P450 binds NADPH-cytochrome P450 reductase accepts an electron, dissociates, binds oxygen and rebinds to the reductase for the second electron (Schenkman and Jansson, 2003). Cytochrome b_5 interacts with NADPH-cytochrome P450 reductase by charge-pairing (Nisimoto and Lambeth, 1985). It also associates with P450 by complementary charge-pairing (Tamburini and Schenkman, 1986). Thus cytochrome b_5 can complex with P450 to form two-hemoprotein and binds to NADPH-cytochrome P450 reductase. Cytochrome b_5 in the complex oxidises ferrous haem iron in the first electron intake making the ferric haem iron to retake the second electron before dissociating from the CPR (Schenkman and Jansson, 2003).

1.4.6.2.5 Electron Facilitator

It was observed in CYP3A4 that binding of cytochrome b_5 induces a structural influence that affect the ability of the P450 to undergo redox changes. These changes facilitate conversion of the oxycytochrome P450 to yield more products and ferricytochrome P450 (Lipscomb et al., 1976).

1.4.7 Reactions Catalyzed by P450s

P450s use the same form of activated oxygen on compound 1 to catalyse various reactions ranging from hydroxylation, oxidation, alkylation, epoxidation, dealkylation, demethylation (Figure 1.18) and many more complex reactions (Isin and Guengerich, 2007). The catalysis via hydroxylations, oxidations and epoxidations of P450s are significant alternative for industrial use because chemical problems such as the use of chlorinated solvents and heavy metals as part of the catalyst are removed (Robins et al., 2009).

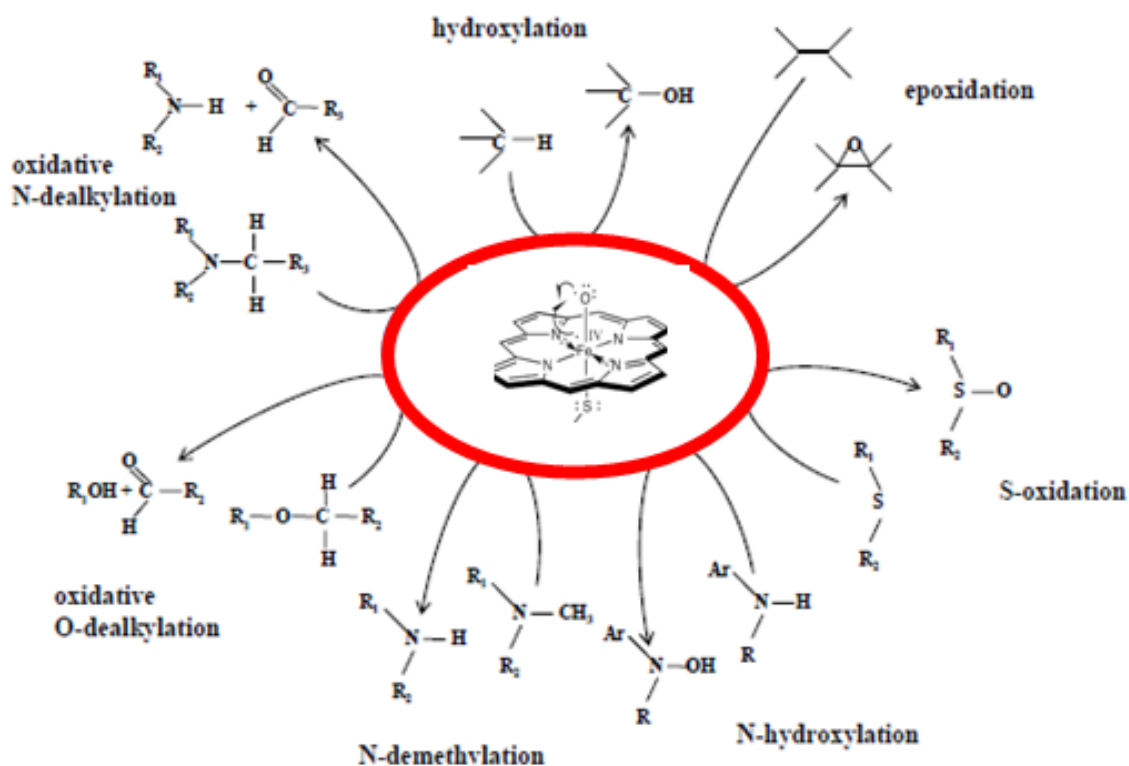


Figure 1.23: Some of the reactions catalysed by P450s.

1.4.8 P450 Distribution in Nature

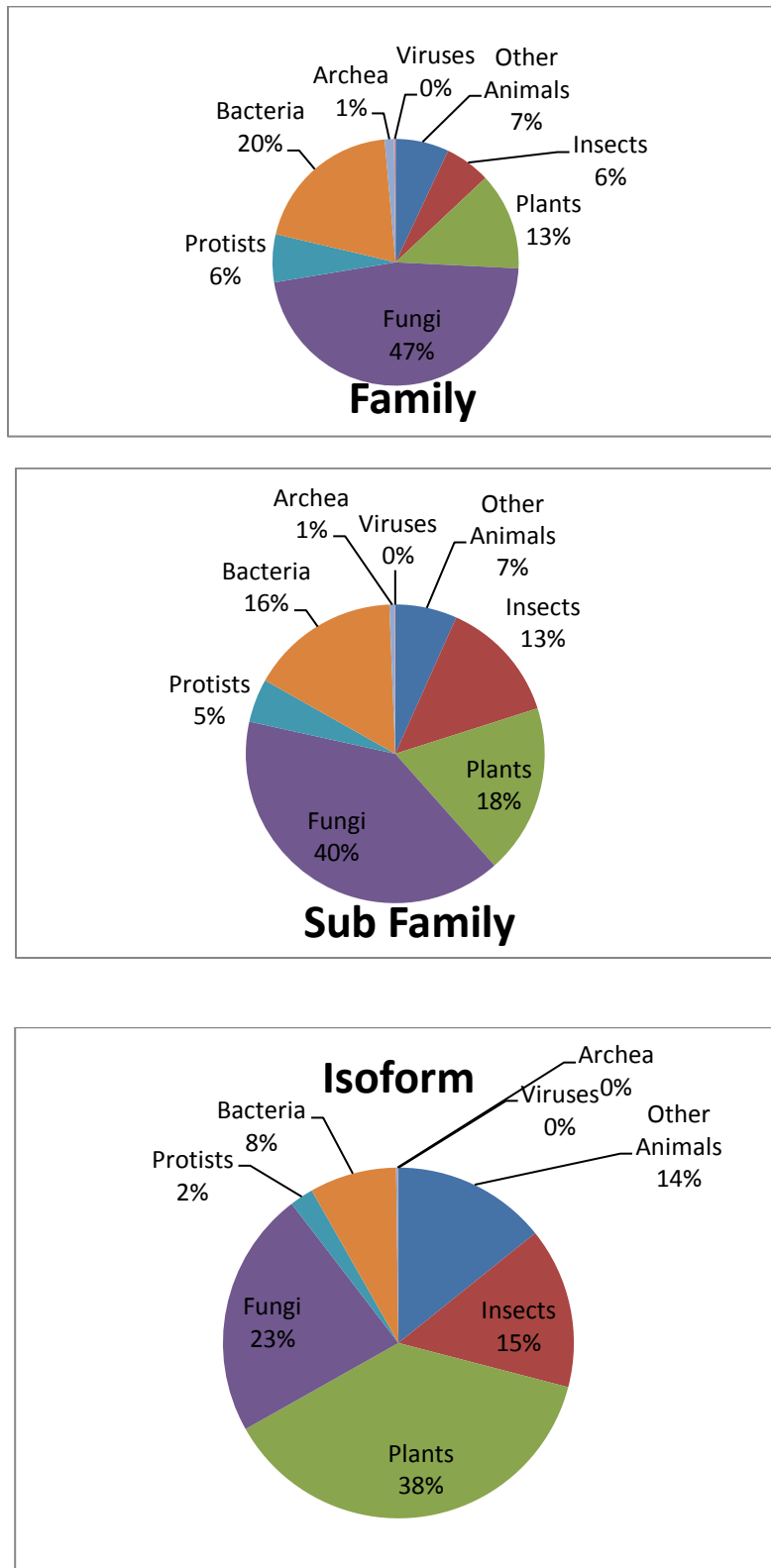


Figure 1.24: Pie charts of P450 distributions in nature

P450 is well distributed in all branches of the tree of life. Over 11,000 genes from 2,526 subfamilies and 985 families have been documented across all the sphere of life (Nelson, 2009). It is not surprising that plants have highest percentage of the P450 genes. They are stationary and could only defend themselves through breaking down of foreign substances having unrestricted access to them. They also synthesise other defence molecules like DIMBOA (2,4-dihydroxy-7-methoxy-1,4-benzoxazin-3-one), a powerful antibiotic (Glawischnig et al., 1999).

1.4.8.1 P450s in human

P450 enzymes are the most well-known group of drug metabolising enzymes in humans. Human P450s are primarily membrane-associated proteins positioned either in the inner membrane of mitochondria or in the endoplasmic reticulum of cells and prominently abundant in the liver (Rendic and Carlo, 1997). These P450s metabolize several endogenous and exogenous chemicals. They are present in most tissues of the body, and play key roles in hormone synthesis and breakdown, cholesterol synthesis, and vitamin D metabolism. P450 enzymes also function to metabolize potentially toxic compounds, including drugs and products of endogenous metabolism such as bilirubin, principally in the liver (Berka et al., 2011). The known clinically relevant human P450s are CYP3A4, CYP2D6, CYP1A2, CYP2C9, CYP2C19 and CYP2E1 (Martin and Fay, 2001). CYP3A4 is the most abundant P450 in the liver (Shimada et al., 1994) and has broad capacity to oxidise structurally diverse substrates (Rendic and Carlo, 1997). Drug-drug interactions between substrates and inhibitors of CYP3A4 can profoundly affect safety or efficacy of drug therapy (Tanaka, 1998).

1.4.8.2 P450s in insects

Insects have a repertoire of over 100 genes of P450s in their genomes (Arensburger et al., 2010, Holt et al., 2002, Nene et al., 2007) thus providing protection against insecticides and xenobiotics. This group of enzymes has been identified to confer insecticide resistance on various vectors by increased metabolism of the insecticides manufactured to eliminate and eradicate the spread of parasites (Feyereisen, 1999, Ranson et al., 2002). The CYP6 family of cytochrome P450 has been reported to be over expressed in most insecticide resistance vectors (Nikou et al., 2003). CYP6A1 of the house fly, *Musca domestica* was first to be implicated in detoxification (Feyereisen et al., 1989). CYP6BQ9 of red flour beetle, *Tribolium castaneum*, was reported to have a major role in deltamethrin resistance (Zhu et al., 2010).

In *Drosophila melanogaster*, CYP6G1 was reported to be over transcribed in all the field isolates of DDT-resistant strains. These CYP6G1-related DDT-resistant strains also show broad cross-resistance to neonicotinoid, growth regulator, organophosphorus and carbamate insecticides (Daborn et al., 2002, Pyke et al., 2004). The CYP6 family was also reported in DDT and cypermethrin depletions in *Musca domestica* and *Helicoverpa zea* (Rupasinghe et al., 2007).

Anopheles gambiae, has been the major mosquito vector of malaria parasite *Plasmodium falciparum* in Africa and has over the years developed resistance to insecticides including dieldrin, DDT (dichlorodiphenyltrichloroethane) and pyrethroids (Coetzee et al., 1999). Microarray studies using fragments of 230 *Anopheles gambiae* genes identified five P450 loci, including CYP4C27, CYP4H15, CYP6Z1, CYP6Z2 and CYP12F1, that showed significantly high expression in DDT-resistant ZANU strain compared with susceptible Kisumu strain (David et al., 2005). Method used by David et al., 2005 is as follows: The microarray analysis was constructed containing fragments of 230 *An. gambiae* genes from families associated with

metabolic-based insecticide resistance. Each gene represented on the microarray was either obtained by PCR amplification or artificially synthesized as a 70-mer antisense oligo (Qiagen, Crawley, U.K.). To keep cross hybridization between closely related genes to a minimum, gene-specific segments were selected by using PRIMEGENS software (<http://compbio.ornl.gov/structure/primegens>). By using software default cut off values, fragments toward the 3' end of the genes between 70 and 300 bp in length were selected as probes for the microarray, provided they matched the criteria of <75% similarity to all other genes in the *An. gambiae* genome. For genes having >75% similarity to another gene, 3' UTRs were used for the probe design. Gene-specific fragments were obtained by PCR amplification from cDNA, cloned into pGEM T-easy vector (Promega), and sequenced. Subsequent PCR amplifications were performed with vector-specific primers, and the products were purified by using the QIAquick PCR purification kit (Qiagen). The 70-mer oligos and artificial spike-in controls were resuspended in nuclease-free water, and both quality and quantity checked on agarose gels before spotting. Arrays were spotted in duplicate onto gamma-amino-propyl-silane-coated glass slides (UltraGaps, Corning) by using a Biorobotics Micro-Grid II printer (BioRobotics, Cambridge, U.K.). All genes were spotted in 50% DMSO (Sigma) at concentrations of 50, 200, and 1,000 ng/μl for spike-in controls, PCR products and 70-mer oligos, respectively. Four replicates of each PCR product and 70-mer oligo were spotted, as were eight replicates of spike-in controls. Printed slides were stored for 24 hours at room temperature in a desiccator before DNA fixation by using a UV auto crosslinker (power 600mJ, Stratagene).

CYP6Z1, CYP6Z2, CYP6M2, CYP6P3 and CYP325A3 were also identified by microarray-based studies to be associated in pyrethroid resistance in *An. gambiae* (David et al., 2005, Müller et al., 2007, Müller et al., 2008, Nikou et al., 2003). CYP6P3 and CYP6M2 out of these P450s, were reported to be most widely over-transcribed in the resistance field populations

(Djouaka et al., 2008) and they have been heterologously expressed and confirmed to metabolise pyrethroids (Müller et al., 2008, Stevenson et al., 2011).

Nikou et al (2003), reported that in *An. gambiae* the genes encoding CYP6Z1, CYP6Z2 and CYP6Z3 are tightly clustered on chromosome 3R. These three CYP6Z genes share common amino acid sequences. CYP6Z2 is 93.5% similar to CYP6Z3 and 69.4% similar to CYP6Z1. CYP6Z1 is in fact 70% and 69% similar to both CYP6Z2 and CYP6Z3 respectively (Chiu et al., 2008). Site directed mutagenesis was used in this study, especially on the amino acid residues at the active site of CYP6Z2 to understand their roles in the activity of this enzyme.

1.5 Mutagenesis

Mutagenesis has made it possible for the functional and structural roles of amino acid residues in proteins of interest to be studied by comparing the characteristic of the mutant strains with the wild type (Ling and Robinson, 1997). Mutagenic agents were used to create mutations on gene of interest with phenotypic or selective screening means before the advent of SDM, which has strengthened the importance and possibility of making individual or combined mutations of the amino acid residues to be studied (Zoller, 1991). The use of polymerase chain reaction or non polymerase chain reaction has made it possible to make desired changes in mutations and expanded the use of mutagenesis to understand structure-function relationship in enzymes (Zoller, 1992). In vitro mutagenesis relies on the DNA template to be copied, short oligonucleotide primer(s) to be extended after binding to the template, DNA ingredients, the building blocks, in the form of the four dNTPs which are dATP, dCTP, dGTP, dTTP, and most importantly the DNA polymerase enzyme.

1.5.1 Site directed mutagenesis (SDM)

SDM is a targeted changes made to DNA sequence in order to characterise gene and protein structure-function relationship, binding domains of proteins, protein-protein interactions or active sites of enzyme. However, changing some specific amino acids may result in a drastic global conformational change or a mistargeting to the protein conserved signature site (Bordo and Argos, 1991). A good example is changing the conserved cysteine at the haem-binding loop needed for the thiolate bond with the haem iron in cytochrome P450.

The PCR methods to generate SDM are:

1.5.1.1 Mutation at the terminal ends

Mutations at the terminus are usually achieved using primers containing the desired mutation and a restriction digestion site. Reverse primer with the mutant codon and a forward primer with just restriction site or vice versa could be used depending on the position of the mutagenesis. The PCR product is digested and ligated into a vector (Vallette et al., 1989).

1.5.1.2 Mutation in the middle of a gene

Several methods could be used to create mutation in the middle of a large DNA, one of the methods uses four primers in two separate PCR. First two primers will be an outside forward primer with a middle reverse primer in the first PCR reaction and then outside reverse primer with inside forward primer. Either of the inside primers could carry the mutation desired. The PCR products will be two separate halves of the gene in tail-to-tail fashion that is then phosphorylated and fused in a ligation reaction (Hayashi et al., 1994).

1.5.1.3 The quickchange SDM method

This method utilises two same mutagenic forward and reverse primers which will annealed to the two strands of the circular DNA and then a nonstrand-displacing thermostable polymerase, e.g. *Pfu* Turbo polymerase will extend the two strands. The PCR product will be nicked circular strands. The PCR product will be separated from the template by digestion with DpnI which digests methylated DNA strands. The circular nicked dsDNA will be repaired when transformed into competent cells (Rabhi et al., 2004).

1.5.1.4 Mutation using megaprimer

Megaprimer method can be used to create mutation anywhere within the gene sequence. In this method, two outside primers, forward and reverse, one middle primer containing the mutation are needed. This follows the method used by Pritchard et al (Pritchard et al., 1997).

1.6 Protein 3-dimensional modelling

Homology modelling is the process of constructing an atomic resolution model of a desired protein from its amino acids sequence using a known experimentally determined three dimensional structure of a homologous protein as a template. Elucidating the structure of a protein is important in the study of the protein function, its interactions with ligands and other proteins (Krieger et al., 2003). Homologous modelling is generally based on the understanding that protein structure is remarkably determined by the sequence of its amino acids (Epstein et al., 1963) and that protein structures are more conserved in evolution than protein sequences (Chothia and Lesk, 1986, Chothia and Lesk, 1987). The many problems posed by experimental elucidation of protein structure through NMR and X-ray crystallography have made the use of modelling useful in *in-silico* study of structure-function of protein (Johnson et al., 1994).

Steps followed in homology modelling are: template recognition, amino acid sequence alignment, alignment correction, backbone generation, loop modelling, side-chain modelling, model optimization and model verification through quality criteria and model quality (Krieger et al., 2004).

1.7 Aims of this project

Cytochrome P450s in mosquitoes are becoming a major challenge for vector control management because of their role in providing a defence mechanism for this vector. However, to date, no insect P450 crystal structures have been published that might provide a molecular framework for rationalising the mechanism of insecticide metabolism.

The aims of this project therefore are as follows:

Through site-directed mutagenesis, examine the functional roles of the amino acid residues at the active sites of *An. gambiae* CYP6Z2 and CYP6P3 as revealed by *in silico* studies of their homology models.

Characterise *An. gambiae* CYP6Z3 and CYP6Z2 with resorufin and diethyl fluorescein substrates and compare their pyrethroids metabolic activities.

Establish expression and purification techniques for the full length 5xHis-tagged CYP6Z2 and investigate the effect of the truncation of the N-terminal hydrophobic domain of 5xHis-tagged CYP6Z2 will have on the proper folding of the enzyme.

Chapter 2

2 Site directed mutagenesis to validate the roles of the amino acid residues identified by homology modelling in the active sites of CYP6P3 & CYP6Z2

2.1 Introduction

Specific CYP families are assigned to insect P450s; five are reported to be specific for insects; CYP6, CYP9, CYP12, CYP18 and CYP4 (Feyereisen, 1999). Other P450s identified in insects are CYP304, CYP314 and CYP325 (David et al., 2013). The involvement of these CYP families in insecticide resistance of mosquitoes was well discussed in the review done by (David et al., 2013). The CYP6 family in mosquitoes has been heterologously expressed and validated to be metabolizers of two major groups of insecticides approved by WHO. DDT has been shown to be metabolised by CYP6Z1 in *An. gambiae* (Chiu et al., 2008), whilst metabolic role of CYP6Z2 in *An. gambiae* and its *Aedes aegypti* orthologue CYP6Z8 have been discovered to be involved in clearance of PBAlc (3-phenoxybenzoic alcohol) and PBAld (3-phenoxybenzaldehyde), which are common metabolites of carboxylesterases (Alexia et al., 2013). Importantly, CYP6P9 and CYP6M7 in *An. funestus* (Riveron et al., 2013, Wondji et al., 2009) and their orthologues in *An. gambiae*, CYP6P3 and CYP6M2 (Müller et al., 2008, Stevenson et al., 2011) have become pyrethroid resistance markers. CYP6P7 and CYP6AA3 also have both been confirmed to metabolise pyrethroids in *An. minimum* (Boonsuepsakul et al., 2008, Duangkaew et al., 2011). CYP6G1 is associated with DDT resistance in *Drosophila* (Daborn et al., 2002), CYP6BQ9 was reported to have a major role in deltamethrin resistance in red flour beetle (Zhu et al., 2010), and CYP6D1 is a confirmed pyrethroid metaboliser in housefly (Zhang and Scott, 1996).

CYP6Z2 in *An. gambiae* (McLaughlin et al., 2008) has been shown to fulfil the two conventional physiological functions of P450, i.e. control of development through hormone

biosynthesis and provision of the potential for xenobiotic metabolism: the main evidence comes from substrate binding and metabolism experiments carried out by these authors (McLaughlin et al., 2008). However, CYP6Z2 has only been shown to bind to permethrin and cypermethrin: it did not metabolise them (McLaughlin et al., 2008). Homology modelling of CYP6Z2 docked with these insecticides examined by McLaughlin et al., 2008 in their *in silico* studies revealed a non-productive binding phenomenon. They also constructed a three dimensional model of CYP6D1 revealing the amino acid residues in the active site and the productive binding of permethrin and cypermethrin.

Comparing the composition of the amino acid residues at the active sites of the homology models of CYP6P3 and CYP6D1, pyrethroid metabolisers, with that of CYP6Z2 revealed three positions with different amino acid residues. Leucine at positions 53 and 216 are in both CYP6P3 and CYP6D1 active sites respectively. In CYP6Z2 phenylalanine replaces leucine at position 212, presenting a potential steric conflict with substrates. Tyrosine 102 in CYP6D1 is retained in CYP6Z2 but is replaced with phenylalanine in CYP6P3. Importantly, arginine, a positively charge amino acid, was seen at position 210 of the active site of CYP6Z2 close to the pyrethroids docked at the active site whereas asparagine, a neutrally charged amino acid, replaced arginine at this position in both CYP6D1 and CYP6P3. These observations made these three substitutions significant for investigations (Figures 2.1 and Table 2.1).

Consequently, CYP6Z2 (F212L) and Y102F mutants were constructed based on the amino acid residues of CYP6P3 at the active site to examine the role of these amino acids at these positions. These residues were also swapped on CYP6P3 by constructing mutants CYP6P3 L216F and F110Y to further establish their functions in the two P450s. The effect of having arginine at the active site of CYP6Z2 instead of asparagine was also investigated with the construction of CYP6Z2 (R210A) mutant.

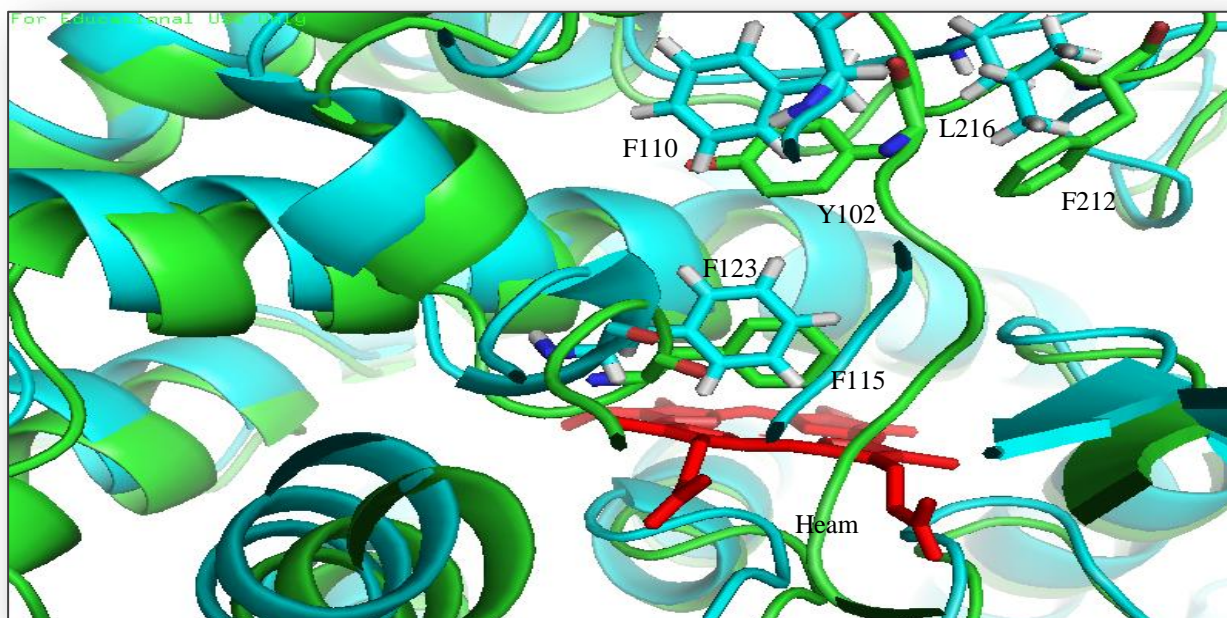


Figure 2.1 Structural alignment of the homology models of CYP6P3 (blue) and CYP6Z2 (green). F110 and L216 in CYP6P3 are replaced with Y102 and F212 in CYP6Z2 respectively. The third position with F123 in CYP6P3 and F115 in CYP6Z2 is 4Å to the haem (red) and are conserved in all CYPs homology models examined.

Table 2.1: Amino acid differences at the active sites of CYP6Z2 and CYP6P3

P450	1 st Position	2 nd Position	3 rd Position
CYP6Z2	F212	Y102	R210
CYP6P3	L216	F110	N217

2.2 Materials & Methods

2.2.1 Site directed mutagenesis

All the CYP6Z2 and CYP6P3 mutants were generated using the Quick change Site-directed mutagenesis kit from Agilent using *Pfu* Turbo DNA polymerase except for CYP6Z2 (R210A) as explained below. The wild type ompACYP6Z2 was used as a template to generate the mutants as described in McLaughlin et al (McLaughlin et al., 2008). ompACYP6P3 and mutants were provided by Dr. Cristina Yunta-Yanes at LSTM. (ompA is a bacterial outer membrane protein A, a leader sequence appended to the N-terminal CYP genes in order to direct the expressed protein to the membrane).

The nucleotide sequence at the point mutation of CYP6Z2 R210A contained six bases that have multiple complementary sites on the pB13 plasmid. The properties of pB13 plasmid are stated in appendix 1. Therefore sequence confirmation of the SDM products gave several unexpected plasmid products. The mega primer method (Ling and Robinson, 1997) was therefore used to generate such mutants. A pCW-ompA 2 forward primer (Table 2.2) was used with the mutagenic reverse primer for R210A and ompACYP6Z2 as template in amplification reactions to generate product of about 700 bp containing the desired mutant. The product was then used in a second PCR with the same pCW-ompA 2 forward primer, but with another pB13 downstream of the original reverse primer and pB13CYP6Z2 template without the ompA component. The product from this second PCR reaction was then digested with *Nde*I and *Eco*R1 and ligated into pB13 plasmid digested with the same pair of restriction enzymes. The nucleotide sequence of the ligated ompACYP6Z2 (R210A) was then obtained by sequencing the PCR product in order to confirm the authenticity of the plasmid. The DNA sequence confirmation of R210A is shown in appendix 2.

Table 2.2: Mutagenic primers for the creation of double mutants CYP6Z2 (F212L,Y102A), CYP6Z2 (F212L,Y102F) and CYP6Z2(R210A)

Mutants	Template	Forward Primer	Reverse Primer
CYP6Z2 (F212L,Y 102F)	pB13omp ACYP6Z2 (F212L)	5' GAT CGC GGT GTC TTC TGC AAT GAA GAG CAC G 3'	5' TCT TCA TTG CAG AAG ACA CCG CGA TCG TGA AAG 3'
CYP6Z2 (F212L,Y 102A)	pB13omp ACYP6Z2 (F212L)	5' GAT CGC GGT GTC GCC TGC AAT GAA GAG CAC G 3'	5' TCT TCA TTG CAG AAG ACA CCG CAA TCG TGA AAG 3'
*CYP6Z2 (R210A)	pB13omp ACYP6Z2	5' CTA ATC GGG GAG CCA ACT TTA TCG 3' (mutagenic)	5' CGA TAA AGT TGG CTC CCC GAT TAG 3' (Mutagenic)
	pB13omp ACYP6Z2	5' GGA GGT CAT ATG AAA AAG ACA G 3' (pCW-ompA 2)	5' CGA TAA AGT TGG CTC CCC GAT TAG 3' (Mutagenic)
	pB13CYP 6Z2	5' GGA GGT CAT ATG AAA AAG ACA G 3' (pCW-ompA 2)	5' CGT ATC ACG AGG CCC TTT CG 3' -pB13 sequencing primer

* In creating this mutant, a “mega primer” was first generated with the reverse mutagenic primer. The product of this PCR reaction was added to the second PCR reaction. The double strand, when denatured during the PCR reaction serves as a primer in combination with the synthetic primer to generate the mutant. The PCR thermal cycle and reaction mixture are shown in appendix 3.

2.2.2 Co-expression of CYP6Z2, wild and mutants with P450 reductase

In order to ensure optimised transformation efficiency for the co-transformations, *E. coli* JM109 cells were initially transformed with pACYC-AgCPR encoding the cytochrome P450 reductase as described elsewhere (McLaughlin et al., 2008). These transformed cells were then subsequently made competent again and a 25 µl aliquot was used for all the co-transformation with wild type and mutant versions of ompACYP6Z2 in pB13. Luria agar plates supplemented with 50 µg/ml ampicillin and 25 µg/ml chloramphenicol were used to screen the colonies. A colony from the co-transformation was then used in overnight culture of Luria-Bertani broth supplemented with same antibiotic concentrations. Then 200 µl of the overnight culture was used to inoculate 200 ml Terrific Broth (1:1000) in a 1litre flask. The inoculated culture was incubated at 37°C with shaking at 200 RPM and growth monitored by absorbance at OD₆₀₀. δ-aminolevulinic acid (ALA), was added to a final concentration of 0.5 mM when the OD₆₀₀ reached between 0.4-0.5 to boost the haem formation. The incubation conditions were maintained until the OD reached 0.9-1.0 and IPTG added to final concentration of 1 mM to induce protein expression. ompACYP6Z2 (wild type) was expressed at 25°C, with shaking at 120 RPM, while all the mutants were expressed at 21°C, 120 RPM. P450 absorbance maxima were monitored at 24 hrs and cells were then harvested at 36 hrs if such a signature absorbance signal at P450 was detected. The incubations at different temperatures were based on observations that the wild type expresses better at 25°C while mutants' expressions are best at temperature 21°C.

Spheroplasts were prepared by centrifuging the 200 ml culture at 2800 x g for 20 minutes at 4°C in pre chilled 250 ml centrifuge bottles using the JLA 16.250 Beckman. The supernatant was discarded and the cell pellets re-suspended in 20 ml of 1x T.S.E. buffer on ice (2 x Tris-Sucrose-EDTA (TSE) buffer was prepared by adding 0.1M Tris-acetate at pH 7.6 with 0.5M sucrose and 0.5mM EDTA. The mixture was then filter sterilized and stored at 4°C). Previously

prepared 20 mg/ml of lysozyme (0.02 g/ml ddH₂O) in water was kept on ice and 250 µl of the prepared lysozyme solution used per 20 ml of cell suspension. The cell suspension was then transferred into an ice cold 50 ml centrifuge tube, gently mixed for 60 minutes while the cell walls are degraded to allow spheroplasts to form. The 50 ml bottles were loaded into the JA 25.50 rotor (Beckman) and centrifuged at 2800 x g for 25 minutes at 4°C. The supernatant was discarded and the pellet(s) retained. The pellets were re-suspended with 8 ml of spheroplast re-suspension buffer and 8 µl of 0.1M DTT.

Protease inhibitors, aprotinin (trypsin inhibitor), leupeptin (cysteine, serine and threonine inhibitor) and PMSF (serine protease inhibitor) were added to the spheroplast preparation to final concentrations of 1 µg/ml for the peptides and 1 mM for the PMSF. The suspension was sonicated three times for 30 seconds (30 seconds on and 30 seconds off/intervals). The sonicated sample was loaded into 50 ml centrifuge tube and centrifuged at 30,000 x g for 20 minutes at 4°C. The supernatant was made up to 16 ml with ice cold ddH₂O and transferred into 70 Ti ultracentrifuge bottles and loaded into a Beckman Ultracentrifuge and centrifuged at 49,600 RPM (180000 x g), for 1hour, at 4°C.

The supernatant was removed using a pasteur pipette: the membranes appeared as a translucent red-brown pellet and the majority of the pellet was transferred to a dounce homogeniser on ice using a glass pasteur pipette to lightly scrape the pellet. Once most of the pellet had been transferred, 1ml of ice-cold 2X TSE buffer and 1 ml of water were added and the same pasteur pipette was used to re-suspend the remaining pellet which was also transferred to the dounce homogeniser. The liquid was loaded from the bottom of the homogeniser to avoid bubbles. Finally, 100 µl aliquots of the homogenised membrane sample were dispensed into eppendroff tubes and stored at -80°C. The total protein was quantified using Bradford reagent (Bradford, 1976). The P450 contents were characterised with respect to Fe²⁺-CO versus Fe²⁺ difference spectrum (Omura and Sato, 1964), and the *Anopheles gambiae* NADPH P450 reductase values

were quantified by cytochrome c reductase activity (Guengerich et al., 2009). The CPR quantifications are shown in appendix 4.

2.2.3 P450 quantification of the CYPs expressed

The expression of P450 was monitored in JM109 cells as follows. First, a 1 ml sample of a broth culture was centrifuged at 16,000 RPM for 5 minutes at 4°C. The pellet was then re-suspended in 1 ml P450 spectrum buffer (100mM Tris, 10mM CHAPS, 20% glycerol and 1mM EDTA) and divided equally into two dark cuvettes labelled blank (B) and experiment (E). A P450 scan program was opened in the UV-Spectrophotometer and each cuvette, B & E, placed in the slots for blank and experiment respectively. A base line was taken and the reading set to zero. The E cuvette was then removed and flushed with CO gas in a fume cupboard. Sodium dithionite salt was then added to the two cuvettes and the instrument set to read the ferrous-CO versus ferrous difference spectrum to quantify the P450. This same procedure was used for the P450 membranes prepared by adding 100 µl of membrane with 900 µl of P450 buffer (ratio 1:10) and the mixture divided into two dark cuvettes labelled blank (B) and experiment (E).

2.2.4 Enzyme assay

The enzyme activity with resorufin derivatives as a substrate and diethyl fluorescein (DEF) were carried out in 96 well plates containing 50 mM potassium phosphate at pH 7.4. 10 pmol of membrane and 5 µmol/l benxyloxyresorufin (BR), metoxyresorufin (MR), ethoxyresorufin (ER), pentoxyresorufin (PR) and 20 µmol/l of diethyl fluorescein (DEF) were used in a total reaction volume of 100 µl. NADPH generating system, to generate steady electrons for the reaction, was prepared with 0.1 mmol/l NADP⁺, 0.25mmol/l MgCl₂, 1mmol/l glucose-6-phosphate and 1U/ml glucose-6-phosphate dehydrogenase. These are final concentrations in the 100µl of reaction volume used in the experiment. For the determination of K_M, with the probes, the reactions were carried out using 1 or 5 pmol of membranes and 0-1.2 µmol/l BR, 0-

4 $\mu\text{mol/l}$ for MR and 0-20 $\mu\text{mol/l}$ for DEF. Fluostar Omega fluoroscan was used set at 30°C with filter combinations of 544 nm excitation and 590 nm emission for the resorufins, 485-12 nm excitation and 520 nm emission for DEF. All reactions were carried out in duplicates and 50-cycle fluorescent readings at a fixed 1500 gain.

2.2.5 Thermostability assay

This assay follows the same protocol as used in the fluorescent assays described in 2.2.4 except that 10 μl of the P450 enzymes to be examined were first incubated for 5 minutes at room temperature, 35°C, 40°C, 45°C, 50°C, 55°C, 60°C and 65°C. After incubation, 10 pmol of the enzymes was then used in 100 μl reaction final volume containing 5 $\mu\text{mol/L}$ BR and NADPH regenerating system.

2.2.6 Inhibition assay

The inhibition assay was carried out with a range of concentrations of deltamethrin against fixed concentration of MR. The reaction mixture contained 50 mM potassium phosphate pH 7.4, an NADPH regenerating system and 10 pmol of enzyme in a final volume of 100 μl . Deionised water was used to replace the NADPH regenerating system for the negative control.

2.2.7 HPLC analysis

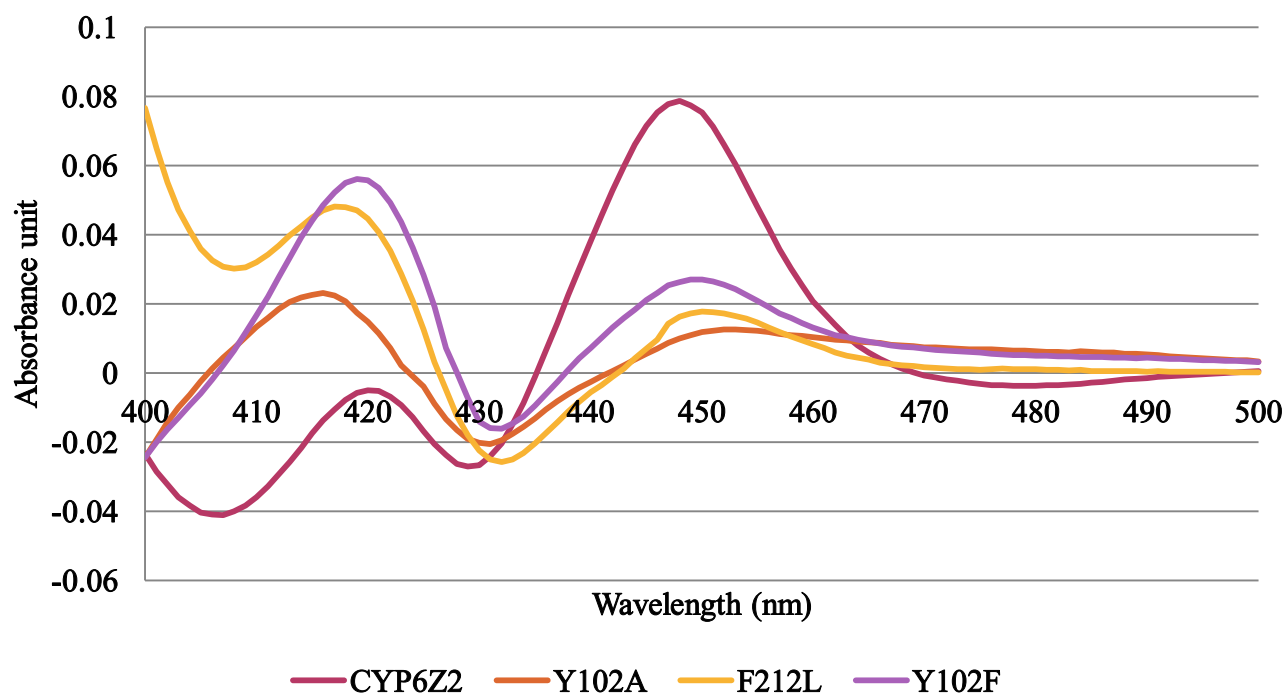
Insecticides concentration of 20 $\mu\text{mol/l}$ were incubated with 20 pmol of P450s at 30°C for 90 minutes in the presence or absence of an NADPH generating system (5 mmol/l glucose 6-phosphate, 1 U glucose 6-phosphate dehydrogenase, 1 mmol/l NADP) in a final volume of 200 μl . The metabolic reactions were terminated by the addition of 200 μl of ice-cold methanol followed by incubation on ice for 10 minutes. The samples were centrifuged at 16,000 $\times g$, and 150 μl of the supernatant transferred into HPLC vials. The substrates peaks eluted from the column were separated using a 250 \times 4.6 mm (5 μm) Supelcosil LC-18-DB column (Supelco, Sigma-Aldrich, Gillingham, U.K.) and detected at 232 nm.

2.3 Results

2.3.1.1 Expression of CYP6Z2 wild type and mutants

All the single mutants of the ompACYP6Z2 created through SDM yielded holoproteins as seen in Figure 2.2. The wild type had the highest P450 content, at 8.4 μM . The P450 content increased with increasing bulkiness of the amino acid residue substituted. Replacing tyrosine with alanine gave the lowest value of 0.7 μM , but the P450 content increased to 1.9 μM when phenylalanine was replaced with leucine. Removal of the hydroxyl group of tyrosine gave a much lower quantity of 2.5 μM when compared to the wild type, but higher than the replacement with alanine or leucine. P450 content is measured at 450 nm and the aromatic rings can influence the reading because they do absorb light in the visible regions of 400 nm – 800 nm (Schmid, 2001). However, Figure 2.2 shows that the wild type is more stable (i.e. folds properly and degrades slowly) than the mutants by yielding more of the holoprotein than the apoprotein as depicted by the appearance of lowest peak at 420 nm. The two double mutants created produced P420, indicative of misfolded cytochrome P450, although, the mutant F212L_Y102A still had activity when tested with BR (Figure 2.3). P420 is the inactive form of P450 resulting from lost of the haem, misfolding or unfolding of the protein.

(A)



(B)

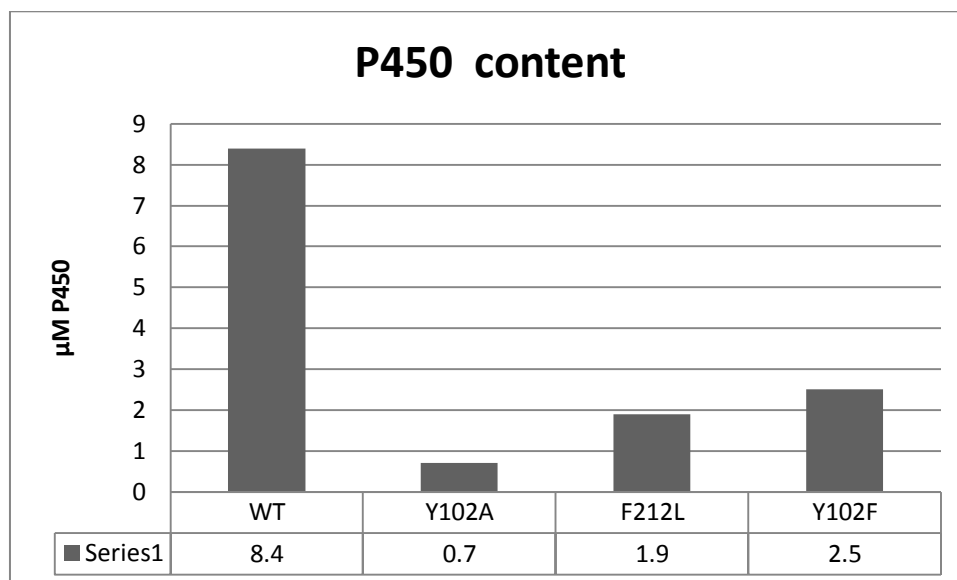


Figure 2.2: (A)- Fe^{2+} -CO vs Fe^{2+} difference spectrum CYP6Z2 and the single mutants. (B)- Bar chart illustrating the increasing P450 content with increase in the size of the amino acid residue substitutions. (n=1)

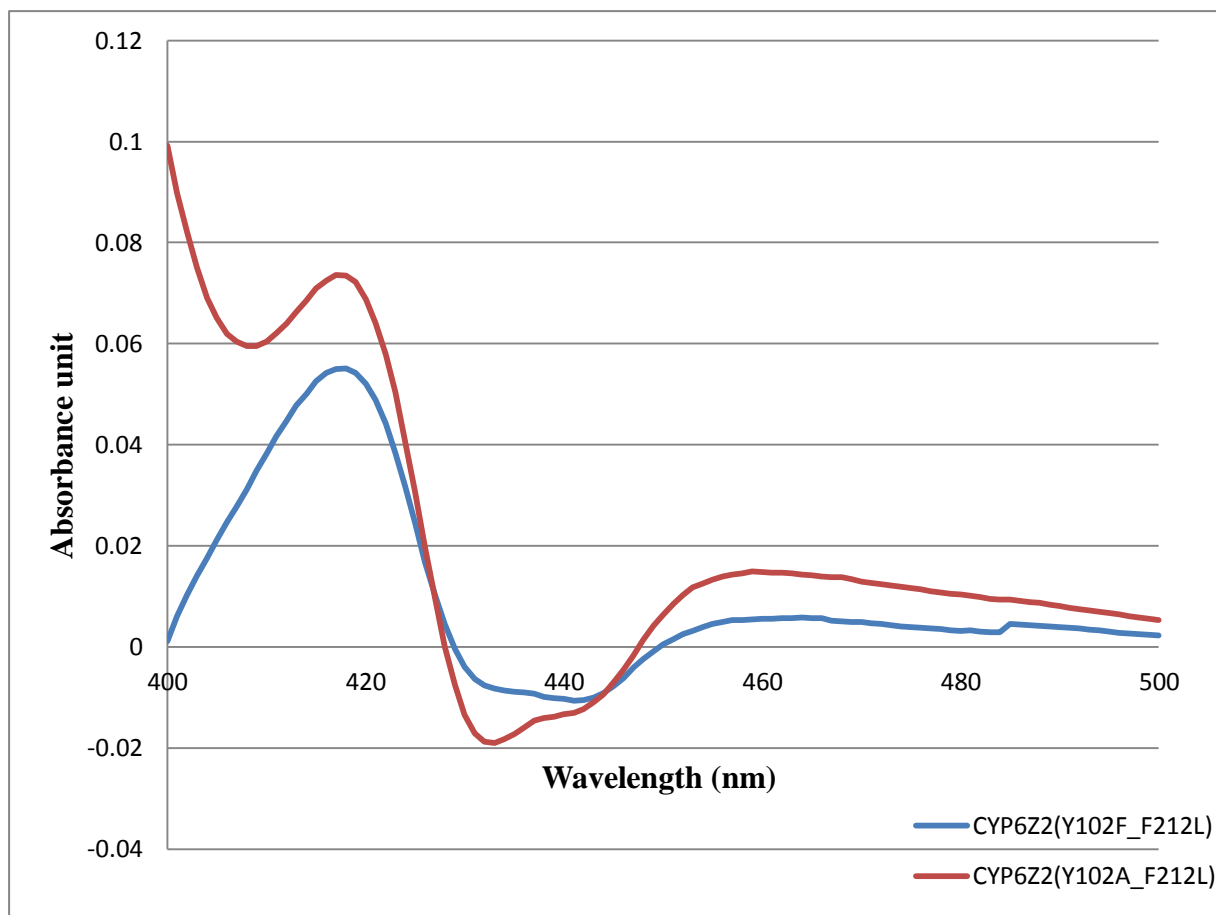


Figure 2.3: Fe^{2+} -CO vs Fe^{2+} difference spectrum of the double mutants showing P450 expression. The P450 quantity computed for the two were negative because the absorbance units at 490 nm were higher than the readings at 450 nm. The amino acid sequence of the double mutants of Y102F_F212L and Y102A_F212L are shown in Appendix 5 and 6 respectively.

2.3.1.2 Comparison of the specific activities of wild type CYP6Z2 and mutants CYP6Z2 (Y102F) & CYP6Z2 (F212L)

Four resorufin substrate probes, benzy-, methoxy-, ethoxy-, and pentoxyresorufin (BR, MR, ER and PR), were tested. The amount of resorufin released was derived from the Resorufin Standard curve shown in appendix 7. The wild type activity with the probes indicated high specific activity and preference for the phenolic group in BR (McLaughlin et al., 2008). The activity was reduced by 2.2-fold when the phenolic group was substituted with methoxy, and the activity progressively lost with increase in the length of the carbon chain in ethoxy and pentoxy derivatives of the probe. However, the phenolic group preference was lost when the aromatic residue of F212 was replaced with leucine F212L and tyrosine changed to phenylalanine Y102F. Although the intolerance to increasing aliphatic chain was retained, both mutants were able to dealkylate methoxy derivatives at higher rates than the phenolic group. The activities of F212L and Y102F were 3-fold and 2-fold respectively higher than the wild type in metabolising methoxy derivative of the resorufin (Figure. 2.4).

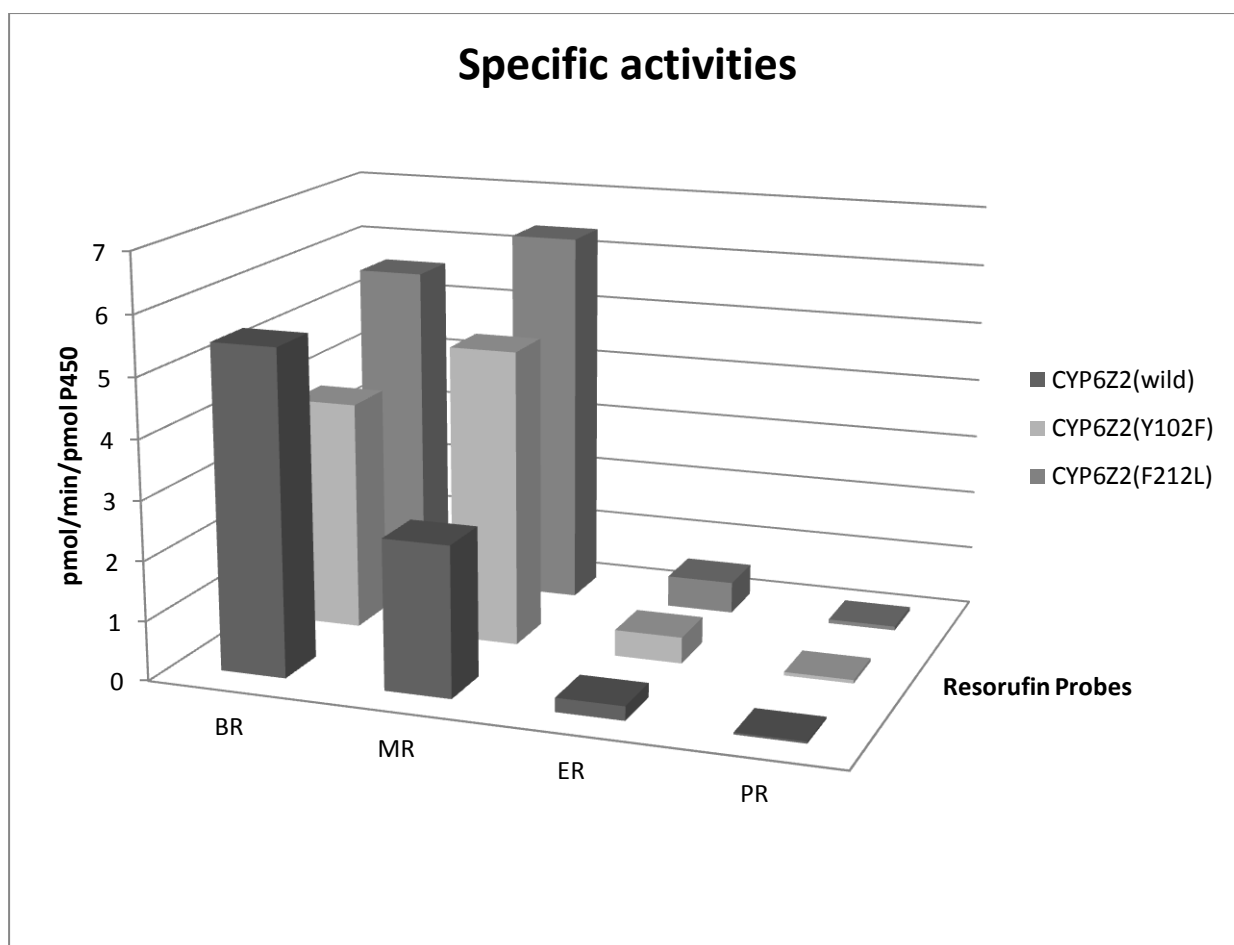


Figure 2.4: Specific activities of CYP6Z2 (wild), CYP6Z2 (Y102F) and CYP6Z2 (F212L) with the resorufin probes. The wild type activity against MR & ER was lowest when compared to the mutants but had highest activity against BR. CYP6Z2 wild type has increased steric screening of oxidation with increasing alkyl chain length of substrate (McLaughlin et al., 2008). The mutants F212L, which is within SRS 2, indicated that deletion of the aromatic side chain may have increased access of substrates into the active site of the enzyme.

Table 2.3: Specific activities of CYP6Z2, CYP6Z2 (Y102F) and CYP6Z2 (F212L) against resorufin probes.

CYP6Z2	BR pmol/min/pmol P450	MR pmol/min/pmol P450	ER pmol/min/pmol P450	PR pmol/min/pmol P450
WT	5.46±0.27	2.52±0.016	0.23±0.0028	0.033±0.0005
Y102F	3.88±0.16	4.99±0.11	0.44±0.009	0.059±0.0009
F212L	5.59±0.17	6.37±0.051	0.53±0.020	0.066±0.0027

(Mean±SE, n=2)

2.3.1.3 Comparison of the kinetic parameters of the wild type CYP6Z2 and mutants CYP6Z2 (Y102F) & CYP6Z2 (F212L) for BR and MR resorufin probes

The affinity for the phenolic derivative of the resorufin did not change significantly in the mutants compared to the wild type except for F212L, which shows a relatively weak affinity when compared with others. The affinity dropped by 1.1-fold and 1.5-fold for Y102F and F212L respectively (Table 2.4). The reduction in affinity in F212L may be due to the introduction of the aliphatic chain of the mutant. However, the turnover number of the mutant Y102F dropped by 1.7-fold when compared to the wild type while F212L was similar to the wild type. The differences in these two parameters compensated for each other in the resultant efficiencies of the two mutants computed from their K_M and k_{cat} values, which were similar, $10.38 \text{ min}^{-1}\mu\text{M}^{-1}$ and $12.74 \text{ min}^{-1}\mu\text{M}^{-1}$ for Y102F and F212L respectively (Table 2.4). The K_M values of the three were relatively low, which may explain why the efficiencies of the two mutants were similar. The catalytic efficiency of the wild type was the highest because of its preference for the phenolic group and high turnover number.

The affinity of the wild type CYP6Z2 and the two mutants examined for MR showed similar results as BR. This may be due to the fact that these two positions are not involved in the binding of the substrates. However, turnover was increased by 2-fold in Y102F and 4-fold in F212L. The efficiencies of the mutants were therefore increased by 3-fold and 4-fold in Y102F and F212L mutants respectively (Table 2.5). All the mutants however have higher catalytic efficiencies with BR than with MR.

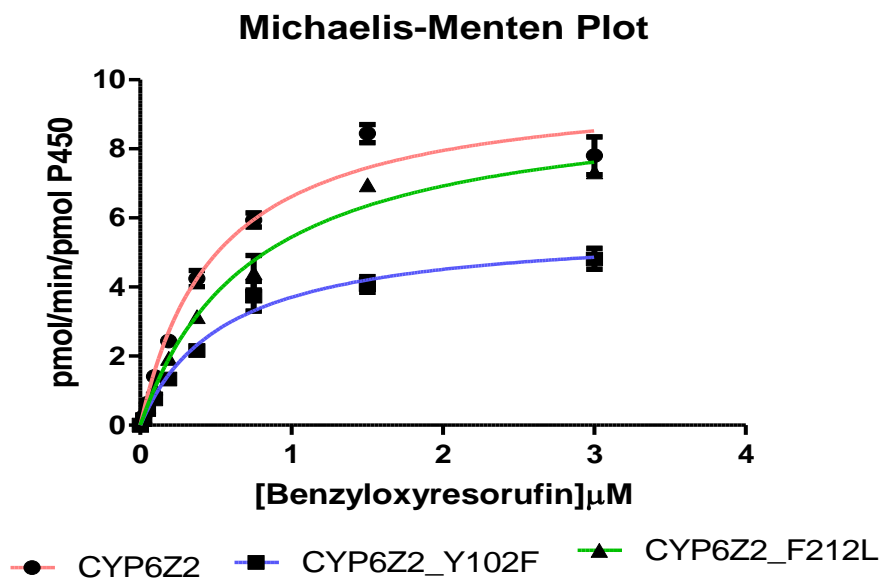


Figure 2.5: Michaelis-Menten plot of CYP6Z2 (wild) CYP6Z2 (Y102F) and CYP6Z2 (F212L)-benzyloxyresorufin kinetics. Curve generated using Graphpad Prism 5 software with R^2 for the curve fittings as 0.97, 0.98 and 0.99 respectively.

Table 2.4: Benzyloxyreorufin kinetics of CYP6Z2 (wild), CYP6Z2 (Y102F) and CYP6Z2 (F212L)

CYP6Z2	K_M (μM)	K_{cat} (min^{-1})	K_{cat}/K_M ($min^{-1} \mu M^{-1}$)
WT	0.51 ± 0.076	9.95 ± 0.52	19.74
Y102F	0.56 ± 0.078	5.76 ± 0.29	10.38
F212L	0.75 ± 0.088	9.51 ± 0.44	12.74

(Mean \pm SE, n=2)

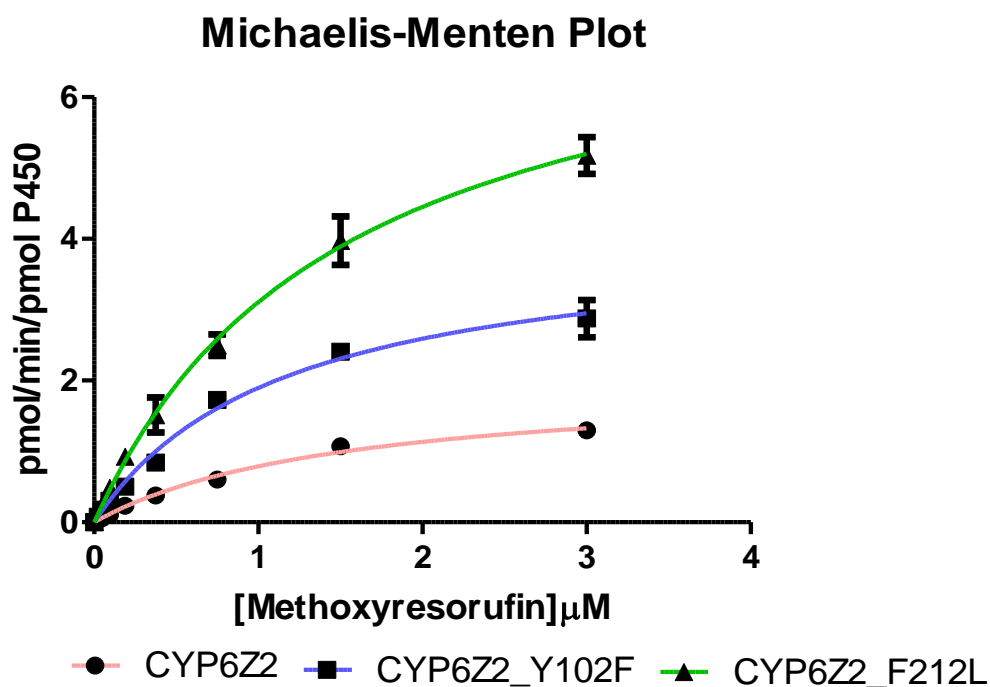


Figure 2.6: Michaelis-Menten plot of CYP6Z2 (wild), CYP6Z2 (Y102F) and CYP6Z2 (F212L)-methoxyresorufin kinetics. Curve generated using Graphpad Prism 5 software with R^2 for the curve fittings as 0.99, 0.99 and 0.99 respectively.

Table 2.5: Methoxyresorufin kinetics of CYP6Z2 (Y102F) and CYP6Z2 (F212L)

CYP6Z2	K_M (μM)	K_{cat} (min^{-1})	K_{cat}/K_M ($\text{min}^{-1} \mu\text{M}^{-1}$)
WT	1.54 ± 0.17	2.01 ± 0.11	1.31
Y102F	1.15 ± 0.16	4.09 ± 0.24	3.6
F212L	1.52 ± 0.19	7.84 ± 0.48	5.15

(Mean \pm SE, n=2)

2.3.1.4 Specific activity of CYP6Z2 (R210A) with the resorufin probes and diethyl fluorescein (DEF)

The equivalent CYP6Z2 R210 position is neutral in CYP6D1 and CYP6P3. Instead of arginine they both have asparagine at the active site. Thus CYP6Z2 R210A, was created to neutralize the positively charged residue and replace the bulky side chain group in the equivalent amino acid position. R210A was created instead of R210N because the amino acids sequence revealed another asparagine at N211 as shown in appendix 8 and appendix 9. Although this side chain was not seen in the active site, however, increasing bulky amino acid close to it may affect the catalytic cavity of the enzyme.

The effect of cytochrome *b*₅ on dealkylation of resorufin substrates by this mutant was also examined to establish if this P450 second redox partner will improve its activity.

Results (Table 2.6) show that compared with wild type, R210A retained a preference for the phenolic derivative of resorufin. Specific activity was 2-fold higher for BR than MR which is similar to the wild type CYP6Z2. Activities with respect to ER and PR were also low for this mutant as were observed in the wild type and the previous mutants investigated. Addition of cytochrome *b*₅ slightly increased the activity of BR by 27% but did not have any effect on MR, ER and PR. However, cytochrome *b*₅ had a 2-fold stimulatory effect on the dealkylation of DEF by R210A. The stimulatory effect of cytochrome *b*₅ with CYP6Z subfamily was further investigated in chapter 3.

Table 2.6: Specific activities of CYP6Z2 (R210A) against the four resorufin probes

Compound	pmol/min/pmol P450 Without b_5	pmol/min/pmol P450 With b_5	% Increase in activity
Benzyloxyresorufin	7.24±0.44	9.24±0.86	27.6
Methoxyresorufin	3.61±0.13	3.46±0.14	-4.21
Ethoxyresorufin	0.29±0.0003	0.26±0.009	-8.65
Pentoxyresorufin	0.053±0.0008	0.049±0.0027	-6.95

(Mean±SE, n=2)

Table 2.7: Specific activity of CYP6Z2 (R210A) with the DEF probe

Compound	RFU/min/pmol P450 Without b_5	RFU/min/pmol P450 With b_5	Fold Increase
DEF	658.70±8.7	1,359±22.5	2-fold

(Mean±SE, n=2)

2.3.1.5 Comparison of the kinetic parameters of wild type CYP6Z2, Y102F & F212L and R210A

The kinetic parameters of R120A were compared with the wild type and the other previously examined mutants, Y102F and F212L using BR probe (Table 2.8).

The K_M of R210A was 0.69 μ M which was within the same range of the wild type, Y102F and F212L. However, the deletion of the positively charged arginine increased the turnover number by 3-fold when compared with both the wild type and mutant F212L and by 6-fold when compared with Y102F.

The deletion of the positively charged amino acid residue also improved the enzyme efficiency, comparing the ratio of K_{cat}/K_M of the mutant with the wild type. The efficiency increased by 2-fold when compared with the wild type and was 4-fold better than Y102F and F212L.

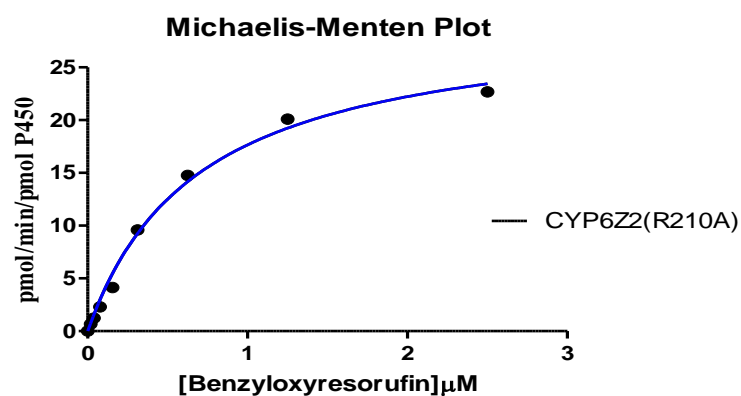


Figure 2.7: Michaelis-Menten plot of CYP6Z2 (R210A)-benzyloxyresorufin kinetics. The curve was generated using Graphpad Prism 5 software. R^2 for the curve fitting is 0.99

Table 2.8: Benzyloxyresorufin kinetic parameters of CYP6Z2 (R210A) compared with the wild type CYP6Z2 and mutants Y102F and F212L

CYP6Z2	K_M (μM)	K_{cat} (min^{-1})	K_{cat}/K_M ($\text{min}^{-1} \mu\text{M}^{-1}$)
WT	0.51 ± 0.076	9.95 ± 0.52	19.74
Y102F	0.56 ± 0.078	5.76 ± 0.29	10.38
F212L	0.75 ± 0.088	9.51 ± 0.44	12.74
R210A	0.69 ± 0.061	30 ± 1.053	43.48

(Mean \pm SE, n=2)

2.3.1.6 Inhibition assay to determine binding ability of the wild type CYP6Z2, Y102F and F212L with deltamethrin

The abilities of the wild type CYP6Z2 and the mutants to bind deltamethrin were tested in the inhibition assay of the enzymes' activities with methoxyresorufin in the presence of the insecticide.

The wild type and the mutants examined exhibited ability to bind to deltamethrin. The insecticide inhibited the activities of the enzymes against the resorufin probe by more than 50% as shown below:

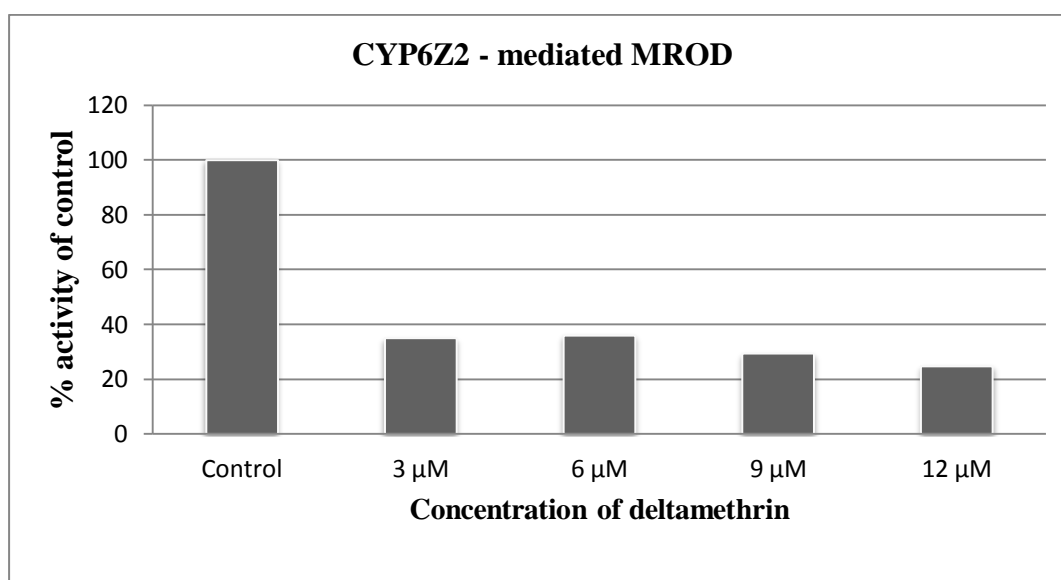


Figure 2.8: Inhibition assay of CYP6Z2-mediated methoxyresorufin O-debenzylation (MROD) reaction with deltamethrin as inhibitory ligand. 6 μ M MR was used and no deltamethrin was added in the control experiment.

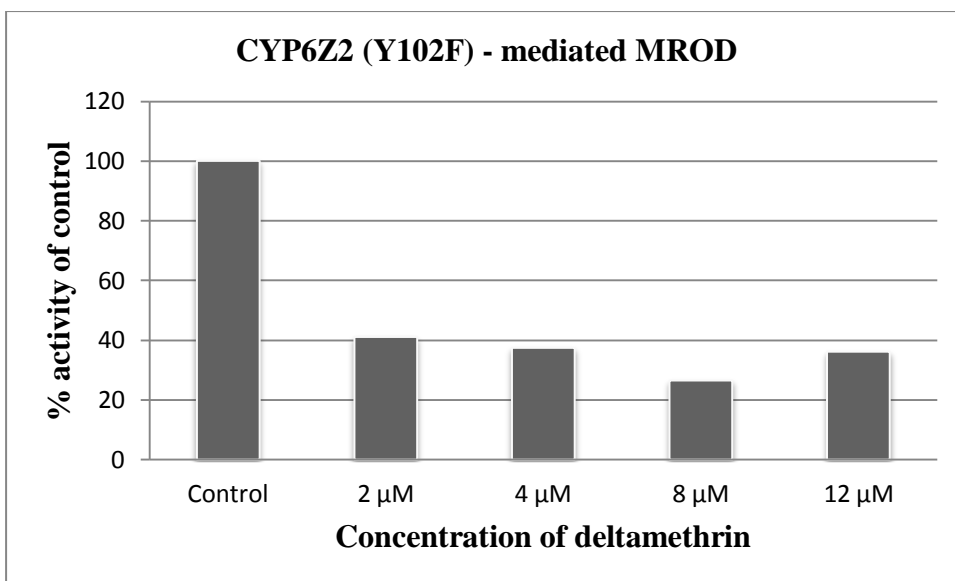


Figure 2.9: Inhibition assay of CYP6Z2(Y102F) -mediated MROD reaction with deltamethrin as inhibitory ligand. 4 μ M MR was used and no deltamethrin was added in the control experiment.

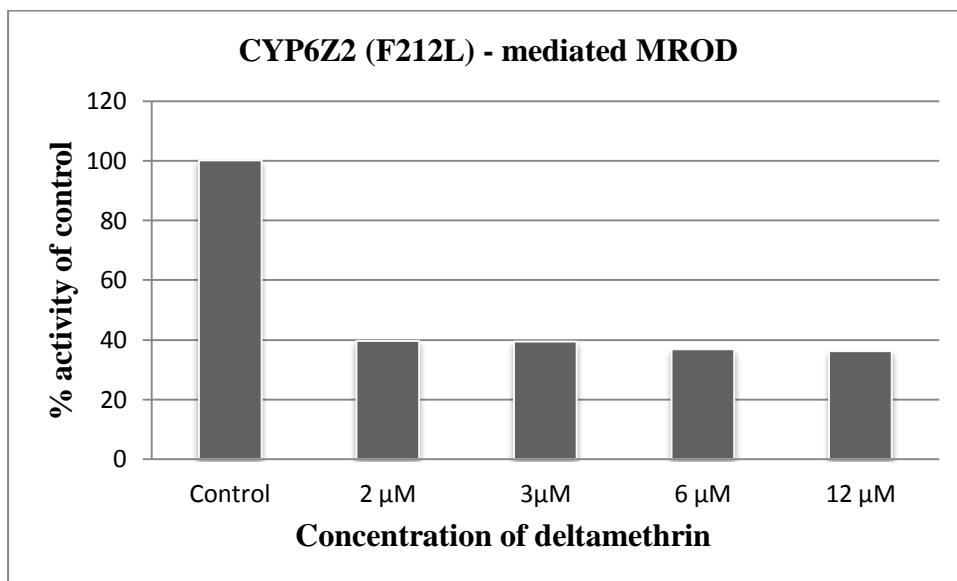


Figure 2.10: Inhibition assay of CYP6Z2(F212L) -mediated MROD reaction with deltamethrin as inhibitory ligand. 3 μ M MR was used and no deltamethrin was added in the control experiment.

2.3.1.7 Metabolic assay with deltamethrin

The abilities of the wild type and the mutants, F212L and Y102F to metabolise deltamethrin was examined. While F212L did not show activity against deltamethrin, Y102F showed improved activity. It achieved 54.6 % depletion (percentage difference in the amount of insecticide in the NADPH negative control and that remaining in the NADPH positive reaction mixture) when freshly prepared membranes were used in the depletion assay. This improved activity was 16.3-fold higher than the activity of the wild type. However, improved activity was only observed when fresh membranes were used. This may be because the enzyme was losing activity when freeze thawed.

Combining the HPLC analysis with Mass Spectrometry analysis of metabolites would provide unequivocal evidence for mutants exhibiting improved insecticide metabolism.

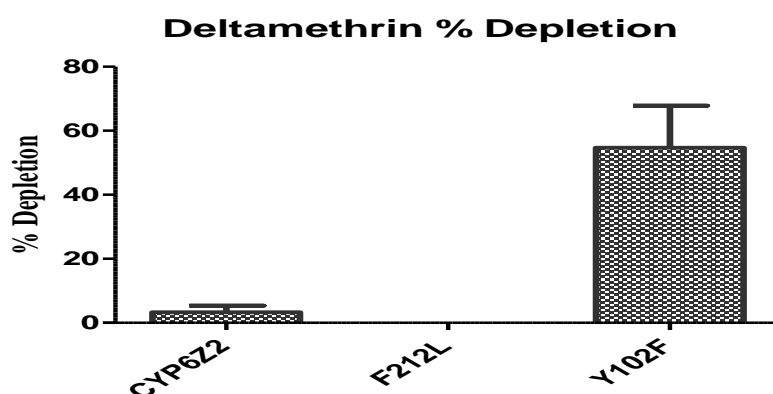


Figure 2.11: Deltamethrin metabolism comparison of wild type CYP6Z2 and mutants F212L and Y102F from freshly prepared enzymes. The mutant Y102F showed improved metabolic activity against deltamethrin while no activity was detected for F212L. (Mean±SE, n=3).

The same pattern was observed with the third mutation at R210A. Three repeated depletion assays were done with the freshly prepared membrane showing 53% depletion of deltamethrin.

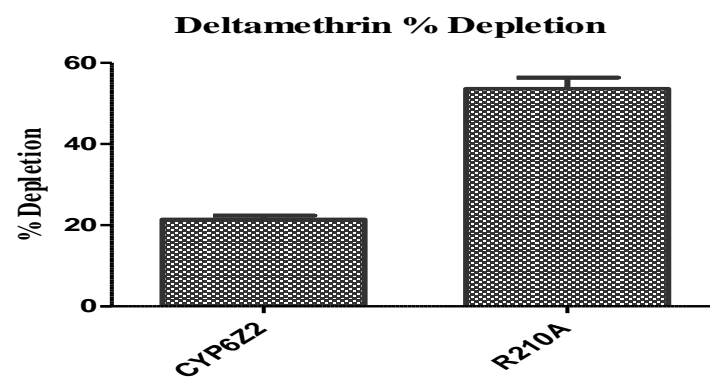


Figure 2.12: Deltamethrin metabolism comparison of wild type CYP6Z2 and mutant R210A from freshly prepared enzymes. R210A showed increased activity against deltamethrin more than the wild type. Mean \pm SE, n=3).

2.3.2 Wild type CYP6P3 and mutants, CYP6P3 (Y110F) and CYP6P3 (L216F)

2.3.2.1 Specific activities of CYP6P3 & the mutants with resorufin probes and DEF

The abilities of CYP6P3 and Y110F and L216F to metabolise resorufin probes were analysed. The amino acid sequence of the wild type CYP6P3 is shown in appendix 10. Only the wild type and L216F indicated low activities against BR and PR even in the presence of cytochrome *b*₅. The presence of cytochrome *b*₅ appears to have inhibitory effect rather than stimulatory for these resorufin probes in the two enzymes. The inhibitory effect with BR substrate was more than with PR. The activities of the wild type and L216F against BR were reduced by 2.5-fold in the presence of *b*₅. The wild type lost 2.5-fold activity against PR in the presence of cytochrome *b*₅.

While the effect of cytochrome *b*₅ was inhibitory with the resorufin probe, the effect was stimulatory for DEF probe. Increase in activities of more than 7-fold were achieved in the wild type and L216F, while cytochrome *b*₅ appeared to have obligate role (i.e. its presence is a must for activity to occur) in the activity of F110Y which had fold increase of over 80 (Schenkman and Jansson, 2003). Changing the side chain at position 216 from aliphatic residue to aromatic residue changed the activity of the native protein significantly by 18.6-fold increase and introducing hydroxyl group into the active site of the native protein at position 110 reduced the activity by 4.2-fold.

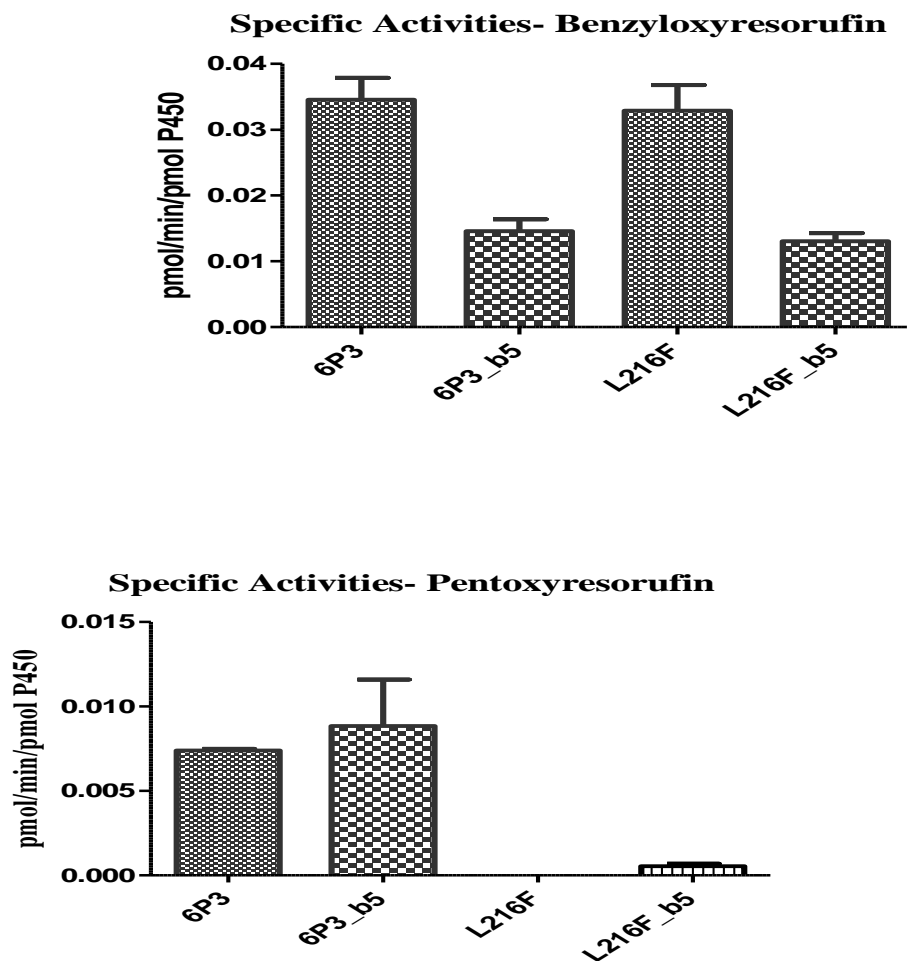


Figure 2.13: Bar chart of specific activities of CYP6P3 and CYP6P3 (L216F) with or without b_5 against BR and PR. The effect of b_5 was clearly seen in the activities of the wild type and mutant against BR. The effect on both isozymes was inhibitory. The activities of the enzymes against PR were too low and almost insignificant for comparison.

Table 2.9: Specific Activities of CYP6P3 and L216F with or without b_5 against BR & PR

CYP6P3	Benzyloxyresorufin pmol/min/pmol P450 Without b_5	Benzyloxyresorufin pmol/min/pmol P450 b_5	Pentoxyresorufin pmol/min/pmol P450 Without b_5	Pentoxyresorufin pmol/min/pmol P450 b_5
Wild	0.035±0.0034	0.0146±0.0018	0.0089±0.003	0.0074±0.0001
F110Y	ND	ND	ND	ND
L216F	0.033±0.0033	0.0131±0.0013	ND	0.00055±0.00015

(Mean±SE, n=2). F110Y did not have activity against any of the resorufins and wild type and L216F did not show activity against MR.

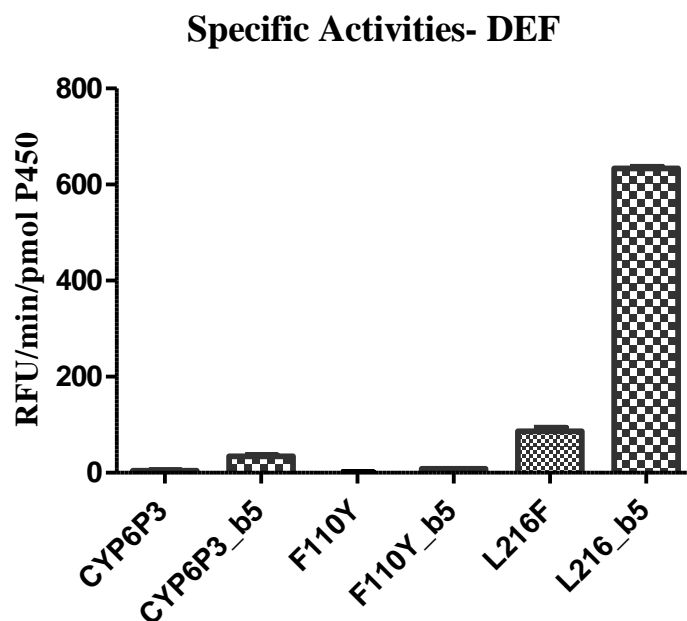


Figure 2.14: Bar chart of the specific activities of CYP6P3, F110Y and L216F with or without b_5 against DEF probe. The presence of b_5 increased the activities of the wild type and mutants against DEF. L216F had the highest activity.

Table 2.10: Specific Activities of CYP6P3, F110Y and L216F with or without b_5 against DEF

CYP6P3	DEF RFU/min/pmol P450 Without b_5	DEF RFU/min/pmol P450 With b_5	Increase
WT	4.65±0.45	34.55±2.05	7.43-fold
F110Y	0.1±1.00	8.35±0.25	83.5-fold
L216F	86.60±7.01	633.70±3.30	7.3-fold

(Mean±SE, n=2)

2.3.2.2 Comparison of kinetic parameters of CYP6P3, mutants F110Y & L216F

F110Y indicated a shift in the affinity of CYP6P3 when hydroxyl group was added to the phenolic ring of the phenylalanine. The affinity of the enzyme to bind DEF probe increased by 6-fold when compared with the wild type and L216F. However, L216F still maintained its huge increase in activity of over 15.3-fold activity over the wild type as indicated by the V_{\max} generated from the Michaelis-Menten equation (Table 2.11).

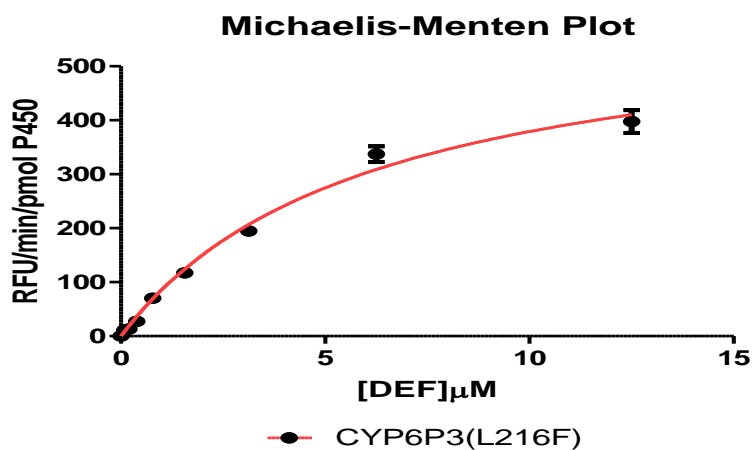
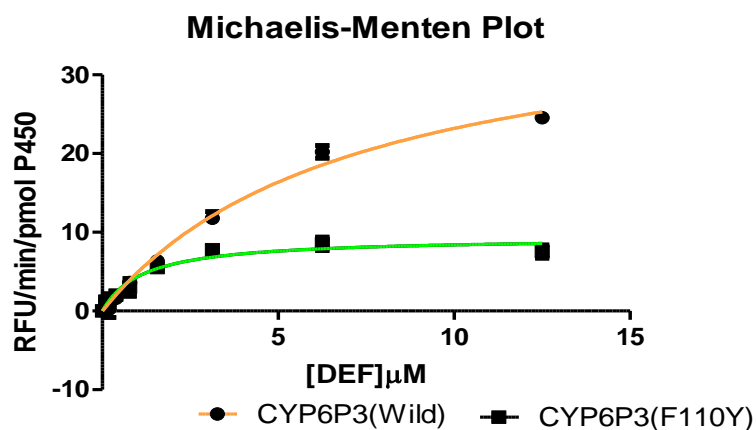


Figure 2.15: Michaelis-Menten plot of CYP6P3, F110Y and 216F -DEF kinetics. The rate of activity of L216F is 15-fold higher than the wild type and 65-fold higher than F110Y. The curves were generated using Graphpad Prism 5 software. R^2 for the curve fittings are 0.98, 0.92 and 0.99 for wild type, F110Y and L216F respectively. ((Mean \pm SE, n=2)

Table 2.11: Kinetic parameters for DEF by CYP6P3, F110Y and L216F

Enzyme	K_M (μM)	V_{max} (RFU/min/pmole P450)
CYP6P3	7.14 \pm 1.06	39.75 \pm 2.99
CYP6P3_F110Y	1.15 \pm 0.28	9.36 \pm 0.67
CYP6P3_L216F	6.12 \pm 0.78	611 \pm 37.73

(Mean \pm SE, n=2)

2.3.2.3 Thermostability of CYP6P3 and the mutants

The addition of phenolic residue in L216F and hydroxyl residue in F110Y improved the thermostability of the native CYP6P3 protein significantly when tested with DEF. The mutant L216F was still 90% active at 50°C and F110Y 80% active at 45°C whereas the wild type completely lost activity at temperatures above 40°C.

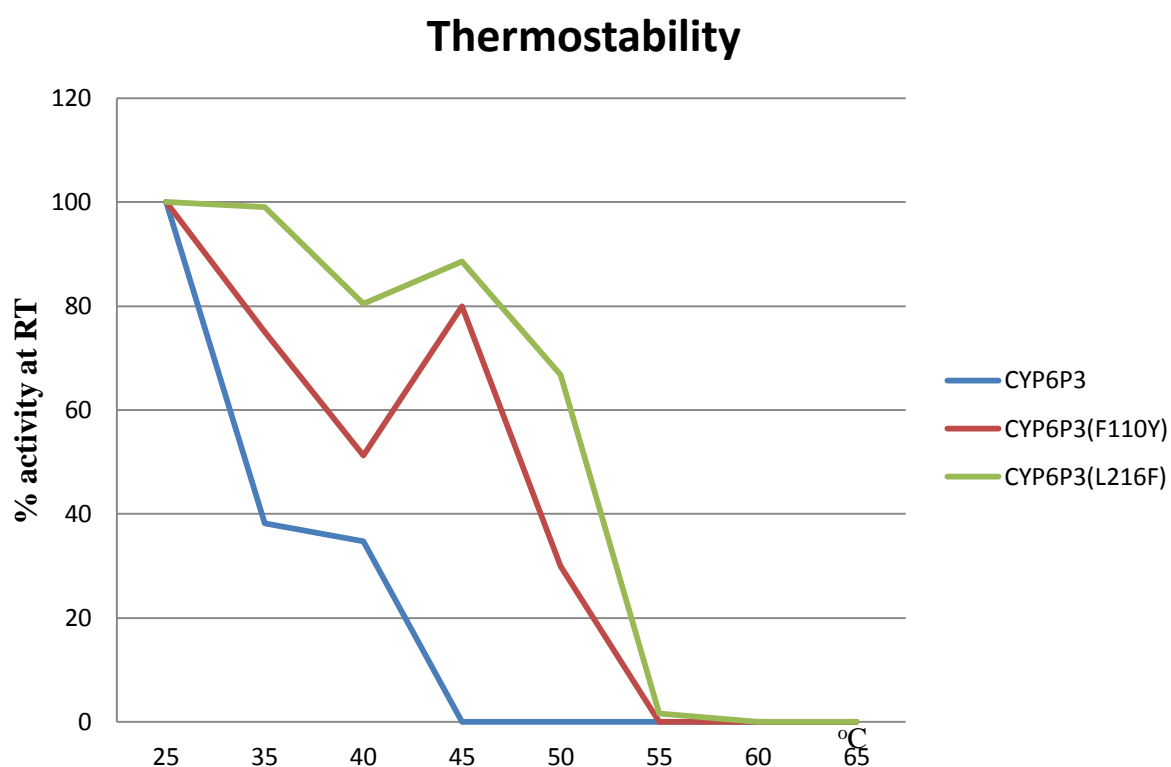


Figure 2.16: Thermostability test of CYP6P3, F110Y and L216F using DEF substrate. The mutants had increased thermostability than the wild type. L216F was more stable than F110Y. The addition of the phenylalanine at this position also improved the metabolic activity of the enzyme.

2.3.2.4 Pyrethroid metabolic profile of CYP6P3 and mutants

The mutants created were examined in their abilities to change the metabolic profile of CYP6P3 against pyrethroids. Both type 1, permethrin, and type 2, deltamethrin & cypermethrin pyrethroids were investigated. The assay measured the disappearance of insecticides in the positive control (NADPH added) compared with the negative control (no NADPH). The chromatograms are displayed in appendix 11.

The increased activity of L216F in the fluorescent probe analysis was also retained in the metabolism of the pyrethroids. This mutant had improved metabolic activity against all the three pyrethroids examined when compared with the wide type. Also, the reduction in activity of the mutant F110Y was reflected in the metabolism of the insecticides. F110Y lost 2.3-fold activity against cis isomer of permethrin and 1.2fold against deltamethrin and cypermethrin.

Table 2.12: Pyrethroid insecticides depletion assay

Insecticide	CYP6P3 % depletion	F110Y % depletion	L216F % depletion
Deltamethrin	100	83.46±8.31	100
Permethrin- Cis	100	42.07±0.44	100
Permethrin -Trans	100	100	100
Cypermethrin	75.4±12.78	58.89±0.38	100

% depletion of substrates (Mean±SE, n=3)

2.4 Discussion

The value of *in silico* methods for predicting the behaviour and or analysing the outcome of site directed mutagenesis experiments, forms the basis of this Chapter. Three specific amino acid residues have been highlighted by a combination of sequence alignment and evaluation of homology models of CYP6D1 and CYP6P3 and differences are suggested with that of CYP6Z2. McLaughlin et al (2008) noted that the active site side chain, F212 of CYP6Z2 is absent from CYP6D1 (McLaughlin et al., 2008): instead L53 is positioned at the active site of CYP6D1, in three dimensional terms. The presence of leucine at the active site of a known pyrethroid metabolizer, CYP6P3 (Müller et al., 2008), supports this judgement, where instead of F212 it has L216 at the same position (again in 3D) in the active site. Also absent at the active site of CYP6P3 is Y102 found in CYP6Z2, which is replaced by F110. In addition, the effect of the positively charged arginine at the active site of CYP6Z2 which is replaced with asparagine in both CYP6D1 and CYP6P3 was examined.

CYP6Z2 binds cypermethrin and permethrin in a non productive binding therefore this enzyme is unable to metabolise the pyrethroid insecticides (McLaughlin et al., 2008). An essential role of clearance of metabolites, PBald (3-phenoxybenzaldehyde) and PBA (3-phenoxybenzoic acids, of carboxylesterases has been confirmed for CYP6Z2 which has linked the enzyme to pyrethroid insecticide resistance (Alexia et al., 2013) . However, similarities of the amino acid residues at the active site with known pyrethroid insecticide metabolisers with just 1 or 2 amino acid difference could make this enzyme to be an artefact: replaced metaboliser (David et al., 2013), or a metaboliser in waiting.

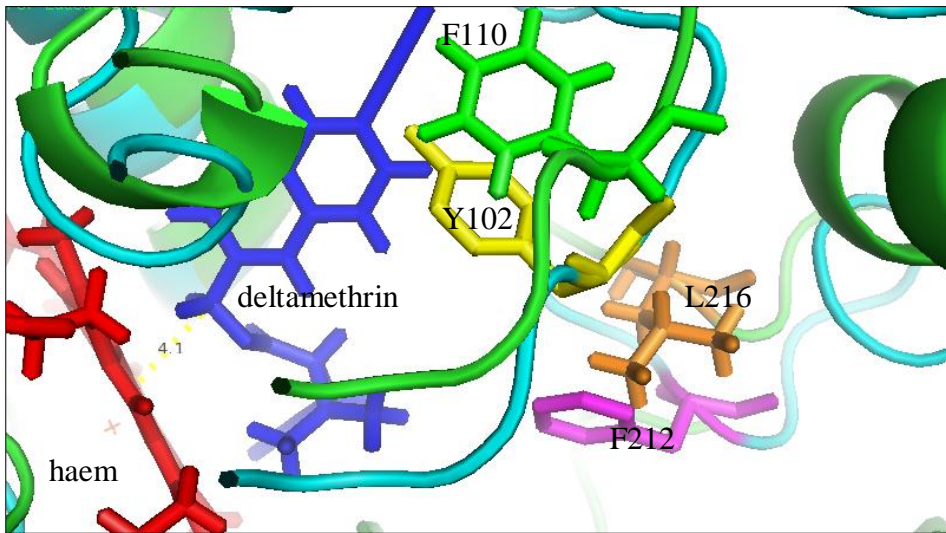
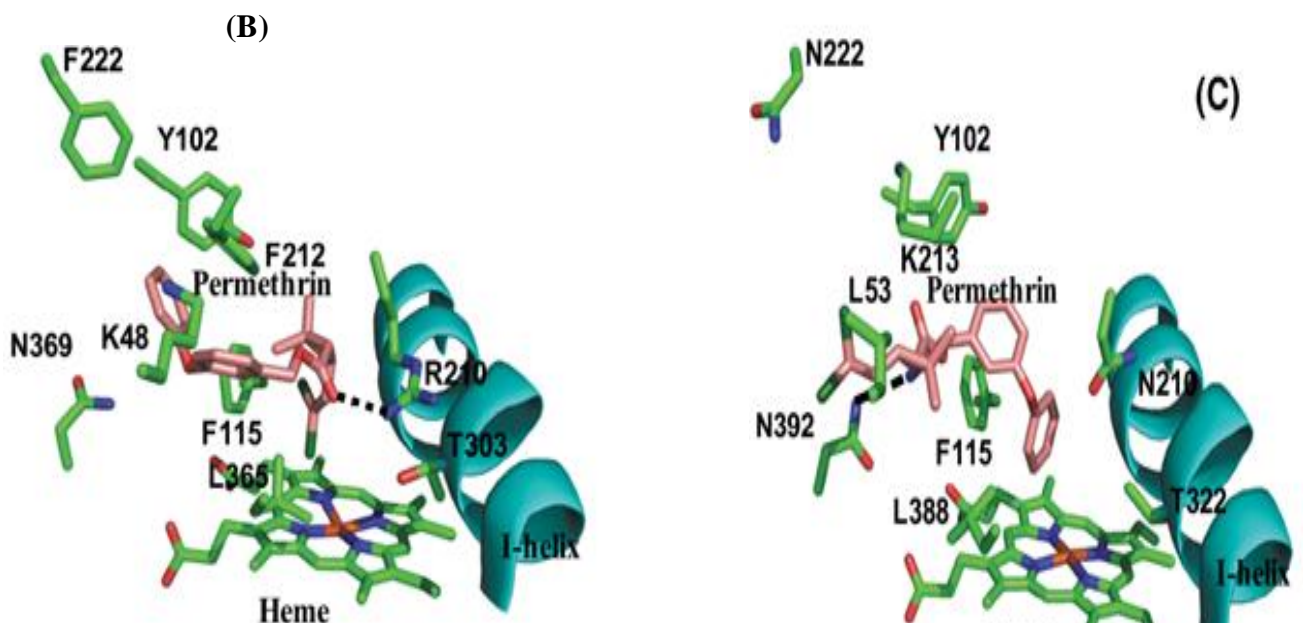


Figure 2.17: Homology models of CYP6P3 overlaid with CYP6Z2 and deltamethrin, in blue, docked at the active site. Haem iron is shown as red and the amino acid residues swapped in the two P450s are shown side by side close to the substrate. CYP6P3 (F110) is shown in green, CYP6Z2 (Y102) in yellow, CYP6P3 (L216) in orange and CYP6Z2 (F212) in magenta. The substrate is 4.1 Å to the haem centre.



Mclaughlin et al. 2008

Figure 2.18: Homology models of (B) CYP6Z2 with permethrin docked in the active site, (C) CYP6D1 with permethrin docked in the active site.

The results in this chapter clearly revealed the roles of the 3 amino acids examined. The affinity of the mutants for their substrates compared with the wild type, as shown by their K_M values, was similar for all the resorufin probes. However, the efficiency of CYP6Z2 increased by 2-fold when the positively charged arginine was replaced with alanine in R210A. Residue R210 was predicted to be involved in protein-ligand hydrogen bonds in permethrin docked in CYP6Z2 (McLaughlin et al., 2008). The exchange of tyrosine for phenylalanine and phenylalanine for leucine in F110Y and L216F mutants respectively in CYP6P3 revealed significant changes in the activities of the native protein. The activities of CYP6P3 and the two mutants were low generally for resorufin probes. However, F110Y completely lost activity to dealkylate BR and L216F did not show significant activity against PR. Cytochrome *b*₅ was inhibitory rather than stimulatory when introduced for these resorufin probes. Conversely, the introduction of cytochrome *b*₅ was stimulatory for DEF substrate. The effect was evidently shown with the increase in activity of L216F with DEF. Activity of F110Y against DEF was much lower when compared with the wild type and L216F but the affinity for DEF was the strongest suggesting this position may be involved in binding of the DEF substrate.

The metabolic activity against deltamethrin of the mutants created in CYP6Z2 was not very clear in this result. However, mutant Y102F and R210A show some level of activities when freshly prepared enzymes were used. Similar mutation of F110Y in CYP6P3 reduced the metabolic activity against the pyrethroids examined. However, a change to phenylalanine from leucine in L216 of CYP6P3 improved the activity to deplete pyrethroids better than the native enzyme. Thermal stability of CYP6P3 was also significantly increased with the introduction of the hydroxyl group in F110Y and the aromatic ring in L216F.

From these results, changing tyrosine to phenylalanine and mutating the arginine in the active site of CYP6Z2 could lead to depletion of pyrethroids.

The ability of P450s to catalyse the insertion of oxygen in a wide variety of substrates has attracted interest in these enzymes by the pharmaceutical industries (Faber and Johnson, 1996, Sono et al., 1996). However, their low stability and the need of redox partners have been the limitations in their technological applications (Joo et al., 1999). The improved thermostability and metabolic activity of CYP6P3 (L216F) suggests that increasing the number of aromatic residue in P450s might improve their stability for industrial use. The number of nucleotide change made and impact on the enzyme activity are shown in appendix 12.

Chapter 3

3 Investigating the role of Phe¹¹⁵ in the CYP6Z subfamily and comparing kinetic parameters and pyrethroid activities of CYP6Z2 and CYP6Z3

3.1 Introduction

Nikou et al (2003) reported that in *An. gambiae* the genes encoding CYP6Z1, CYP6Z2 and CYP6Z3 are tightly clustered on chromosome 3R. The different expression levels of these three CYP6Zs in the three developmental stages of *An. gambiae* suggested diverse roles for these P450s in this insect (McLaughlin et al., 2008). CYPZ1 is predominantly expressed in the adult stage (Nikou et al., 2003) and has been heterologously expressed to confirm it metabolises DDT (Chiu et al., 2008). CYP6Z1 may thus have a protective role in metabolising and detoxifying DDT in the adult mosquito.

CYP6Z2 is found expressed at high level in the larvae and at a reduced level in the adult stage (Nikou et al., 2003). *An. gambiae* is an aquatic herbivorous feeder during the larval stage and CYP6Z2 can metabolise plant toxins such as α -naphtho-flavone (ANF), thus may play a chemoprotective role during the aquatic life stage (McLaughlin et al., 2008). CYP6Z2 also binds to JH-III hormone, which is involved in insect development and metamorphosis (McLaughlin et al., 2008). CYP6Z2 has been confirmed to have secondary role in pyrethroid metabolism in processing metabolites generated by carboxylesterase led (and possibly P450) metabolism of pyrethroids (Alexia et al., 2013). CYP6Z2 has also been shown to metabolise carbaryl, a carbamate insecticide (Chiu et al., 2008). Finally, CYP6Z3 is expressed predominantly in larvae and pupae stages (Nikou et al., 2003). Muller et al identified CYP6Z3 among those P450s whose gene expression was associated with pyrethroid resistant *An. gambiae* strain from Ghana (Müller et al., 2007). However, this P450 has yet to be functionally characterised.

These three CYP6Z genes share common amino acid sequences. CYP6Z2 is 93.5% similar to CYP6Z3 and 69.4% similar to CYP6Z1. CYP6Z1 is in fact 70% and 69% similar to both CYP6Z2 and CYP6Z3 respectively (Chiu et al., 2008). The amino acid residues of the P450s are 494, 490, and 492 for CYP6Z1, CYP6Z2 and CYP6Z3 respectively as stated in appendix 13, 14 and 15. However, CYP6Z1 can metabolise DDT and CYP6Z2 cannot (Chiu et al., 2008). The ability of CYP6Z1 to metabolise pyrethroid insecticides has not been reported. Efforts were made here to express CYP6Z1 in *E. coli* as for CYP6Z2 (McLaughlin et al., 2008), but these attempts were unsuccessful.

Phe¹¹⁵ is well conserved in the three CYP6Z isoforms and it is positioned in the substrate recognition site 1 (SRS1) in between B-C loop. The residue protrudes into the active site over the haem iron (Chiu et al., 2008), and it is 4.1Å close to one of the pyrrolic groups of the haem (Figure 3.1). The effect of this aromatic ring and its pi electrons close to the porphyrin of the haem was investigated using SDM technique to mutate the Phenylalanine to other related and unrelated amino acid residues.

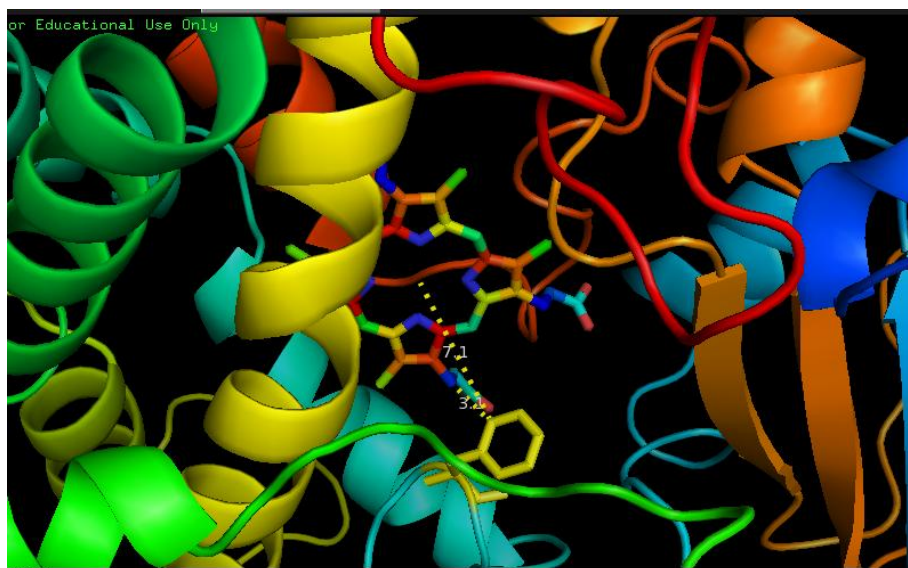


Figure 3.1 Homology model of CYP6Z2 viewed with Pymol showing the haem in rainbow colour and Phe¹¹⁵ residue in yellow at a 7.1 Å to the haem center and 3.1 Å to the pyrrole of the haem.

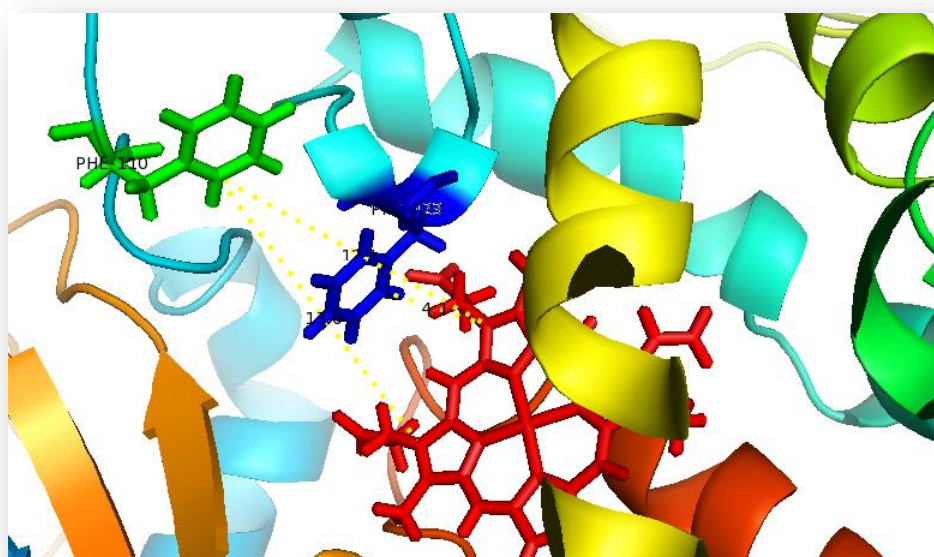


Figure 3.2: Homology model of CYP6P3 showing the haem in red colour, Phe¹¹⁰ in green and Phe¹²³ in blue. Phe¹¹⁰ is 12.1 Å and 13.6 Å to the nearest pyrroles of the haem, while Phe¹²³ is 4.1 Å to the nearest pyrrole of the haem. Phe¹²³ of CYP6P3 occupies the same position as Phe¹¹⁵ of CYP6Z2 when the two were compared.

3.2 Materials & Methods

3.2.1 Site directed mutagenesis

The protocol described in Chapter 2 was used to generate all the mutants created in this chapter: the primers and templates are stated in Table 3.1.

3.2.2 Thermostability assay

As described in chapter 2.

3.2.3 Effects of a range of concentrations of cytochrome *b*₅ on CYP6Z family

Two reaction mixtures following the fluorescent assay protocol were used to evaluate concentration of cytochrome *b*₅ needed in the activity of CYP6 family used in this experiment against DEF probe. Reaction mixture 1 contained 100 pmol of cytochrome *b*₅ as used in 1:10 reaction ratio, 10 pmol membrane, 20 μmol/l DEF and NADPH regenerating system (as describe in chapter 2). Reaction mixture 2 contains 10 pmole of membrane, 20 μmol/l DEF and regenerating system without cytochrome *b*₅. Reaction mixture 2 was used in serial dilution of reaction mixture 1 to achieve 50% downward dilution reaction mixtures.

Table 3.1: F115 mutagenic primers for CYP6Z2 and CYP6Z3

Mutants	Template	Forward Primer	Reverse Primer
CYP6Z2(F115A)	pB13ompACYP6Z2	5' TTC TCG GCC AAT CTG GCC GCT CTG CCC GGT CAG 3'	5' CTG ACC GGG CAG AGC GGC CAG ATT GGC CGA GAA 3'
CYP6Z2(F115L)	pB13ompACYP6Z2	5' TCG GCC AAT CTG CTC GCT CTG CCC GGT 3'	5' ACC GGG CAG AGC GAG CAG ATT GGC CGA 3'
CYP6Z2(F115Y)	pB13ompACYP6Z2	5' TCG GCC AAT CTG TAC GCT CTG CCC GGT 3'	5' ACC GGG CAG AGC GTA CAG ATT GGC CGA 3'
CYP6Z2(F115W)	pB13ompACYP6Z2	5' TCG GCC AAT CTG TGG GCT CTG CCC GGT 3'	5' ACC GGG CAG AGC CCA CAG ATT GGC CGA 3'
CYP6Z2(F115H)	pB13ompACYP6Z2	5' TCG GCC AAT CTG CAC GCT CTG CCC GGT 3'	5' ACC GGG CAG AGC GTG CAG ATT GGC CGA 3'
CYP6Z3(F115A)	pB13ompACYP6Z3	5' GTC GGC CAA CCT GGC CGC CCT GCC CGG CC 3'	5' GGC CGG GCA GGG CGG CCA GGT TGG CCG AC 3'

3.2.4 Cloning and expression of CYP6Z1 in JM109

cDNA of CYP6Z1 in pGEM-T easy holding vector was used in the subcloning carried out in this experiment. To confirm the gene and plasmid from previous cloning construct, the plasmid was digested with *EcoRI*. This digestion is expected to cut out the gene from the plasmid since the vector has two unique *EcoRI* sites. DNA mini-prep of the gene (prepared as described in chapter 4) was then sent for sequencing with information to the sequencing lab, SienceBiolab, to use standard primers of T7 promoters (forward and reverse). JM109 *ompA*-leader sequence was directly copied from the JM109 cells being used for the P450 expression. This was done by using *ompA* 2 forward primer with a reverse primer designed to have the reverse of the C-terminal of *ompA* leader sequence fused with the reverse sequence of the N-terminal of CYP6Z1. The genomes in JM109 cells were used as template in the first PCR reaction. The PCR product was ran on agarose to confirm product. Then the product was recovered from the gel and purified using Qiagen miniprep kit. The purified product then served as part of the 2nd PCR. In the 2nd PCR, another reverse primer was designed to have the reverse sequence of the C-terminal of CYP6Z1 with *EcoRI* site. This reverse primer was then used with *ompA* forward primer in the 2nd PCR comprising the short oligo product from the first PCR and the pGEM-Teasy plasmid with the cDNA of CYP6Z1 serving as template. The PCR product was run on gel and purified and subjected to *EcoRI* and *NdeI* digestions (restriction endonuclease enzymes). The digested product was then ligated into pB13 plasmid digested with same restriction endonuclease enzymes. CYP6Z1 gene was reconstructed in another subcloning when this construct was not producing holoprotein. The DNA sequence of CYP6Z1 is shown in appendix 16.

This new construct was made to have a chimera truncation of the N-terminal hydrophobic region of the CYP6Z1 by replacing it with the modified N-terminal sequence of CYP6Z2. This

was achieved by designing a reverse primer with 21 nucleotides from the end of the 21 amino acid residues of the N-terminal of CYP6Z2 fused to the 21 nucleotide of the beginning of the 22nd amino acid of CYP6Z1 as shown below. ompA forward primer was used with pB13CYP6Z2 as template in a PCR reaction to generate oligo having ompA leader with the N-terminal sequence of CYP6Z2 linked to part of the CYP6Z1 sequence starting from the 22nd amino acid residue.

Forward Primer: 5'GGAGGTGCATAGAAAAGACAG 3'

Reverse Primer: 5' **CCCCTGTCGATCCCAGTACGAGTAGATGTAGCGGAGCACGAG**



The oligo product was ran on agarose gel, confirmed, purified and used as part of the 2nd PCR reaction with pGEM-Teasy plasmid holding the cDNA of CYP6Z1 as template, CYP6Z1 reverse primer and ompA forward primer. The length of the PCR product was confirmed on agarose gel, recovered, purified and digested with *EcoR1* and *Nde1* and then ligated into pB13 plasmid. The new construct was then sent for sequencing.

The method for inducing the expression of CYP6Z2 and CYP6Z3 as described in chapter 2 was used. Two other expression methods, cold shock induction and heat shock induction were also employed. In the cold shock induction, 1µg/ml tetracycline was added alongside IPTG while 6ml ethanol was added for the induction of the heat shock (Kusano et al., 1999).

3.3 Results

3.3.1 P450 contents of expressed mutant isoforms of CYP6Z2

Functional mutants F115A, F115L, F115Y and F115W were expressed in *E.coli* (Figure 3.3). F115A shows highest peak at 420nm than the rest indicating fast conversion to apoprotein (Flanagan et al., 2004). This mutant was later discovered to degrade faster than the other mutant isoforms expressed as evidenced by the P450 peak being lost within 3months at -80°C. The introduction of a charged residue through F115H mutant did not yield P450 peak.

3.3.2 Specific activities of CYP6Z2 and mutants against resorufin & DEF probes

The fluorescent probes, BR, MR, ER, PR and DEF were used to test the enzyme activities of the mutants that expressed P450 peaks. Only F115A isoform had activity with BR (Figure 3.5). The BR activity of the mutant F115A was reduced by 13-fold when compared with the wild type. No activity was detected for any of the mutants against the DEF probe.

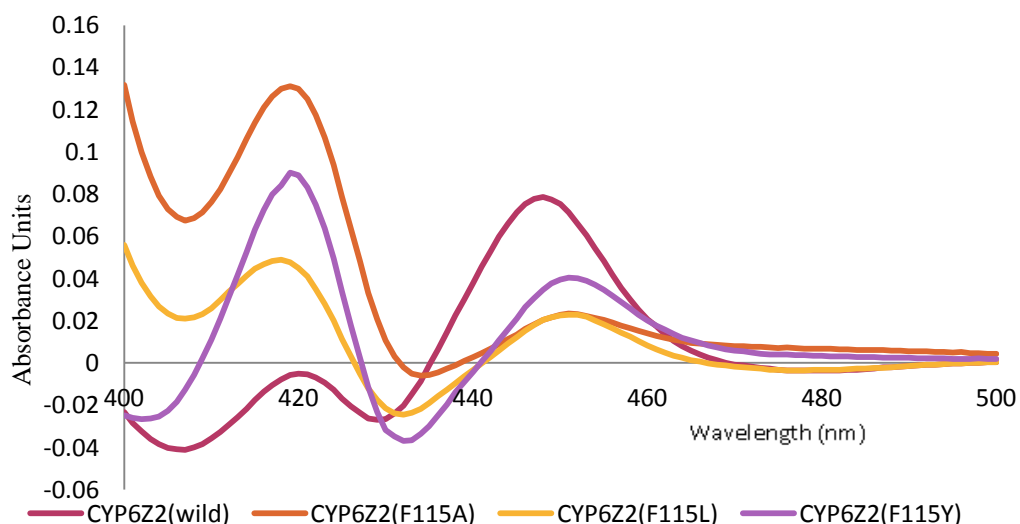


Figure 3.3: Fe^{2+} -CO vs Fe^{2+} difference spectrum of CYP6Z2 and the mutants, F115A, F115L and F115Y. The wild type had more intact holoprotein than the mutants. The spectral shift observed is because P450 exhibits spectrum between 448 – 452nm (Schenkman and Jansson, 2006).

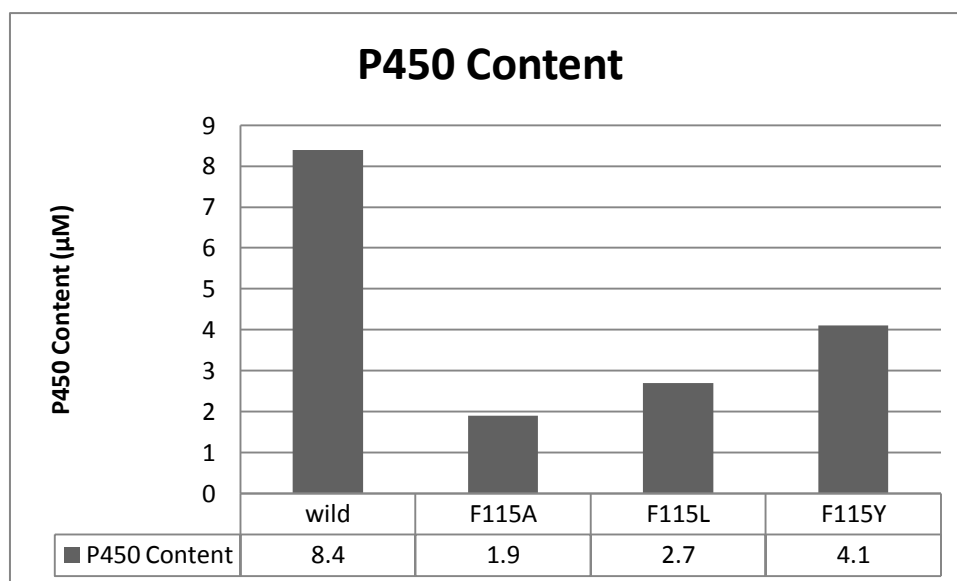


Figure 3.4: A- Fe^{2+} -CO vs Fe^{2+} difference spectrum CYP6Z2 and F115A, F115L, and F115Y- P450 contents in (μM). The bar-chart of the peaks at 450nm of the wild type and mutants to show the quantities of the intact holoprotein expressed for the membrane prepared. Expression was carried out at optimised conditions and n=1.

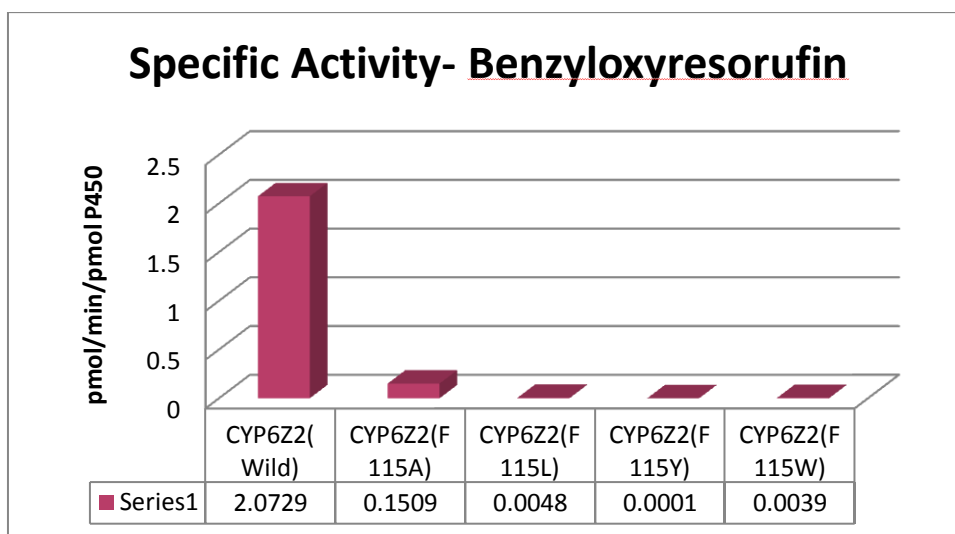


Figure 3.5: Specific activities of CYP6Z, F115A, F115L, F115Y and F115W against BR. The wild type and mutants that expressed intact holoprotein were tested with P450 probe, BR. Only F115A had activity.

3.3.3 Optimisation of cytochrome b_5 concentration for metabolic assay

Serial dilution of b_5 concentrations used with 1 pmole of CYP6Z2 and CYP6Z3 indicated that ratio 1:10 combination of the enzymes produced highest dealkylation of DEF substrate. The activity reduced to 40% and 80% in ratio 1:5 for CYP6Z2 and CYP6Z3 respectively.

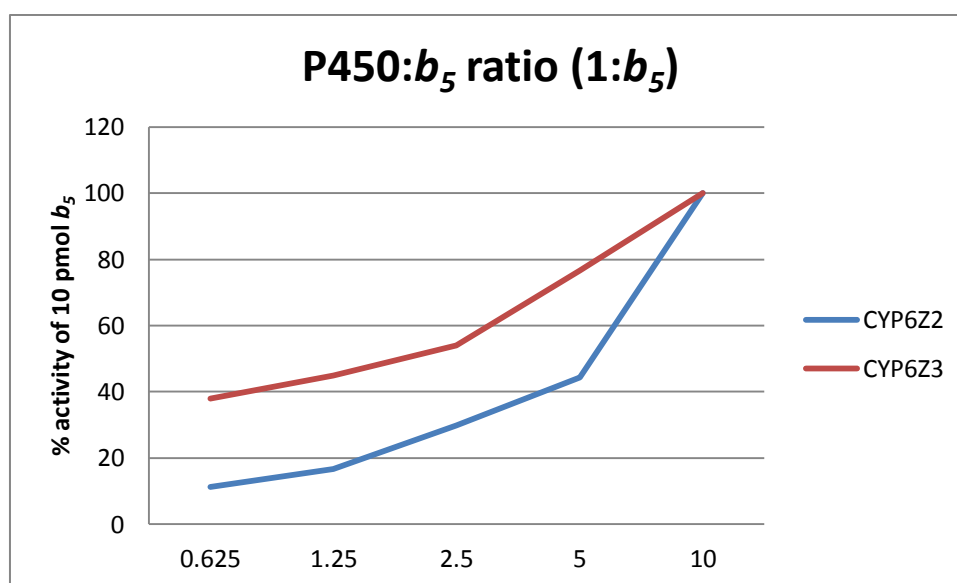


Figure 3.6: Serial dilution of cytochrome b_5 concentrations against 1 pmol of P450 in DEF dealkylation reaction. CYP6Z3 had higher activity against DEF than CYP6Z2 however they both showed similar reaction rates with the increasing concentrations of b_5 . Highest enzyme activity was recorded at ratio 1:10 for the two P450s.

3.3.4 Comparison of specific activities of wild type CYP6Z2 and wild type CP6Z3 with resorufin probes and DEF with and without cytochrome *b*₅

CYP6Z2 and CYP6Z3 retained their preference for the phenolic derivatives of resorufin. However, activities of CYP6Z3 against the four resorufin probes were higher when compared with CYP6Z2 (Table 3.2).

Table 3.2: Comparison of dealkylation of resorufin probes between CYP6Z3 and CYP6Z2

	CYP6Z2	CYP6Z3	Increase
	pmol/min/pmol P450	pmol/min/pmol P450	
BR	5.46±0.27	25.19±1.3	4.6-fold
MR	2.52±0.016	18.46±0.63	7.3-fold
ER	0.23±0.003	1.9±0.033	8.2-fold
PR	0.033±0.0005	0.098±0.013	3-fold

(Mean±SE, n=2)

The effect of cytochrome *b*₅ was on BR activity was examined. The addition of cytochrome *b*₅ did not have any effect on the activities of either CYP6Z2 or CYP6Z3 to dealkylate BR (Table 3.3).

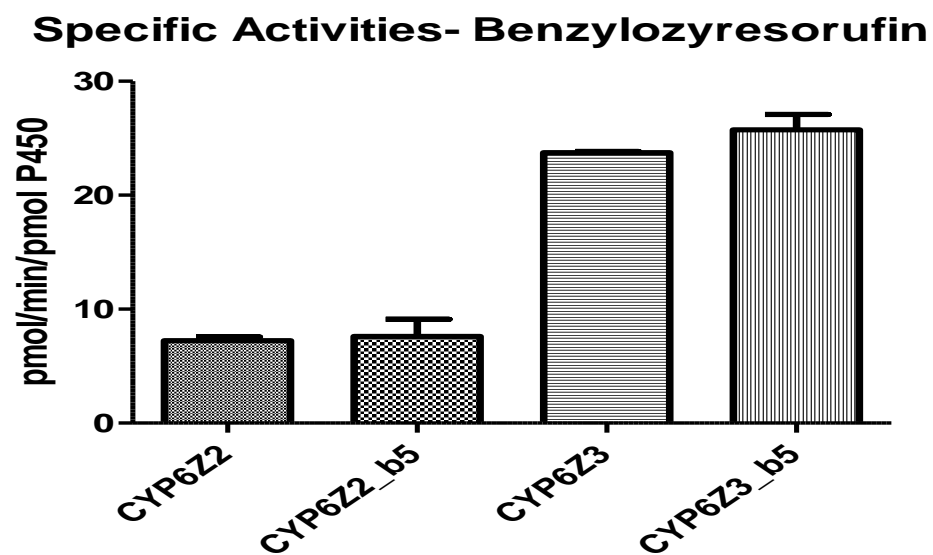


Figure 3.7: Effect of b_5 on P450 activity. Bar chart of specific activities of CYP6Z3 and CYP6Z2 against BR with or without b_5 . The presence of b_5 did not have noticeable effect in both dealkylation reactions.

Table 3.3: Specific activities of CYP6Z3 and CYP6Z2 against BR with or without b_5

Enzyme	Without b_5	b_5
	pmol/min/pmol P450	pmol/min/pmol P450
CYP6Z2	7.24±0.32	7.61±1.51
CYP6Z3	23.73±0.10	25.73±1.36

(Mean±SE, n=2)

However, the addition of cytochrome b_5 increased the activities of both enzymes when DEF was used as a substrate. The activity of CYP6Z2 was increased by 3.5-fold while CYP6Z3's activity was increased by 1.8-fold as shown below.

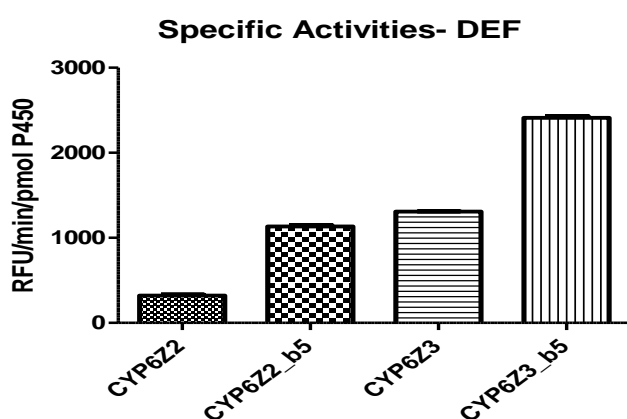


Figure 3.8: The influence of cytochrome b_5 on the specific activity of CYP6Z3 and CYP6Z2 against DEF, with or without b_5 investigating effect of addition of cytochrome b_5 to the reactions

Table 3.4: Specific activities of CYP6Z3 and CYP6Z2 against DEF with or without b_5

Enzyme	Without b_5	b_5	Increase
	RFU/min/pmol P450	RFU/min/pmol P450	
CYP6Z2	320.7 ± 12.00	1,134 ± 13.15	3.5-fold
CYP6Z3	1,310 ± 1.35	2,411 ± 21.30	1.8-fold

(Mean ± SE, n=2)

3.3.5 Comparing kinetic parameters of CYP6Z2 and CYP6Z3

The kinetic parameters of CYP6Z2 and CYP6Z3 were examined and compared using BR and MR. Both enzymes maintained their preference for BR. CYP6Z3 achieved 2-fold activity and 7-fold efficiency in dealkylation for BR and MR respectively. CYP6Z2 had 8-fold activity and 14-fold efficiency against BR and MR respectively

Overall CYP6Z3 proved to be more active and more efficient than CYP6Z2. It had 2-fold turnover rate and 5-fold higher enzyme effectiveness than CYP6Z2 in the dealkylation of BR, and 8-fold and 10-fold in turnover rate and efficiency respectively for MR.

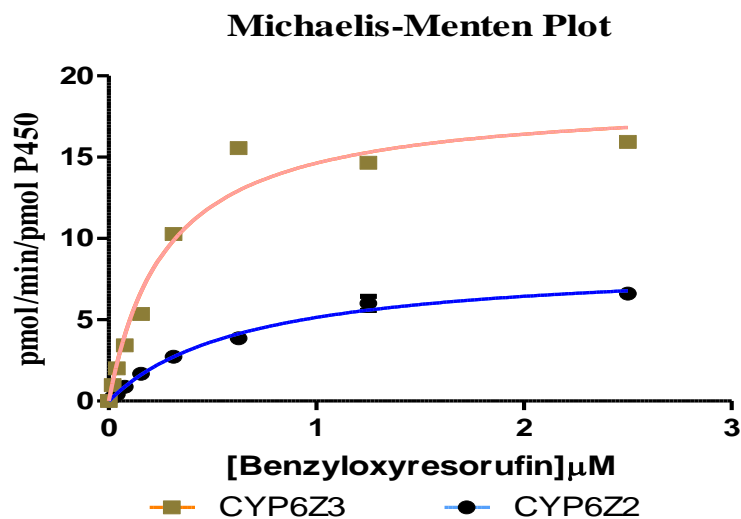


Figure 3.9: Michaelis-Menten plot of CYP6Z3 & CYP6Z2 -BR kinetics. CYP6Z3 showed higher turnover number and affinity for BR than CYP6Z2. The curve was generated using Graphpad Prism 5 software. R^2 for the curve fitting are 0.99 and 0.95 for CYP6Z3 and CYP6Z2 respectively.

Table 3.5: Kinetic parameters of BR dealkylation by CYP6Z3 and CYP6Z2.

Enzyme	K_M (μM)	K_{cat} (min^{-1})	K_{cat}/K_M ($min^{-1} \mu M^{-1}$)
CYP6Z2	0.68 ± 0.069	8.62 ± 0.35	12.72
CYP6Z3	0.28 ± 0.056	18.70 ± 1.17	67.15

(Mean \pm SE, n=2)

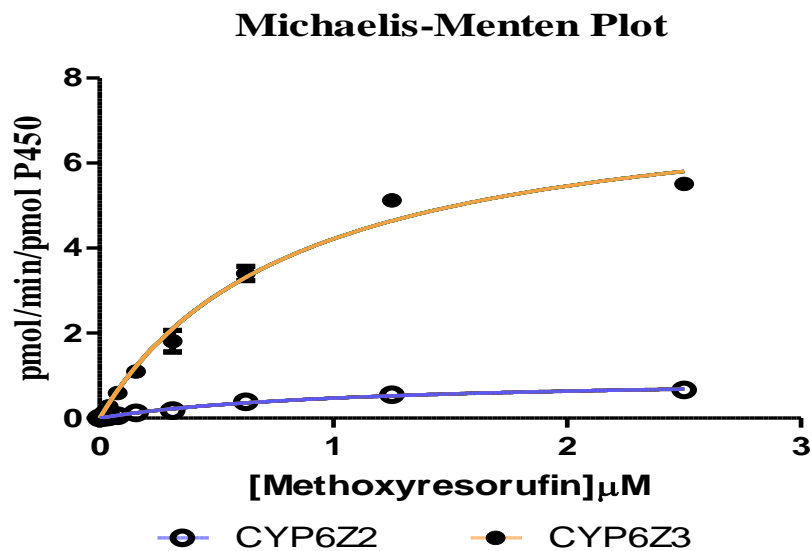


Figure 3.10: Michaelis-Menten plot of CYP6Z3 & CYP6Z2 -MR kinetics. CYP6Z3 showed higher turnover number and affinity for MR than CYP6Z2. The curve was generated using Graphpad Prism 5 software. R^2 for the curve fitting are 0.99 and 0.99 for CYP6Z3 and CYP6Z2 respectively.

Table 3.6: Kinetic parameters for MR dealkylation of CYP6Z2 and CYP6Z3

Enzyme	K_M (μM)	K_{cat} (min^{-1})	K_{cat}/K_M ($min^{-1} \mu M^{-1}$)
CYP6Z2	1.07±0.15	0.97±0.06	0.9
CYP6Z3	0.84±0.11	7.75±0.43	9.22

(Mean±SE, n=2)

3.3.6 Thermostability of CYP6Z2, CYP6Z3 and CYP6P3 compared

The thermostability of the three enzymes was tested using DEF. CYP6Z3 was most stable, maintaining 100% of its activity until 55°C. CYP6Z2 had lost 70% of its activity at same 55°C and CYP6P3 was no more active at this temperature just above 40 °C.

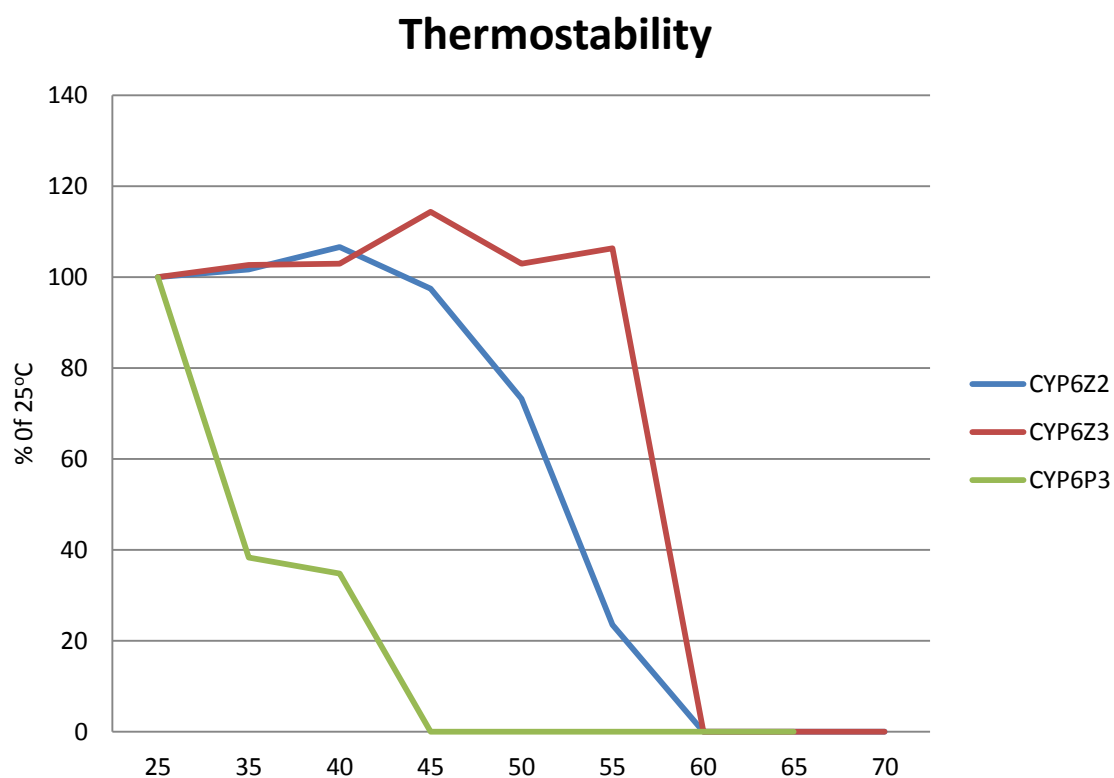


Figure 3.11: Thermostability of CYP6Z2, CYP6Z3 and CYP6P3 compared as a percentage of activity against DEF at 25°C. CYP6Z3 had highest thermostability and CYP6P3 the least.

3.3.7 Pyrethroid insecticides metabolic profiles of CYP6Z2 and CYP6Z3 compared with CYP6P3

The abilities of the two isoforms to metabolise pyrethroid insecticides were examined side by side with CYP6P3, a known pyrethroid metaboliser (Müller et al., 2008).

CYP6Z3 was able to achieve 50% of the metabolic activities of CYP6P3 in depleting pyrethroid insecticides. It also showed 100% depletion of pyriproxyfen, a pyridine-based pesticide.

Table 3.7: Insecticide metabolic activities of CYP6Z3 and CYP6Z2 compared with CYP6P3 as control

Insecticide	CYP6Z2 % depletion	CYP6Z3 % depletion	CYP6P3 % depletion
Deltamethrin	13.22±4.25	58.61±2.56	100
Permethrin- Cis	11.50±0.85	55.79±1.49	100
Permethrin -Trans	5.98±1.17	25.52±2.66	100
Cypermethrin	5.31±1.77	40.99±1.36	75.4±12.78
Pyriproxyfen	-	100±0	59.29±5.66

% depletion of substrate (Mean±SE, n=3)

3.3.8 Effect of mutating F115 on the kinetic parameters of CYP6Z2 and CYP6Z3

The two P450 isoforms, CYP6Z2 and CYP6Z3, were mutated to their F115A mutant isoforms. The DNA sequence confirmation of CYP 6 Z3 F115A is shown in appendix 17. The mutation was done at this position to further establish that the aromatic residue close to the haem may be involved in the stability of the formation of the activated oxygen (compound 1) used by P450s for catalytic activities.

The turnover numbers of the mutants were reduced significantly when compared with the wild types. CYP6Z2 (F115A) activity was reduced 2.3-fold and CYP6Z3 (F115A) 19.7-fold compared with the wild types. The efficiency of CYP6Z2 (F115A) was reduced by 14-fold and CYP6Z3(F115A) by 50-fold when compared with the wild type in BR dealkylation reaction (Table 3.8).

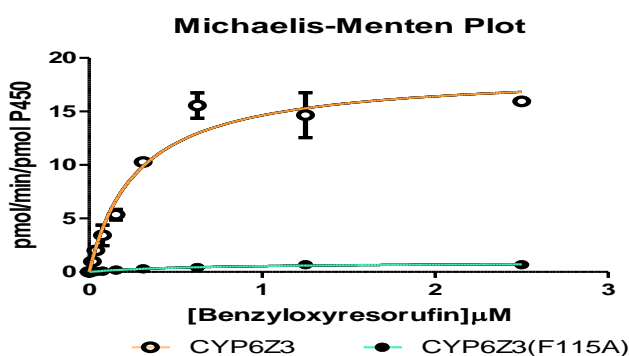
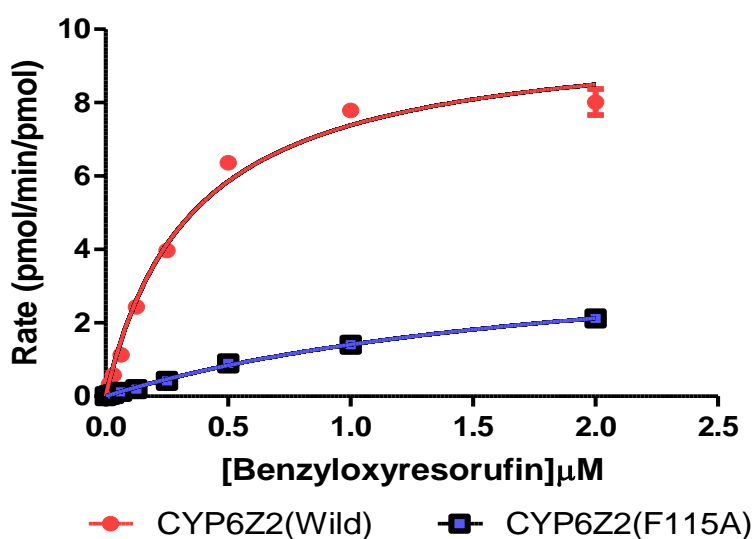


Figure 3.12: Michaelis-Menten plots: A- CYP6Z2 and CYP6Z2 (F115A), B- CYP6Z3 and CYP6Z3 (F115A). -BR kinetics. Substitutions of phenylalanine in both enzymes reduced the turnover rates of the enzymes. The curves were generated using Graphpad Prism 5 software. R^2 for the curve fitting are 0.99 and 0.99 for CYP6Z2 and CYP6Z2 (F115A) respectively and 0.96 and 0.95 for CYP6Z3 and CYP6Z3 (F115A) respectively.

Table 3.8: Kinetic parameters for BR dealkylation of CYP6Z2, CYP6Z2 (F115A), CYP6Z3 and CYP6Z3 (F115A)

Enzyme	K_M (μM)	K_{cat} (min^{-1})	K_{cat}/K_M ($\text{min}^{-1}\mu\text{M}^{-1}$)
CYP6Z2	0.35 ± 0.038	9.99 ± 0.37	28.54
CYP6Z2(F115A)	2.078 ± 0.20	4.311 ± 0.25	2.07
CYP6Z3	0.28 ± 0.05	18.70 ± 1.18	67
CYP6Z3(F115A)	0.67 ± 0.14	0.91 ± 0.07	1.34

(Mean \pm SE)

3.3.9 Effect of mutating F115 on pyrethroid insecticide metabolic profiles of CYP6Z3

The effect of the loss of activity with the mutation at F115 was also tested in the ability of CYP6Z3 in retaining its metabolic profiles of pyrethroid insecticides. The results show that the mutant lost 44-fold of its activity against deltamethrin and 16-fold against cypermethrin, type-2 pyrethroids. While the mutant recorded 3.6-fold lost in activity against permethrin, a type-1 pyrethroid.

Table 3.9: Metabolic assay with pyrethroid insecticides

Insecticide	CYP6Z3 % depletion	F115A % depletion	Reduction
Deltamethrin	62.74	1.40±0.85	44-fold
Permethrin- Cis	55.79±1.49	15.10±0.98	3.6-fold
Permethrin -Trans	25.52±2.66	7.52±3.81	3.4-fold
Cypermethrin	40.99±1.36	2.50±1.10	16-fold

% depletion of substrate (Mean±SE, n=3)

3.3.10 Comparison of the thermostability of mutant CYP6Z3 (F115A), CYP6Z2 (Y102F), CYP6Z2 (F212L) and CYP6Z2 (R210A)

The thermostability of CYP6Z3 (F115A) and the wild type was investigated and compared with the thermostability of mutations created at other positions on CYP6Z2. This was done to further investigate if the phenylalanine 4Å to the haem is contributing to the stability of the activated oxygen. The phenylalanine mutation at other positions away from the haem is not expected to have effect on the thermostability of the mutants. There was a visible 5°C shift to the left in the stability of the enzyme when Phe¹¹⁵ was mutated to alanine. This stability shift was not observed in the other mutations created away from the haem as illustrated below:

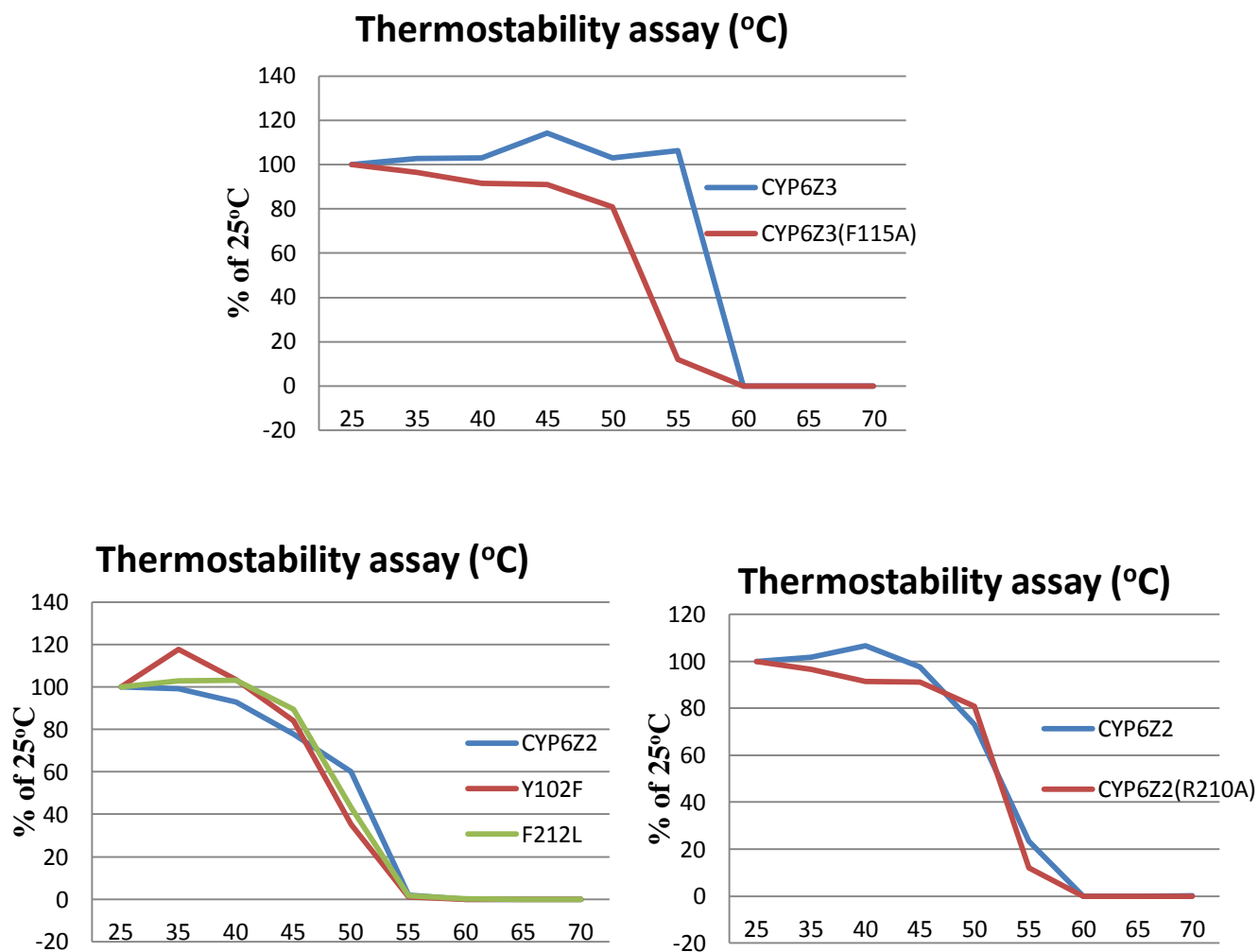


Figure 3.13: Thermostability assay of: A- CYP6Z3 and mutant F115A. B- CYP6Z2 and mutants Y102F ,F212L. C- CYP6Z2 and mutant R210A. Y axis computed as a percentage of the reaction activity of each enzyme against BR at 25°C.

3.4 Discussion

CYP6Z1 from *An. gambiae* was expressed successfully in Sf9 insect cells and was confirmed as a DDT metaboliser (Chiu et al., 2008). However, the ability of the enzyme to metabolise pyrethroid insecticides have not been documented. This may be due to the fact that heterologous expression of the enzyme in *E.coli* has been difficult. CYP6Z1 shares 69% primary structural similarity with both CYP6Z2 and CYP6Z3. CYP6Z2 was successfully expressed in *E. coli* but only after, the cDNA was modified by changing the second amino acid codon from phenylalanine to alanine and making the subsequent seven amino acids AT rich by “silent” mutagenesis (McLaughlin et al., 2008). The modified cDNA subcloned into the expression vector, pB13, yielded holoprotein and the enzyme’s substrates and inhibitors have been characterised (McLaughlin et al., 2008). The only modification made to CYP6Z3 used in this experiment was the change of the second amino acid from phenylalanine to alanine and was successfully expressed in *E. coli* using pB13 plasmid. However, similar efforts made with CYP6Z1 did not produce holoprotein even when N-terminal chimera of the modified sequence of CYP6Z2 was created. The wild type ompACYP6Z1 and the CYP6Z2-N-terminal chimera variant were also induced under cold shock response (this involves translational regulation), using tetracycline selection, and heat shock response (associated with protein folding through molecular chaperons), using ethanol, but none produced holoprotein.

These methods were used successfully to express “recalcitrant” P450 cDNAs (Kusano et al., 1999). CYP6Z1 may be more different from the other two isoforms at the translational level and its amino acids assembling may be facing codon usage bias when expressed in *E.coli*. Expressing the gene in a bacterial strain fortified with plasmids expressing the rare tRNAs, or in a yeast host, may improve the protein expression prospects.

Both CYP6Z2 and CYP6Z3 expressed in this thesis shared the same metabolic behaviour with the fluorescent probes used in the characterisation of *An. gambiae* CYP6Z2 with its inhibitors and substrates (McLaughlin et al., 2008). The two isoforms do not need cytochrome *b*₅ in the dealkylation reactions with the resorufin probes and both have their activity enhanced significantly with cytochrome *b*₅ in the dealkylation of DEF. However, CYP6Z3 has higher activity, is more thermostable and indicated higher metabolic activity against pyrethroids than CYP6Z2. Although CYP6Z2 shares 94% identity with CYP6Z3, the differences in the amino acid residues starts at SRS 2 with 2 out of 7 amino acids similar. SRS 2 is involved in the substrate access (Schuler and Berenbaum, 2013) and affects the entry and exit of substrate.

Phe¹¹⁵, is conserved in these three isoforms and predicted by homology modelling to be close to the haem (Chiu et al., 2008). P450s have relatively high proportions of occurrence of phenylalanine at the active site as part of the hydrophobic core. CYP3A4 has a unique 7 phenylalanine-cluster, with five of them involved in “closing of the roof” of the active site above the haem (Yano et al., 2004). In human CYP2D6, Phe^{481, 483}, located in the β1-4 loop and Phe¹²⁰ in B'-C loop were described to have a concerted or individual role for the phenolic group in ligand orientation (Flanagan et al., 2004). Phe¹²⁰ in human CYP2D6 was mutated to F120A, F120L, F120H and F120S by Flanagan et al to investigate its role in substrate binding and catalysis. All these mutants created via SDM expressed holoenzymes, including the mutant to histidine residue and their kinetic parameters with bufuralol established. (Flanagan et al., 2004). However, similar mutations in CYP6Z2 at F115 to F115A, F115L, F115Y, F115W and F115H produced holoprotein except for F115H. However, only F115A, a neutral substitution both in terms of steric and charge effects, was able to show activity against resorufin probes. F115L, F115Y and F115W (Figure 3.4) expressed stable holoprotein but did not have activity against the resorufin probes (Figure 3.5). Similar mutation on CYP6Z2 (F212L) gave activity against resorufin probe and CYP6P3 (F110Y) was still able to metabolise pyrethroid

insecticides as shown in chapter 2. Residue F212 in CYP6Z2 and residue F110 in CYP6P3 are at their respective active sites and are 12.1Å and 13.4Å away from the porphyrin of the haem (Figure 3.2). The Phe¹¹⁵ in CYP6Z2 was suggested to be involved in substrate positioning for catalysis (Alexia et al., 2013), this study has however revealed that this residue may be involved in stabilising the coupling of the oxygen on the haem-iron for catalysis to occur because of its proximity to the porphyrin of the haem. The porphyrin is important in the activation of the oxygen on the haem iron by donating electron for the O-O cleavage and the resultant formation of the active iron oxide complex known as compound 1 (Dolphin et al., 1997, Goh and Nam, 1999, Stillman, 2000). Phe¹¹⁵ is 4.1Å close to the haem (Figure 3.1) and its π -electrons may be contributing to the stability of compound 1. This may be the reason why mutants F115L, F115Y and F115W could not dealkylate the probes because there may be uncoupling of the oxygen at the catalytic cycle. The same mutation created in CYP6Z3 (F115A) supported this argument with the lost in activity of this mutant against pyrethroids when compared with the wild type. Further experiments to examine the presence of peroxide or superoxide anion (both products of uncoupling events) in F115L, F115L, F115W dealkylation reaction is however required to ascertain which of the shunt is at play in the uncoupling events. The shift in the thermostability of the mutants is also an indication of the stability role being played by Phe¹¹⁵.

Chapter 4

4 Establishing suitable expression and purification methods for full length 5xHis-tagged CYP6Z2 & the N-terminal truncated isoforms

4.1 Introduction

Insecticide resistance conferred on insects, especially mosquitoes, by P450s is increasingly threatening the gains made from vector control programs (Hemingway and Ranson, 2000). The WHO report of 2013 established that over 3.4 billion people are at risk of becoming infected with the malaria parasite transmitted by mosquitoes (World Health Organization, 2013). This potential loss of lives has been the driving force in efforts to understand the structural basis of those P450s responsible for the resistances of the insecticides approved to be used by WHO. However, no crystal structure of insect P450 has been solved to date and the knowledge of the molecular structure of the insect P450s have only been possible through homology modelling (Jones et al., 2010, Karunker et al., 2009, Lertkiatmongkol et al., 2011). Conversely, *in silico* homology modelling study is at best an explanatory tool rather than predictive tool (Szklarz et al., 1995). Although, the sequence of the side chains thought to constitute the active site conformation of P450s are well conserved, the spatial relationships of the residues of known crystal structures varies (Podust et al., 2001). These variations underscore the importance of a definitive crystal structure of a representative P450 from each family for better understanding of the structure- function of this enzyme class (Scott et al., 2001).

P450s in eukaryotes are membrane bound enzymes and their heterologous expression in *E. coli* typically results in low yields, because *E. coli* does not have an internal membrane system appropriate to accommodate the large microsomal recombinant proteins being expressed (Li and Chiang, 1991). More importantly is the effect of the dominant hydrophobic N-terminal

signal domain of eukaryotic P450s on the solubility of the expressed recombinant protein (Sagara et al., 1993).

The first P450 to be purified in quantities sufficient for crystallisation trials was camphor P450 from *Pseudomonas putida* (Poulos et al., 1987). The lack of an N-terminal trans-membrane region in prokaryotes is thought to be a key factor in increasing their solubility in cytosol and P450BM3 was also crystallised 6 years after P450CAM (Ravichandran et al., 1993). More prokaryotic P450 crystal structures have been subsequently determined and they have provided useful templates on which molecular models of eukaryotic P450s were created, until the first eukaryotic crystal structure was published (Scott et al., 2001). The latter was in large part made possible by modifications of the N-terminal trans-membrane region.

The first mammalian P450 to be crystallised was rabbit CYP2C5 (Poulos and Johnson, 2005). The authors deleted the N-terminal trans-membrane domain and created a chimeric enzyme that contains amino acid substitutions from CYP2C3. These substitutions were known to convert CYP2C5 to a monomer in high salt buffers (Cosme and Johnson, 2000). N-terminal truncations of CYP2C3 and CYP2C5 alone produced dimers and tetramers respectively in high salt buffers without the use of detergent (von Wachenfeldt et al., 1997). This engineering of the N-terminal deletions and modifications have made it possible for more eukaryotic P450s, in sub families 2B, 2C and 3A, to be crystallised (Schoch et al., 2004, Scott et al., 2003, Wester et al., 2003, Williams et al., 2004, Williams et al., 2003, Yano et al., 2004). However, deletion of N-terminal trans-membrane sequence in CYP2C1 did not produce a properly folded P450 (Hsu et al., 1993) and truncated CYP2D6 was expressed in a multimeric form in the absence of detergent (Kempf et al., 1995). Improvements have been observed in the expression of N-terminal trans-membrane truncated isomers of CYP2B subfamily through additional modification, including the insertion of positively charged amino acids at the N-terminus. However the holoprotein expressed formed large aggregates and only achieved 100%

monomeric status in the presence of 0.25% cholate (Scott et al., 2001). Human CYP3A4 however was successfully crystallised with just the deletion of the N-terminal domain without any further modifications (Yano et al., 2004).

The aim in this chapter is to develop expression and purification methods for the full length CYP6Z2 with 5 histidines attached to the C-terminal to aid purification by affinity chromatography, and to examine the effect of truncating the N-terminal trans-membrane sequence on the folding and expression of the truncated isomers.

The full length 5xHis-tagged CYP6Z2 and two N-terminal truncations of this full length, by 11 and 22 amino acids independently, were used in this experiment. While the full length expressed as holoprotein, the two truncated isoforms expressed as apoprotein.

4.2 Materials & Methods

4.2.1 Transformation and plasmid preparation and analysis

The nucleotide sequence of the construct pB13, expressing His-tagged CYP6Z2 was obtained to confirm its authenticity. pB13 is a modified form of pCW Ori (Barnes et al., 1991). Competent DH5a cells, (CaCl₂ method) were transformed with the plasmid by the heat shock method. The transformed cells were then spread on agar plates containing 100 µg/ml ampicillin and incubated at 37°C overnight. A colony was picked and inoculated in 3.5 ml LB medium with 100µg/ml ampicillin overnight at 37°C. A glycerol stock of 800 µl of incubated culture and 200 µl of glycerol was prepared and stored at -80°C. The remaining culture was used to prepare plasmid DNA using a Qiagen miniprep kit. The plasmid extracted was subjected to single and double restriction digestions using *Eco*RI and *Nde*I and the products examined on a 1% agarose gel electrophoresis to confirm the predicted sizes.

4.2.2 Primer design for pB13 insert sequencing

Three oligonucleotides were designed and synthesised as sequencing primers for the gene cloned into pB13. The forward and reverse primers were complementary to pB13 DNA sequences approximately 100 bases flanking on both sides of the multiple cloning regions. The middle primer was complementary to the centre of the CYP6Z2 gene. These primers were used to confirm the DNA sequences of all genes cloned into pB13 used in this project, using the Corefacility Centre, Medical School, Sheffield.

Sequencing Primers:

Forward: 5' ACA GGA TCA GCT TAC TCC CC 3'

Reverse: 5' CGT ATC ACG AGG CCC TTT CG 3'

Middle: 5' GCC GTG CTA ATC GGG GAC GC 3'

4.2.3 Modification to the histidine sequence attached to the CYP6Z2 gene.

Nucleotides encoding the run of 5 histidines were identified from the sequencing data, attached in frame, downstream of the 3' end of the CYP6Z2 cDNA. However, there was an unintentional addition of a base pair after the fifth histidine codon which would cause a shift of the stop codon during protein expression. Therefore, the gene was further modified with the following mutagenic primers to delete the unwanted base pair.

Mutagenic primers for modification:

Forward: 5' CAT CAC CAT CAC CAT TGA GAA TTC CCG GG 3'

Reverse: 5' CCC GGG AAT TCT CAA TGG TGA TGG TGA TG 3'

4.2.4 SDM procedure for the plasmid modification

The single mutagenic reverse primer SDM method (Vallette et al., 1989) was used to effect this reversion because the required SDM position has 7 nucleotides complementary to 2 other locations in pB13. In this method the mutagenic reverse primer, the forward primer, from the sequencing primer, and the His-tagged CYP6Z2, as template, were all used for the first PCR. The PCR product was then digested since the reverse primer has an *EcoRI* site at the 3' end and the forward primer generated the *NdeI* at the 5' end. The digested product was then ligated into a similarly digested product of pB13.

4.2.5 Construction and cloning of truncated versions of 5xHis-tagged CYP6Z2

Table 4.1: Primers and template for the creation of truncated 5xHis-tagged CYP6Z2 isomers

	Template	Forward primer	Reverse primer	Amino acids deleted
5xHis-tagged CYP6Z2Δ3-25	5xHis-tagged CYP6Z2	5' CAT ATG GCT GGA CTT CCT CAT CTA AAG CCA GA 3'	5' CCC GGG AAT TCT CAA TGG TGA TGG TGA TG 3'	23
5xHis-tagged CYP6Z2Δ3-13(5H)	5xHis-tagged CYP6Z2	5' CAT ATG GCT TTT CTC GTG CTC CGC TAC ATC TA 3'	5' CCC GGG AAT TCT CAA TGG TGA TGG TGA TG 3'	11

The start codon and the second amino acid codon are mutated to alanine codons to increase expression, were retained in the truncated isomers as highlighted.

The PCR for the generation of truncated mutants was carried out using Phusion High Fidelity Polymerase as described in appendix 3. The PCR product was purified and excised from a 1% agarose gel using a Qiagen gel extraction kit. The purified product and pB13CYP6Z2 were digested with *EcoR1* and *Nde1* to produce compatible flanking ends on both the truncated PCR products and digested pB13. The mixtures, after incubation at 37°C for 1 hour, were run and excised from a 1% agarose gel and the key bands purified as above and then ligated using T4 ligase enzyme. DH5α competent cells were transformed with the ligation mixture and the recovered plasmids were sent for sequencing.

4.2.6 Expression of the full length 5xHis-tagged CYP6Z2 and the truncated isomers

A modified form of the protocols for expression and purification of CYP2B subfamily (Scott et al., 2001) were utilised in this experiment.

The confirmed plasmids were used to transform *E.coli* JM109 K made competent with transformation buffer 1, (prepared with 100 mM RbCl, 50 mM MnCl₂, 30 mM potassium acetate, 10 mM CaCl₂, 15% glycerol, pH adjusted to 5.8 with acetic acid) and transfer buffer 2, (prepared with 10 mM MOPS, 10 mM RbCl, 75 mM CaCl₂, 15% glycerol, pH adjusted to 6.8 with KOH) using the heat shock method of transformation. A single colony from the transformation plate was used to inoculate a 20 ml LB supplemented with 100 µg/ml ampicillin and incubated at 37°C overnight. Then, 15 ml of the overnight culture was used to inoculate 250 ml of terrific broth supplemented with 100 µg/ml ampicillin, which was then grown to an OD₆₀₀ of 1–1.5 at 37°C (Scott et al., 2001). Expression was induced by adding IPTG to 1 mM. ALA was added to 80 mg/l as a precursor for haem synthesis. Imidazole was added to 5 mM at the time of induction to stabilize the holoprotein. The culture was grown for additional 24 hours at 30°C with shaking at 120 RPM. The cells were harvested by spinning at 5000 RPM for 15 minutes at 4°C with a JA-14 fixed angle rotor in a Beckman JA-21 centrifuge.

4.2.1 Affinity chromatography and purification of full length 5xHis-tagged CYP6Z2

Purification was performed at 4°C. Cell pellets were re-suspended in 500 mM potassium phosphate, 10% glycerol, 10 mM β-mercaptoethanol (βME) with 0.4% sodium cholate, pH7.4 and homogenised using a hand homogeniser. The homogenate was then sonicated for 30 seconds and 45 seconds cooling on ice three times, followed by centrifugation for 35minutes at 31,000 RPM (113,000 x g) using a fixed-angle Ti 50.2 rotor in a Beckman Ultracentrifuge. The supernatant was applied to a Ni²⁺-NTA column previously equilibrated with 500 mM potassium phosphate, 10% glycerol 10 mM βME with 0.4% sodium cholate at pH 7.4. The column was washed with the following buffers: (1) 500 mM buffer A with 0.1% sodium

cholate, (2) 10 mM buffer (A) with 20 mM imidazole, and (3) 10 mM buffer (A) with 40 mM imidazole. The protein was eluted with 10 mM buffer (A) plus 500 mM imidazole. 0.5M NaCl was added to the elution buffer (buffer (A): potassium phosphate, 10% glycerol, and 10mM β -ME). All the fractions collected were run on SDS-PAGE and were subsequently analysed by Western Blotting.

4.2.2 Ion exchange purification of the partially purified full length 5xHis-tagged CYP6Z2

The DNA sequence of the CYP6Z2(5H) was translated into its ORF in order to calculate its Isoelectric Point(pI), which is the pH at which full length 5xHis-tagged CYP6Z2 carries no net charge. Online ExPASy - Compute pI/Mw tool was used. The pI was 8.04 and at working pH of 7.4 the protein is expected to have net positive charge. Both cationic and anionic ion exchange, SP Sepharose and Q Sepharose respectively were used to further purify the expressed full length 5xHis-tagged CYP6Z2.

4.2.3 SDS-PAGE analysis

In this experiment, 10% SDS- PAGE resolving gel was used by preparing 3.3 ml of 30% acrylamide solution, 2.5 ml of resolving gel buffer (1.5 M Tris plus 0.4% SDS, pH 8.8) 4 ml distilled water, 10 μ l TEMED and 200 μ l of 10% ammonium persulphate. The stacking gel was prepared using 1 ml 30% acrylamide solution, 1.5 ml stacking buffer (0.5 M Tris plus 0.4% SDS pH 6.8), 3.4 ml water, 10 μ l TEMED and 100 μ l of 10% ammonium persulphate. The gel was ran with running buffer (25 mM tris base, 250 mM glycine and 0.1% SDS) for the first 10min at 80V to allow the sample stack properly and then the voltage increased to 100 Volts for another 60minutes. Standard Protein Ladder was run with the samples. The SDS gel was either stained using Coomassie staining solution or used for immunoblotting.

4.2.4 Immunoblotting

Nitrocellulose membrane was cut to the size of the gel and packed into the immunoblotting cassette with absorbent papers, filter pads, all previously soaked in the transfer/running buffer, Towbin Transfer Buffer (25 mM tris base, 192 mM glycine, 20% methanol). The cassette was then loaded into the immunoblotting tank and ran for 90 minutes at 200 mA. The nitrocellulose paper with the transferred samples from the SDS gel was first rinsed in phosphate buffer saline, PBS, (80 mM di-sodium hydrogen orthophosphate, 20 mM sodium di-hydrogen orthophosphate and 100 mM NaCl) and then blocked with 1% BSA in T-PBS (0.1% tween-20 in PBS prepared) at room temperature for 1hour. The BSA blocked nitrocellulose membrane was then rinsed in T-PBS for 5minutes and then incubated for another 1hour with the antibody, Hisprobe-HRP in 1% BSA in T-PBS buffer. HisProbe-HRP is a nickel (Ni^{2+})-activated derivative of horseradish peroxidase (HRP) that enables direct detection of His-tagged proteins and other histidine-rich proteins in western blots. After the incubation the membrane was rinsed with T-PBS first and then PBS to remove the tween detergent. ECL kit reagent (Amersham ECL Prime Western Blotting Detection Reagent (*GE-Healthcare*)) was then used to develop the probe for capturing in the dark room on the developing machine.

4.2.5 Bradford total protein quantification

Bradford reagent from BioRad protein assay solution was used to quantify the total protein content. The method is based on Coomassie blue G-250: the solution is red-brown in its acidic solution when not bound to protein. However, when proteins bind to the dye, the pKa of the dye shifts causing the dye to become blue and then measured at 595 nm (Bradford, 1976). Protein standard curve was prepared using known concentrations of prepared BSA and the quantity of the protein samples derived from the standard curve (Appendix 18). The samples were diluted in 100-fold dilution to fit into the curve.

4.2.6 P450 quantification of the full length 5xHis-tagged CYP6Z2 expressed

Quantification of the expressed P450 was carried out as described in chapter 2.

4.3 Results

4.3.1 Confirmation of Insert and Plasmid

The plasmid pB13 5xHis-tagged CYP6Z2 is a variant of the gene cloned and described by McLaughlin et al. (McLaughlin et al., 2008). However, this clone variant did not have the bacteria ompA leader sequence. The CYP6Z2 insert is flanked at the 5' end by *Nde*I and at the 3' with *Eco*RI. It has total length of 1.5kbp and the pB13 5kbp as shown below in the 1% agarose gel confirming the plasmid and the insert.

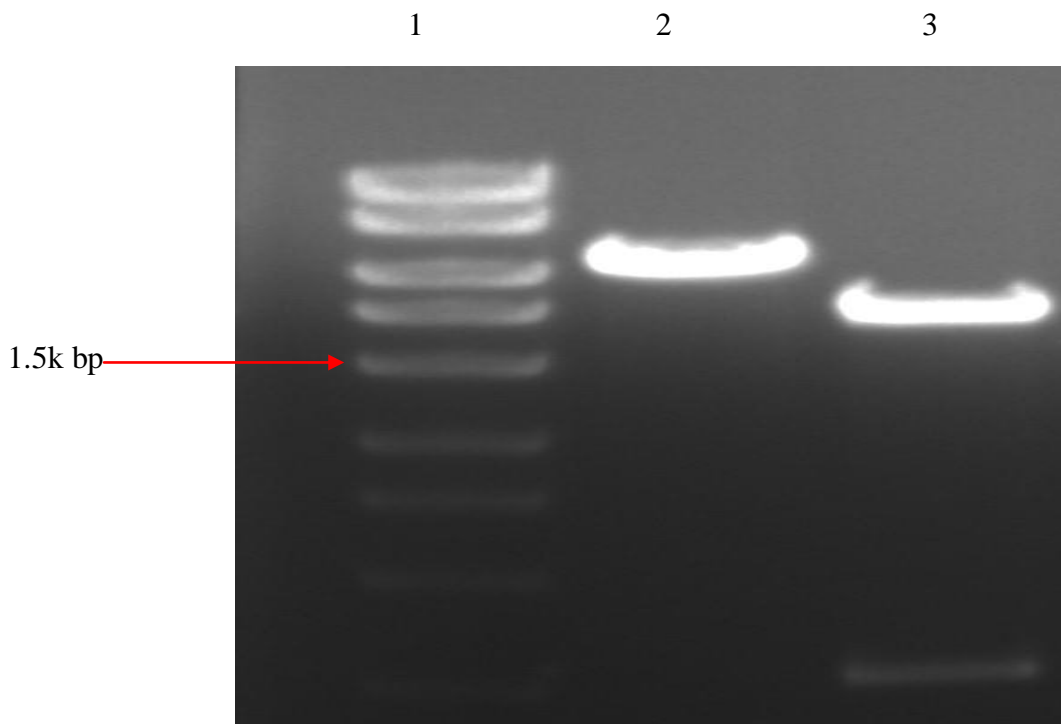


Figure 4.1: 1% agarose gel image of the digested sample with standard DNA markers for size confirmation. Lane1 is hyperladder, lane 2 is *Eco*RI digestion, lane 3 is *Eco*RI and *Nde*I digestions, showing the CYP6Z2 cut out of pB13. The insert is 1.5k bp while the pB13 plasmid is 5k bp.

4.3.2 Expressed full Length 5xHis-tagged CYP6Z2 and the truncated isoforms

The yield of P450 holoenzyme expression was monitored under a range of growth conditions. Expression of the full length at 25°C with shaking at 150 RPM yielded 33.18 nmol/l culture of P450 after 24 hours of incubation. The quantity increased by 3.9-fold at 48hrs but the expressed P450 was lost at 72hours. The truncated isoforms did not give properly folded protein in all of these experimental conditions used.

Cells of the full length grown at 30°C and shaking at 200 RPM yielded 146.7 nmol/l culture of P450 after 24 hours incubation but this was progressively lost by 1.2-fold after 48hours and by 1.5-fold at 72 hours. The third set of growth conditions at 30°C and shaking at 120 RPM gave 119.12 nmol/l culture of P450 after incubation for 24 hours and progressively increased by 2.6-fold at 48 hours and 5.3-fold at 72 hours (Figure 4.2)

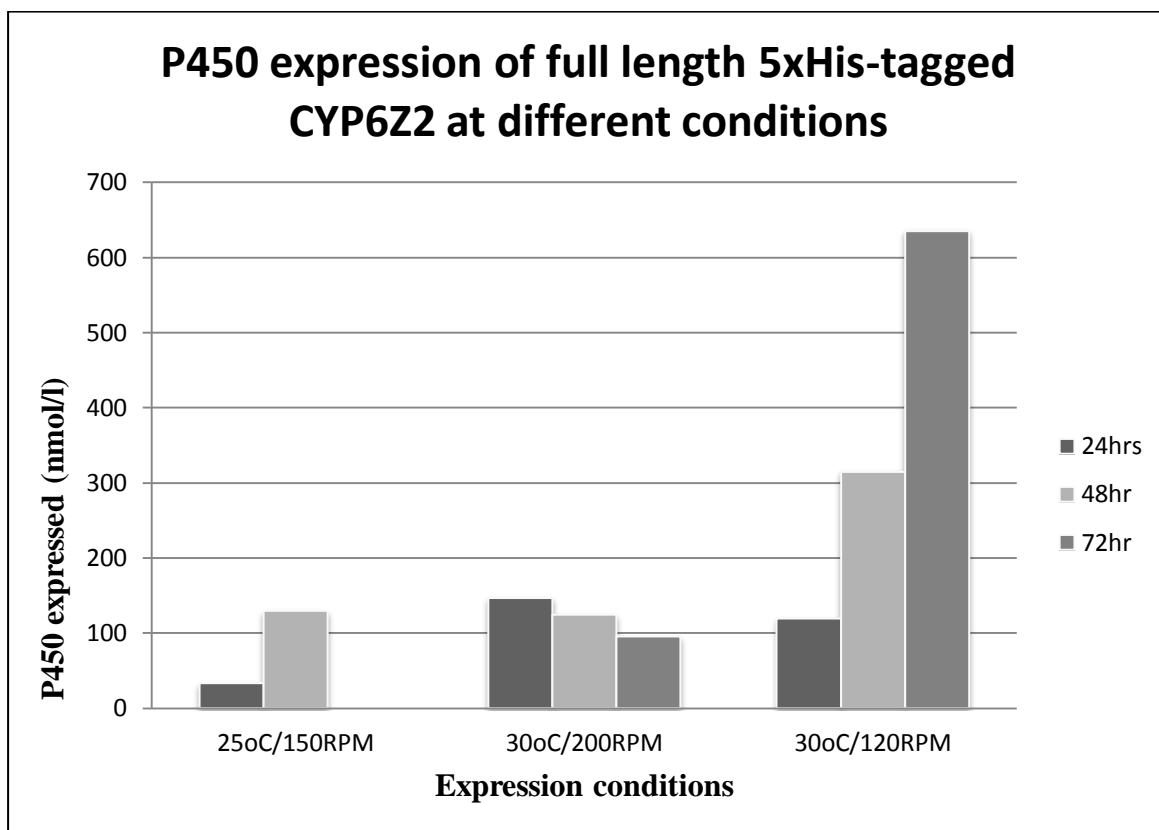


Figure 4.2: The P450 yield at different incubation temperature, shaking and time. The yield at 30°C and shaking at lower speed was highest and seems the best condition for JM109 *E. coli* cells in expressing the P450 and for the formation of the thiolate bond needed in the formation of properly folded CYP6Z2.

The expressed full length CYP6Z2 yielded P450 holoenzyme and also showed peak at 420nm, indicating degradation of the enzyme being expressed. The two truncated isomers however, did not produce P450 peak. The peak at 420nm also indicated that the truncated enzymes had very low expression when the Soret bands at 420nm were compared with that of the full length (Figure 4.3). The full length produced P450 content of 0.598 nmol/ml of total protein expressed.

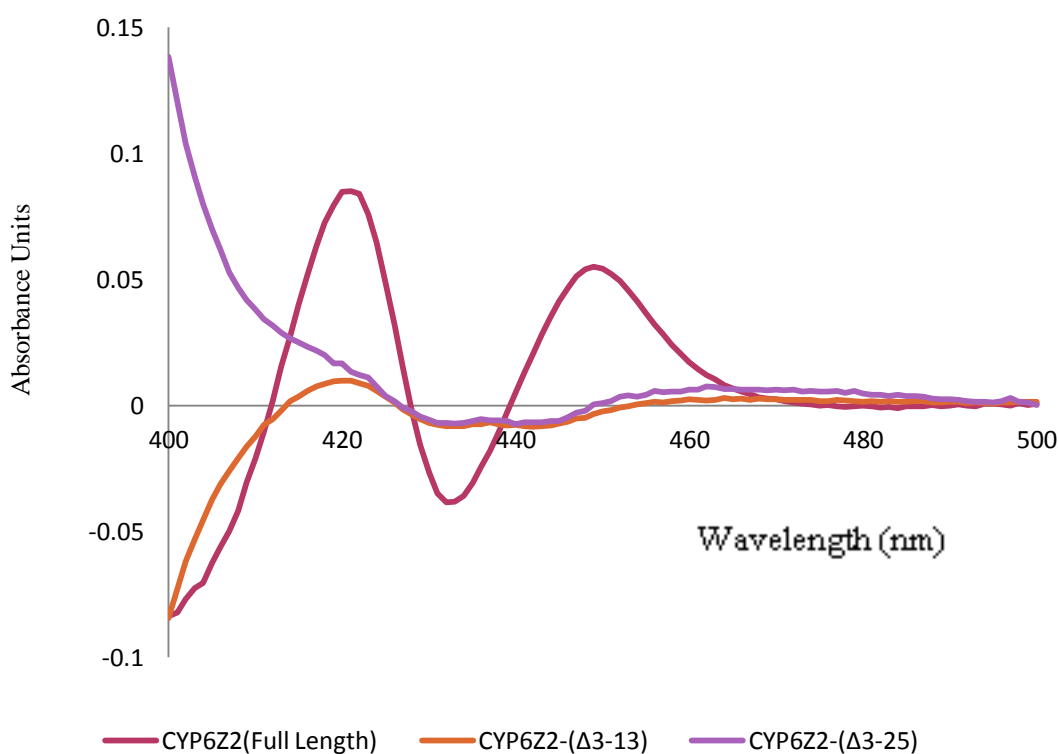


Figure 4.3: Fe²⁺-CO vs Fe²⁺ difference spectrum of the full length 5xHis-tagged CYP6Z2 and the truncated isoforms, CYP6Z2(Δ3-13) & CYP6Z2(Δ3-25) showing the P450 & P420 folding patterns. The truncated isozymes did not fold properly.

4.3.3 SDS-PAGE and immunoblotting of expressed 5xHis-tagged CYP6Z2

The expressed full length CYP6Z2 was loaded on two SDS-PAGE. One was stained with Coomassie staining solution and the other used for the immunoblotting assay to confirm distributions and purity of the expressed protein in the various purification steps. CYP6Z2 is approximately 56 kDa.

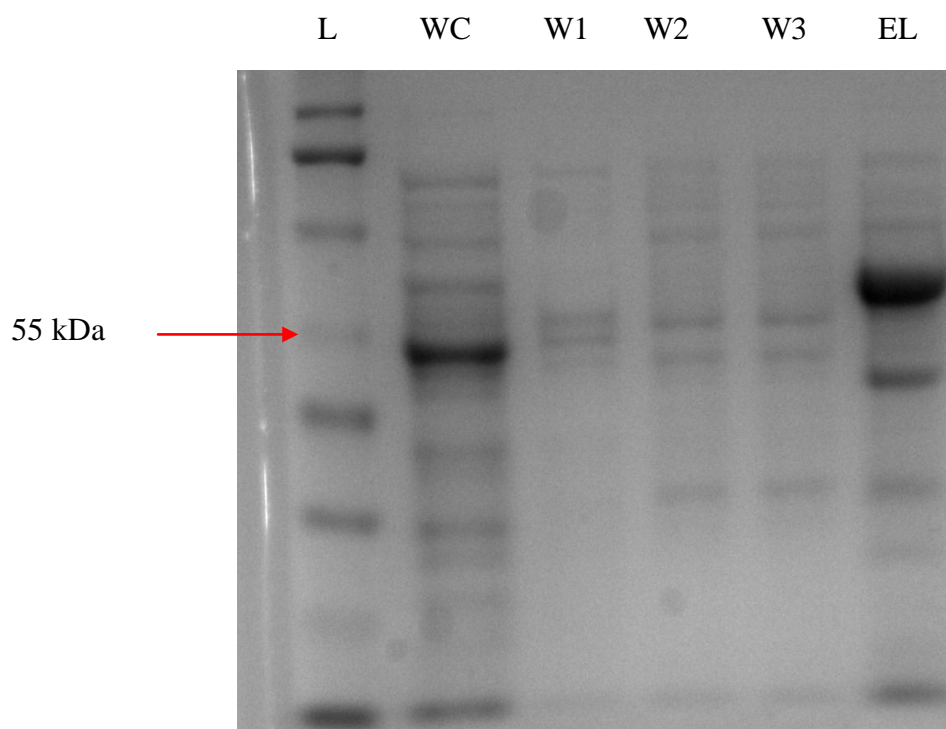


Figure 4.4: The SDS-PAGE of the expressed CYP6Z2 stained with coomassie blue dye. The lanes are; protein ladder (L), whole cell lysate (WC), 1st washing step with 0.1% sodium cholate (W1), 2nd washing step with 20mM imidazole (W2), 3rd washing step with 40mM imidazole (W3), and eluted fraction with 500mM imidazole (EL)

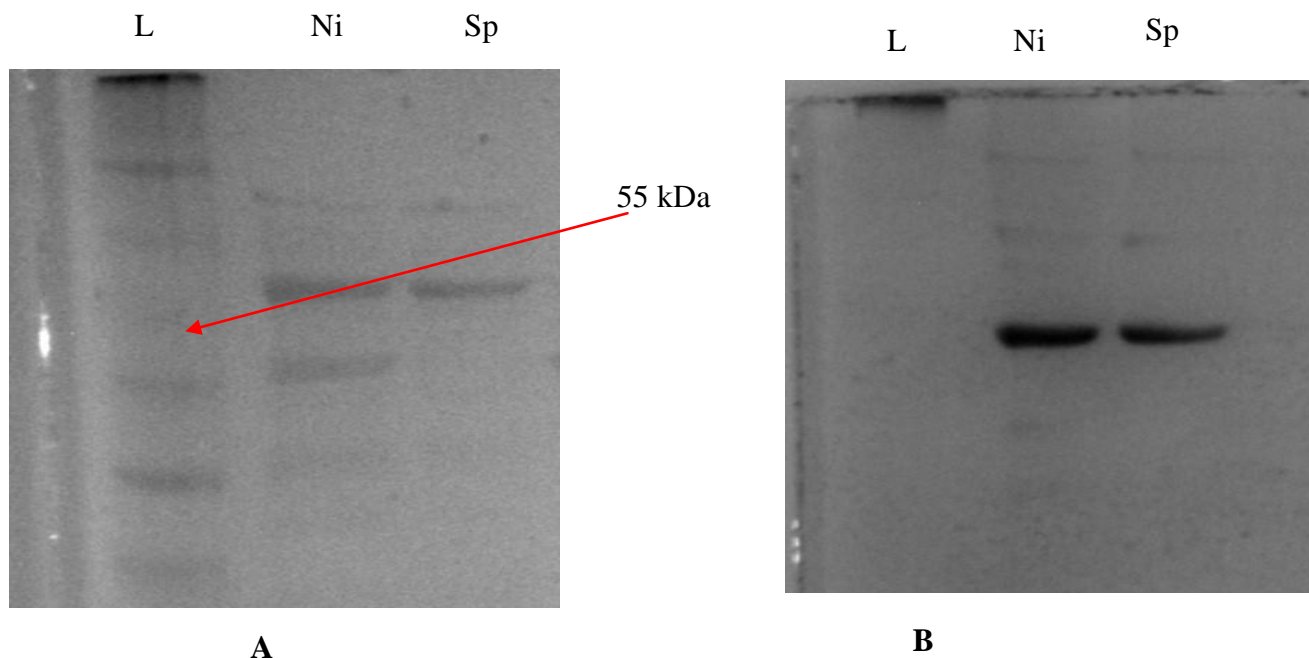


Figure 4.5: SDS-PAGE stained with coomassie blue dye (A) and western blot (B) of the purified CYP6Z2 on affinity chromatography and further purification on SP sepharose. The protein ladder is in lane 1(L), Ni-NTA affinity column (Ni) and SP sepharose column (SP). The protein is seen here to be 90% pure with the ion exchange used to further purify it after affinity chromatography.

The final purified sample yielded 1.57 mg/ml of protein, quantified with Bradford reagent using BSA standard curve. The P450 content of the purified full length 5xHis-tagged CYP6Z2 is therefore 0.38 nmol P450/mg protein.

4.4 Discussion

The relatively high hydrophobic nature of P450s, especially at the N-terminal region, was a great concern in designing strategies for expressing and purifying CYP6Z2 in *E.coli*. The N-terminus has been shown to interact with the bacterial membrane and rendering the P450 less soluble in cytosolic extracts (Scott et al., 2001). Therefore various protocols for overcoming these problems with expression of soluble P450 were investigated.

The level of expression was very low when, ALA, the haem precursor, was omitted and only iron was added to the LB. A protocol used by Modi et al. using 20mM Tris buffer, 2mM CHAP detergent and ALA to purify CYP2D6 (Modi et al., 1996), improved yield of the protein, but the expressed protein failed to bind to a Nickel NTA column as expected. At this point β -mercaptoethanol (β ME) and urea were added separately to the impure fraction, prior to Ni-NTA affinity chromatography. Samples from the two procedures were retained on the resin as anticipated indicating that the C-terminus of the protein where the histidines were appended, may be inaccessible in their absence. β ME was then used in combination with high salt phosphate buffer and sodium cholate during cell lysis. The affinity column was equilibrated with sodium cholate prior to loading the sample and NaCl was omitted from the washing buffers and was added only to the elution buffer in order to improve the binding of the protein on the column (Scott et al., 2001).

The presence of impurities after stringent washing during the affinity chromatography step indicates partial degradation (Fig. 4.4 & 4.5) of the purified protein or interaction of the protein with other lipoprotein from the *E. coli* cells which necessitated the use of the second purification step.

The isoelectric point computed using the amino acid sequence of 5xHis-tagged CYP6Z2 specified a protein with net positive charge at pH 7.4 of the buffer. However, when the sample was loaded on Q-Sepharose, an ionic exchanger, the sample bound to the column indicating a protein with net negative charge. The sample was expected to flow through since the resin of Q-sepharose is positively charged and then some of the impurities that are negatively charged to be held on the column. The differences in the behaviour of the isoelectric point computed and the one observed may be due to the effect of the presence of the cofactor. The sample however passed through SP Sepharose without binding to the resin and protein of nearly 90% purity was obtained.

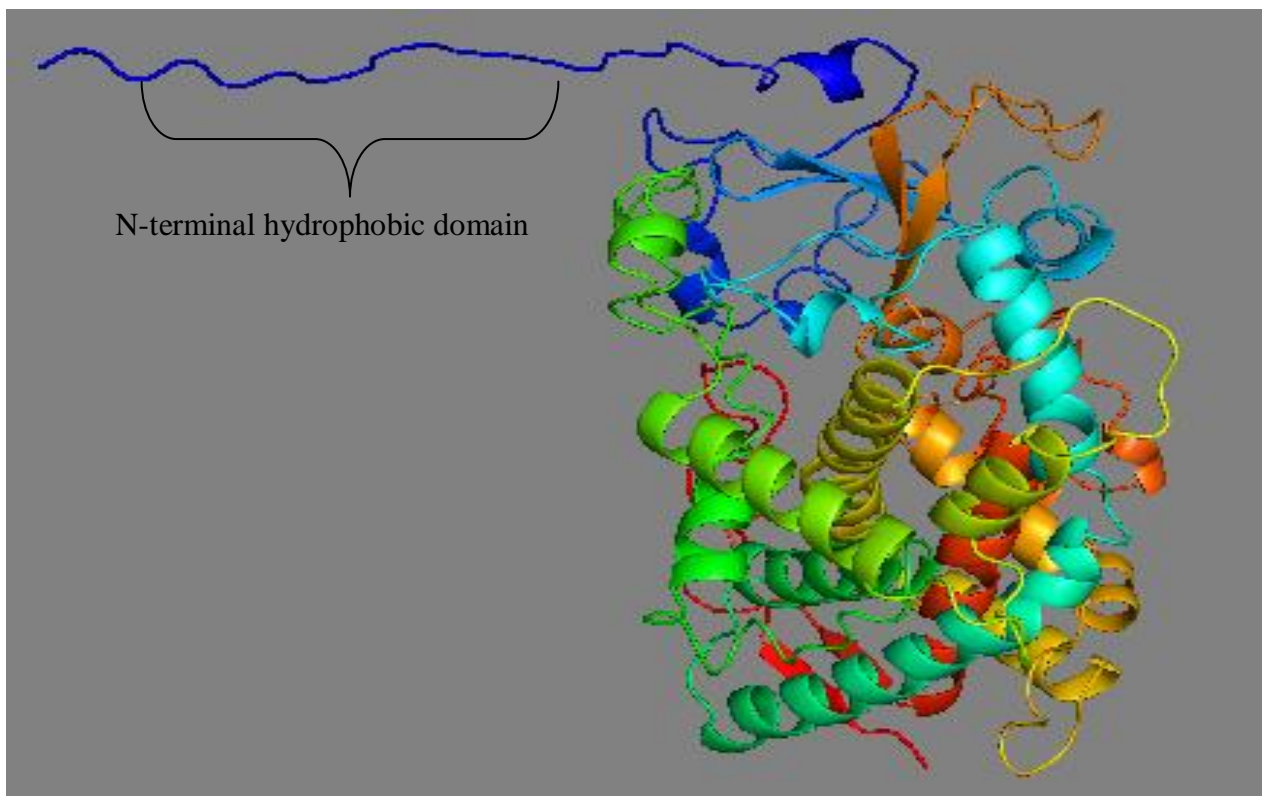


Figure 4.6: Homology model of CYP6Z2 showing the three dimensional structure of the full length CYP6Z2. The N-terminal hydrophobic domain truncated is the extended domain in blue.

The three dimensional homology model of CYP6Z2 shown in Figure 4.6 shows the folding pattern and the extending N-terminal domain of the P450. In vivo, microsomal P450s are targeted to the endoplasmic reticulum membrane using this hydrophobic domain (Monier et al., 1988). The region also serves as anchor to the membrane and positions the catalytic domain to face the cytoplasmic side (Chen et al., 1997). The hydrophobic nature of this domain represents a major challenge for expressing and solubilising the protein in the hydrophilic environment of the cytosol of the *E.coli*. Recombinant P450s form large aggregates when expressed in the absence of detergent (Scott et al., 2001). Although most P450s form smaller aggregates when the trans-membrane regions are deleted, but they still form oligomer when purified and monomer is only achieved in the presence of detergent (Scott et al., 2001).

As important as deletion of this domain is for solubility, it also appears to be important in the proper folding of the P450s. Hsu et al, have suggested that the N-Terminal of CYP2C1 may be contributing to the structural requirement for the proper folding and stability of the enzyme (Hsu et al., 1993). However, the truncation and solubilisation of CYP3A4 for crystallographic studies was different. The N-terminal residues 3-23 were deleted and the truncated gene was expressed successfully in DH5 α . No other mutation or modification was made to the truncated CYP3A4 to produce the crystal structure (Yano et al., 2004). These structural studies revealed that CYP3A4 has a unique hydrophobic region the 7 “phenylalanine-cluster” (Williams et al., 2004) and since the hydrophobic effect is one of the key determinants of protein folding (Southall et al., 2002), CYP3A4 may not depend on the N-terminal hydrophobic region to fold properly.

The two hydrophobic N-terminal domain truncations made in this project did not fold properly. This region may be interacting with the remaining part of CYP6Z2 for proper folding of the holoprotein (Hsu et al., 1993).

Chapter 5

5 General discussion and conclusions

5.1 The N-terminal hydrophobic region of insect P450s may be a requirement for structural stability and integrity

The challenges encountered in producing recombinant insect P450 suitable for crystallisation and subsequent X-ray structural analysis may be in large part a consequence of the nature of the N-terminal hydrophobic sequence of these microsomal P450s. Indeed, the function of N-terminal hydrophobic region of some P450s may not just be for targeting the molecule for co-translational insertion into the microsomal membranes by signal recognition particles (Sakaguchi et al., 1984): this region may be essential for proper folding of the enzymes and deletion of part or whole of this domain may affect the enzyme's structural stability (Hsu et al., 1993). Introduction of several positively charged residues after deleting the N-terminal hydrophobic region may increase expression and solubility as carried out in the expression of CYP2B1 (Scott et al., 2001), but the success of this strategy in eliciting proper folding was not elucidated and similar modification on CYP2B6 (Gillam et al., 1994) did not improve the expression levels of this modified isoform over the full length in *E. coli* (Hanna et al., 2000). The addition of the positively charged amino acids after the deletion of the N-terminal in CYP2E1 and CYP2B4 was suggested to improve the solubility of the expressed P450s by altering the subcellular location of CYP2E1 and CYP2B4 to mainly cytosolic (Pernecky et al., 1993, Scott et al., 2001). Therefore, addition of the positively charged amino acids to the N-terminal domain seems to further reduce the attachment of the P450 from interacting with the *E. coli* membrane after deleting the hydrophobic N-terminal domain and not for proper folding of the P450 being expressed.

Human CYP2C2 had been shown to have a spacer sequence domain between the N-terminal signal anchor and the catalytic domain (Chen et al., 1997). This spacer region is glycine-rich region between residues 22-28 and has a proline-rich region between residues 30 to 37 which contains the conserved PPGP sequence (Chen et al., 1997). Proline and glycine in combination, are α -helix breakers found in bends supporting structural folding in proteins (Engelman et al., 1986). The PPGP is well conserved in CYP2B (Scott et al., 2001) and may be contributing to the proper folding of the truncated isoforms.

Table 5.1: Comparisons of the amino acid sequences of the N-terminal hydrophobic domain of CYP2B sub-family with CYP6Z2

CYP	Sequence	P450 Yield (nmol/l)
2B1	<u>MAPS</u> ILL LL LALLVGF LL LLLV RG HPKSRGNF <u>PPGP</u>	20 – 40
2B1 Δ 3-20	<u>MA</u> <u>KKTSSK</u> <u>GKL</u> <u>PPGP</u>	800 – 1000
2B4	<u>MALLLAVLLA</u> FLAG LL LL LL FRGHPKAHGRL <u>PPGP</u>	30 - 40
2B4 Δ 3-20	<u>MA</u> <u>KKTSSK</u> <u>GKL</u> <u>PPGP</u>	200 – 400
2B6	<u>MALLLAVRL</u> LALLTGL LL LLLVQRHPNTHDRL <u>PPGP</u>	<1
2B6 Δ 3-20	<u>MA</u> <u>KKTSSK</u> <u>GKL</u> <u>PPGP</u>	50 – 100
2B11	<u>MALLLAVLL</u> LALLTGL LL LLMARGHPKAYGHL <u>PPGP</u>	100
2B11 Δ 3-20	<u>MA</u> <u>KKTSSK</u> <u>GKL</u> <u>PPGP</u>	300 – 600
6Z2	<u>MA</u> VYTLALVA AV IFLVLRYIYSHWERHGLPHLKP	598
6Z2 Δ 3-13	<u>MA</u> FLVLRYIYSHWERHGLPHLKP	0
6Z2 Δ 3-25	<u>MA</u> RHGLPHLKP	0

The amino acid modifications in the isoforms are underlined. Δ represents the truncated isoforms and the spaces in the sequences show the amino acids deleted. The yields for CYP2B were from (Scott et al., 2001). The conserved PPGP in the CYP2B is absent in CYP6Z2.

The truncations created in CYP6Z2 in this project were without the addition of the positively charged amino acids (Table 5.1) just as it was created in CYP3A4. CYP3A4 formed holoprotein when this domain was deleted without any other modifications. The main challenge faced in expression of CYP3A4 was the need for detergent for solubility. The solubility issue was however resolved by using CHAPS to release the expressed truncated P450 from the membrane and then substitute the detergent with CYMAL6, a mild detergent, and erythromycin during purification steps. CYMAL6 was eventually removed in the buffer used in concentrating the protein for crystallisation (Yano et al., 2004).

Although the two truncated N-terminal CYP6Z2 created did not produce properly folded P450, the set aim of establishing expression and purification techniques for the full length was however achieved. The protocols yielded 598 nmol/l of the full length 5xHis-tagged CYP6Z2.

5.2 Site directed mutagenesis of amino acid residues at the active sites of CYP6Z2 and CYP6P3 predicted to be involved in metabolic activity, by *in silico* modelling.

Homology modelling has some limitations as a purely predictive method (Szklarz et al., 1995) but its importance in the investigation of structure function of difficult proteins that are tough to crystallise cannot be over emphasised. Homology models of CYP6Z2, CP6D1 and CYP6P3, created using CYP3A4 as template (McLaughlin et al., 2008), made it possible for the amino acid residues at the active sites of the pyrethroid insecticides metabolisers to be compared with CYP6Z2. Deltamethrin, permethrin and cypermethin docked in the active sites of the models revealed the amino acid residues that may be interacting with the substrates. Most importantly, the orientation of the substrate and proximity to the haem iron could be evaluated. The composition of the amino acids at the active site of CYP6Z2 close to the substrates and the haem iron lack leucine and asparagines in positions 212 and 210 respectively when compared with the active site of CYP6D1. CYP6Z2 has phenylalanine and arginine instead. The positively charged amino acid replaced asparagine at position 210 in the SRS1 site and is predicted to be a point of protein-ligand hydrogen bond in the docking of permethrin (McLaughlin et al., 2008). The arrangement of the amino acids in CYP6P3 compared with CYP6Z2 differs in three positions: tyrosine (102), phenylalanine (212) and arginine (210): these were replaced with phenylalanine (110), leucine (216) and asparagine (210) respectively in CYP6P3.

The mutations at F212, Y102 and R210 revealed that these residues are involved in the metabolic activities of CYP6Z2. The metabolic roles of these positions were further supported with the swapping of the amino acids composition of CYP6Z2 in CYP6P3. The mutants CYP6P3 (F110Y) and CYP6P3 (L216F) acquired significantly increased metabolic activities. Changing the long chain hydrophobic side chain to aromatic ring in L216F caused an increase in the thermostability of the mutant by 10°C when compared with the wild type. The unique clustering of aromatic residues running down one side of the structure of CYP119, a

thermophilic P450, was suggested to be the structural basis for its thermostability (Poulos and Johnson, 2005). CYP119 can withstand temperature up to 90°C (McLean et al., 1998) and mutations of one of the aromatic residues reduced this melting temperature by 10 °C (Park et al., 2002). It appears that the L216F substitution confers enhanced structural stability and it also (in turn) increases the rate of insecticide metabolism of this mutant.

Identifications of these amino acid residues were made possible through homology modelling of the P450s examined in this thesis. Homology modelling has therefore proved to be a useful tool in the studies of structure-function of enzymes in the absence of crystal structures.

5.3 The role of cytochrome b_5 in P450 metabolism depends on both the substrates and the P450 enzymes

Cytochrome b_5 plays a pleiotropic function in P450 related metabolic activities (Schenkman and Jansson, 1999). It has been suggested that such a requirement for cytochrome b_5 in P450 reaction is dependent upon both the substrate being oxidised and the nature of the oxidising enzyme (Kuwahara and Omura, 1980). The presence of b_5 did not detectably alter the activities of CYP6Z2 and CYP6Z3 with resorufin probes; however their activities with the DEF probe were increased by 3.5-fold and 1.8-fold respectively upon the addition of b_5 . Whereas addition of b_5 in CYP6P3 reduced its activity with BR by 2.4-fold but increased its activity with DEF by 7.4-fold. Therefore, b_5 increased the activities of all the three enzymes with DEF, reduced the activities of only CYP6P3 with resorufin probes and seems to have no effect with the activities of both CYP6Z2 and CYP6Z3 with resorufin probes.

The positive effect of b_5 in the activities of CYP6Z2 and CYP6Z3 with the DEF probe and the insensitivity exhibited with resorufin probes may be due to the differences in the reaction mechanism required to produce the fluorescent moiety for detection in the two classes of probes (Figure 5.1 & 5.2).

Resorufin derivative probes require only one dealkylation reaction step to release the resorufin for detection and quantification:

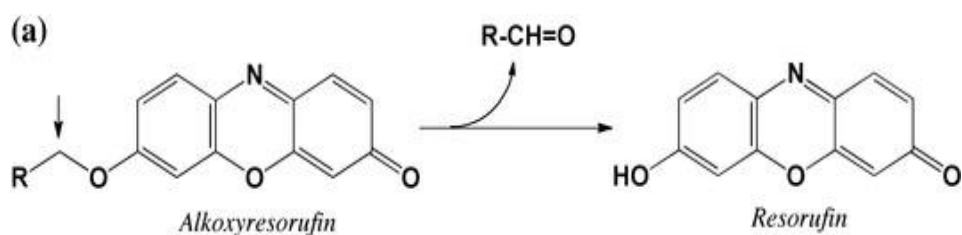


Figure 5.1: One step dealkylation reaction of P450 against resorufin derivative probes.

However, fluorescein derivative probes require two dealkylation reaction steps and formation of an intermediate to release the fluorescein for detection and quantification.

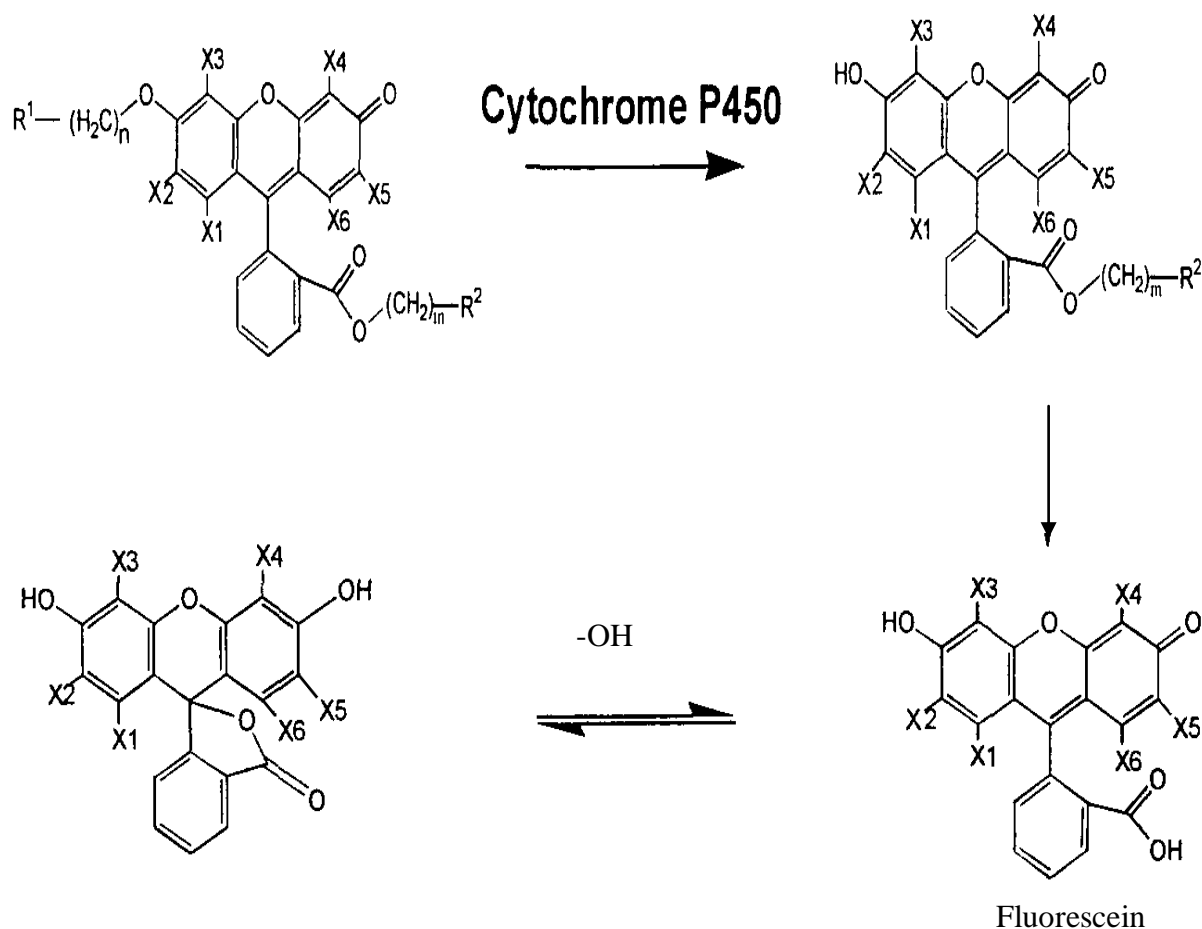


Figure 5.2: Two-step dealkylation reaction of P450 against fluorescein derivative probes

Cytochrome b_5 has been proposed to complex with P450 and allow two-electron transfer during a single interaction with reductase (Schenkman and Jansson, 2003). This would improve the rate of formation of compound 1 and increase reaction activities which may be required in substrates like DEF. The same complex may be formed with the resorufin probes but the effect may not be having significant impact because of the one-step reaction rate.

5.4 Phenylalanine residue 4.0 Å to porphyrin may be involved in stabilising coupling of the oxygen on the haem iron.

Porphyrin plays a major role in donating an electron for oxygen bond cleavage bound to the haem for the activated oxygen of compound 1 to be formed (Goh and Nam, 1999, Stillman, 2000). The proximity of phenylalanine residues close to the porphyrin of the P450s as shown in Table 5.2 suggests they may be engaged in π - π interactions with the porphyrin ring, and contribute to the electrons being supplied for the formation of the activated oxygen.

This possibility was established with the mutation of the phenylalanine to other amino acid residues on CYP6Z2. The mutants, F115L, F115W, F115Y and F115A, produced properly folded P450s but only F115A had sufficient activity to dealkylate BR. Both F115W and F115Y have aromatic rings but the presence of oxygen in tyrosine and the nitrogen in the indole of tryptophan, also electron withdrawing groups, will affect the flow of the π electrons in their aromatic ring. Leucine in F115L has no π electron to contribute except for its long hydrophobic chain which could be involved in steric interaction with the haem. F115A has no π electron, no charge and no steric interaction to contribute or withdraw. This may be the reason why it was able to retain some level of metabolic activity but less stable P450 structure.

Significant loss of activity observed in CYP6Z3 when it was mutated to F115A also suggested that mutations of any of the phenylalanine in Table 5.2 or any that is 4Å close to the porphyrin in P450 may be involved in the stability of the coupling of the activated oxygen to the haem. The mutations created to understand the role of F120 in CYP2D6 were similar to the ones created on CYP6Z2 in this project. F120A, F120L, F120H and F120S were all active against dextromethorphan and bufuralol (Flanagan et al., 2004). However, F120 is 8.2Å (Table 5.2) away from the haem. Therefore, depletion of the aromatic ring did not affect the activity of the

enzyme. The aromatic ring close to the porphyrin that may have effect on the π - π interactions is F436, which is 4.1Å away from the haem and may be the phenylalanine stabilising the activated oxygen in CYP2D6. The ability of F212L to retain its metabolic activity after the replacement of the aromatic ring as seen in chapter 2 of this thesis supports the assumption that only the phenylalanine close to the porphyrin may be contributing to the π - π interactions.

Table 5.2: Predicted phenylalanine in some P450s and their closeness to the porphyrin of the haem.

CYP	Phe position	Distance to porphyrin
6Z1	115	4.0Å
6Z2	115	4.1Å
6Z3	115	4.0Å
6P3	123	4.1Å
6M2	124	4.3Å
2D6	436	4.1Å
2D6	120	8.2Å
6Z2	212	27Å

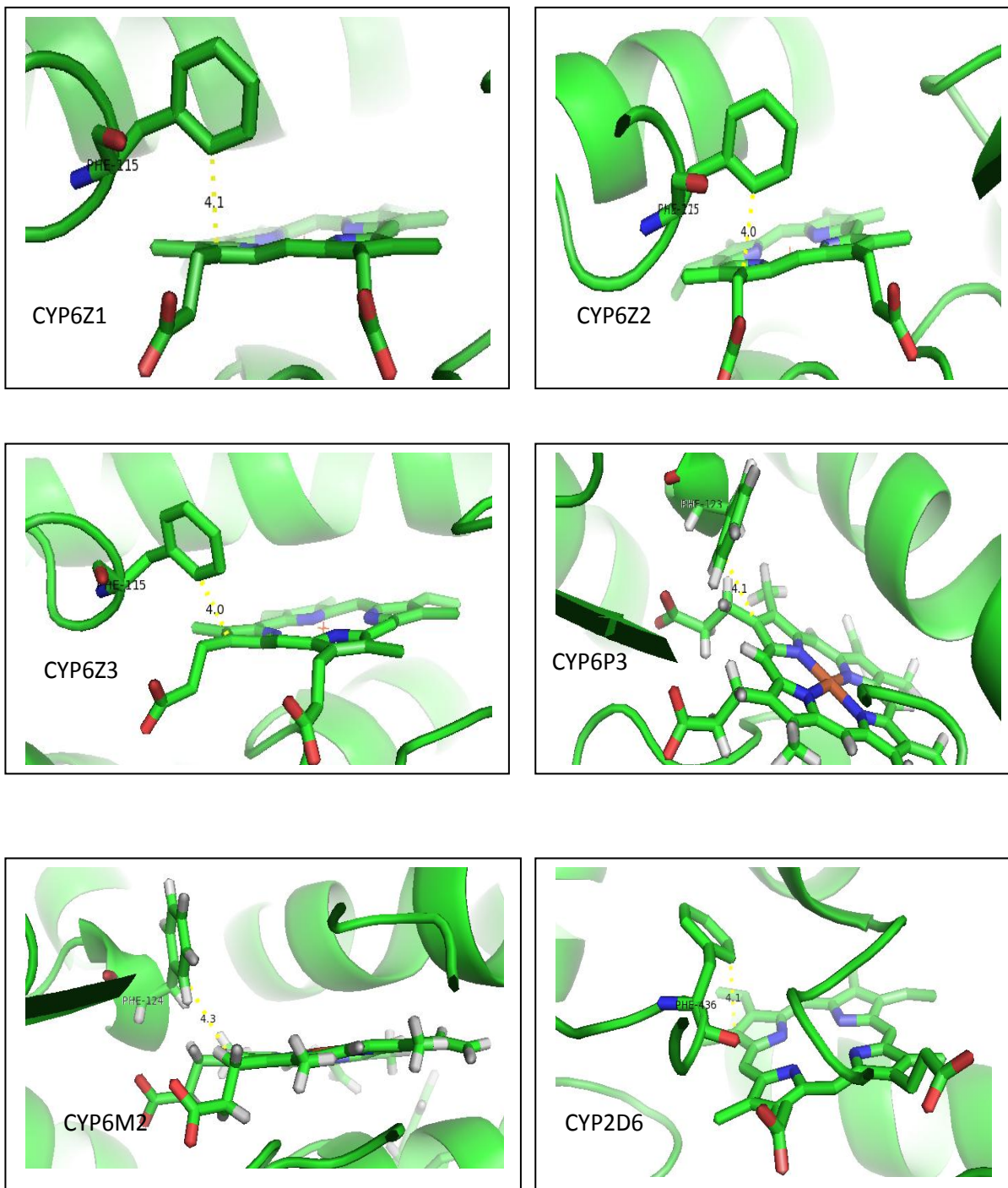


Figure 5.3: Predicted phenylalanine that may be involved in π - π interactions with the porphyrin of the haem in CYP6Z1, CYP6Z2, CYP6Z3, CYP6P3, CYP6M2 and CYP2D6.

5.5 CYP6Z3 has higher metabolic activity than CYP6Z2

Comparative kinetics reveal that CYP6Z3 exhibits greater catalytic efficiency with equivalent substrates compared with the isoform CYP6Z2 and may therefore represent a threat to any malaria control program, because its metabolic activity against pyrethroid insecticides was higher than CYP6Z2, as confirmed in this study. This study also discovered the unique metabolic activity of CYP6Z3 against pyriproxyfen, a pyridine-based pesticides effective against various arthropoda, which prevent larvae from developing into adulthood (Ishaaya and Horowitz, 1995) and this could prove as a marker in pyriproxyfen resistance vectors.

5.6 Conclusions

The results in this thesis have shown that *in silico* studies of homology models of enzymes can be used to investigate structure-function especially when their three-dimensional structures have not been determined.

The amino acids at the three positions examined in CYP6Z2 and CYP6P3 are important in the activities of the P450s. The introduction of phenylalanine increased activity and changing of phenylalanine, 4Å to the heam, may inactivate the activities of P450s.

This information will be useful in quick identification of resistant mosquitoes in single nucleotide polymorphism (SNP) mapping carried out in the field, and in the design of new insecticides to eradicate malaria disease in the future.

Increased thermostability coupled with increase in rate of reaction are important to the industrial applications of P450s and a single nucleotide change, as seen in this study, could achieve both.

5.7 Recommendations

The current absence of a crystal structure of an insect P450 represents a major omission from the arsenal of knowledge required to understand and potentially manipulate insecticide resistance activities with respect to P450 for these disease vectors. The effort made in this study to produce a soluble, properly folded P450 has demonstrated that the N-terminal hydrophobic residues of insect P450s remain a barrier to facilitating the proper folding of heterologously expressed enzyme in all hosts tested, here and by others. However, since this study has been able to establish the expression and purification methods yielding authentically folded full length CYP6Z2; confirming the aggregation state of the purified protein will be of great value. Investigation of the purified full length enzyme with size exclusion chromatography will reveal the concentrations of detergent needed to have a monomer that could be used in high-throughput crystallization screens.

The three amino acid residues targeted in this study, are involved in the metabolic activities of CYP6Z2. Two mutations, R210A and Y102F have shown a tendency to increase cellular metabolism in respect of deltamethrin. The substitution of phenylalanine for tyrosine in CYP6P3 reduced its metabolic activity, indicating the effect of the hydroxyl group at this position. Moreover, the absence of the positively charged arginine at the active sites of both CYP6P3 and CYP6D1 suggests the impact that this side chain may have in reducing the metabolic activity associated with CYP6Z2. It would be interesting to combine these two mutations (CYP6Z2 (Y102L_R210A)) and verify if the metabolic activity against pyrethroid insecticides would improve.

Establishing the exact point in the P450 kinetic cycle where the impact of the loss of activities of mutants CYP6Z2 (F115L), F115Y and F115W, is an important next objective. The presence

of superoxide or hydrogen peroxide will indicate where on the catalytic steps the uncoupling of the oxygen is occurring.

The importance of the aromatic ring, and its close proximity to the haem as predicted in Table 5.2 should be investigated further. It may hold the key to turning off the activities of P450s.

CYP6Z3 indicated its ability to metabolise pyrethroids and importantly have stronger activity against pyriproxyfen. These metabolic activities were established by comparing the amount of substrate left in the NADPH plus and NADPH minus depletion reactions. The use of HPLC analysis combined with Mass Spectrometry analysis would further improve the knowledge of the metabolic activities of these P450 enzymes especially with assays where both the substrates and the metabolites cannot be simultaneously detected with HPLC alone.

CYP6Z2 and CYP6Z3 both have similar amino acids sequences at SRS 1, SRS 4 and SRS 5. The differences in amino acids are in SRS 2, SRS 3 and SRS 6. SRS 2 and SRS 3 are involved with substrates access channel while SRS 6 is involved with catalytic activity.

SRS 2

CYP6Z2 - N R G R N F I
CYP6Z3 - I K S R K F M

SRS 3

CYP6Z2 - M T S L Q P E L
CYP6Z3 - I T S L P P E L

SRS 6

CYP6Z2 - A A T V G L T
CYP6Z3 - V A T V V V T

The megaprimer mutation method could be used to create chimera of CYP6Z2 having these SRSs substituted for that of CYP6Z3. The chimera that gives similar activity as CYP6Z3 will reveal the SRS(s) responsible for the higher activities observed in CYP6Z3.

Chimera of CYP6Z3 on CYP6Z1 could also be created as well using the megaprimer method.

We may be able to get CYP6Z3 to metabolise DDT since CYP6Z1 does.

References

- Agnandji, S. T., Lell, B., Soulanoudjingar, S. S., Fernandes, J. F., Abossolo, B. P., Conzelmann, C., Methogo, B., Doucka, Y., Flamen, A. & Mordmüller, B. 2011. First results of phase 3 trial of RTS, S/AS01 malaria vaccine in African children. *The New England journal of medicine*, 365, 1863-75.
- Agosin, M. 1985. Role of microsomal oxidations in insecticide degradation. *Comprehensive insect physiology, biochemistry and pharmacology*, 12, 647-712.
- Alexia, C.-P., Jaclyn, B., Myriam, R.-K., Jessica, R., Emilie, G.-C., Rodolphe, P., Muhammad, A. R., Mark, P., Chantal, D.-V. & Stephane, R. 2013. The central role of mosquito cytochrome P450 CYP6Zs in insecticide detoxification revealed by functional expression and structural modelling. *Biochemical Journal*, 455, 75-85.
- Anand, S. S., Bruckner, J. V., Haines, W. T., Muralidhara, S., Fisher, J. W. & Padilla, S. 2006. Characterization of deltamethrin metabolism by rat plasma and liver microsomes. *Toxicology and applied pharmacology*, 212, 156-166.
- Arensburger, P., Megy, K., Waterhouse, R. M., Abrudan, J., Amedeo, P., Antelo, B., Bartholomay, L., Bidwell, S., Caler, E. & Camara, F. 2010. Sequencing of *Culex quinquefasciatus* establishes a platform for mosquito comparative genomics. *Science*, 330, 86-88.
- Atieli, F. K., Munga, S. O., Ofulla, A. V. & Vulule, J. M. 2010. The effect of repeated washing of long-lasting insecticide-treated nets (LLINs) on the feeding success and survival rates of *Anopheles gambiae*. *Malar J*, 9, 29.
- Bale, J., Van Lenteren, J. & Bigler, F. 2008. Biological control and sustainable food production. *Philosophical Transactions of the Royal Society B: Biological Sciences*, 363, 761-776.

- Bassat, Q., Guinovart, C., Sigaúque, B., Aide, P., Sacarlal, J., Nhampossa, T., Bardají, A., Nhacolo, A., Macete, E. & Mandomando, I. 2008. Malaria in rural Mozambique. Part II: children admitted to hospital. *Malaria journal*, 7, 37.
- Berka, K., Hendrychová, T., Anzenbacher, P. & Otyepka, M. 2011. Membrane position of ibuprofen agrees with suggested access path entrance to cytochrome P450 2C9 active site. *The journal of physical chemistry A*, 115, 11248-11255.
- Black, S. D., French, J. S., Williams, C. H. & Coon, M. J. 1979. Role of a hydrophobic polypeptide in the N-terminal region of NADPH-cytochrome P-450 reductase in complex formation with P-450LM. *Biochemical and biophysical research communications*, 91, 1528-1535.
- Bonfils, C., Balny, C. & Maurel, P. 1981. Direct evidence for electron transfer from ferrous cytochrome b5 to the oxyferrous intermediate of liver microsomal cytochrome P-450 LM2. *Journal of biological chemistry*, 256, 9457-9465.
- Boonsuepsakul, S., Luepromchai, E. & Rongnoparut, P. 2008. Characterization of Anopheles minimus CYP6AA3 expressed in a recombinant baculovirus system. *Archives of insect biochemistry and physiology*, 69, 13-21.
- Bordo, D. & Argos, P. 1991. Suggestions for “safe” residue substitutions in site-directed mutagenesis. *Journal of molecular biology*, 217, 721-729.
- Bradford, M. M. 1976. A rapid and sensitive method for the quantitation of microgram quantities of protein utilizing the principle of protein-dye binding. *Analytical biochemistry*, 72, 248-254.
- Brash, A. R. 2009. Mechanistic aspects of CYP74 allene oxide synthases and related cytochrome P450 enzymes. *Phytochemistry*, 70, 1522-1531.

- Caraballo, H. & King, K. 2014. Emergency department management of mosquito-borne illness: malaria, dengue, and West Nile virus. *Emergency medicine practice*, 16, 1-23; quiz 23-4.
- Chapman, A. D. 2009. Numbers of living species in Australia and the world.
- Chen, C.-D., Doray, B. & Kemper, B. 1997. Efficient assembly of functional cytochrome P450 2C2 requires a spacer sequence between the N-terminal signal anchor and catalytic domains. *Journal of Biological Chemistry*, 272, 22891-22897.
- Chiu, T.-L., Wen, Z., Rupasinghe, S. G. & Schuler, M. A. 2008. Comparative molecular modeling of *Anopheles gambiae* CYP6Z1, a mosquito P450 capable of metabolizing DDT. *Proceedings of the National Academy of Sciences*, 105, 8855-8860.
- Chothia, C. & Lesk, A. M. 1986. The relation between the divergence of sequence and structure in proteins. *The EMBO journal*, 5, 823.
- Chothia, C. & Lesk, A. M. 1987. Canonical structures for the hypervariable regions of immunoglobulins. *Journal of molecular biology*, 196, 901-917.
- Coetzee, M., Horne, D., Brooke, B. & Hunt, R. 1999. DDT, dieldrin and pyrethroid insecticide resistance in african malaria vector mosquitoes: An historical review and implications for future malaria control in southern africa. *South African Journal of Science*, 95, 215-218.
- Collins, W. E. 2012. *Plasmodium knowlesi*: A Malaria Parasite of Monkeys and Humans*. *Annual review of entomology*, 57, 107-121.
- Connell, D., Lam, P., Richardson, B. & Wu, R. Introduction to Ecotoxicology, 1999. Blackwell Science Ltd, Oxford.
- Correia, M. A. & Mannering, G. 1973. Reduced Diphosphopyridine Nucleotide Synergism of the Reduced Triphosphopyridine Nucleotide-Dependent Mixed-Function Oxidase

- System of Hepatic Microsomes I. Effects of Activation and Inhibition of the Fatty Acyl Coenzyme A Desaturation System. *Molecular pharmacology*, 9, 455-469.
- Cosme, J. & Johnson, E. F. 2000. Engineering microsomal cytochrome P450 2C5 to be a soluble, monomeric enzyme mutations that alter aggregation, phospholipid dependence of catalysis, and membrane binding. *Journal of Biological Chemistry*, 275, 2545-2553.
- Daborn, P., Yen, J., Bogwitz, M., Le Goff, G., Feil, E., Jeffers, S., Tijet, N., Perry, T., Heckel, D. & Batterham, P. 2002. A single P450 allele associated with insecticide resistance in *Drosophila*. *Science*, 297, 2253-2256.
- David, J.-P., Ismail, H. M., Chandor-Proust, A. & Paine, M. J. I. 2013. Role of cytochrome P450s in insecticide resistance: impact on the control of mosquito-borne diseases and use of insecticides on Earth. *Philosophical Transactions of the Royal Society B: Biological Sciences*, 368, 20120429.
- David, J.-P., Strode, C., Vontas, J., Nikou, D., Vaughan, A., Pignatelli, P. M., Louis, C., Hemingway, J. & Ranson, H. 2005. The *Anopheles gambiae* detoxification chip: a highly specific microarray to study metabolic-based insecticide resistance in malaria vectors. *Proceedings of the National Academy of Sciences of the United States of America*, 102, 4080-4084.
- Dawson, J., Holm, R., Trudell, J., Barth, G., Linder, R., Bunnenberg, E., Djerassi, C. & Tang, S. 1976. Letter: Oxidized cytochrome P-450. Magnetic circular dichroism evidence for thiolate ligation in the substrate-bound form. Implications for the catalytic mechanism. *Journal of the American Chemical Society*, 98, 3707.
- Denisov, I. G., Makris, T. M., Sligar, S. G. & Schlichting, I. 2005. Structure and chemistry of cytochrome P450. *Chemical reviews*, 105, 2253-2278.

- Djimdé, A., Doumbo, O. K., Cortese, J. F., Kayentao, K., Doumbo, S., Diourté, Y., Coulibaly, D., Dicko, A., Su, X.-Z. & Nomura, T. 2001. A molecular marker for chloroquine-resistant falciparum malaria. *New England journal of medicine*, 344, 257-263.
- Djouaka, R. F., Bakare, A. A., Coulibaly, O. N., Akogbeto, M. C., Ranson, H., Hemingway, J. & Strode, C. 2008. Expression of the cytochrome P450s, CYP6P3 and CYP6M2 are significantly elevated in multiple pyrethroid resistant populations of *Anopheles gambiae* ss from Southern Benin and Nigeria. *BMC genomics*, 9, 538.
- Dolphin, D., Traylor, T. G. & Xie, L. Y. 1997. Polyhaloporphyrins: unusual ligands for metals and metal-catalyzed oxidations. *Accounts of chemical research*, 30, 251-259.
- Dondorp, A. M., Yeung, S., White, L., Nguon, C., Day, N. P., Socheat, D. & Von Seidlein, L. 2010. Artemisinin resistance: current status and scenarios for containment. *Nature Reviews Microbiology*, 8, 272-280.
- Donnelly, M. J., Corbel, V., Weetman, D., Wilding, C. S., Williamson, M. S. & Black Iv, W. C. 2009. Does kdr genotype predict insecticide-resistance phenotype in mosquitoes? *Trends in parasitology*, 25, 213-219.
- Duangkaew, P., Pethuan, S., Kaewpa, D., Boonsuepsakul, S., Sarapusit, S. & Rongnoparut, P. 2011. Characterization of mosquito CYP6P7 and CYP6AA3: differences in substrate preference and kinetic properties. *Archives of insect biochemistry and physiology*, 76, 236-248.
- Dunlap, T. R. 1981. DDT: Science, Citizens, and Public Policy. Princeton: Princeton University Press. viii.
- Engelman, D., Steitz, T. & Goldman, A. 1986. Identifying nonpolar transbilayer helices in amino acid sequences of membrane proteins. *Annual review of biophysics and biophysical chemistry*, 15, 321-353.

- Enoch, H. & Strittmatter, P. 1979. Cytochrome b5 reduction by NADPH-cytochrome P-450 reductase. *Journal of Biological Chemistry*, 254, 8976-8981.
- Epstein, C. J., Goldberger, R. F. & Anfinsen, C. B. The genetic control of tertiary protein structure: studies with model systems. Cold Spring Harbor symposia on quantitative biology, 1963. Cold Spring Harbor Laboratory Press, 439-449.
- Estabrook, R. W. 1996. I Serial Reviews I.
- Faber, K. & Johnson, C. 1996. Biotransformations in Organic Chemistry. *Synthesis-Journal of Synthetic Organic Chemistry*, 791.
- Fantuzzi, A., Fairhead, M. & Gilardi, G. 2004. Direct electrochemistry of immobilized human cytochrome P450 2E1. *Journal of the American Chemical Society*, 126, 5040-5041.
- Feyereisen, R. 1999. Insect P450 enzymes. *Annual review of entomology*, 44, 507-533.
- Feyereisen, R., Koener, J., Carino, F. & Daggett, A. 1990. Biochemistry and molecular biology of insect cytochrome P450. *Molecular Insect Science*. Springer.
- Feyereisen, R., Koener, J. F., Farnsworth, D. E. & Nebert, D. W. 1989. Isolation and sequence of cDNA encoding a cytochrome P-450 from an insecticide-resistant strain of the house fly, *Musca domestica*. *Proceedings of the National Academy of Sciences*, 86, 1465-1469.
- Flanagan, J., Marechal, J., Ward, R., Kemp, C., Mclaughlin, L., Sutcliffe, M., Roberts, G., Paine, M. & Wolf, C. 2004. Phe120 contributes to the regiospecificity of cytochrome P450 2D6: mutation leads to the formation of a novel dextromethorphan metabolite. *Biochem. J*, 380, 353-360.
- Gilbert, L. I., Iatrou, K. & Gill, S. S. 2005. Comprehensive molecular insect science.
- Gillam, E. M., Guo, Z. & Guengerich, F. P. 1994. Expression of Modified Human Cytochrome P450 2E1 in *Escherichia coli*, Purification, and Spectral and Catalytic Properties. *Archives of biochemistry and biophysics*, 312, 59-66.

- Glawischnig, E., Grün, S., Frey, M. & Gierl, A. 1999. Cytochrome P450 monooxygenases of DIBOA biosynthesis: specificity and conservation among grasses. *Phytochemistry*, 50, 925-930.
- Goh, Y. M. & Nam, W. 1999. Significant electronic effect of porphyrin ligand on the reactivities of high-valent iron (IV) oxo porphyrin cation radical complexes. *Inorganic chemistry*, 38, 914-920.
- Gotoh, O. 1992. Substrate recognition sites in cytochrome P450 family 2 (CYP2) proteins inferred from comparative analyses of amino acid and coding nucleotide sequences. *Journal of Biological Chemistry*, 267, 83-90.
- Greenwood, B. M., Bojang, K., Whitty, C. J. & Targett, G. A. 2005. Malaria. *Lancet*, 365, 1487-98.
- Guengerich, F. P., Martin, M. V., Sohl, C. D. & Cheng, Q. 2009. Measurement of cytochrome P450 and NADPH-cytochrome P450 reductase. *Nature protocols*, 4, 1245-1251.
- Gullan, P. J. & Cranston, P. S. 2009. *The insects: an outline of entomology*, John Wiley & Sons.
- Haines, D. C., Tomchick, D. R., Machius, M. & Peterson, J. A. 2001. Pivotal role of water in the mechanism of P450BM-3. *Biochemistry*, 40, 13456-13465.
- Hammock, B., Kerkut, G. & Gilbert, L. 1985. Comprehensive Insect Physiology, Biochemistry, and Pharmacology. *GA Kerkut and LI Gilbert, Pergamon Press, New York*, 431-472.
- Hanna, I. H., Reed, J. R., Guengerich, F. P. & Hollenberg, P. F. 2000. Expression of Human Cytochrome P450 2B6 in *Escherichia coli*: Characterization of Catalytic Activity and Expression Levels in Human Liver. *Archives of biochemistry and biophysics*, 376, 206-216.

- Hasemann, C. A., Kurumbail, R. G., Boddupalli, S. S., Peterson, J. A. & Deisenhofer, J. 1995. Structure and function of cytochromes P450: a comparative analysis of three crystal structures. *Structure*, 3, 41-62.
- Hayaishi, O., Katagiri, M. & Rothberg, S. 1955. Mechanism of the pyrocatechase reaction. *Journal of the American Chemical Society*, 77, 5450-5451.
- Hayashi, N., Welschhof, M., Zewe, M., Braunagel, M., Dübel, S., Breitling, F. & Little, M. 1994. Simultaneous mutagenesis of antibody CDR regions by overlap extension and PCR. *Biotechniques*, 17, 310, 312, 314-5.
- Hemingway, J. & Ranson, H. 2000. Insecticide resistance in insect vectors of human disease. *Annual review of entomology*, 45, 371-391.
- Holt, R. A., Subramanian, G. M., Halpern, A., Sutton, G. G., Charlab, R., Nusskern, D. R., Wincker, P., Clark, A. G., Ribeiro, J. C. & Wides, R. 2002. The genome sequence of the malaria mosquito *Anopheles gambiae*. *Science*, 298, 129-149.
- Hougard, J.-M., Duchon, S., Darriet, F., Zaim, M., Rogier, C. & Guillet, P. 2003. Comparative performances, under laboratory conditions, of seven pyrethroid insecticides used for impregnation of mosquito nets. *Bulletin of the World Health Organization*, 81, 324-333.
- Hsu, L., Hu, M.-C., Cheng, H.-C., Lu, J.-C. & Chung, B. 1993. The N-terminal hydrophobic domain of P450c21 is required for membrane insertion and enzyme stability. *Journal of Biological Chemistry*, 268, 14682-14686.
- Ishaaya, I. & Horowitz, A. R. 1995. Pyriproxyfen, a novel insect growth regulator for controlling whiteflies: mechanisms and resistance management. *Pesticide Science*, 43, 227-232.
- Isin, E. M. & Guengerich, F. P. 2007. Complex reactions catalyzed by cytochrome P450 enzymes. *Biochimica et Biophysica Acta (BBA)-General Subjects*, 1770, 314-329.

- Johnson, M. S., Srinivasan, N., Sowdhamini, R. & Blundell, T. L. 1994. Knowledge-based protein modeling. *Crit Rev Biochem Mol Biol*, 29, 1-68.
- Jones, R. T., Bakker, S. E., Stone, D., Shuttleworth, S. N., Boundy, S., McCart, C., Daborn, P. J. & Van Den Elsen, J. M. 2010. Homology modelling of Drosophila cytochrome P450 enzymes associated with insecticide resistance. *Pest management science*, 66, 1106-1115.
- Joo, H., Lin, Z. & Arnold, F. H. 1999. Laboratory evolution of peroxide-mediated cytochrome P450 hydroxylation. *Nature*, 399, 670-673.
- Karunker, I., Morou, E., Nikou, D., Nauen, R., Sertchook, R., Stevenson, B. J., Paine, M. J., Morin, S. & Vontas, J. 2009. Structural model and functional characterization of the Bemisia tabaci CYP6CM1vQ, a cytochrome P450 associated with high levels of imidacloprid resistance. *Insect biochemistry and molecular biology*, 39, 697-706.
- Kempf, A. C., Zanger, U. M. & Meyer, U. A. 1995. Truncated Human P450 2D6P: Expression in Escherichia coli, Ni²⁺-Chelate Affinity Purification, and Characterization of Solubility and Aggregation. *Archives of biochemistry and biophysics*, 321, 277-288.
- Klein, E. 2013. Antimalarial drug resistance: a review of the biology and strategies to delay emergence and spread. *International journal of antimicrobial agents*, 41, 311-317.
- Klingenberg, M. 1958. Pigments of rat liver microsomes. *Archives of biochemistry and biophysics*, 75, 376-386.
- Krieger, E., Darden, T., Nabuurs, S. B., Finkelstein, A. & Vriend, G. 2004. Making optimal use of empirical energy functions: Force-field parameterization in crystal space. *Proteins: Structure, Function, and Bioinformatics*, 57, 678-683.
- Krieger, E., Nabuurs, S. B. & Vriend, G. 2003. Homology modeling. *Methods of biochemical analysis*, 44, 509-524.

- Kusano, K., Waterman, M. R., Sakaguchi, M., Omura, T. & Kagawa, N. 1999. Protein Synthesis Inhibitors and Ethanol Selectively Enhance Heterologous Expression of P450s and Related Proteins in *Escherichia coli*. *Archives of biochemistry and biophysics*, 367, 129-136.
- Kuwahara, S.-I. & Omura, T. 1980. Different requirement for cytochrome *b*₅ in NADPH-supported O-deethylation of p-nitrophenetole catalyzed by two types of microsomal cytochrome P-450. *Biochemical and biophysical research communications*, 96, 1562-1568.
- Lertkiatmongkol, P., Jenwitheesuk, E. & Rongnoparut, P. 2011. Homology modeling of mosquito cytochrome P450 enzymes involved in pyrethroid metabolism: insights into differences in substrate selectivity. *BMC research notes*, 4, 321.
- Li, Y. C. & Chiang, J. 1991. The expression of a catalytically active cholesterol 7 alpha-hydroxylase cytochrome P450 in *Escherichia coli*. *Journal of Biological Chemistry*, 266, 19186-19191.
- Ling, M. M. & Robinson, B. H. 1997. Approaches to DNA mutagenesis: an overview. *Analytical biochemistry*, 254, 157-178.
- Lipscomb, J. D., Sligar, S., Namtvedt, M. & Gunsalus, I. 1976. Autooxidation and hydroxylation reactions of oxygenated cytochrome P-450cam. *Journal of Biological Chemistry*, 251, 1116-1124.
- Losey, J. E. & Vaughan, M. 2006. The economic value of ecological services provided by insects. *Bioscience*, 56, 311-323.
- Lu, G., Lindqvist, Y., Schneider, G., Dwivedi, U. & Campbell, W. 1995. Structural Studies on Corn Nitrate Reductase: Refined Structure of the Cytochrome *b*₅ Reductase Fragment at 2.5 Å, its ADP Complex and an Active-site Mutant and Modeling of the Cytochrome *b*₅ Domain. *Journal of molecular biology*, 248, 931-948.

- Martin, J. & Fay, M. 2001. Cytochrome P450 drug interactions: are they clinically relevant? *Australian Prescriber*, 24, 10-12.
- Mclaughlin, L., Niazi, U., Bibby, J., David, J. P., Vontas, J., Hemingway, J., Ranson, H., Sutcliffe, M. & Paine, M. 2008. Characterization of inhibitors and substrates of *Anopheles gambiae* CYP6Z2. *Insect molecular biology*, 17, 125-135.
- Mclean, M. A., Maves, S. A., Weiss, K. E., Krepich, S. & Sligar, S. G. 1998. Characterization of a Cytochrome P450 from the Acidothermophilic Archaea *Sulfolobus solfataricus*. *Biochemical and biophysical research communications*, 252, 166-172.
- Modi, S., Paine, M., Sutcliffe, M., Lian, L.-Y., Primrose, W., Wolf, C. & Roberts, G. 1996. A model for human cytochrome P450 2D6 based on homology modeling and NMR studies of substrate binding. *Biochemistry*, 35, 4540-4550.
- Momenteau, M. & Reed, C. A. 1994. Synthetic heme-dioxygen complexes. *Chemical reviews*, 94, 659-698.
- Monier, S., Van Luc, P., Kreibich, G., Sabatini, D. & Adesnik, M. 1988. Signals for the incorporation and orientation of cytochrome P450 in the endoplasmic reticulum membrane. *The Journal of cell biology*, 107, 457-470.
- Mueller, I., Zimmerman, P. A. & Reeder, J. C. 2007. *Plasmodium malariae* and *Plasmodium ovale*—the ‘bashful’ malaria parasites. *Trends in parasitology*, 23, 278-283.
- Müller, P., Donnelly, M. J. & Ranson, H. 2007. Transcription profiling of a recently colonised pyrethroid resistant *Anopheles gambiae* strain from Ghana. *BMC genomics*, 8, 36.
- Müller, P., Warr, E., Stevenson, B. J., Pignatelli, P. M., Morgan, J. C., Steven, A., Yawson, A. E., Mitchell, S. N., Ranson, H. & Hemingway, J. 2008. Field-caught permethrin-resistant *Anopheles gambiae* overexpress CYP6P3, a P450 that metabolises pyrethroids. *PLoS Genetics*, 4, e1000286.

- Munro, A. W., Leys, D. G., Mclean, K. J., Marshall, K. R., Ost, T. W., Daff, S., Miles, C. S., Chapman, S. K., Lysek, D. A. & Moser, C. C. 2002. P450 BM3: the very model of a modern flavocytochrome. *Trends in biochemical sciences*, 27, 250-257.
- Nebert, D. W. & Gonzalez, F. 1987. P450 genes: structure, evolution, and regulation. *Annual review of biochemistry*, 56, 945-993.
- Nelson, D. R. 2009. The cytochrome p450 homepage. *Human genomics*, 4, 59.
- Nene, V., Wortman, J. R., Lawson, D., Haas, B., Kodira, C., Tu, Z. J., Loftus, B., Xi, Z., Megy, K. & Grabherr, M. 2007. Genome sequence of *Aedes aegypti*, a major arbovirus vector. *Science*, 316, 1718-1723.
- Nikou, D., Ranson, H. & Hemingway, J. 2003. An adult-specific CYP6 P450 gene is overexpressed in a pyrethroid-resistant strain of the malaria vector, *Anopheles gambiae*. *Gene*, 318, 91-102.
- Nisimoto, Y. & Lambeth, J. D. 1985. NADPH-cytochromeP450 reductase-cytochrome *b₅* interactions: Crosslinking of the phospholipid vesicle-associated proteins by a water-soluble carbodiimide. *Archives of biochemistry and biophysics*, 241, 386-396.
- Noshiro, M., Harada, N. & Omura, T. 1980. Immunochemical study on the route of electron transfer from NADH and NADPH to cytochrome P-450 of liver microsomes. *Journal of biochemistry*, 88, 1521-1535.
- Omura, T. & Sato, R. 1962. A new cytochrome in liver microsomes. *Journal of Biological Chemistry*, 237, PC1375-PC1376.
- Omura, T. & Sato, R. 1964. The carbon monoxide-binding pigment of liver microsomes. I. Evidence for its hemoprotein nature. *J. biol. Chem*, 239, 2370-2378.
- Paine, M. J., Scrutton, N. S., Munro, A. W., Gutierrez, A., Roberts, G. C. & Wolf, C. R. 2005. Electron transfer partners of cytochrome P450. *Cytochrome P450*. Springer.

- Park, S.-Y., Yamane, K., Adachi, S.-I., Shiro, Y., Weiss, K. E., Maves, S. A. & Sligar, S. G. 2002. Thermophilic cytochrome P450 (CYP119) from *Sulfolobus solfataricus*: high resolution structure and functional properties. *Journal of inorganic biochemistry*, 91, 491-501.
- Pears, F. & Cranshaw, W. 2010. Mosquito Management (Supplement to Fact Sheet 5.526).
- Pernecky, S. J., Larson, J. R., Philpot, R. M. & Coon, M. J. 1993. Expression of truncated forms of liver microsomal P450 cytochromes 2B4 and 2E1 in *Escherichia coli*: influence of NH₂-terminal region on localization in cytosol and membranes. *Proc Natl Acad Sci U S A*, 90, 2651-5.
- Phyo, A. P., Nkhoma, S., Stepniewska, K., Ashley, E. A., Nair, S., Mcgready, R., Ler Moo, C., Al-Saai, S., Dondorp, A. M. & Lwin, K. M. 2012. Emergence of artemisinin-resistant malaria on the western border of Thailand: a longitudinal study. *The Lancet*, 379, 1960-1966.
- Podust, L. M., Poulos, T. L. & Waterman, M. R. 2001. Crystal structure of cytochrome P450 14 α -sterol demethylase (CYP51) from *Mycobacterium tuberculosis* in complex with azole inhibitors. *Proceedings of the National Academy of Sciences*, 98, 3068-3073.
- Poulos, T. L., Finzel, B. C. & Howard, A. J. 1987. High-resolution crystal structure of cytochrome P450cam. *Journal of molecular biology*, 195, 687-700.
- Poulos, T. L. & Johnson, E. F. 2005. Structures of cytochrome P450 enzymes. *Cytochrome P450*. Springer.
- Presnell, S. R. & Cohen, F. E. 1989. Topological distribution of four-alpha-helix bundles. *Proceedings of the National Academy of Sciences*, 86, 6592-6596.
- Price, R. & Nosten, F. 2001. Drug resistant falciparum malaria: clinical consequences and strategies for prevention. *Drug resistance updates*, 4, 187-196.

- Pritchard, M. P., Ossetian, R., Li, D. N., Henderson, C. J., Burchell, B., Wolf, C. R. & Friedberg, T. 1997. A General Strategy for the Expression of Recombinant Human Cytochrome P450s in *Escherichia coli* Using Bacterial Signal Peptides: Expression of CYP3A4, CYP2A6, and CYP2E1. *Archives of biochemistry and biophysics*, 345, 342-354.
- Pyke, F. M., Bogwitz, M. R., Perry, T., Monk, A., Batterham, P. & McKenzie, J. A. 2004. The genetic basis of resistance to diazinon in natural populations of *Drosophila melanogaster*. *Genetica*, 121, 13-24.
- Pylypenko, O. & Schlichting, I. 2004. Structural aspects of ligand binding to and electron transfer in bacterial and fungal P450s. *Annual review of biochemistry*, 73, 991-1018.
- Qian, W., Sun, Y.-L., Wang, Y.-H., Zhuang, J.-H., Xie, Y. & Huang, Z.-X. 1998. The influence of mutation at Glu44 and Glu56 of cytochrome b 5 on the protein's stabilization and interaction between cytochrome c and cytochrome b 5. *Biochemistry*, 37, 14137-14150.
- Raag, R. & Poulos, T. L. 1989. The structural basis for substrate-induced changes in redox potential and spin equilibrium in cytochrome P-450CAM. *Biochemistry*, 28, 917-922.
- Rabhi, I., Guedel, N., Chouk, I., Zerria, K., Barbouche, M. R., Dellagi, K. & Fathallah, D. M. 2004. A novel simple and rapid PCR-based site-directed mutagenesis method. *Molecular biotechnology*, 26, 27-34.
- Ranson, H., Claudianos, C., Orтели, F., Abgrall, C., Hemingway, J., Sharakhova, M. V., Unger, M. F., Collins, F. H. & Feyereisen, R. 2002. Evolution of supergene families associated with insecticide resistance. *Science*, 298, 179-181.
- Ravichandran, K. G., Boddupalli, S. S., Hasermann, C., Peterson, J. A. & Deisenhofer, J. 1993. Crystal structure of hemoprotein domain of P450BM-3, a prototype for microsomal P450's. *Science*, 261, 731-736.

- Rendic, S. & Carlo, F. J. D. 1997. Human cytochrome P450 enzymes: a status report summarizing their reactions, substrates, inducers, and inhibitors. *Drug metabolism reviews*, 29, 413-580.
- Ricoux, R., Raffy, Q. & Mahy, J.-P. 2007. New biocatalysts mimicking oxidative hemoproteins: Hemoabzymes. *Comptes Rendus Chimie*, 10, 684-702.
- Riveron, J. M., Irving, H., Ndula, M., Barnes, K. G., Ibrahim, S. S., Paine, M. J. & Wondji, C. S. 2013. Directionally selected cytochrome P450 alleles are driving the spread of pyrethroid resistance in the major malaria vector *Anopheles funestus*. *Proceedings of the National Academy of Sciences*, 110, 252-257.
- Robert, L. 2002. Metcalf Insect Control in Ullmann's Encyclopedia of Industrial Chemistry" Wiley-VCH. Weinheim.
- Roberts, L. S. & Janovy, J. 2005. *Gerald D. Schmidt & Larry S. Roberts' Foundations of Parasitology*, McGraw-Hill Higher Education Boston.
- Robins, K. T., Osorio-Lozada, A., Avi, M. & Meyer, H.-P. 2009. Lonza: biotechnology—a key ingredient for success in the future. *CHIMIA International Journal for Chemistry*, 63, 327-330.
- Roper, C., Pearce, R., Bredenkamp, B., Gumede, J., Drakeley, C., Mosha, F., Chandramohan, D. & Sharp, B. 2003. Antifolate antimalarial resistance in southeast Africa: a population-based analysis. *The Lancet*, 361, 1174-1181.
- Rupasinghe, S. G., Wen, Z., Chiu, T.-L. & Schuler, M. A. 2007. Helicoverpa zea CYP6B8 and CYP321A1: different molecular solutions to the problem of metabolizing plant toxins and insecticides. *Protein Engineering Design and Selection*, 20, 615-624.
- Sagara, Y., Barnes, H. & Waterman, M. 1993. Expression in *Escherichia coli* of Functional Cytochrome P450 Lacking Its Hydrophobic Amino-Terminal Signal Anchor. *Archives of biochemistry and biophysics*, 304, 272-278.

- Sakaguchi, M., Mihara, K. & Sato, R. 1984. Signal recognition particle is required for co-translational insertion of cytochrome P-450 into microsomal membranes. *Proceedings of the National Academy of Sciences*, 81, 3361-3364.
- Schenkman, J. B. & Jansson, I. 1999. Interactions between cytochrome P450 and cytochrome b5. *Drug metabolism reviews*, 31, 351-364.
- Schenkman, J. B. & Jansson, I. 2003. The many roles of cytochrome b₅ *Pharmacology & therapeutics*, 97, 139-152.
- Schenkman, J. B. & Jansson, I. 2006. Spectral analyses of cytochromes P450. *Cytochrome P450 Protocols*. Springer.
- Schmid, F. X. 2001. Biological Macromolecules: UV-visible Spectrophotometry. *eLS*.
- Schoch, G. A., Yano, J. K., Wester, M. R., Griffin, K. J., Stout, C. D. & Johnson, E. F. 2004. Structure of human microsomal cytochrome P450 2C8 Evidence for a peripheral fatty acid binding site. *Journal of Biological Chemistry*, 279, 9497-9503.
- Schuler, M. A. & Berenbaum, M. R. 2013. Structure and function of cytochrome P450S in insect adaptation to natural and synthetic toxins: insights gained from molecular modeling. *J Chem Ecol*, 39, 1232-45.
- Scott, E. E., He, Y. A., Wester, M. R., White, M. A., Chin, C. C., Halpert, J. R., Johnson, E. F. & Stout, C. D. 2003. An open conformation of mammalian cytochrome P450 2B4 at 1.6-Å resolution. *Proceedings of the National Academy of Sciences*, 100, 13196-13201.
- Scott, E. E., Spatzenegger, M. & Halpert, J. R. 2001. A truncation of 2B subfamily cytochromes P450 yields increased expression levels, increased solubility, and decreased aggregation while retaining function. *Archives of biochemistry and biophysics*, 395, 57-68.
- Scott Mathews, F. 1985. The structure, function and evolution of cytochromes. *Progress in biophysics and molecular biology*, 45, 1-56.

- Shaik, S., Kumar, D., De Visser, S. P., Altun, A. & Thiel, W. 2005. Theoretical perspective on the structure and mechanism of cytochrome P450 enzymes. *Chemical reviews*, 105, 2279-2328.
- Shimada, T., Yamazaki, H., Mimura, M., Inui, Y. & Guengerich, F. P. 1994. Inter individual variations in human liver cytochrome P-450 enzymes involved in the oxidation of drugs, carcinogens and toxic chemicals: studies with liver microsomes of 30 Japanese and 30 Caucasians. *Journal of Pharmacology and Experimental Therapeutics*, 270, 414-423.
- Sligar, S. G. 1976. Coupling of spin, substrate, and redox equilibriums in cytochrome P450. *Biochemistry*, 15, 5399-5406.
- Sono, M., Roach, M. P., Coulter, E. D. & Dawson, J. H. 1996. Heme-containing oxygenases. *Chemical Reviews*, 96, 2841-2888.
- Southall, N. T., Dill, K. A. & Haymet, A. 2002. A view of the hydrophobic effect. *The Journal of Physical Chemistry B*, 106, 521-533.
- Stephenson, G. R., Ferris, I. G., Holland, P. T. & Nordberg, M. 2006. Glossary of terms relating to pesticides (IUPAC Recommendations 2006). *Pure and Applied Chemistry*, 78, 2075-2154.
- Stevenson, B. J., Bibby, J., Pignatelli, P., Muangnoicharoen, S., O'neill, P. M., Lian, L.-Y., Müller, P., Nikou, D., Steven, A. & Hemingway, J. 2011. Cytochrome P450 6M2 from the malaria vector *Anopheles gambiae* metabolizes pyrethroids: Sequential metabolism of deltamethrin revealed. *Insect biochemistry and molecular biology*, 41, 492-502.
- Stillman, M. 2000. Formation and electronic properties of ring-oxidized and ring-reduced radical species of the phthalocyanines and porphyrins. *Journal of Porphyrins and Phthalocyanines*, 4, 374-376.

- Szklarz, G. D., He, Y. A. & Halpert, J. R. 1995. Site-directed mutagenesis as a tool for molecular modeling of cytochrome P450 2B1. *Biochemistry*, 34, 14312-14322.
- Tamburini, P. P., Jansson, I., Favreau, L. V., Backes, W. L. & Schenkman, J. B. 1986. Differences in the spectral interactions between NADPH-cytochrome P-450 reductase and a series of cytochrome P-450 enzymes. *Biochemical and biophysical research communications*, 137, 437-442.
- Tamburini, P. P. & Schenkman, J. B. 1986. Mechanism of interaction between cytochromes P450 RLM5 and *b*₅: Evidence for an electrostatic mechanism involving cytochrome *b*₅ heme propionate groups. *Archives of biochemistry and biophysics*, 245, 512-522.
- Tanaka, E. 1998. Clinically important pharmacokinetic drug–drug interactions: role of cytochrome P450 enzymes. *Journal of clinical pharmacy and therapeutics*, 23, 403-416.
- Valette, F., Mege, E., Reiss, A. & Adesnik, M. 1989. Construction of mutant and chimeric genes using the polymerase chain reaction. *Nucleic acids research*, 17, 723-733.
- Van Den Berg, H. 2009. Global status of DDT and its alternatives for use in vector control to prevent disease. *Environmental Health Perspectives*, 117, 1656-1663.
- Von Wachenfeldt, C., Richardson, T. H., Cosme, J. & Johnson, E. F. 1997. Microsomal P450 2C3 Is Expressed as a Soluble Dimer in *Escherichia coli* Following Modifications of Its N-terminus. *Archives of biochemistry and biophysics*, 339, 107-114.
- Wellems, T. E. & Plowe, C. V. 2001. Chloroquine-resistant malaria. *Journal of Infectious Diseases*, 184, 770-776.
- Wester, M. R., Johnson, E. F., Marques-Soares, C., Dansette, P. M., Mansuy, D. & Stout, C. D. 2003. Structure of a substrate complex of mammalian cytochrome P450 2C5 at 2.3 Å resolution: evidence for multiple substrate binding modes. *Biochemistry*, 42, 6370-6379.

- Whitaker, I. S., Twine, C., Whitaker, M. J., Welck, M., Brown, C. S. & Shandall, A. 2007. Larval therapy from antiquity to the present day: mechanisms of action, clinical applications and future potential. *Postgraduate medical journal*, 83, 409-413.
- Williams, P. A., Cosme, J., Vinković, D. M., Ward, A., Angove, H. C., Day, P. J., Vonrhein, C., Tickle, I. J. & Jhoti, H. 2004. Crystal structures of human cytochrome P450 3A4 bound to metyrapone and progesterone. *Science*, 305, 683-686.
- Williams, P. A., Cosme, J., Ward, A., Angove, H. C., Vinković, D. M. & Jhoti, H. 2003. Crystal structure of human cytochrome P450 2C9 with bound warfarin. *Nature*, 424, 464-468.
- Wondji, C. S., Irving, H., Morgan, J., Lobo, N. F., Collins, F. H., Hunt, R. H., Coetzee, M., Hemingway, J. & Ranson, H. 2009. Two duplicated P450 genes are associated with pyrethroid resistance in *Anopheles funestus*, a major malaria vector. *Genome research*, 19, 452-459.
- World Health Organization 1982. Manual on environmental management for mosquito control, with special emphasis on malaria vectors.
- World Health Organization 2010. First WHO report on neglected tropical diseases: working to overcome the global impact of neglected tropical diseases. *First WHO report on neglected tropical diseases: Working to overcome the global impact of neglected tropical diseases*. WHO.
- World Health Organization 2013. *Malaria entomology and vector control*, World Health Organization.
- Yadouleton, A. W., Padonou, G., Asidi, A., Moiroux, N., Bio-Banganna, S., Corbel, V., N'guessan, R., Gbenou, D., Yacoubou, I. & Gazard, K. 2010. Insecticide resistance status in *Anopheles gambiae* in southern Benin. *Malar J*, 9, 11186.

- Yano, J. K., Wester, M. R., Schoch, G. A., Griffin, K. J., Stout, C. D. & Johnson, E. F. 2004. The structure of human microsomal cytochrome P450 3A4 determined by X-ray crystallography to 2.05-Å resolution. *Journal of Biological Chemistry*, 279, 38091-38094.
- Yoshio, I. 1981. The roles of cytochrome *b*₅ in reconstituted monooxygenase systems containing various forms of hepatic microsomal cytochrome P-450. *Journal of biochemistry*, 89, 351-362.
- Zhang, M. & Scott, J. G. 1996. Cytochrome *b*₅ Is Essential for Cytochrome P450 6D1-Mediated Cypermethrin Resistance in LPR House Flies. *Pesticide biochemistry and physiology*, 55, 150-156.
- Zhu, F., Parthasarathy, R., Bai, H., Woithe, K., Kaussmann, M., Nauen, R., Harrison, D. A. & Palli, S. R. 2010. A brain-specific cytochrome P450 responsible for the majority of deltamethrin resistance in the QTC279 strain of *Tribolium castaneum*. *Proceedings of the National Academy of Sciences*, 107, 8557-8562.
- Zoller, M. J. 1991. New molecular biology methods for protein engineering. *Current Opinion in Structural Biology*, 1, 605-610.
- Zoller, M. J. 1992. New recombinant DNA methodology for protein engineering. *Current opinion in biotechnology*, 3, 348-354.

Appendix 1: Plasmid pB13

All plasmids used in this project were provided by Dr. Mark Paine of Liverpool School of Tropical medicine, LSTM.

pB13 is a modified vector of pCW ori. The Chemotaxis gene(500bp) on pCW was cut out using Nde I and Xba I and was replaced with a pair of linker oligos (LINK48 and LINK49) to create additional restriction sites on the new vector. This vector is also known as pCWmod1(10) or pCWmod1 (Barnes et al; 1991).

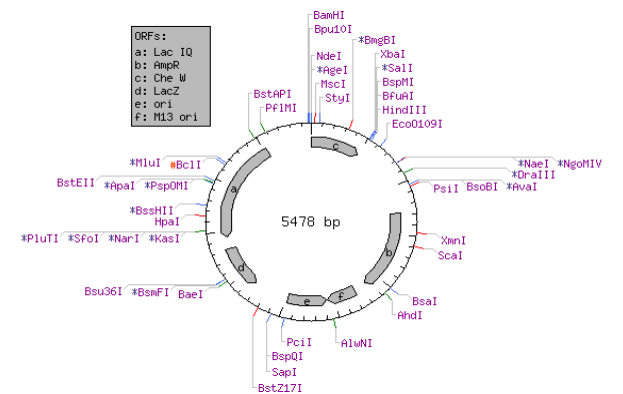


Fig. A2.1 Plasmid map of pCW ori

Sequence of MCS:

CAT ATG GAA GTG AAT TCC CGG GTA CCG AGG CTC TAG AGT CGA

Nde I

Eco RI

Kpn I

Xba I Acc I, Sal I

Xma I, Sma I

CCT GCA GCC CAA GCT TAT CGA TGA TAA G

Pst I

Hind III

Cla I

Properties:-

Ptac Ptac (Tac promoter):- Hybrid of trp and lac promoters

M13:- Bacteriophage origin of replication

Lac Z:- β -galactosidase gene

Lac IQ:- Mutation in the promoter of the lacI gene of *E. coli* for increased transcription and higher levels of lac repressor within cells

Ori :- Origin of replication, uses host's replicating protein for replication

Amp r:- Ampicillin resistant gene, selectable marker

MCS:- Multiple cloning site

Appendix 2: DNA Sequence confirmation of SDM of CYP6Z2(R210A)

SDM Primer	CATATGAAAAAGACAGCTATCGCGATTGCAGTGGCACTGGCTGGTTTCGCTACCGTAGCG	60
CYP	----- CATATGAAAAAGACAGCTATCGCGATTGCAGTGGCACTGGCTGGTTTCGCTACCGTAGCG	60
SDM Primer	CAGGCCGCTCCGATGGCTGTTTATACTCTTGCTCTTGTGCGGCCGTGATCTTTCTCGTG	120
CYP	----- CAGGCCGCTCCGATGGCTGTTTATACTCTTGCTCTTGTGCGGCCGTGATCTTTCTCGTG	120
SDM Primer	CTCCGCTACATCTACTCTCACTGGGAGAGGCATGGACTTCCGCATCTAAAGCCAGAGATT	180
CYP	----- CTCCGCTACATCTACTCTCACTGGGAGAGGCATGGACTTCCGCATCTAAAGCCAGAGATT	180
SDM Primer	CCGTACGGCAACATACGCACCGTTGCCGAGAAGAAAGAATCATTCGGCACTGCCATCAAC	240
CYP	----- CCGTACGGCAACATACGCACCGTTGCCGAGAAGAAAGAATCATTCGGCACTGCCATCAAC	240
SDM Primer	AACCTGTACCACAAGTCGTCGACCGTCTGCTGGGAATCTACCTGTTCTTCCGCCCTGCT	300
CYP	----- AACCTGTACCACAAGTCGTCGACCGTCTGCTGGGAATCTACCTGTTCTTCCGCCCTGCT	300
SDM Primer	ATCTTGATTTCGCGATCCTCATCTCGCGAAGCGTATTATGGTAAACGACTTCCAGAACTTT	360
CYP	----- ATCTTGATTTCGCGATCCTCATCTCGCGAAGCGTATTATGGTAAACGACTTCCAGAACTTT	360
SDM Primer	CACGATCGCGGTGTCGCCTGCAATGAAGAGCAGATCCCTTCTCGGCCAATCTGTTTCGCT	420
CYP	---GATCGCGGTGTCGCCTGCAATGAAGAGCAG--- CACGATCGCGGTGTCGCTACTGCAATGAAGAGCAGATCCCTTCTCGGCCAATCTGTTTCGCT	31 420

SDM Primer	CTGCCCGGTTCAGCGGTGGAAGAACTTGCCTGCGAAGCTCACGCCGACCTTCACGTCCGGA	480
CYP	----- CTGCCCGGTTCAGCGGTGGAAGAACTTGCCTGCGAAGCTCACGCCGACCTTCACGTCCGGA	480
SDM Primer	CAACTGCGTAACATGCTCCCCACCCTGCTGGACGTCGGAAACAAGTTGATCGATCGTATG	540
CYP	----- CAACTGCGTAACATGCTCCCCACCCTGCTGGACGTCGGAAACAAGTTGATCGATCGTATG	540
SDM Primer	AACAAGTGGCCGACGAGAAGGCGATCGTCGATATGCGTGATATGCGTCACGGTTTGTG	600
CYP	----- AACAAGTGGCCGACGAGAAGGCGATCGTCGATATGCGTGATATGCGTCACGGTTTGTG	600
SDM Primer	CTCGACACGATCGCTTCGGTGTCTTCGGCTTTGAGGCAAACGTATTCAACAACCGGAA	660
CYP	----- CTCGACACGATCGCTTCGGTGTCTTCGGCTTTGAGGCAAACGTATTCAACAACCGGAA	660
SDM Primer	GATCCCTTCCTATCGACACTGCGCCGTGCTAATCGGGGACGCAACTTTATCGATAACTTC	720
CYP	----- GATCCCTTCCTATCGACACTGCGCCGTGCTAATCGGGGACGCAACTTTATCGATAACTTC	720
SDM Primer	CGTTCGCTCGGTGATTTATTTGTCCCGGCTGTTGAAGCTTACCCGCATGACATCTCTC	780
CYP	----- CGTTCGCTCGGTGATTTATTTGTCCCGGCTGTTGAAGCTTACCCGCATGACATCTCTC	780
SDM Primer	CAGCCTGAATTGATTAAGTTTGTGATGGAGATCATCACCCATCAGATTGATCATCGCGAG	840
CYP	----- CAGCCTGAATTGATTAAGTTTGTGATGGAGATCATCACCCATCAGATTGATCATCGCGAG	840
SDM Primer	AAGAACCAGATCACTCGCAAAGACTTTGTTTCAGCTACTGATTGATCTGCGTCGTGAAGCT	900
CYP	----- AAGAACCAGATCACTCGCAAAGACTTTGTTTCAGCTACTGATTGATCTGCGTCGTGAAGCT	900

SDM	GATAAAGGTTTCGGAAGAAGCACTTACAATCGAACAGTGTGCAGCCAATGTGTTTCCTGTTT	960
Primer	-----	
CYP	GATAAAGGTTTCGGAAGAAGCACTTACAATCGAACAGTGTGCGGCCAATGTGTTTCCTGTTT	960
SDM	TACATTGNCCGNNCGGAAACGTCAACAGCAACGATCTCGTTCACGCTCCACGAGCTTTC	1020
Primer	-----	
CYP	TACATTGCCGGTTCGGAACGTCAACAGCAACGATCTCGTTCACGCTCCACGAGCTTTCG	1020
SDM	GCACAATCCAGAAGCGATGGCAAACACTGCAGCAAGAAATTGACGA-----	1064
Primer	-----	
CYP	CACAATCCAGAAGCGATGGCAAACACTGCAGCAAGAAATTGACGAGATGATGGAGCGATAT	1080

Appendix 3: PCR reactions

Phusion Polymerase was used to create the two truncations in a thermal Cycle of 35 as follows:

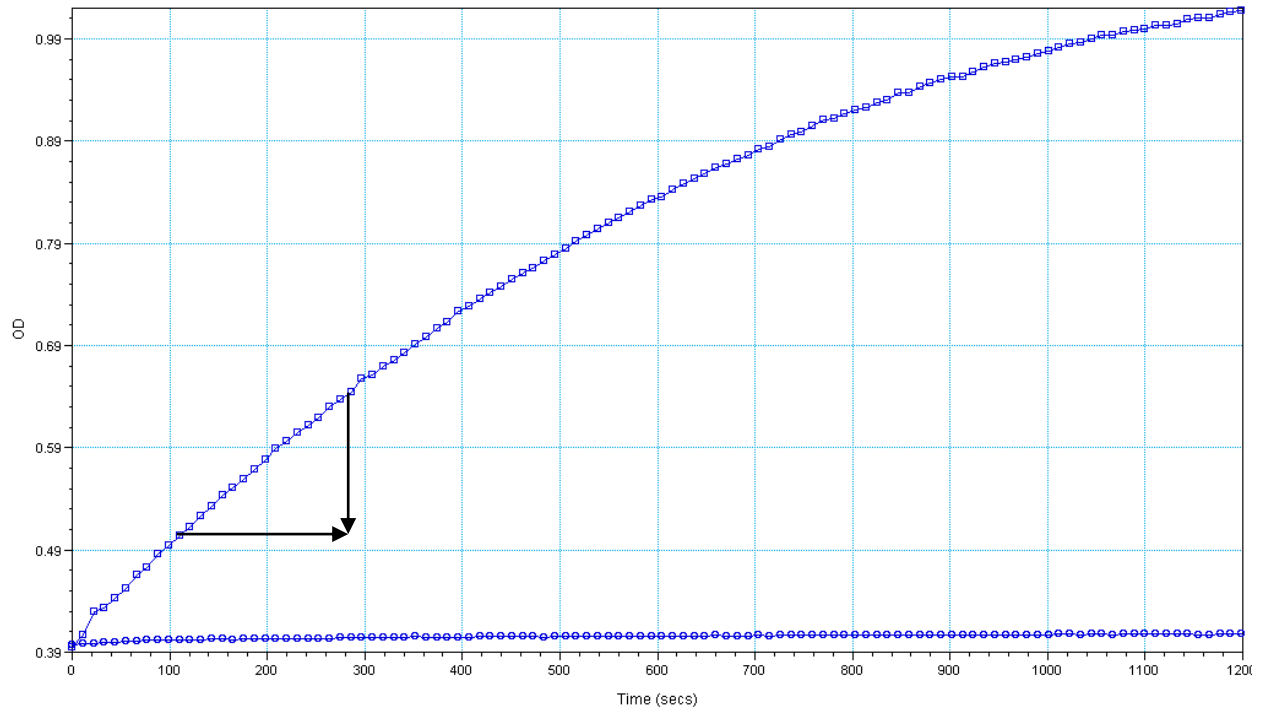
Reaction Mixture	Volume
10 x buffer	2.5ul
Forward Primer	1ul
Reverse Primer	1ul
Template	1ul
DNTPs	0.5ul
Phusion Polymerase	0.5ul
Water	18.5ul
Total Volume	25ul

Phusion high fidelity polymerase thermal Cycle

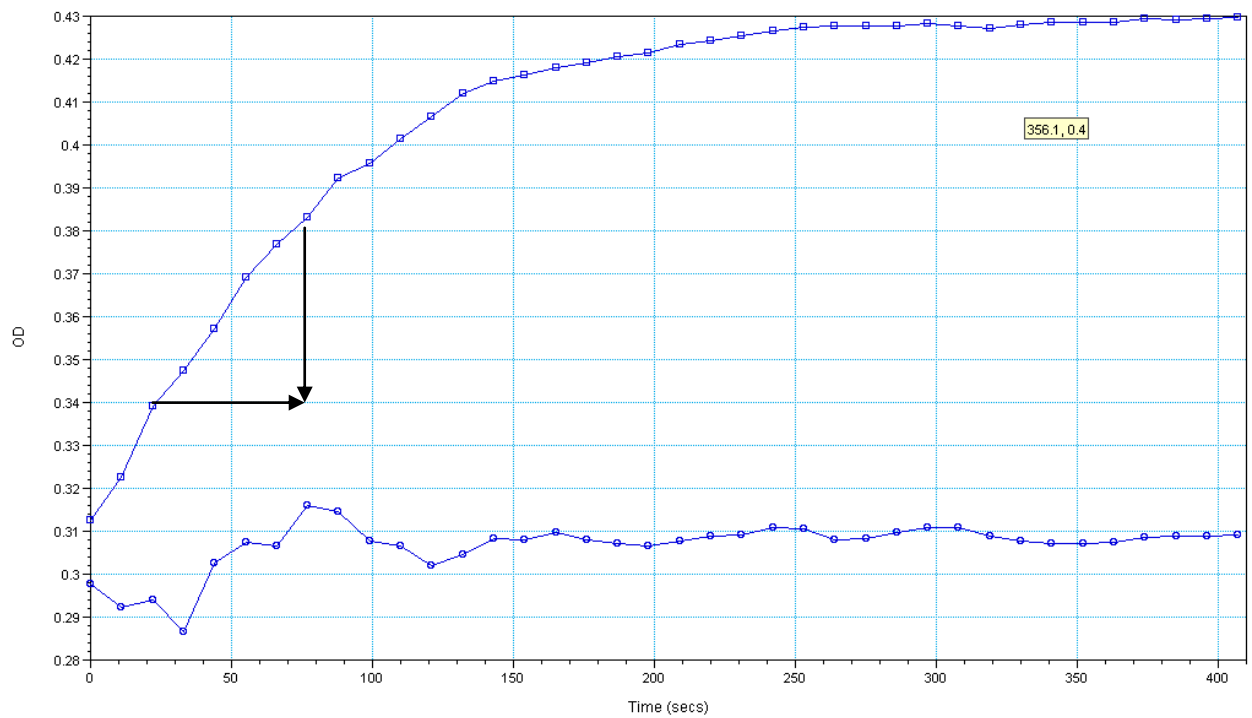
	Temperature	Time	Cycle
Initial Denaturation	90°C	30s	1
Denaturation	90°C	10s	35
Annealing	65°C	5s	
Extention	72°C		
Final Extention	72°C	10min	1
Hold	4°C		1

Appendix 4: CPR quantification graphs and total protein evaluations

NADPH – Cytochrome C Reduction Assay Co-expressed with CYP6Z2(Wild Type)



NADPH – Cytochrome C Reduction Assay Co-expressed with CYP6Z2(F115A)



CYP6Z2 TYPE	TOTAL PROTEIN (mg/ml)	P450 CONTENT (μ M)	P450 CONTENT (nmol/mg protein)	P450 REDUCTASE ACTIVITY(n mol/min/mg)
CYP6Z2(wild)	49.37	8.43	0.171	25.14
CYP6Z2(F115A)	36.36	1.889	0.052	29.47
CYP6Z2(F115L)	32.66	2.633	0.082	18.51
CYP6Z2(F115Y)	35.62	4.089	0.115	20.05
CYP6Z2(Y102A)	38.61	0.712	0.018	18.50
CYP6Z2(Y102F)	49.92	1.91	0.038	28.62
CYP6Z2(F212L)	46.70	2.486	0.053	18.04

CYP6P3	TOTAL PROTEIN (mg/ml)	P450 CONTENT (μ M)	P450 CONTENT (nmol/mg protein)	P450 REDUCTASE ACTIVITY(n mol/min/mg protein)
Wild –CYP6P3	15.80	1.364	0.0863	721.04
Mutant CYP6P3 (F110Y)	16.33	0.6478	0.039	772.31
Mutant CYP6P3 (L216F)	18.27	2.188	0.119	401.62

Appendix 5: Amino Acid sequence confirmation of double mutant CYP6Z2 (F212L,Y102F)

Amino Acid Alignment ompACYP6Z2

```

CYP6Z2      MKKTAIAIAVALAGFATVAQAAPMAVYTLALVAAVIFLVLRYIYSHWERHGLPHLKPEIP 60
SDM         MKKTAIAIAVALAGFATVAQAAPMAVYTLALVAAVIFLVLRYIYSHWERHGLPHLKPEIP 60
*****

CYP6Z2      YGNIRTVAEKKESFGTAINNLYHKSSDRLLGIYLFRRPAILIRDPHLAKRIMVNDQNFH 120
SDM         YGNIRTVAEKKESFGTAINNLYHKSSDRLLGIYLFRRPAILIRDPHLAKRIMVNDQNFH 120
*****

CYP6Z2      DRGVFCNEEHDPFSANLFFALPGQRWKNLRAKLTPTFTSGQLRNMLPTLLDVGNKLIDRMN 180
SDM         DRGVFCNEEHDPFSANLFFALPGQRWKNLRAKLTPTFTSGQLRNMLPTLLDVGNKLIDRMN 180
*****

CYP6Z2      KVADEKAIIVDMRDIASRFVLDTIASVFFGFEANCIHNSEDPFLLSTLRRANRGRNLFIDNFR 240
SDM         KVADEKAIIVDMRDIASRFVLDTIASVFFGFEANCIHNSEDPFLLSTLRRANRGRNLFIDNFR 240
*****

CYP6Z2      SSGVFICPGLLKLTRMTSLQPELIKVFMEIITHQIDHREKNQITRKDFVQLLIDLREAD 300
SDM         SSGVFICPGLLKLTRMTSLQPELIKVFMEIITHQIDHREKNQITRKDFVQLLIDLREAD 300
*****

CYP6Z2      KGSEEALTIEQCAANVFLFYIAGAETSTATISFTLHELHSHNPEAMAKLQQEIDEMMERYN 360
SDM         KGSEEALTIEQCAANVFLFYIAGAETSTATISFTLHELHSHNPEAMAKLQQEIDEMMERYN 360
*****

CYP6Z2      GEITYENIKEMKYLDLCVKETLRKYPGLPILNRECTIDYKVPDSDVVIRKGTQVIIPLLS 420
SDM         GEITYENIKEMKYLDLCVKETLRKYPGLPILNRECTIDYKVPDSDVVIRKGTQVIIPLLS 420
*****

CYP6Z2      ISMNEKYFPDPELYSPERFDEATKNYDADAYYFPGAGPRNCIGLRQGVLVSKIIGLVFLLS 480
SDM         ISMNEKYFPDPELYSPERFDEATKNYDADAYYFPGAGPRNCIGLRQGVLVSKIIGLVFLLS 480
*****

CYP6Z2      KFNFAQATTPAKVKFAAATVGLTPDAGFPMRIDHRK 515
SDM         KFNFAQATTPAKVKFAAATVGLTPDAGFPMRIDHRK 515
*****

```

Appendix 6: Amino acid sequence confirmation of double mutant CYP6Z2(F212L,Y102A)

```

CYP6Z2_Wild_Type_      MKKTAIAIAVALAGFATVAQAAPMAVYTLALVAAVIFLVLRYYIYSHWERHGLPHLKPEIP 60
CYP6Z2_Y102A_F212L_  MKKTAIAIAVALAGFATVAQAAPMAVYTLALVAAVIFLVLRYYIYSHWERHGLPHLKPEIP 60
*****

CYP6Z2_Wild_Type_      YGNIRTVAEKKESFGTAINNLYHKSSDRLLGIYLFRRPAILIRDPHLAKRIMVNDFQNFH 120
CYP6Z2_Y102A_F212L_  YGNIRTVAEKKESFGTAINNLYHKSSDRLLGIYLFRRPAILIRDPHLAKRIMVNDFQNFH 120
*****

CYP6Z2_Wild_Type_      DRGVYCNEEHDPFSANLALPGQRWKNLRAKLTPTFTSGQLRNMLPTLLDVGNKLIDRMN 180
CYP6Z2_Y102A_F212L_  DRGVAACNEEHDPFSANLALPGQRWKNLRAKLTPTFTSGQLRNMLPTLLDVGNKLIDRMN 180
**** *****

CYP6Z2_Wild_Type_      KVADEKAIIVDMRDIASRFVLDTIASVFFGFEANCIHNSEDPFLSTLRRANRGRNLIDNFR 240
CYP6Z2_Y102A_F212L_  KVADEKAIIVDMRDIASRFVLDTIASVFFGFEANCIHNSEDPFLSTLRRANRGRNLIDNFR 240
*****

CYP6Z2_Wild_Type_      SSGVFICPGLLKLTRMTSLQPELIKVFMEIITHQIDHREKNQITRKDFVQLLIDLRRREAD 300
CYP6Z2_Y102A_F212L_  SSGVFICPGLLKLTRMTSLQPELIKVFMEIITHQIDHREKNQITRKDFVQLLIDLRRREAD 300
*****

CYP6Z2_Wild_Type_      KGSEEALTIEQCAANVFLFYIAGAETSTATISFTLHELSHNPEAMAKLQQEIDEMMERYN 360
CYP6Z2_Y102A_F212L_  KGSEEALTIEQCAANVFLFYIAGAETSTATISFTLHELSHNPEAMAKLQQEIDEMMERYN 360
*****

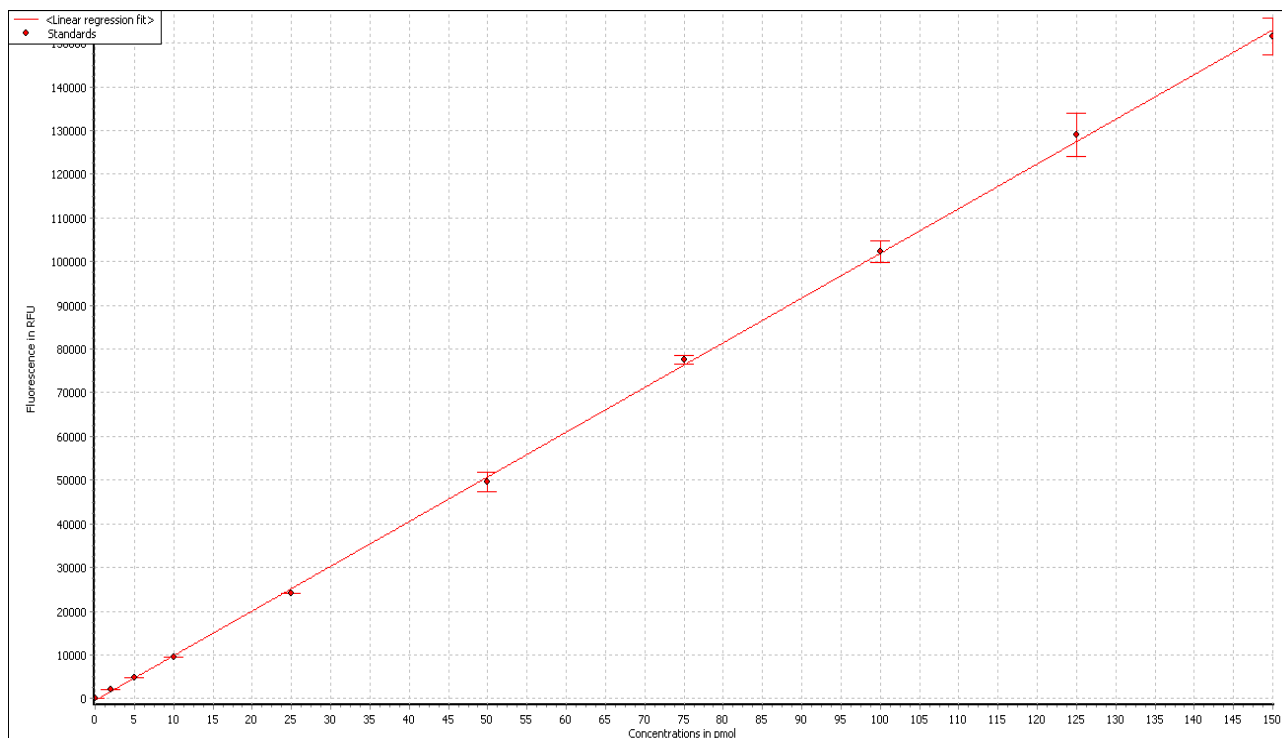
CYP6Z2_Wild_Type_      GEITYENIKEMKYLDLCVKETLRKY PGLPILNRECTIDYKVPDSDVIRKGTQVIIPLLS 420
CYP6Z2_Y102A_F212L_  GEITYENIKEMKYLDLCVKETLRKY PGLPILNRECTIDYKVPDSDVIRKGTQVIIPLLS 420
*****

CYP6Z2_Wild_Type_      ISMNEKYFPDPELYSPERFDEATKNYDADAYYPFGAGPRNCIGLRQGVLVSKIGLVFLLS 480
CYP6Z2_Y102A_F212L_  ISMNEKYFPDPELYSPERFDEATKNYDADAYYPFGAGPRNCIGLRQGVLVSKIGLVFLLS 480
*****

CYP6Z2_Wild_Type_      KFNFQATTPAKVKFAAATVGLTPDAGFPMRIDHRK 515
CYP6Z2_Y102A_F212L_  KFNFQATTPAKVKFAAATVGLTPDAGFPMRIDHRK 515
*****

```

Appendix 7: Resorufin standard curve



$$1 \text{ unit of activity} = \frac{\Delta \text{FLU}/\text{min} \times \text{dilution factor of sample}}{(\text{pmole}/\text{ml}/\text{min}) \quad (\text{FLU}/\text{pmole})}$$

Appendix 8: DNA sequence alignments of documented alleles of CYP6Z2 amino acid with the gene used in this project.

```

CYP6Z2_Q7PNB5_ -----MFVYTLALVAAVIFLVLRYIYSHWERHGLPHLKPEIP 37
CYP6Z2_A8I285_ -----MFVYTLALVAAVIFLVLRYIYSHWERHGLPHLKPEIP 37
CYP6Z2_Q8T625_ -----MFVYTLALVAAVIFLVLRYIYSHWERHGLPHLKPEIP 37
SDM MKKTAIAIAVALAGFATVAQAAMAVYTLALVAAVIFLVLRYIYSHWERHGLPHLKPEIP 60
      * *****

omp
CYP6Z2_Q7PNB5_ YGNIRTVAEKKESFGTAINNLYHKSSDRLLGIYLFRRPAILIRDPHLAKRIMVNDQNFH 97
CYP6Z2_A8I285_ YGNIRTVAEKKESFGTAINNLYHKSSDRLLGIYLFRRPAILIRDPHLAKRIMVNDQNFH 97
CYP6Z2_Q8T625_ YGNIRTVAEKKESFGTAINNLYHKSSDRLLGIYLFRRPAILIRDPHLAKRIMVNDQNFH 97
SDM YGNIRTVAEKKESFGTAINNLYHKSSDRLLGIYLFRRPAILIRDPHLAKRIMVNDQNFH 120
      *****

CYP6Z2_Q7PNB5_ DRGVYCNEEHDPFSANL FALPGQRWKNLRAKLTPTFTSGQLRNMLPTLLDVGNKLIDRMN 157
CYP6Z2_A8I285_ DRGVYCNEEHDPFSANL FALPGQRWKNLRAKLTPTFTSGQLRNMLPTLLDVGNKLIDRMN 157
CYP6Z2_Q8T625_ DRGVYCNEEHDPFSANL FALPGQRWKNLRAKLTPTFTSGQLRNMLPTLLDVGNKLIDRMN 157
SDM DRGVYCNEEHDPFSANL FALPGQRWKNLRAKLTPTFTSGQLRNMLPTLLDVGNKLIDRMN 180
      *****

SDM
F115
L
CYP6Z2_Q7PNB5_ KVADEKAI VDMRDIASRFVLDTIASVFFGFEANCIHNSEDPFLSTLRRANRGRNFIDNFR 217
CYP6Z2_A8I285_ KVADEKAI VDMRDIASRFVLDTIASVFFGFEANCIHNSEDPFLSTLRRANRGRNFIDNFR 217
CYP6Z2_Q8T625_ KVADEKAI VDMRDIASRFVLDTIASVFFGFEANCIHNSEDPFLSTLRRANRGRNFIDNFR 217
SDM KVADEKAI VDMRDIASRFVLDTIASVFFGFEANCIHNSEDPFLSTLRRANRGRNFIDNFR 240
      *****;*****

CYP6Z2_Q7PNB5_ SSGVFCPGLLKLTRMTSLQPELIKFMVEI ITHQIDHREKNQITRKDFVQLLIDLRRREAD 277
CYP6Z2_A8I285_ SSGVFCPGLLKLTRMTSLQPELIKFMVEI ITHQIDHREKNQITRKDFVQLLIDLRRREAD 277
CYP6Z2_Q8T625_ SSGVFCPGLLKLTRMTSLQPELIKFMVEI ITHQIDHREKNQITRKDFVQLLIDLRRREAD 277
SDM SSGVFCPGLLKLTRMTSLQPELIKFMVEI ITHQIDHREKNQITRKDFVQLLIDLRRREAD 300
      *****

CYP6Z2_Q7PNB5_ KGSEEALTIEQCAANVFLFYIAGAETSTATISFTLHELSHNPEAMAKLQQEIDEMMERYN 337
CYP6Z2_A8I285_ KGSEEALTIEQCAANVFLFYIAGAETSTATISFTLHELSHNPEAMAKLQQEIDEMMERYN 337
CYP6Z2_Q8T625_ KGSEEALTIEQCAANVFLFYIAGAETSTATISFTLHELSHNPEAMAKLQQEIDEMMERYN 337
SDM KGSEEALTIEQCAANVFLFYIAGAETSTATISFTLHELSHNPEAMAKLQQEIDEMMERYN 360
      *****

CYP6Z2_Q7PNB5_ GEITYENIKEMKYLDLCVKETLRKYPGLPILNRECTIDYKVPDSDVVIRKGTQVI I PLLS 397
CYP6Z2_A8I285_ GEITYENIKEMKYLDLCVKETLRKYPGLPILNRECTIDYKVPDSDVVIRKGTQVI I PLLS 397
CYP6Z2_Q8T625_ GEITYENIKEMKYLDLCVKETLRKYPGLPILNRECTIDYKVPDSDVVIRKGTQVI I PLLS 397
SDM GEITYENIKEMKYLDLCVKETLRKYPGLPILNRECTIDYKVPDSDVVIRKGTQVI I PLLS 420
      *****

CYP6Z2_Q7PNB5_ ISMNEKYFPDPELYSPERFDEATKNYDADAYYPFGAGPRNCIGLRQGVLVSKI GLVFLLS 457
CYP6Z2_A8I285_ ISMNEKYFPDPELYSPERFDEATKNYDADAYYPFGAGPRNCIGLRQGVLVSKI GLVFLLS 457
CYP6Z2_Q8T625_ ISMNEKYFPDPELYSPERFDEATKNYDADAYYPFGAGPRNCIGLRQGVLVSKI GLVFLLS 455
SDM ISMNEKYFPDPELYSPERFDEATKNYDADAYYPFGAGPRNCIGLRQGVLVSKI GLVFLLS 480
      *****

CYP6Z2_Q7PNB5_ KFKFQATTPAKVKFAAATVGLTPDAGFPMRIDHRK 492
CYP6Z2_A8I285_ KFKFQATTPAKVKFAAATVGLTPDAGFPMRIDHRK 492
CYP6Z2_Q8T625_ KFNQATTPAKVKFAAATVGLTPDAGFPMRIDHRK 490
SDM KFNQATTPAKVKFAAATVGLTPDAGFPMRIDHRK 515
      **;*****

```

Appendix 9: Analysis of mutations observed in the polymorphism of CYP6Z2

Swissprot accession code	Amino Acid	Position 1	Position 2	Position 3	Position 4	No of mutations- To working gene
CYP6Z2_Q7PNB5	492	S201	L441	R442	K460	1
CYP6Z2_A8I285	492	T201	L441	R442	K460	2
CYP6Z2_Q8T625	490	S201	NA	NA	N458	2
Working Gene	492	S201	L441	R442	N460	

The closest to the working gene is CYP6Z2_Q7PNB5 with 1 mutation at K60N.

Nucleotide Alignment with CYP6Z2_Q7PNB5

```

CYP6Z2_Q7PNB5      ATGTTTGTTTTACTCTCGCGCTCGTGGCGGCCGTGATCTTTCTCGTGCTCCGCTACATC 60
Working            ATGGCTGTTTATACTCTTGCTCTTGTGCGGCCGTGATCTTTCTCGTGCTCCGCTACATC 60
                    ***  *****  *****  *  *  *  *  *****  *****

CYP6Z2_Q7PNB5      TACTCTCACTGGGAGAGGCATGGACTTCCCATCTAAAGCCAGAGATTCGGTACGGCAAC 120
Working            TACTCTCACTGGGAGAGGCATGGACTTCCGCATCTAAAGCCAGAGATTCGGTACGGCAAC 120
                    *****  *****

CYP6Z2_Q7PNB5      ATACGCACCGTTGCCGAGAAGAAAGAATCATTCGGCACTGCCATCAACAACCTGTACCAC 180
Working            ATACGCACCGTTGCCGAGAAGAAAGAATCATTCGGCACTGCCATCAACAACCTGTACCAC 180
                    *****

CYP6Z2_Q7PNB5      AAGTCGTCGGACCGTCTGCTGGGAATCTACTGTCTTCCGCCCTGCTATCTTGATTTCGC 240
Working            AAGTCGTCGGACCGTCTGCTGGGAATCTACTGTCTTCCGCCCTGCTATCTTGATTTCGC 240
                    *****

CYP6Z2_Q7PNB5      GATCCTCATCTCGCGAAGCGTATCATGGTAAACGACTTCCAGAACTTTCACGATCGCGGT 300
Working            GATCCTCATCTCGCGAAGCGTATCATGGTAAACGACTTCCAGAACTTTCACGATCGCGGT 300
                    *****

CYP6Z2_Q7PNB5      GTCTACTGCAATGAAGAGCAGCATCCCTTCTCGGCAATCTGTTTCGCTCTGCCCGGTCAG 360
Working            GTCTACTGCAATGAAGAGCAGCATCCCTTCTCGGCAATCTGTTTCGCTCTGCCCGGTCAG 360
                    *****

CYP6Z2_Q7PNB5      CGGTGGAAGAAGCTTACGTGCGAAGCTCACGCCGACCTTACGTCGGGACAACACGTAAC 420
Working            CGGTGGAAGAAGCTTACGTGCGAAGCTCACGCCGACCTTACGTCGGGACAACACGTAAC 420
                    *****

CYP6Z2_Q7PNB5      ATGCTCCCCACTCTCCTGGACGTCGGCAACAAGCTGATCGATCGTATGAACAAGGTGGCC 480
Working            ATGCTCCCCACTCTCCTGGACGTCGGCAACAAGCTGATCGATCGTATGAACAAGGTGGCC 480
                    *****

CYP6Z2_Q7PNB5      GACGAGAAGGCGATCGTTGATATGCGTGATATTGCGTCACGGTTTGTGCTCGACACGATC 540
Working            GACGAGAAGGCGATCGTTGATATGCGTGATATTGCGTCACGGTTTGTGCTCGACACGATC 540
                    *****

CYP6Z2_Q7PNB5      GCTTCGGTGTCTTCGGCTTCGAGGCCAACTGTATTCACTCGGAAGATCCCTTCCTA 600
Working            GCTTCGGTGTCTTCGGCTTCGAGGCCAACTGTATTCACTCGGAAGATCCCTTCCTA 600
                    *****

```

CYP6Z2_Q7PNB5 Working TCGACACTGCGCCGTGCTAATCGGGGACGCAACTTTATCGATAACTTCCGTTTCGTCTGGT 660
TCGACACTGCGCCGTGCTAATCGGGGACGCAACTTTATCGATAACTTCCGTTTCGTCTGGT 660

CYP6Z2_Q7PNB5 Working GTATTTATTTGTCC TGGG TTGTTGAAGCTTACCCGCATGACATCTCTCCAGCTGAATTG 720
GTATTTATTTGTCC CGGG CTGTTGAAGCTTACCCGCATGACATCTCTCCAGCTGAATTG 720

CYP6Z2_Q7PNB5 Working ATTAAGTTTGTGATGGAGATCATCACCATCAGATTGATCATCGCGAGAAGAA TCAATC 780
ATTAAGTTTGTGATGGAGATCATCACCATCAGATTGATCATCGCGAGAAGAA CCAATC 780

CYP6Z2_Q7PNB5 Working ACTCGCAAAGACTTTGTG T CAGCTACTGATTGATCTGCGTCTGTAAGCTGATAAAGGTTTCG 840
ACTCGCAAAGACTTTGTG T CAGCTACTGATTGATCTGCGTCTGTAAGCTGATAAAGGTTTCG 840

CYP6Z2_Q7PNB5 Working GAAGAAGCACTTACAATCGAACAGTGTGC G GCAATGTGTTCTCTGTT TACATTGCCGGT 900
GAAGAAGCACTTACAATCGAACAGTGTGC A GCAATGTGTTCTCTGTT TACATTGCCGGT 900

CYP6Z2_Q7PNB5 Working GCAGAAACATCAAC G GCAACGATCTCGTTTCACTCCATGAA CTTTCGCACAATCCAGAA 960
GCGGAAACG TCAAC A GCAACGATCTCGTTTCACTCCACGAG CTTTCGCACAATCCAGAA 960
** *****

CYP6Z2_Q7PNB5 Working GCGATGGCAAAGCTGCAGCAAGAAATGACGAGATGATGGAGCGATATAACGGCGAAATC 1020
GCGATGGCAAAGCTGCAGCAAGAAATGACGAGATGATGGAGCGATATAACGGCGAAATC 1020

CYP6Z2_Q7PNB5 Working ACGTATGAGAACATAAAAGAGATGAAGTACTTGGATTTGTGCGTGAA A GAAACGCTTCGA 1080
ACGTATGAGAACATAAAAGAGATGAAGTACTTGGATTTGTGCGTGAA G GAAACGCTTCGA 1080

CYP6Z2_Q7PNB5 Working AAGTATCC G GGCTTCCGATCTTGAACCGAGAGTGCACGATCGACTACAAAGTCCCGGAC 1140
AAGTATCC T GGCTTCCGATCTTGAACCGAGAGTGCACGATCGACTACAAAGTCCCGGAC 1140

CYP6Z2_Q7PNB5 Working AGTGATGTTGTGATACGCAAGGGAAGTCTCAGGTGATCATACCGTTGTTGAGTATCAGTATG 1200
AGTGATGTTGTGATACGCAAGGGAAGTCTCAGGTGATCATACCGTTGTTGAGTATCAGTATG 1200

CYP6Z2_Q7PNB5 Working AACGAGAAGTACTTCCCCGATCCAGAGCTCTATTCTCCAGAGCGGTTTGACGAGGCCACG 1260
AACGAGAAGTACTTCCCCGATCCAGAGCTCTATTCTCCAGAGCGGTTTGACGAGGCCACA 1260

CYP6Z2_Q7PNB5 Working AAGAACTACGATGCAGATGCGTACTATCCGTTCCGAGCTGGTCCTCGCAATGTCATCGGC 1320
AAGAACTACGATGCAGATGCGTACTATCCGTTCCGAGCTGGTCCTCGCAATGTCATCGGC 1320

CYP6Z2_Q7PNB5 Working CTTCGACAAGGTGTATTGGTGTCCAAAATAGG GCTTGTCTTCTTGCTGTCAAAGTTCAAG 1380
CTTCGACAAGGTGTATTGGTGTCCAAAATAGG ACTTGTCTTCTTGCTGTCAAAGTTCAAG 1380

CYP6Z2_Q7PNB5 Working TTCCAG GCCACAACCTCTGCAAAAGTAAAGTTTGC A GCCGCTACTGTAGGTCTCACTCCA 1440
TTCCAG GCCACAACCTCTGCAAAAGTAAAGTTTGC C GCCGCTACTGTAGGTCTCACTCCA 1440

CYP6Z2_Q7PNB5 Working GACGCTGGATTCCCAATGAGGATAGACCATAGAAAGTGA 1479
GACGCTGGATTCCCAATGAGGATAGACCATAGAAAGTGA 1479

The alignment above shows 33 mutations. 32 of the mutations are silent, thus are synonymous SNPs. However, the mutation at position 1380, from G to C caused a non-synonymous SNP by changing the amino acid from Lysine to Asparagine.

Conclusion

My working gene is a closer allele of CYP6Z2_Q7PNB5.

NB:

Please note that the mutations observed at the beginning of the gene were deliberately done to improve the expression of the working gene.

Appendix 10: Amino acid sequence confirmation of CYP6P3

```

Primers      MKKTAIAIAVALAGFATVAQAGMELINAVLAAFI FAVSIVYLFIRNKHNYWKDNGFPYAP 60
CYP6P3      -----MELINAVLAAFI FAVSIVYLFIRNKHNYWKDNGFPYAP 38
                *****

Primers      NPHFLFGHAKGQAQTRHGADIHQELYRYFKQRGERYGGISQFIVPSVLVIDPELAKTILV 120
CYP6P3      NPHFLFGHAKGQAQTRHGADIHQELYRYFKQRGERYGGISQFIVPSVLVIDPELAKTILV 98
                *****

Primers      KDFNVFHDHGVFTNAKDDPLTGHLFALEGQPWRLMRQKLTPTFTSGRMKQMFGTIWDVGL 180
CYP6P3      KDFNVFHDHGVFTNAKDDPLTGHLFALEGQPWRLMRQKLTPTFTSGRMKQMFGTI RDVGL 158
                *****

Primers      ELEKCMESYNQPEVEMKDILGRFTT DVI GTCAFGIECNTLKT DSEFRKYGNKAFELNT 240
CYP6P3      ELEKCMESYNQPEVEMKDILGRFTT DVI GTCAFGIECNTLKT DSEFRKYGNKAFELNT 218
                *****

Primers      MIMMKTFLASSYPTLVRNLHMKITYNDVERFFLDIVKETVDYREANNVKNRDNFMNMLQI 300
CYP6P3      MIMMKTFLASSYPTLVRNLHMKITYNDVERFFLDIVKETVDYREANNVKNRDNFMNMLQI 278
                *****

Primers      KNKGKLLDSDDG SVGKGEVGMTQNELAAQAFVFFLAGFETSSTTQSFCLYELAKNPDIQE 360
CYP6P3      KNKGKLLDSDDG S GKGEVGMTQNELAAQAFVFFLAGFETSSTTQSFCLYELAKNPDIQE 338
                *****

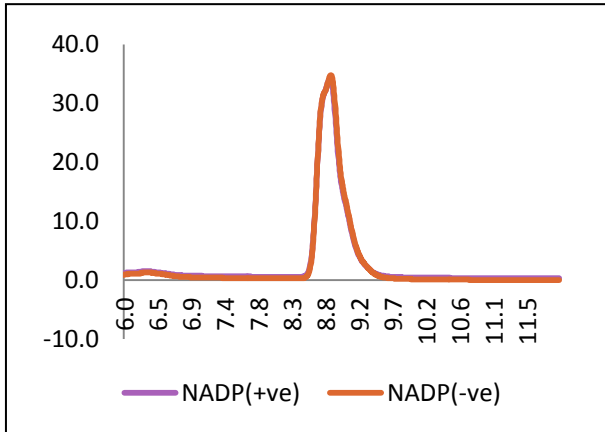
Primers      RLREEINRAIAENGGEV TYDVMN I KYLDNVIDETLRKYPPVESLTRVPSVDYLI PGTKH 420
CYP6P3      RLREEINRAIAENGGEV TYDVMN I KYLDNVIDETLRKYPPVESLTRVPSVDYLI PGTKH 398
                *****

Primers      VIPKRTL VQIPAYAIQRDPDHYDPERFNPDRFLPEEVKRRHPFTFIPFGEGPRICIGLR 480
CYP6P3      VIPKRTL VQIPAYAIQRDPDHYDPERFNPDRFLPEEVKRRHPFTFIPFGEGPRICIGLR 458
                *****

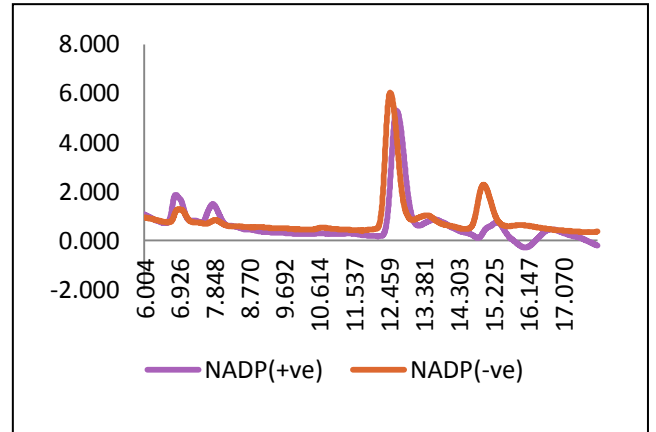
Primers      FGLMQTKVGLITLLRKRFRFSPSARTPERVEYDPKMITIAPKAGNYLKVEKLHHHHHH 537
CYP6P3      FGLMQTKVGLITLLRKRFRFSPSARTPERVEYDPKMITIAPKAGNYLKVEKL----- 509

```

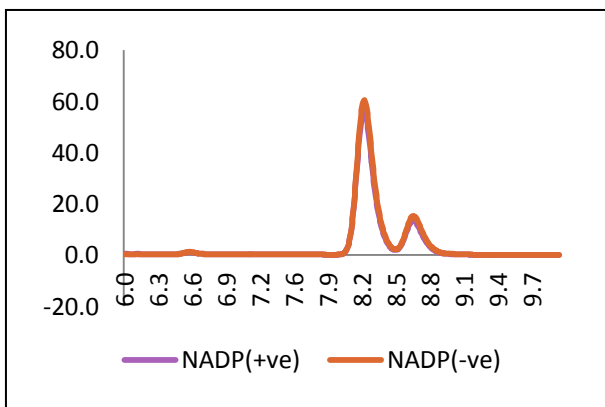
Appendix 11: HPLC Chromatograms



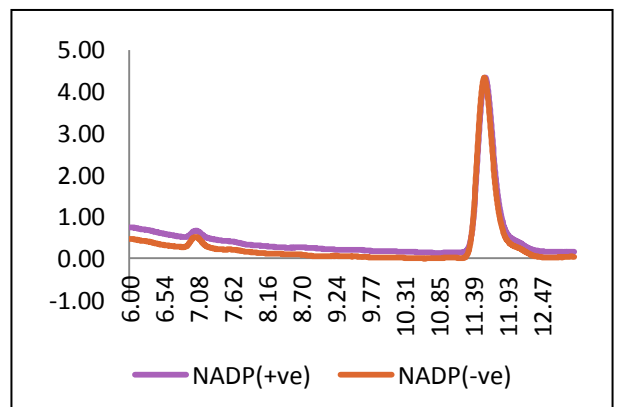
CYP6Z2 Deltamethrin Depletion



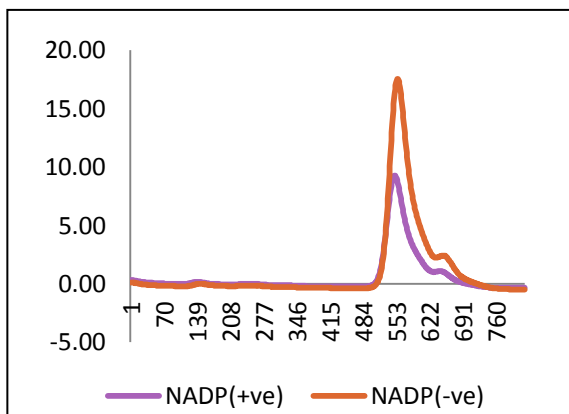
CYP6Z2 Permethrin Depletion Assay



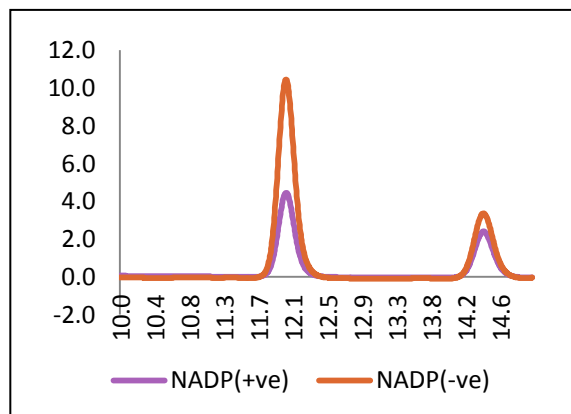
CYP6Z2 Cypermethrin Depletion



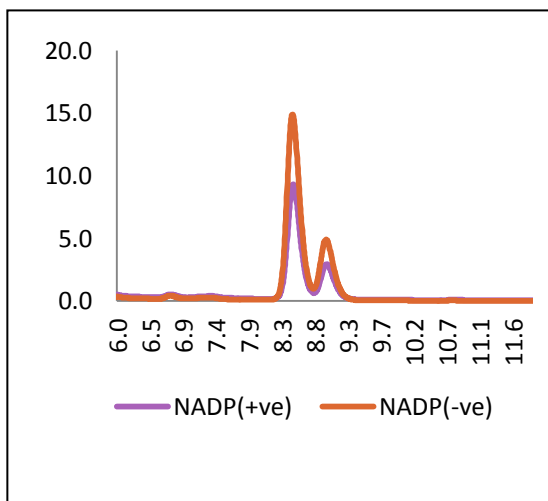
CYP6Z2 DDT Depletion Assay



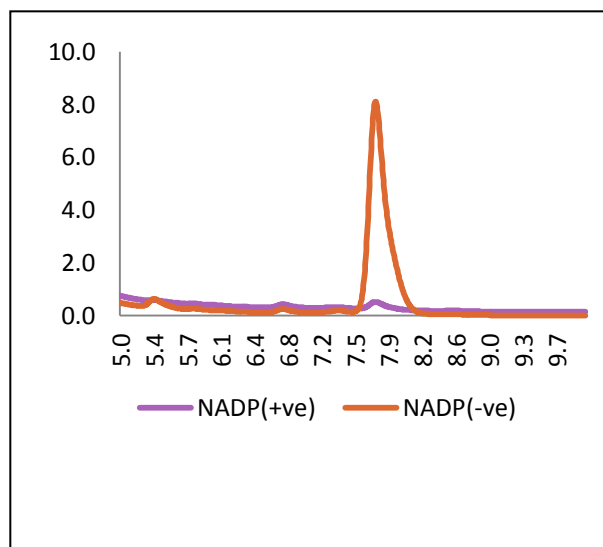
CYP6Z3-Deltamethrin Depletion



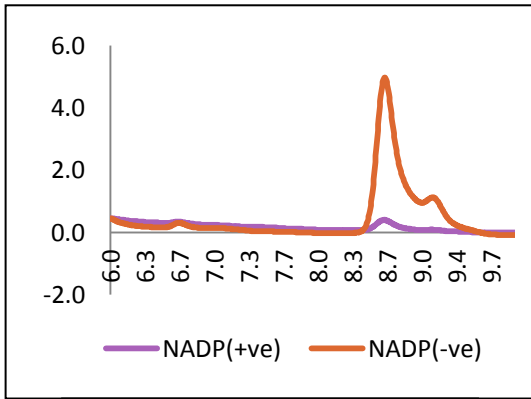
CYP6Z3-Permethrin Depletion



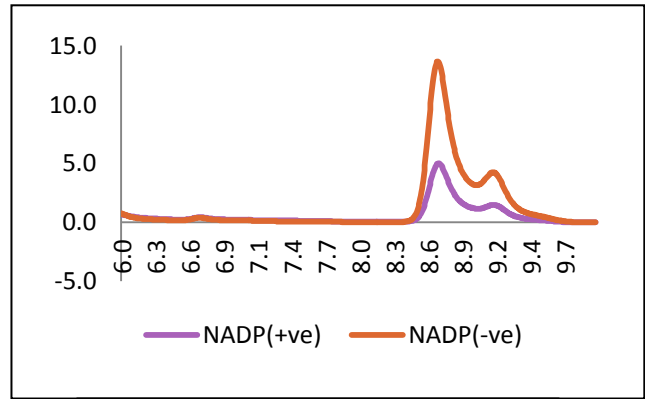
CYP6Z3-Cypermethrin Depletion Assay



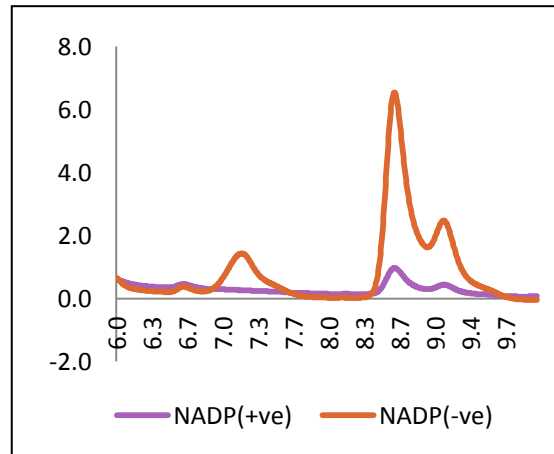
CYP6Z3-Pyriproxyfen Depletion Assay



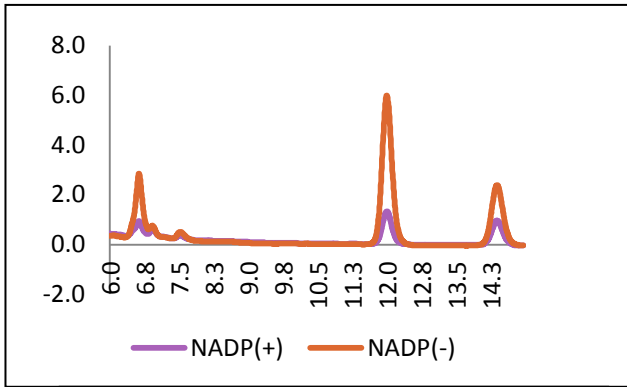
CYP6P3-Deltamethrin assay



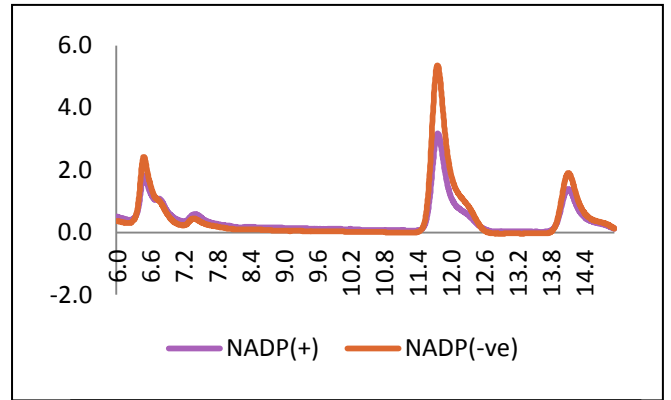
CYP6P3(F110Y)-Deltamethrin



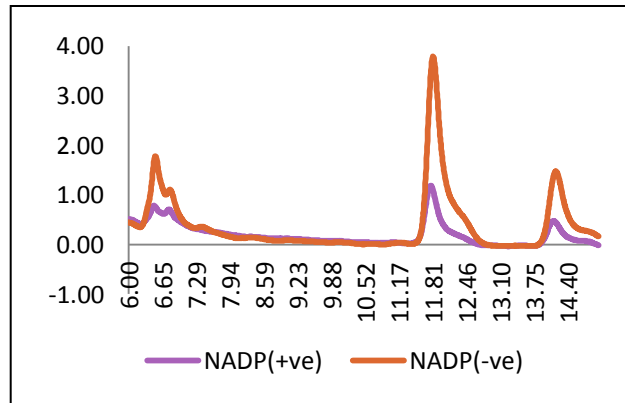
CYP6P3(L216F)-Deltamethrin



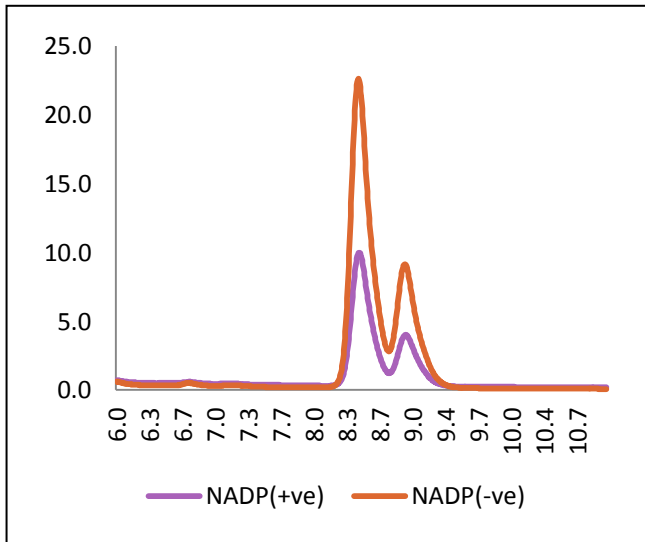
CYP6P3-Permethrin depletion assay



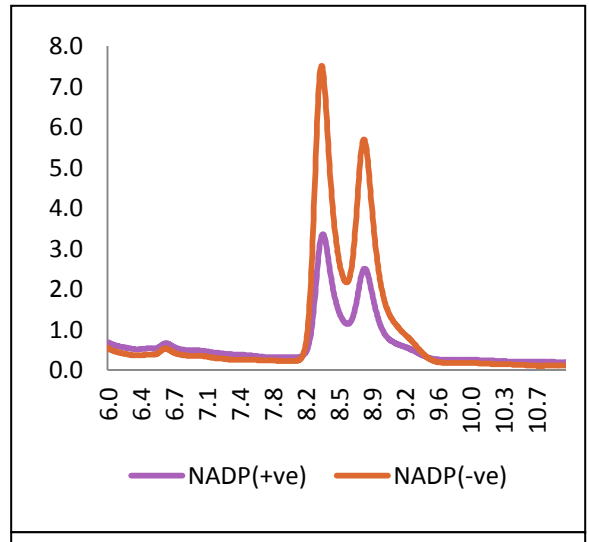
CYP6P3(F110Y)-Permethrin depletion



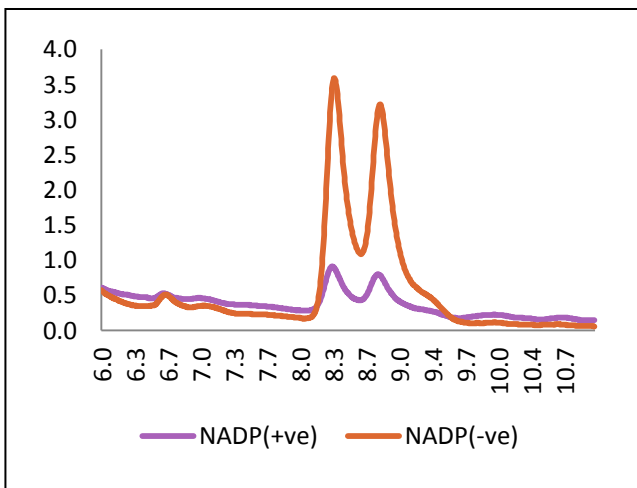
CYP6P3(L216F)-Permethrin depletion



6P3-Cypermethrin depletion assay








6P3(F110Y)-Cypermethrin depletion



6P3(L216F)-Cypermethrin depletion

Appendix 12: No of nucleotide change and the effects on enzyme activities.

Sequence Alignment of wild type and mutants	No of base mutated	Fold increase
AAGGCGTTCGAGTTGAATACGATGATCATGATGAAGA -CYP6P3 (wild) CAAGGCGTTCGAGTTCAATACGATGATCATGATGAAG - CYP6P3 (L216F) *****	1	 15- Fold (DEF)
GATCACGGCGTGTTTACCAATGCAAAGGACGACC -CYP6P3 (wild) GATCACGGCGTGTATACCAATGCAAAGGACGACC -CYP6P3 (F110Y) *****	1	 4-Fold (DEF)
GATCGCGGTGTCTACTGCAATGAAGAGCACG - CYP6Z2 (wild) GATCGCGGTGTCTTCTGCAATGAAGAGCACG - CYP6Z2 (Y102) *****	1	 2-Fold (MR)
AATCGGGGACGCAACTTTATCGATAACTTCCG CYP6Z2 (wild) AATCGGGGACGCAACTTGATCGATAACTTCCG CYP6Z2 (f2121) *****	1	 4-Fold (MR)
GTGCTAATCGGGGACGCAACTTTATCGATAAC - CYP6Z2 (wild) GTGCTAATCGGGGAGCCAACTTTATCGATAAC - CYP6Z2 (R210A) *****	2	 2-Fold (BR)

Appendix 13: Amino acids sequence alignment of CYP6Z1, CYP6Z2 & CYP6Z3

```
1 MLYTTIGLIVAFVFLALKYVYSYWDRQGLPNLRPEIPYGNLRILAQKKESFNVAINDLYD 60 Q8T631 Q8T631_ANOGA
1 MFVYTLALVAAVIFLVLRYIYSHWERHGLPHLKPPEIPYGNIRTVAEKKESFGTAINNLYH 60 Q8T625 Q8T625_ANOGA
1 MFVYTLALVAAVIFLVLRYIYSHWERHGLPHLKPPEIPYGNIRTVAEKKESFGTAINNLYH 60 Q86LT6 Q86LT6_ANOGA
*:*:*:*:*:*:*:*:*:*:*:*:*:*:*:*:*:*:*:*:*:*:*:*:*:*:*:*:*:*:*:
61 RSSERLVGVYLFRRPAILVRDAHLAKRIMVNDQFNHFDHFRGVYCNEHSDFMSANLFALPGQ 120 Q8T631 Q8T631_ANOGA
61 KSSDRLLGIYLFRRPAILIRDPHLAKRIMVNDQFNHFDHFRGVYCNEHDFPFSANLFALPGQ 120 Q8T625 Q8T625_ANOGA
61 KSSDRLLGIYLFRRPAILIRDPHLAKRIMVNDQFNHFDHFRGVYCNEHDFPFSANLFALPGQ 120 Q86LT6 Q86LT6_ANOGA
*:*:*:*:*:*:*:*:*:*:*:*:*:*:*:*:*:*:*:*:*:*:*:*:*:*:*:*:*:*:*:
121 RWKNLRAKLTPTFTSGQLRHMLPTFLAVGSKLEQYLERLANEKQIVDMRDIVSRVLDVV 180 Q8T631 Q8T631_ANOGA
121 RWKNLRAKLTPTFTSGQLRNMLPTLLDVGNKILDRMNKVADEKAIVDMRDIASRFVLDTI 180 Q8T625 Q8T625_ANOGA
121 RWKNLRAKLTPTFTSGQLRNMLPTLLDVGNKILDRMNKVADEKAIVDMRDIASRFVLDTI 180 Q86LT6 Q86LT6_ANOGA
*:*:*:*:*:*:*:*:*:*:*:*:*:*:*:*:*:*:*:*:*:*:*:*:*:*:*:*:*:*:*:
181 ASVFFGFEANCLHDPDDAFRVALRDLNPNPDSFMNNIRTAGVFLCPGLLKFTGINSLSPPM 240 Q8T631 Q8T631_ANOGA
181 ASVFFGFEANCIHNSEDPFLLSTLRRANRGRNFIDNFRSSGVFICPGLLKLTRMTSLQPEL 240 Q8T625 Q8T625_ANOGA
181 ASVFFGFEANCIHNSEDPFLLSTLQRLTKSRKFMDFNRTSGVFICPGLLKLTTRITSLPEL 240 Q86LT6 Q86LT6_ANOGA
*:*:*:*:*:*:*:*:*:*:*:*:*:*:*:*:*:*:*:*:*:*:*:*:*:*:*:*:*:*:*:
241 KKFTEVEISSHLHQRETQVVRKDFIQMLTDLRRKAGSSGEETLTDQAANVFLFYGAG 300 Q8T631 Q8T631_ANOGA
241 IKFVMEIITHQIDHREKNQITRKDFVQLLIDLRREADKGSSEALITIEQCAANVFLFYIAG 300 Q8T625 Q8T625_ANOGA
241 ISFVMEIITHQIDHREKNQITRKDFVQLLIDLRREAENGSEKALSIEQCAANVFLFYIAG 300 Q86LT6 Q86LT6_ANOGA
*:*:*:*:*:*:*:*:*:*:*:*:*:*:*:*:*:*:*:*:*:*:*:*:*:*:*:*:*:*:*:
301 ADTSTGTITFTLHELTHNAEAMAKLQREVDEMMEHGHGEITYDNITGMKYLDLCVKETLR 360 Q8T631 Q8T631_ANOGA
301 AETSTATISFTLHELHSHNPEAMAKLQQEIDEMMERYNGEITYENIKEMKYLDLCVKETLR 360 Q8T625 Q8T625_ANOGA
301 AETSTATISFTLHELHSHNPEAMAKLQQEIDEMMERYNGEITYENIKEMKYLDLCVKETLR 360 Q86LT6 Q86LT6_ANOGA
*:*:*:*:*:*:*:*:*:*:*:*:*:*:*:*:*:*:*:*:*:*:*:*:*:*:*:*:*:*:*:
361 IYPALAVLNRECTIDYKVPDSDTVIRKGTQMIIPLLGISMNEKYFPPELYSPERFDEAT 420 Q8T631 Q8T631_ANOGA
361 KYPGLPILNRECTIDYKVPDSDVIRKGTQVIIPLLSISMNEKYFPPELYSPERFDEAT 420 Q8T625 Q8T625_ANOGA
361 KYPGLPILNRECTIDYKVPDSDVIRKGTQVIIPLWSISMNEKYFPPELYSPERFDEAT 420 Q86LT6 Q86LT6_ANOGA
*:*:*:*:*:*:*:*:*:*:*:*:*:*:*:*:*:*:*:*:*:*:*:*:*:*:*:*:*:*:*:
421 KNYDADAYYPFGAGPRNCIGLRQGLLSKIALVMMLSRFNFSATIPRKIKFEPVSITLAP 480 Q8T631 Q8T631_ANOGA
421 KNYDADAYYPFGAGPRNCIG--QGLVSKIGLVFLLSKFNFAAAATVGLTP 478 Q8T625 Q8T625_ANOGA
421 KNYDADAYYPFGAGPRNCIGLRQGVFVSKIGLVLLSKYFNFAAATVAVVVTVP 480 Q86LT6 Q86LT6_ANOGA
*:*:*:*:*:*:*:*:*:*:*:*:*:*:*:*:*:*:*:*:*:*:*:*:*:*:*:*:*:*:*:
481 KGGLPMRIENRVKH 494 Q8T631 Q8T631_ANOGA
479 DAGFPMRIDHRK-- 490 Q8T625 Q8T625_ANOGA
481 EDGFP MRVEHRC-- 492 Q86LT6 Q86LT6_ANOGA
*:*:*:*:*:*
```

Amino Acids sequence alignment of CYP6Z1, CYP6Z2 and CYP6Z3. Asterisks represent identical residues, colons represent conserved residues, and dots represent semi conserved residues in the three sequences. The alignment indicates 332 identical positions and 116 similar positions. The amino acid identity of the three proteins is 67.206%. (Swissprot accession codes are Q8T631, Q8T625 and Q86LT6 respectively) - UniProtKB/Swiss-Prot. www.uniprot.org

Appendix 14: Amino acids sequence alignment of CYP6Z1, CYP6Z2 & CYP3A4

		A'		A	
CYP6Z1	MILY	<u>TIGLIVAFVFLAL</u>	<u>KYVYSY</u>	<u>WDRQGLPNLRPEIPY</u>	-GNLRILAQKKESFNVAINDLY 59
CYP6Z2	MFVY	<u>TLALVAAVIFLVL</u>	<u>RYIYSH</u>	<u>WERHGLPHLKPEIPY</u>	-GNIRTVAEKKESFGTAINNLY 59
CYP3A4	-----	<u>HS</u>	<u>GLFK</u>	<u>LGI</u>	<u>PGPTP-LPFLGNILSYHKGFCMFDMECHKKY 68</u>
		:	* * *	* * *	: * . . . *
		B		SRS1	
CYP6Z1	DRSS	<u>ERLVGVYLF</u>	<u>FRPA</u>	<u>ILVRDAHLAKRIMVND</u>	-FQHFHD <u>RGVYCNEHSDPMSANL</u> <u>FALP</u> 118
CYP6Z2	HKSS	<u>DRLLGIYLF</u>	<u>FRPA</u>	<u>ILIRDPHLAKRIMVND</u>	-FQNFH <u>DRGVYCNEEHDPFSANL</u> <u>FALP</u> 118
CYP3A4	GK----	<u>VW</u>	<u>GFYD</u>	<u>GQQPVL</u>	<u>AITDPDMIKTVLVKECYSVFTNRRPFGPVGF--MKS</u> <u>AI</u> <u>SIAE</u> 122
		:	* * *	* * *	: * . . . *
		C		D	E
CYP6Z1	<u>GQRW</u>	<u>KNLRAKL</u>	<u>TPTFTSGQLRHML</u>	<u>PTFLAVGSKLEQYLERLANEKQIVDMRDIVSRYVLD</u>	178
CYP6Z2	<u>GQRW</u>	<u>KNLRAKL</u>	<u>TPTFTSGQLRNML</u>	<u>PTLLDVGNKLIDRMNKVADEKAIVDMRDIASRFVLD</u>	178
CYP3A4	<u>DEEW</u>	<u>KRLRSL</u>	<u>SPTFTSGKLE</u>	<u>KEMVPIIAQYGDVLRNLRREAETGKPVTLKDVFGAYSMD</u>	182
		. . . * . * . *	* : * * * * * : * . * * . *	. . . * . * . *	. . . * . * . *
		F	SRS2	F'	G'
CYP6Z1	VVAS	<u>VFP</u>	<u>GF</u>	<u>FEANCLHDPDDAF</u>	<u>VALRDLN</u>
CYP6Z2	TIAS	<u>VFP</u>	<u>GF</u>	<u>FEANCIHNS</u>	<u>EDPFLSTLRRANRGRNFI</u>
CYP3A4	VITST	<u>SPGVNIDSLN</u>	<u>NPQDPF</u>	<u>VENTKLLRFD</u>	<u>FLDPFFLSITVFPFLIP-ILEVLN</u> <u>ICVF</u> 241
		. . . * . * . *	. . . * . * . *	. . . * . * . *	. . . * . * . *
		SRS3	G	H	I SRS4
CYP6Z1	<u>SPPM</u>	<u>KKFTTE</u>	<u>VISSHLHQR</u>	-ETGQVMRKDFIQMLTDLRRKAGSSGEETLTD <u>ACCAANVFL</u>	295
CYP6Z2	<u>QP</u>	<u>ELIKFVMEI</u>	<u>ITHQIDHR</u>	-EKNQITRKDFVQLLIDLRRREADKGSSEALTI <u>EQCAANVFL</u>	295
CYP3A4	<u>PREVTN</u>	<u>FLRKS</u>	<u>VKRMKES</u>	<u>RL</u>	<u>LEDTQKHRVDFLQLMID----</u>
		: . . * . . . *	. . . * . * . *	. . . * . * . *	. . . * . * . *
		J		K	
CYP6Z1	<u>FYGA</u>	<u>GADT</u>	<u>STGTIT</u>	<u>FTLHEL</u>	<u>THNAEAMAKLQREVD</u>
CYP6Z2	<u>FYLA</u>	<u>GAET</u>	<u>ST</u>	<u>ATISFTLHEL</u>	<u>SHNPEAMAKLQREID</u>
CYP3A4	<u>FIFAG</u>	<u>YETTS</u>	<u>SVLS</u>	<u>FIMYELATH</u>	<u>PDVQQLQEEIDAVLPN-KAPPTYD</u>
		* ** : * *	: * * * . . . *	* * * . * * . *	: . . * * * . * * * . *
		SRS5		K'	K''
CYP6Z1	<u>KETL</u>	<u>RINPA</u>	<u>AVLNRE</u>	<u>CTIDYKVPDSDTVIRKGTQMI</u>	<u>IPLLGISMNEKYFPEPELYSPER</u> 415
CYP6Z2	<u>KETL</u>	<u>RKY</u>	<u>PGLPILNRE</u>	<u>CTIDYKVPDSDVIRKGTQVII</u>	<u>IPLLSISMNEKYFPDPPELYSPER</u> 415
CYP3A4	<u>NETL</u>	<u>RLPPIAM</u>	<u>RLE</u>	<u>RVCKDVEI--</u>	<u>NGMFI</u>
		: * * * * . *	* * * . * . *	. . . * * * . * * * . *	. . . * * * . * * * . *
		Heme binding L			
CYP6Z1	<u>FDEATK</u>	-NYDADAYYPFGAGPRNCIGLRQGLLLSKIALVMMLSRFNFSATIPRKIKFEPV			474
CYP6Z2	<u>FDEATK</u>	-NYDADAYYPFGAGPRNCIGLRQGLVLSKIGLVFLLSKFKFQATTPAKVKFAAA			474
CYP3A4	<u>F</u>	<u>SKKNKDNIDP</u>	<u>YIYTPFGSGPRNCIGMRFALMNMKLALIRVLQNF</u>	<u>SFKPCKETQIPLKLS</u>	478
		* . . * * * . *	* * * * * * * * * * . *	. . . * . * . *	. . . * . * . *
		SRS6			
CYP6Z1	<u>SIT</u>	<u>LA</u>	-PKGGLPMRIENRVKH		494
CYP6Z2	<u>TVGLT</u>	-PDAGFPMRIDHRK--			492
CYP3A4	<u>LG</u>	<u>LLQPEK</u>	<u>PVVLKVESRDGT</u>		498
		* * *			

Amino Acids sequence alignment of CYP6Z1, CYP6Z2, and CYP3A4. *An. Gambiae* CYP6Z1 from the RSP-ST strain (GenBank accession no. AF487535), *An. Gambiae* CYP6Z2 from the PEST strain (GenBank accession no. XP_317252), and human CYP3A4 (Protein Data Bank ID code 1TQN) are shown with underlines representing α -helices and gray blocks representing SRS regions. Asterisks represent identical residues, colons represent conserved residues, and dots represent semi conserved residues in the three sequences. Residues in the CYP6Z1 sequence predicted to exist within 4.5 Å of DDT are boxed (Chiu et al. 2008).

Appendix 15: % amino acids identities between CYP6Z1, CYP6Z2, CYP6Z3 and CYP3A4

Swissprot Accession Code	Enzyme	Amino Acids Length	Amino Acids % Identity to CYP6Z1	Amino Acids % Identity to CYP6Z2	Amino Acids % Identity to CYP6Z3	Amino Acids % Identity to CYP3A4
Q8T631	CYP6Z1	494	-	69.433	68.623	27.132
Q8T625	CYP6Z2	490	69.433	-	93.699	28.185
Q86LT6	CYP6Z3	492	68.623	93.699	-	29.207
P08684	CYP3A4	503	27.132	28.185	29.207	-

Appendix 16: DNA Sequence confirmation of ompACYP6Z1

```

6z1template -----
forward      CATATGAAAAGACAGCTATCGCGATTGCAGTGGCACTGGCTGGTTTCGCTACCGTAGCG 60
6z1template -----ATGATCCTTTACACGATCGGACTGATCGTGGCGTTTGTTCCTCGCC 48
forward      CAGGCCGCTCCGATGATCCTTTACACGATCGGACTGATCGTGGCGTTTGTTCCTCGCC 120
                *****
6z1template  CTCAAGTACGTCTACTCGTACTGGGATCGACAGGGGCTGCCGAATTTGAGGCCGAAATT 108
forward      CTCAAGTACGTCTACTCGTACTGGGATCGACAGGGGCTGCCGAATTTGAGGCCGAAATT 180
                *****
6z1template  CCCTACGGCAATCTACGCATTCTAGCCCAAAGAAAGAATCCTTCAATGTGGCTATTAAC 168
forward      CCCTACGGCAATCTACGCATTCTAGCCCAAAGAAAGAATCCTTCAATGTGGCTATTAAC 240
                *****
6z1template  GATCTGTACGACCGTTCCAGTGAACGGTTGGTTGGAGTTTATCTGTTCTCCGCCCAGCG 228
forward      GATCTGTACGACCGTTCCAGTGAACGGTTGGTTGGAGTTTATCTGTTCTCCGCCCAGCG 300
                *****
6z1template  ATCCTGGTCCGGGATGCGCATCTCGCCAAGCGGATAATGATGAACGATTTCCAGCACTTT 288
forward      ATCCTGGTCCGGGATGCGCATCTCGCCAAGCGGATAATGATGAACGATTTCCAGCACTTT 360
                *****
6z1template  CACGACCGTGGCGTCTACTGCAACGAGCACAGTGATCCGATGTCGGCCAACCTGTTCGCC 348
forward      CACGACCGTGGCGTCTACTGCAACGAGCACAGTGATCCGATGTCGGCCAACCTGTTCGCC 420
                *****
6z1template  CTGCCCGGCCAGCGGTGGAAAAATCTGCGTGCGAAGCTTACACCAACCTTCACCTCCGGC 408
forward      CTGCCCGGCCAGCGGTGGAAAAATCTGCGTGCGAAGCTTACACCAACCTTCACCTCCGGC 480
                *****
6z1template  CAGTACGGCACATGCTGCCAACGTTTCTGGCAGTGGGCAGCAAGCTCGAGCAGTATCTC 468
forward      CAGTACGGCACATGCTGCCAACGTTTCTGGCAGTGGGCAGCAAGCTCGAGCAGTATCTC 540
                *****
6z1template  GAACGCTTGGCAAACGAAAAACAGTCCG---ACATGCGTGACATCGTTTCGCGCTACGTG 525
forward      GAACGCTTGGCAAACGAAAAACAGTCCG---ACATGCGTGACATCGTTTCGCGCTACGTG 597
                *****
6z1template  CTCGATGTGGTGGCTTCAGTGTTCGCGCTTCGAAGCCAACTGTCTGCACGATCCCGAC 585
forward      CTCGATGTGGTGGCTTCAGTGTTCGCGCTTCGAAGCCAACTGTCTGCACGATCCCGAC 657

```

```

*****
6z1template      GATGCGTTCGGTGTGGCGTTGCGTGATCTTAACAATCCGGACAGCTTCATGAACAACATC 645
forward          GATGCGTTCGGTGTGGCGTTGCGTGATCTTAACAATCCGGACAGCTTCATGAACAACATC 717
*****
6z1template      CGAACAGCCGGCGTTTTTCTGTGTCCCGGCTGCTAAAGTTTACCGGCATCAAATCGCTA 705
forward          CGAACAGCCGGCGTTTTTCTGTGTCCCGGCTGCTAAAGTTTACCGGCATCAAATCGCTA 777
*****
6z1template      TCGCCTCCGATGAAAAAGTTTACCACAGAAGTGATCAGTCCCATCTGCACCAGCGTGAG 765
forward          TCGCCTCCGATGAAAAAGTTTACCACAGAAGTGATCAGTCCCATCTGCACCAGCGTGAG 837
*****
6z1template      ACGGGCCAGGTGATGCGCAAGGACTTTATCCAGATGCTAACGGATCTGCGCCGCAAGGCT 825
forward          ACGGGCCAGGTGATGCGCAAGGACTTTATCCAGATGCTAACGGATCTGCGCCGCAAGGCT 897
*****
6z1template      GGTAGCAGTGGGAAGAAACGCTCACCGATGCACAGTGTGCGCCAATGTGTTTCTGTTT 885
forward          GGTAGCAGTGGGAAGAAACGCTCACCGATGCACAGTGTGCGCCAATGTGTTTCTG--- 954
*****

```

Appendix 17: DNA Sequence confirmation of SDM of CYP6Z3 (F115A)

FW Primer 1

```

primer      CATATGAAAAAGACAGCTATCGCGATTGCAGTGGCACTGGCTGGTTTCGCTACCGTAGCG 60
Template    -----

primer      CAGGCCGCTCCGATGGCTGTTTACACTCTCGCGCTCGTGGCGGCCGTGATCTTTCTCGTG 120
Template    -----ATGTTTGTTTACACTCTCGCGCTCGTGGCGGCCGTGATCTTTCTCGTG 48
              ***      *****

primer      CTCCGCTACATCTACTCTCACTGGGAGAGGCATGGACTTCCGCATCTAAAGCCAGAGATT 180
Template    CTCCGCTACATCTACTCTCACTGGGAGAGGCATGGACTTCCGCATCTAAAGCCAGAGATT 108
              *****

primer      CCGTACGGCAACATACGCACCGTTGCCGAGAAGAAAGAATCATTCGGAATTGCCATCAAC 240
Template    CCGTATGGCAACATACGCACCGTTGCCGAGAAGAAAGAATCATTCGGAATTGCCATCAAC 168
              *****

primer      AACCTGTACCACAAGTCGTCCGACCGTCTGCTGGGAATCTACCTGTTCTTCGGCCCTGCT 300
Template    AACCTGTACCACAAGTCGTCCGACCGTCTGCTGGGAATCTATCTGTTCTTCGGCCCTGCT 228
              *****

primer      ATCTTGATTTCGCGATCCTCATCTCGCGAAGCGTATTATGGTAAACGACTTCCAGAACTTT 360
Template    ATCTTGATTTCGCGATCCTCATCTCGCGAAGCGTATTATGGTAAACGACTTCCAGAACTTT 288
              *****

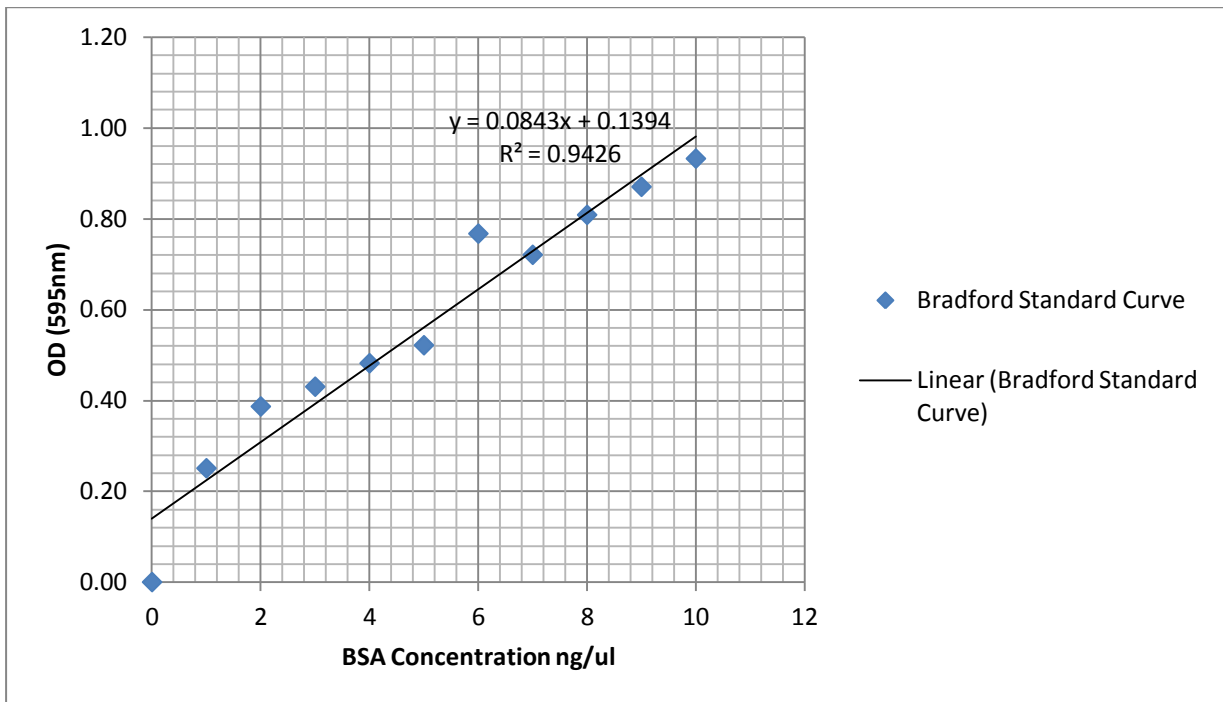
primer      CACGATCGCGGTGTCTACTGCAACGAAGAGCACGATCCCTTCTCGGCCAATCTGGCCGCT 420
Template    CACGATCGCGGTGTCTACTGCAATGAAGAGCACGATCCCTTCTCGGCCAATCTGTTTCGCT 348
              *****

primer      CTGCCCAGTACGCGGTGGAAGAAGTGGCGTGCAGGCTCACGCCGACCTTACGTCGCGGA 480
Template    CTGCCCAGTACGCGGTGGAAGAAGTGGCGTGCAGGCTCACGCCGACCTTACGTCGCGGA 408
              *****

primer      CAACTGCGTAACATGCTCCCNCCCTGCTGGACGTCGGCAACAAGCTGATCGATCGTATG 540
Template    CAACTGCGTAACATGCTCCCNCCCTGCTGGACGTCGGCAACAAGCTGATCGATCGTATG 468
              *****

```

Appendix 18: Protein standard curve



BSA Standard Curve